MISSISSIPPI ACADEMY OF SCIENCES

Supplemental Issue

33rd Annual Southern Biomedical Engineering Conference

Digest of Papers

March 17-19, 2017

Courtyard by Marriott Beachfront,

Gulfport, MS

Major Sponsor

Mississippi Academy of Science

Journal of the Mississippi Academy of Sciences

Volume 62 April 2017 Supplemental Issue 1

The Journal of the Mississippi Academy of Sciences (ISSN 0076-9436) is published in January (annual meeting abstracts), April, July, and October, by the Mississippi Academy of Sciences. Members of the Academy receive the journal as part of their regular (nonstudent) membership. Inquiries regarding subscriptions, availability of back issues, and address changes should be addressed to The Mississippi Academy of Sciences, Post Office Box 55709, Jackson, MS 39296-5709, telephone 601-977-0627, or email msacademyofscience@comcast.net.

Contents

156 HISTORY – SOUTHERN BIOMEDICAL ENGINEERING CONFERENCE

157 KEYNOTE SPEAKERS

PAPERS

161 **USING POLYMER BULK DIFFUSION AS A MECHANISM FOR ADVANCING TISSUE ENGINEERING APPLICATIONS**

Kelsey Phelan and Bryant Hollins
Louisiana Tech University, Ruston, LA, USA

164 **BENEFICIAL EFFECTS OF SEMEN PURIFICATION WITH MAGNETIC NANOPARTICLE**

Casey Durfey[1], Sabrina Swistek[1,2], Wei Tan[3], Henry Clemente[*], Peter Ryan[1,4], Scott Willard[1,2], and Jean Feugang[1]
[1]Departments of Animal and Dairy Sciences, [2]Biochemistry and Molecular Biology & Entomology and Plant Pathology, [3]Basic Sciences, 4Pathobiology and Population Medicine at Mississippi State University, [*]Clemente Associates, Madison, CT, USA

168 **EFFECT OF MUSCLE ENGAGEMENT AND MEASUREMENT POSITION ON ELECTRICAL IMPEDANCE OF THIGH MUSCLES**

Joseph Mathews and Todd Freeborn
The University of Alabama Tuscaloosa, AL, USA

172 **VARIABILITY OF ELECTRICAL IMPEDANCE MEASUREMENTS COLLECTED FROM HUMAN FOREARM USING MULTIPLE ELECTRODE CONFIGURATION**

Shelby Critcher and Todd Freeborn
The University of Alabama, Tuscaloosa, AL, USA

176 **A NEW METHOD FOR EARLY DIAGNOSIS OF COLON CANCER USING FLUORESCENCE EXCITATION-SCANNING HYPERSPECTRAL IMAGING**

Malvika Lall[1,6], Joshua Deal[1,3], Shante Hill[4], Paul Rider[5], Carole Boudreaux[4], and Thomas Rich[2]
[1]Chemical and Biomolecular Engineering, University of South Alabama, Mobile, AL, USA; [2]Pharmacology, University of South Alabama, Mobile, AL, USA; [3]Center of Lung Biology, University of South Alabama Mobile, AL, USA; [4]Pathology, University of South Alabama, Mobile, AL, USA; [5]Surgery, University of South Alabama, Mobile, AL, USA; [6]Biomedical Sciences, University of South Alabama, Mobile, AL, USA

181 **FUNCTIONAL ANALYSIS OF AIF-1 IN ASSOCIATION WITH CARDIAC ISCHEMIA REPERFUSION (IR)**

Olga McDaniel[1], Allen Simeone[1], Kathy Alvarez[2], Madeleine Cunningham[2], and Larry McDaniel[1]
[1]University of Mississippi Medical Center, Jackson, MS, USA and [2]University of Oklahoma Health Science Center, Oklahoma City, OK, USA

Contents Continued

183 **EFFECT OF MUSCLE FATIGUE ON ELECTRICAL IMPEDANCE OF BICEP MUSCLES DURING EXERCISE OF VARYING INTENSITY: A CASE STUDY**
Tim Crenshaw and Todd Freeborn
The University of Alabama, Tuscaloosa, AL, USA

188 **APPLICATIONS OF INERTIAL MICRO-ELECTRO-MECHANICAL SYSTEMS ON AMERICAN FOOTBALL PLAYERS AND EQUIPMENT**
Derius Galvez and Jamel Alexander
Mississippi State University, Starkville, MS, USA

192 **BIOCOMPATIBILITY OF NOVEL COPPER-CONTAINING BIOCOMPOSITES IN QUANTIFIABLE MODEL CELL SYSTEM**
Kahla St Marthe, Mark DeCoster, Neha Karekar, and Anik Karan
Louisiana Tech University, Rushton, LA, USA

196 **IN VIVO EVALUATION OF THE EFFECT OF RESONANCE FREQUENCY ON DELIVERING INSULIN NON-INVASIVELY USING ULTRASOUND**
Khaldon Lweesy
Jordan University of Science and Technology, Irbid, Jordan

200 **BEHAVIORAL RISK FACTORS ASSOCIATED WITH ADULT OBESITY AND INFLUENCE OF THE BUILT ENVIRONMENT**
Shelia Baitey and Elgenaid Hamadain
University of Mississippi Medical Center, Jackson, MS, USA

206 **COMPARING COLORECTAL CANCERS IN MISSISSIPPI BY RACE, STAGE, AGE, REGION, AND AREA-BASED SOCIOECONOMIC STATUS**
Deirdre Rogers and Elgenaid Hamadain
University of Mississippi Medical Center, Jackson, MS, USA

213 **ANTICOAGULANT EFFECTS ON PURE PLATELET-RICH PLASMA**
Sofia Galdames, Andrea Shimojo, Angela Luzo, and Maria Santana
Unicamp Campinas, SP, Brazil

217 **PREVALENCE AND TRENDS OF EARLY CHILDHOOD CARIES EXPERIENCE AND UNTREATED CARIES IN THE MISSISSIPPI HEAD START POPULATION**
Kristin Nalls, Elgenaid Hamadain, and Denise Krause
University of Mississippi Medical Center, Jackson, MS USA

223 **TAILORING GITLAB FOR COMPUTER SCIENCE PROGRAMMING COURSES**
Mesafint Fanuel[1] and Tzusheng Pei[1*], Ali Abu El Humos[1], Andrew Villarrubia[1], and Hyunju Kim[2]
[1]Jackson State University, Jackson, MS, USA and [2]Department of Mathematics and Computer Science, Wheaton College, Wheaton, IL, USA

227 **INCREASED GLUTHATIONE in CAOV-3 OVARIAN CANCER CELLS FOLLOWING DELIVERY OF THYMOQUINONE**
Jennifer Harpole, Michelle Tucci, and Hamed Benghuzzi
University of Mississippi Medical Center, Jackson, MS, USA

Contents Continued

230 **NANOCERIA AND CATALASE CONJUGATES AS A FREE-RADICAL SCAVENGING SYSTEM**

Brendan Ward[1], Dmitry Gil[1], Vladimir Ivanov[2], and Vladimir Reukov[1,3]
[1]Department of Bioengineering, Clemson University Clemson, SC USA; [2]Kurnakov Institute of General and Inorganic Chemistry Moscow Russia; [3] Institute for Biological Interfaces of Engineering, Clemson University Clemson, SC USA

234 **NONLINEAR FINITE ELEMENT ANALYSIS OF MICRO-LATTICE STRUCTURES FOR PATIENT SPECIFIC IMPLANTS**

Prashant Athanker and Amit Singh
MNIT Jaipur, India

239 **A NEW EXCITATION-BASED TECHNIQUE FOR ESTIMATING FRET EFFICIENCY**

John Robert Griswold, Naga Annamdevula, Joshua Deal, Thomas Rich, and Silas Levesley
University of South Alabama, Mobile, AL, USA

243 **MIRROR THERAPY FOR LOWER EXTREMITY RECOVERY AND GAIT IN SUBACUTE STROKE: A RANDOMIZED CONTROL TRIAL**

Lisa J. Barnes and Kim Curbow Wilcox
University of Mississippi Medical Center, Jackson, MS, USA

245 **THE EFFECTS OF AQUATIC THERAPY ON FATIGUE AND QUALITY OF LIFE IN PATIENTS WITH MULTIPLE SCLEROSIS: A SYSTEMATIC REVIEW**

Kimberly Willis and Lisa J. Barnes
University of Mississippi Medical Center, Jackson, MS, USA

247 **THE EFFECTS OF THERAPEUTIC ULTRASOUND ON ADULT PATIENTS WITH NON-SPECIFIC CHRONIC LOW BACK PAIN: A SYSTEMATIC REVIEW**

Sherry Colson and Lisa J. Barnes
University of Mississippi Medical Center, Jackson, MS, USA

252 **THE EFFECTS OF HIPPOTHERAPY ON GROSS MOTOR FUNCTION IN CHILDREN WITH CEREBRAL PALSY: A SYSTEMATIC REVIEW**

Janet Slaughter and Lisa J. Barnes
University of Mississippi Medical Center, Jackson, MS USA

255 **THE EFFECT OF DRY NEEDLING ON PAIN CONTROL AND POSSIBLE MECHANISM**

Felix Adah, Min Huang, and Mark Weber
University of Mississippi Medical Center, Jackson, MS, USA

261 **THE EFFECT OF COMBINATION TREATMENTS OF EPIGALLOCATECHIN-3-GALLATE, THYMOQUINONE, AND 5-FLUOROURACIL ON FADU NASOPHARYNGEAL CARCINOMA CELLS**

Sharita Williams, Hamed Benghuzzi, and Michelle Tucci
University of Mississippi Medical Center, Jackson, MS, USA

265 **THE EVALUATION OF ANTIHYPERTENSIVE AGENTS USING CARDIOMYOCYTES**

Shana Nelson, Hamed Benghuzzi and Michelle Tucci
University of Mississippi Medical Center, Jackson, MS, USA

269 **TOWARDS THE PREVENTION OF OXIDATIVE DAMAGE VIA NOVEL ANTIOXIDANT CONJUGATES**

Jeannette Rodriguez, Dmitry Gil[1], Vladimir Ivanov[2], and Vladimir Reukov[1,3]
[1] Department of Bioengineering, Clemson University Clemson, SC USA; [2]Kurnakov Institute of General and Inorganic Chemistry Moscow Russia; [3] Institute for Biological Interfaces of Engineering, Clemson University Clemson, SC, USA

272 **DEVELOPING AN APPARATUS TO TREAT PLANTAR FASCIITIS**

Jack McGreevey, Benjamin Shumpert, Eddie Bear, Bryce Kunkle, Jushawn Macon, Vladimir Reukov
Clemson University, Clemson, SC, USA

275 **THE RESPONSE OF INTERLEUKIN-STIMULATED A549 HUMAN ALVEOLAR BASAL EPITHELIAL CELLS UPON EXPOSURE TO HYDROCORTISONE IN CULTURE**

Jana Bagwell
University of Mississippi Medical Center, Jackson, MS, USA

278 **LOW LEVEL LASER THERAPY IMPROVES MICROCIRCULATION IN SKELETAL MUSCLE VASCULAR BEDS IN ZUCKER RATS**

Silu Lu, Lusha; Xiang, Robert L. Hester, Lisa Barnes, Ham Benghuzzi, and Min Huang
Departments of Physical Therapy, Physiology and Biophysics, University of Mississippi Medical Center, Jackson, MS, USA

283 **SULFORAPHANE, A DIETARY COMPONENT OF BROCCOLI SPROUTS ATTENUATES HYPERTENSION AND MAITAINS RENAL STRUCTURE ON SHRsp RATS**

Ali Banigesh[1], Ramlah Iqbal[1], Adam Murabit[1], Kaushik Desai[2] and Adel Mohamed[1]
[1]Department of Anatomy and Cell Biology, College of Medicine, University of Saskatchewan, Saskatoon, Saskatchewan, Canada, and Department of Pharmacology, College of Medicine, University of Saskatchewan, Saskatoon, Saskatchewan, Canada.

Hamed A. Benghuzzi, Ph.D.
Department of Diagnostic and Clinical Health Sciences
University of Mississippi Medical Center
Jackson, MS 39216

Michelle A. Tucci, Ph.D.
Department of Anesthesiology
University of Mississippi Medical Center
Jackson, MS 39216

Program Committee

Amol Janorkar, Ph.D.
Ibrahim Farah, Ph.D.
Joseph A. Cameron, Ph.D.
Felix Adah, Ph.D.
Gerri Wilson, Ph.D.$_c$
Tom Rich, Ph.D.
Ken Butler, Ph.D.
Lynne Jones, Ph.D.
Lir-Wan Fan, Ph.D.
Adel Mohamed, M.D.
Jafar Vossoughi**,** Ph.D.
Elgenaid Hamadain, Ph.D.
Tom Fields, MS
Olga McDaniel, Ph.D.
Larry McDaniel, Ph.D.
Angelia Garner, Ph.D.
Zelma Cason, Ph.D.

Scientific Committee

Michelle Tucci, Ph.D. (Chair)
Hamed Benghuzzi, Ph.D.
Amol Janorkar, Ph.D.
Tom Rich, Ph.D.
Adel Mohamed, M.D.
Olga McDaniel, Ph.D.
Ibrahim Farah, Ph.D.
Ken Butler, Ph.D.
Jafar Vossoughi, Ph.D.
Larry McDaniel, Ph.D.
Joseph A. Cameron, Ph.D.
Lynne Jones, Ph.D.
Elgenaid Hamadain, Ph.D.
Lir-Wan Fan, Ph.D.
Tom Fields, MS
Zelma Cason, Ph.D.
Subrata Saha, Ph.D.
Bryant Hollins, Ph.D.
Teresa Murray, Ph.D.
Saami Yazdani, Ph.D.
Leon Iaesmidis, Ph.D.
Min Huang, Ph.D
Jamil Ibrahim, Ph.D.
C. Lashan Simpson, Ph.D.
Ramesh Patel, M.D.
Elgenaid Hamadain, Ph.D.
Pradip Biswas, Ph.D.
Ahmed El-Ghannam, Ph.D.
Vinoy Thomas, Ph.D.
Gene Bidwell, Ph.D.
Silas Levesley, Ph.D.
Ali Abu El Humos, Ph.D.
Xiaoli Dai, M.D.
Jens Rosenberg, Ph.D.
Mohammed Benalla, Ph.D.
Angelia Garner, Ph.D.
Felix Adah, Ph.D.
Alamgir Hossain, Ph.D.

SBEC HISTORY

The Southern Biomedical Engineering Conference (SBEC) series was conceived by bioengineering professionals from academia and industry located primarily in the South of the United States in 1982. The first Southern Biomedical Engineering Conference was held at the LSU Medical Center, Shreveport, Louisiana, in 1982. Since then it has been held annually in different cities, mostly in the southern United States, and has grown to become a global event that regularly attracts attendees from all over the world. Submitted Papers are peer-reviewed, and those papers accepted for presentation and publication appear in the yearly issue of SBEC proceedings.

The SBEC serves a special purpose by emphasizing participation from young professionals and advanced students. Since established investigators present papers in the same sessions with the students, it encourages a high level of professionalism as a standard for young investigators and students. Submission of papers from individuals from around the world is encouraged. However, if their papers are accepted, an author or co-author must attend the conference to present their work and to interact with other attendees. In keeping with the emphasis on student participation, the SBEC presents best paper and presentation awards to undergraduate, graduate, and professional students.

Keynote Speaker – I

"Multifunctional Bioceramics for Innovative Therapy"

Ahmed El-Ghannam, Ph.D.

President, International Society for Ceramics in Medicine
Associate Editor, Journal of Biomedical Materials Research
Associate Professor of Tissue Engineering and Biomaterials,
Department of Mechanical Engineering and Engineering Science,
University of North Carolina at Charlotte

Dr. Ahmed El-Ghannam holds a BSc in Chemistry, MSc in Glass Science and Technology, and an MS and Ph.D. in Bioengineering from the University of Pennsylvania. He has over 30 years of experience in material science and bioceramics engineering. He has six US patents, many world-renowned collaborators, and has been invited as a keynote and plenary speaker to various national and international meetings. He is the Associate. Editor for the Journal of Biomedical Materials and a leader in various prestigious societies. Dr. El-Ghannam's lab focuses on the development of bioceramics for multifaceted applications in drug delivery to treat cancer and infection, augment soft tissue and reconstruct bone. Dr. El-Ghannam's team includes clinicians, molecular biologists, and scientists who are widely published.

Keynote Speaker – II

"Clinical Trial of Medical Devices"

Jafar Vossoughi, Ph.D.

President, Biomedical Research Foundation
President, Engineering and Scientific Research Associates
Adjunct Professor, Fischell Department of Bioengineering University of Maryland,
Fellow: American Institute of Medical and Biological Engineers
Fellow: American Society of mechanical Engineers
Fellow: European Academy of Sciences
Fellow: Washington Academy of Sciences

Dr. Vossoughi received his Ph.D. degree in Applied Mechanics and Biomechanics from the Catholic University of America in Washington, DC in 1989. He has been a faculty member at the Catholic University of America, University of District of Columbia, and the University of Maryland. Dr. Vossoughi has taught many engineering, biomedical, and clinical courses to engineering students, residents, and physicians. For his work in the area of applied biomechanics he has been recognized by numerous professional societies, including the Arthur Guyton Award on Cardiovascular Physiology, Samuel Sideman Award of Cardiovascular Biomechanics, C. William Hall Research Award in Biomedical Engineering, and several dedicated service awards. He serves as a guest scientist and consultant to the FDA Center for Devices and Radiological Health along with several other government and private agencies. He has published over 250 peer reviewed papers, 14 book chapters, and 16 books.

"Scientific Writing and Publishing"

Dr. Larry McDaniel

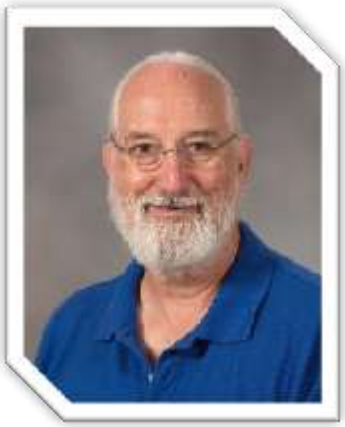

After completing his education and training, Dr. McDaniel has held teaching positions at the University of Mississippi Medical Center, the University of Southwestern Louisiana, University of Oklahoma and the University of Alabama at Birmingham, as well as other positions in the private sector. He is active with editorial service and holds several patents. Dr. McDaniel's research interests include host pathogen interactions and molecular basis of infectious disease. The goal of the workshop is to initiate the development of skills needed to write and submit a scientific manuscript. Insight will be provided into the processes required to successfully publish a scientific article. A brief discussion of ethics in scientific writing will be presented.

"Power and Sample Size Analysis: Importance in Research and Approaches to Best Practices"

Dr. Elgenaid Hamadain

Dr. Hamadain obtained both his MS and PhD degrees from Mississippi State University in the area of Entomology/Toxicology/Statistics. He has held faculty positions at Jackson State University (JSU) and at the University of Mississippi Medical Center (UMMC). During his tenure at JSU he established and was director of an NIH funded Biostatistical Support Unit. As Director of the Core he provided statistical advice to faculty and graduate students within the College of Science, Engineering, and Technology. Dr. Hamadain joined the UMMC faculty in 2006 and has been instrumental in the development and implementation of the biostatistical core courses in the Clinical Health Science graduate program. He has served as the major advisor for 15 students and has been on the advisory committee for over 50 graduate students. He provides statistical advice on all aspects of experimental design, including sample sizedetermination, probability and hypothesis testing, regression and correlation analysis, and parametric and non-parametric analysis. He has significant experience with data analysis using SAS, MINITAB, STATA, and SPSS statistical packages with particular emphasis on experimental design, factorial analysis, Factor Analysis, ANCOVA, logistic and probit analysis, survival analysis, and analysis of risk factors associated with diseases. Dr. Hamadain has conducted biostatistical educational workshops and seminars at local and state level meetings. His interests and publications are in the areas of outcome, epidemiology, analysis of health surveys, and meta-analysis research. The goal of this workshop is to enlighten graduate students and faculty on the importance of power analysis prior to implementing the experiment.

Keynote Speaker– III

"Computational Tools for Prediction Toxicity of Nanomaterials"

Dr. Jerzy Leszczynski

Professor of Chemistry
President's Distinguished Fellow
Director, NSF Interdisciplinary Nanotoxicity CREST Center
Jackson State University
Jackson, MS, USA

Dr. Leszczynski, a computational quantum chemist, joined the faculty of the JSU Department of Chemistry in 1990. He attended the Technical University of Wroclaw (TUW) in Wroclaw, Poland where he obtained his MS (1972) and Ph.D. (1975) degrees. Two areas of his most notable research contributions are: investigations of DNA fragments and development of novel techniques for investigation of properties and toxicity of nanomaterials.

Dr. Leszczynski has served as referee for over 50 journals and has published about 900 refereed papers and over 70 book chapters. He has given about 1000 presentations, with over 200 of those being invited presentations. His papers have been cited about 20,000 times and, according to the Web of Science, his Hirsh Index amounts to 64. He is the recipient of the White House Millennium Award for Teaching and Research Excellence in Mathematics, Science, and Engineering. Other selected awards include Member of the European Academy of Sciences, 2002; Guest Professorship, Chinese Academy of Sciences, Shanghai, 2002; Honorary Doctorate, Dnipropetrovsk National University, 2003; and Honorary Professorship\. He is the chairman of the organizing committee for the annual International Conference Series on Current Trends in Computational Chemistry (since 1992); chairman of the organizing committee for Southern Schools on Computational Chemistry and Material Sciences Series (since 2001); editor and member of editorial boards of eight journals; editor of a total of 36 books including four book series: "**Computational Chemistry: Reviews of Current Trends**" World Scientific; **"Challenges and Advances in Computational Chemistry and Physics,"** (Springer); **"Practical Aspects of Computational Chemistry"** (Springer); and editor of two editions of the "**Handbook of Computational Chemistry"** (Springer); **"Lecture Notes in Chemistry"** (Springer).

Keynote Speaker – IV

"Translational Research and Major Challenges to Basic Scientists"

Dr. Hamed Benghuzzi

Dr. Benghuzzi is a professor at the University of Mississippi Medical Center. He is known nationally and internationally as a pioneer in ceramic drug delivery systems. He has over 250 PubMed indexed articles and over 700 abstracts detailing the release characteristics of various biologicals from the bioceramic carriers. He has trained more than 35 Ph.D. students who are actively involved in academic careers. He has mentored students at all levels (from high school, undergrad, grad, post doc and faculty). He has served as a mentor for residents and faculty on more than 10 funded grants. He has served in leadership roles in many organizations such as President of the Academy of Surgical Research, Vice President of the Rocky Mountain Bioengineering Society, President of Mississippi Academy of Sciences (MAS), and Executive Director-MAS; he has also organized and chaired several regional, national and international society programs. He has also served on numerous NIH special emphasis panels including R-25, K01, KO8, T-35, and the P-60 center grants. In addition, he has received numerous awards from various organizations during his career. A few of his awards include: (1) the Presidential Award from the RMBS, (2) the Presidential Award from SEM International, (3) the Endocrine Society's Outstanding Investigator Award, (4) the MAS Contribution to Science Award, (5) The MAS Dudley Peeler Award, (6) the HEADWAE Award, (7) the C. William Hall Award- Outstanding Contribution to Biomedical Engineering (32nd SBEC), and (8) the ISCM Excellence Award from the International Society for Ceramics in Medicine. He was invited as a keynote/plenary speaker at state, national and international levels including recent invitations in France, Italy, Spain, Greece, China, Poland, Dubai and Canada. He is a fellow of the American Institute for Medical and Biological Engineering (AIMBE) as well as an International Fellow of Biomaterials Science and Engineering (FBSE).

Keynote Speaker – V

"Historical Perspective of SBEC"

Dr. Subrata Saha

Editor-in-Chief, Journal of Long Term Effects of Medical Implants; Ethics in Biology; Engineering & Medicine
Director, Biomedical Engineering Program, School of Graduate Studies
Research Professor and Director of Musculoskeletal Research.
Department of Orthopaedic Surgery and Rehabilitation Medicine.
Professor, Dept. Physiology & Pharmacology
SUNY Downstate Medical Center

Dr. Subrata Saha was the Director of Musculoskeletal Research and Research Professor in the Department of Orthopaedic Surgery & Rehabilitation Medicine at SUNY Downstate Medical Center in Brooklyn, New York. Dr. Saha received a BS in Civil Engineering from Calcutta University in 1963, an MS in Engineering Mechanics from Tennessee Technological University in 1969, and Engineering and PhD degrees in Applied Mechanics from Stanford University in 1972 and 1974, respectively. He has been a faculty member at Yale University, Louisiana State University Medical Center, Loma Linda University, Clemson University, and Alfred University. Dr. Saha has received many awards from professional societies, including Orthopedic Implant Award, Dr. C. P. Sharma Award, Researcher of the Year Award, C. William Hall Research Award in Biomedical Engineering, Award for Faculty Excellence, Research Career Development Award from NIH, and Engineering Achievement Award. He is a Fellow of the Biomedical Engineering Society (BMES), The American Society of Mechanical Engineers (ASME), and the American Institute for Medical and Biological Engineering (AIMBE). He currently chairs the Bioethics Committee of the International Federation of Medical and Biological Engineering (IFMBE) and the Development Committee of Sigma Xi, and is Co-Chair of the International Committee of AIMBE. He is the immediate past chair of the Ethics Committee of the American Association of Dental Research (AADR).

He has received numerous research grants from federal agencies (NIH and NSF), foundations, and industry. Dr. Saha is the founder of the Southern Biomedical Engineering Conference Series, and he also started the International Conference on Ethical Issues in Biomedical Engineering. Dr. Saha has published over 118 papers in journals, 45 book chapters and edited volumes, 382 papers in conference proceedings, and 151 abstracts. His research interests are bone mechanics, biomaterials, orthopedic and dental implants, drug delivery systems, rehabilitation engineering, and bioethics.

USING POLYMER BULK DIFFUSION AS A MECHANISM FOR ADVANCING TISSUE ENGINEERING APPLICATIONS

Kelsey Phelan and Bryant C. Hollins
Biomedical Engineering, Louisiana Tech University, Ruston, LA, USA

ABSTRACT

Advances in biopolymers have long been sought to advance fields of biomedical engineering, with particular focus in biomicrofluidics and tissue engineering. We recently demonstrated that PDMS, a commonly used polymer in biological applications, can be used to intentionally leach molecules into a sample. In this work, we characterized the diffusion of fluorescein into water from the bulk PDMS, with a focus on calculating the diffusion rate of molecules from the polymer bulk into its surrounding aqueous environment. We look at diffusion from the bulk over a period of days in an attempt to formulate a fluorescein diffusion model from PDMS. Our results can guide future work in tissue engineering application studies, as we established a framework with fluorescein for determining the properties of molecules capable of diffusion from bulk PDMS. This strategy can be used as a tool for creating self-regulating microfluidic chambers for drug discovery, cell culture, and chemical monitoring applications, as well as a substrate for guiding cell growth and migration in tissue engineering applications.

Keywords: PDMS; biomicrofluidics; bulk diffusion; tissue engineering; leaching; biopolymer

INTRODUCTION

Polydimethylsiloxane (PDMS) continues to generate successful research findings regarding various devices, as the polymer has ideal characteristics for microenvironment applications. The material's flexibility, ease of creation, optical clarity, and inexpensive manufacturing aids in its common usage [1-2]. The material has been used as a basis for cell cultures and probing microenvironments [3]. A study completed by Toepke and Beebe showed that PDMS can absorb hydrophobic molecules, which could be used as a potential mechanism for removing unwanted species from a solution [4]. Recently, we demonstrated that fluorescein, a small molecule, was capable of being released into an aqueous solution following doping PDMS with the molecule [5]. The results of that study indicated the potential for this process to be regulated by a diffusive mechanism. The aim of our study was to characterize the diffusion of fluorescein from bulk PDMS. We hypothesized this diffusion was driven by Fick's Law, shown below in equation 1.

$$J=-D\nabla C \quad \text{(eq.1)}$$

As shown in equation 1, flux (J) is equal to the product of the diffusion coefficient (D) and the concentration gradient (∇C), accounting for the potential direction dependence on diffusion. The diffusion coefficient is expressed in units, mm2/sec, indicating a dependence on surface area and time, as shown in equation 2.

$$D= SA/t \quad \text{(eq.2)}$$

We assumed the PDMS bulk to be uniform throughout and therefore assumed isotropic diffusion properties within the bulk (i.e. diffusion rate is the same in all directions from the bulk into the solution). Our aim was to characterize the diffusion coefficient of fluorescein from the bulk PDMS, with a target of creating a fundamental model to describe and predict the qualities of molecules that can diffuse from PDMS. The significance of this model could range from the creation of self-regulating PDMS microchambers for applications in drug discovery, cell culture incubation, and medical diagnostics to tissue engineering applications, where gradients of diffusive molecules can be created to guide cell growth and migration, targets that are currently unachievable in traditional cell culture. PDMS micro-devices could also benefit from further diffusion knowledge by determining how the molecules and surface characteristics interact with the solution stream.

MATERIAL AND METHODS

Materials: The Sylgard 184 Elastomer Kit (PDMS) used was purchased from Dow Corning Corporation, Midland, MI. Fluorescein was purchased from Pfaltz & Bauer Inc., Waterbury, CT. Water purified through reverse osmosis was used as the solvent for all studies.

PDMS Sample Preparation: PDMS cubes doped with fluorescein of either 600 or 632 mm^2 surface areas were prepared according to the method outlined by Stone and Hollins [5]. Briefly, the PDMS prepolymer and curing agent was mixed according to manufacturer's instructions and the desired amount of fluorescein (1 mg per 1 g of PDMS) was added, getting a consistent color throughout. The mixture was degassed and poured into small dishes for curing at 80 °C. After curing, rectangular slices of PDMS were cut to the appropriate surface area. Prior to placing the sample into the tube for diffusion studies, each cube was washed with water. This step was taken to ensure the data was not influenced by unbound fluorescein that was on the surface of the sample after the slices were cut. The cubes were rinsed under flowing water for 30 seconds to remove any free fluorescein from

the surface. In addition to measuring the dimensions of the cubes, each cube was also weighed prior to the diffusion study, so that we would be able to map the mass of fluorescein measured in the solvent back to the lost mass of the PDMS cube after the diffusion study was completed.

Diffusion Study Protocol: Each doped PDMS slice was placed in a conical tube with 5 mL of water. To prevent potential photobleaching, the samples were stored in a dark room. Every 24 hours, the fluorescence of the tube solvent (water) was measured using the Nanodrop 3300 (in triplicate), measuring fluorescein at 515 nm using a blue excitation source. This process was repeated for four days. The results obtained from the Nanodrop were compared to a standard calibration curve generated in lab. Briefly, measurements were taken of known fluorescein concentrations ranging from 0.5 nM to 10 µM. A linear fit was created and interpolation was used for determining the concentration of the fluorescein in the tube solvent.

RESULTS

Figure 1 shows our expected model of diffusion of fluorescein from the bulk PDMS. We assume that diffusion through PDMS is not directionally dependent, due to the uniform properties of the PDMS mixture. We also assume that fluorescein is uniformly distributed throughout the bulk PDMS; therefore, no areas of the PDMS will have a larger concentration than any others. Because we are looking at diffusion from PDMS into the solvent, we establish a control volume around the doped PDMS. Mass conservation tells us that mass must be constant in this system. Following the four day experiment, we weighed the samples used for the diffusive studies. We found an average mass gain of 1.3 mg and 3.22 mg for 600 and 632 mm^2 samples, respectively.

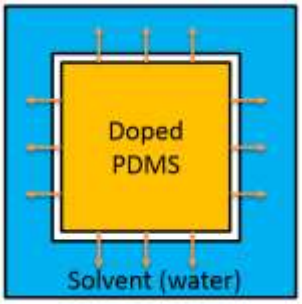

Figure 1: Our expected model of diffusion from the doped PDMS into the solvent. The diffusion occurs across the infinitesimally small control volume surrounding the cube (shown in white). Diffusion was assumed to be constant in all directions.

At the start of the experiment, there was no fluorescein present in the water. Since this scenario generated the largest concentration gradient, we expected the fastest diffusion from the doped PDMS into the solvent to occur during the first 24 hours. The results in Figure 2 support that expectation. Diffusion rate slowed between subsequent days. Since we did not prepare a fresh solvent sample each day, this reduction in diffusion was expected according to Fick's Law of diffusion (eq. 1.), as the concentration between the doped PDMS and the water was reduced each day. At the conclusion of the four days, we obtained a final concentration of fluorescein in the solvent of 3.62 and 3.31 µM for the 600 and 632 mm^2 surface areas, respectively. This concentration, in a 5 mL volume, correlated to a mass of 6.01 and 5.50 µg, respectively, using a molecular weight of 332.31 g/mol for fluorescein. The mass in solution correlated poorly with the mass gain from the doped PDMS samples, suggesting that an additional parameter, such as solvent inflow, is occurring in this system that our model (Figure 1) did not take into account.

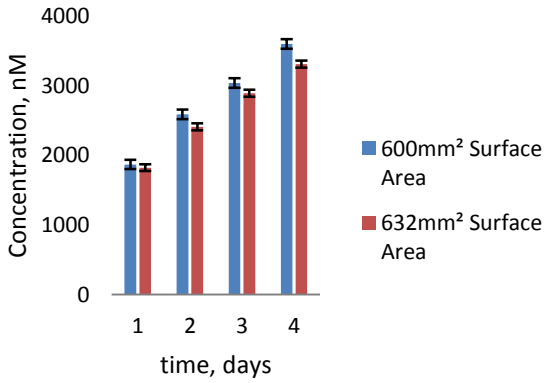

Figure 2: Average concentration diffused from the bulk PDMS (600 mm^2, n =5; 632 mm^2, n=6) into the solvent per day over the period of four days. The rate of diffusion slows between subsequent days as the concentration gradient driving diffusion was not as great over time.

DISCUSSION

The results established some fundamental understanding of fluorescein diffusion through PDMS. At first glance, this model appears to be in violation of the law of mass conservation, which implies we are not capturing all the necessary variables in our current setup. However, this increase in mass could be accounted for by the solvent. PDMS is known to swell when exposed to solvents; therefore, the increased weight of PDMS due to solvent absorption could explain the increased weight,

allowing for mass of the system to remain constant. This suggests that diffusion out of the bulk PDMS may not be completely dependent on concentration gradient, as some of the dopant can be "pushed" out of the bulk by the solvent. Our current model, shown in Figure 1, does not account for solvent inflow. Therefore, future revisions to the model must account for solvent inflow into PDMS. In addition, the experimental setup shows a relationship between concentration and time as opposed to Fick's Law, which shows a relationship between flux and concentration gradient. While Figure 2 shows the expected outcome, it does not explicitly show flux.

CONCLUSIONS

This research provides initial mechanistic insight into diffusion of fluorescein from bulk PDMS. Future work involving fluorescein includes measuring diffusion consistency by loading the samples into fresh solvent daily and analyzing how long it takes for a sample equilibrium to be reached with the solvent. However, this project is envisioned to move toward biologically relevant applications. In order to achieve that, future work will include using this preliminary model and adding additional parameters, such as solvent pH, solvent temperature, and molecular characteristics such as size and charge. These additions will allow for the establishment of a more robust model and make some of the applications listed earlier in the report achievable, namely, self-regulating microfluidic chambers and intentionally designed gradient generators for controlling cell growth and migration in tissue engineering applications.

ACKNOWLEDGMENTS

We thank Sawyer Stone for his contributions to intellectual discussion of the process, and for advice concerning troubleshooting the instrumentation.

REFERENCES

[1] S. Hu, X. Ren, M. Bachman, C. E. Sims, G. P. Li, and N. Allbrittion, "Surface modification of poly(dimethylsiloxane) microfluidic devices by ultraviolet polymer grafting". *Anal Chem*¸ vol. 74, no. 16, pp. 4117-23, Aug. 2002.

[2] S. Hemmila, J. V. Cauich-Rodriguez, J. Kreutzer, and P. Kallio, "Rapid, simple, and cost-effective treatments to achieve long-term hydrophilic PDMS surfaces," Appl. Surf. Sci., vol. 258, no. 24, pp. 9864–75, Oct. 2012

[3] H.-W. Wu, C.-C. Lin, and G.-B. Lee, "Stem cells in microfluidics," Biomicrofluidics, vol. 5, no. 1, p. 13401, Jan. 2011.

[4] Toepke MW, Beebe DJ (2006) PDMS absorption of small molecules and consequences in microfluidic applications. Lab Chip 6:1484–1486.

[5] S. D. Stone and B. C. Hollins, "Doping poly(dimethylsiloxane) for intentional leaching of small molecules into microchannels". *Proc 32nd Southern Biomedical Egnineering Conference*, 43-44, 2016.

BENEFICIAL EFFECTS OF SEMEN PURIFICATION WITH MAGNETIC NANOPARTICLES

Casey Durfey[1], Sabrina Swistek[1,2], Wei Tan[3], Henry Clemente[4], Peter Ryan[1,3], Scott Willard[1,2], and Jean Feugang[1]

[1] Departments of Animal and Dairy Sciences, Mississippi State University
[2]Biochemistry, Molecular Biology, Entomology, & Plant Pathology, Mississippi State University
[3]Basic Sciences, Pathobiology and Population Medicine at Mississippi State University
[4]Clemente Associates, Madison, CT

ABSTRACT

Introduction: Semen contain both viable and non-viable spermatozoa which equilibrium affects male fertility. Current techniques for detecting non-viable spermatozoa in semen ejaculates lack specific targeting for their subtraction. Here we used magnetic nanoparticle conjugates to selectively target and remove non-viable spermatozoa, and assess the motion characteristics and viability of residual spermatozoa. **Methods:** Boar semen were mixed with (nanopurified) or without (control) magnetic nanoparticle conjugates and incubated to allow specific targeting of non-viable (or moribund) spermatozoa. Afterwards, mixtures were placed against a powerful magnet trapping moribund spermatozoa and permitting elution of viable spermatozoa. Before and after incubation, sperm motion and viability parameters were respectively analyzed with a Computer-Assisted-Sperm-Analyzer and flow cytometry after specific staining to evaluate the viability status of spermatozoa. Data (mean±sem) were compared with SAS package. **Results and Discussion:** The proportion of static sperm significantly decreased after purification (8.9±0.5% vs. 11.3±0.5% for the control; $P<0.05$). Motion parameters (total and progressive motility, straightness, linearity, straight line velocity or VSL, and beat cross frequency or BCF) of nanopurified spermatozoa were significantly increased, while the amplitude lateral head displacement or ALH was decreased ($P<0.05$). Sperm viability parameters (plasma and acrosome membrane integrity and mitochondrial potential) were comparable between both groups ($P>0.05$). **Conclusions**: Findings indicate the successful removal of moribund (static) spermatozoa without impairing the viability of eficial effects on sperm motion has potential improving male fertility.
Acknowledgements: Work supported by USDA-ARS Biophotonics Initiative #58-6402-3-018.

Keywords: Boar, Nanoparticles, Pig, Sperm motility, Sperm viability

INTRODUCTION

Spermatozoa provide the source for male genetic potential, serving as essential biomarkers for male fertility. Physical and physiological properties of spermatozoa are dependent upon intrinsic and extrinsic factors to the male, creating a heterozygous population of viable and non-viable (damaged or moribund) sperm cells [1]. Commonly, sperm aggregates are formed as a result of large proportions of damaged spermatozoa, impeding the migration and fertilization potential of spermatozoa both in vitro and in vivo [2, 3]. Male infertility can be a distressing issue in humans with significant genetic and economic impacts in livestock.

Various technical methodologies have been developed to improve assisted reproductive technology (ART) outcomes in livestock. Nonetheless, the elimination or substantial decrease of proportions of non-viable spermatozoa from semen ejaculates prior to artificial insemination (AI) remains an unachieved goal for maximizing semen fertility. Conversely, recent developments in nanotechnology now permit for novel sperm purification approaches. For instance, magnetic nanoparticles (MNP) have shown success for reproductive applications, through a magnetic semen purification technique, termed "nanopurification"[4, 5]. These studies conducted in boar and bull species eliminated (nanopurified) spermatozoa bearing a single morphologically damaging factor (acrosome reaction), disregarding the variable assorted possibilities of spermatozoal impairments. The incidence of apoptosis is another damaging factor of spermatozoa which combined with a pre-matured acrosome reaction constitutes the majority of sperm damage, and thus, the non-viable sperm population. Here, we developed MNP conjugates targeting two nanopurification steps, apoptotic and acrosome reacted spermatozoa through respective binding to annexin V and lectins (PNA/PSA) [6] and to assess the motility and viability of nanopurified spermatozoa.

MATERIAL AND METHODS

Nanoparticle Synthesis: Iron oxide (Fe3O4) magnetic nanoparticles (MNP) were synthesized and coated with annexin V (Sigma Aldrich, St Louis, MO, USA) or lectins (PNA/ PSA), allowing selective binding to early apoptotic spermatozoa and glycans exposed by damaged acrosome membrane (or premature capacitated), respectively.

Sperm Labeling, Purification With Nanoparticles, And Motility Characteristics: Freshly harvested and extended semen doses (~ 3 × 109 spermatozoa/dose) were obtained from a local boar stud. A total of 0.3 mg of annexin V- and lectin-conjugated MNP was successively mixed with each semen dose to target 0.6 x 10^9 moribund spermatozoa. Starting with the targeting of apoptotic (annexin V) and following each mixture, a co-incubation was performed at 37°C with a gentle rotation to allow sperm-MNP interactions. After, semen mixtures were placed against a magnet for at room temperature for the trapping of free and sperm-bound MNP's. Free unbound, or intact spermatozoa were subsequently eluted into new tubes. This separation process was repeated twice (total of 3 purification steps) for each MNP conjugate. Aliquots of control (not purified), and double-nanopurified semen samples were obtained for motility analysis using a Computer-Assisted Sperm Analyzer (IVOS; Hamilton-Thorne Biosciences; Beverly, MA, USA).

Viability analysis of nanopurified spermatozoa: Nanopurified spermatozoa were immediately diluted to 30 x 10^6 cells/ml with a pre-warmed phosphate-buffered saline solution. Sperm suspensions were allocated to various staining for viability assessment: propidium iodide (PI, 1 mg/ml in PBS) for plasma membrane integrity, PNA-FITC (100 mg/ml in PBS) for acrosome reaction, JC-1 (500mg/ml; Cayman Chemical Co., Ann Arbor, MI, USA) for mitochondrial integrity, and H2DCFDA (1 mM in DMSO) for reactive oxygen species (ROS) accumulation within cells. All samples were incubated and diluted with pre-warmed PBS before immediate analyses with a flow cytometer (Becton–Dickinson FACSDiva version 6.1.3) set for 10,000 total events per analysis. Sample aliquots were mounted onto microscope slides and visualized under an epifluorescence microscope (EVOS FL-Auto, Thermo Fisher Scientific, Hampton, NH, USA) to validate proper staining.

Statistical analysis: All data were analyzed and compared using A Statistical-Analytical-Software (SAS). Nano-purification influences on sperm motility characteristics and viability parameters were analyzed using a two-way ANOVA and a student's t-test. Data are expressed as mean ± standard error mean (sem) of 4 independent replicates. $P \leq 0.05$ were held as the threshold of significance.

RESULTS

Motility characteristics of nanopurified spermatozoa. In comparison to the control, sperm nanopurification significantly increased the proportions of motile, progressive (forward-moving), and rapid (fast) spermatozoa while decreasing the proportions of static (non-motile) spermatozoa ($P<0.05$; Figure 1). Nanopurified sperm showed increased sperm velocity parameters, compared to the control group (VAP, VSL and VCL, $P >0.05$). Other spermatozoal directional parameters such as straightness (55.7±0.6% vs. 60.4± 0.8%), and linearity (27.3±0.4% vs. 29.8±0.7%) were variably increased with the lateral head amplitude (ALH; 7.9±0.1 vs. 7.5 ±0.1) decreased, following nanopurification ($P<0.05$).

Viability assessment of nanopurified spermatozoa through flow cytometry: Control and nanopurified (annexin V and lectin) spermatozoa exhibited comparable proportions of high mitochondrial membrane potential, low reactive oxygen species (ROS) levels, and intact acrosome and plasma membrane ($P>0.05$). Following nanopurification, the mean relative fluorescence intensities (RFI) associated with ROS production (H2DCFDA) and damaged plasma membrane (PI) were non- significantly decreased, while the mitochondrial membrane (JC-1) intensity were increased ($P>0.05$; Table 1). Successful staining was confirmed through fluorescence microscopy (not shown).

.

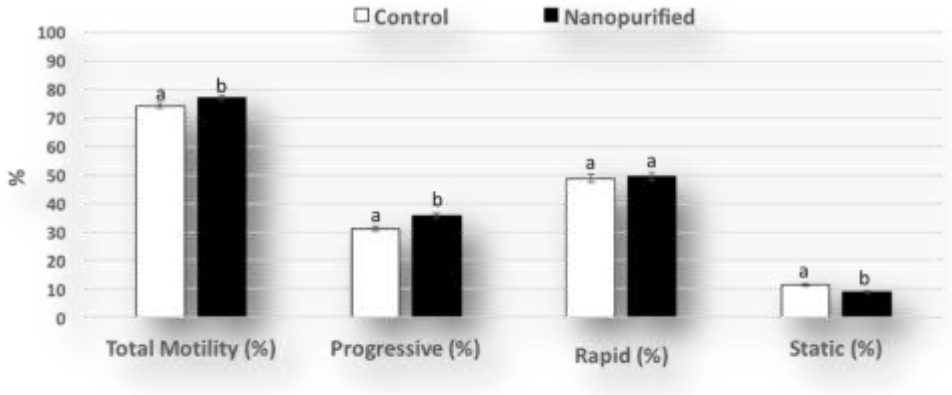

(Data are means±sem; a,b indicate significant differences; $P < 0.05$)

Table 1: Relative fluorescence intensities (RFI; mean±sem) of labeled spermatozoa.

Staining	Control (RFI)	Nanopurified (RFI)
ROS production (DCHF-DA)	1068.93 ± 200.26	864.42 ± 200.26
Plasma membrane integrity (PI)	11.892 ± 25.62	8.638 ± 25.62
Mitochondrial membrane integrity (JC-1)	425.89 ± 200.26	897.81 ± 223.9

DISCUSSION

The two-step nanopurification procedure conducted in this study showed no significant impairments of resulted spermatozoa but rather motility and velocity improvements. The findings were consistent with a previous study using single MNP-lectin nanopurification of boar spermatozoa [5]. Significant decreased proportions of static spermatozoa succeeding nanopurification revealed successful elimination of non-motile sperm from MNP purification (nanopurification). This removal was likely cause for improved velocity, directionality, and increased proportion of fast forward-moving (straight) spermatozoa following nanopurification. This enhanced performance of spermatozoa suggests a potential greater activity within the female genital tract, leading to better fertility potential [7, 8].

Viability assessments showed no added impairments of nanopurified spermatozoa, with the proportions of viable spermatozoa remaining comparable to the control. Interestingly, nanopurified semen showed lower fluorescence intensity for ROS production that contrasted with higher plasma and mitochondrial membrane integrity; these observations indicated more stable plasma and mitochondrial membranes. Ultimately, results revealed better sperm robustness for improved fertility potential [8].

CONCLUSIONS

This study used a two-step MNP sperm nanopurification method to target two major molecular defectsof mature spermatozoa. Data indicate effective removal of targeted spermatozoa with improved performance and fertility potential of nanopurified semen. Although further large-scale *in vivo* studies are still needed, these preliminary findings indicate promising applications of this two-step nanopurification technique for improved male fertility in livestock productions.

ACKNOWLEDGMENTS

The authors thank Prestage Farms Inc., Mississippi Division for providing semen; Dr. Robert Willis and Ms. Wei Tan at The College of Veterinary Medicine at Mississippi State University for their respective assistance in statistical data and flow cytometry analyses. This work was funded by the United States Department of Agriculture – Agricultural Research Service (USDA-ARS grant # 8-6402-3-018), the College of Agricultural and Life Sciences – Undergraduate Research Scholar Program, the Office of Research and Economic Development (ORED), and Mississippi Agriculture, Forestry and Extension Service (MAFES) of Mississippi State University.

REFERENCES

1. Bungum, M., P. Humaidan, Anna Axmon, M. Spano, Leif Bungum, Juris Erenpreiss, and Aleksander Giwercman., *Sperm DNA integrity assessment in prediction of assisted reproduction technology outcome.* Human Reproduction, 2007. **22**(1): p. 5.

2. Sharma, R.K., and Ashok Agarwal, *Role of reactive oxygen species in male infertility.* Urology 1996. **48**(6): p. 15.

3. Saleh, R.A., Ashok Agarwal, Essam A. Nada, Mohamed H. El-Tonsy, Rakesh K. Sharma, Andrew Meyer, David R. Nelson, and Anthony J. Thomas, *Negative effects of increased sperm DNA damage in relation to seminal oxidative stress in men with idiopathic and male factor infertility.* Fertility and Sterility, 2003. **79**: p. 8.

4. Odhiambo, J.F., J. M. DeJarnette, Thomas W. Geary, Chelsey E. Kennedy, Susan S. Suarez, Miriam Sutovsky, and Peter Sutovsky, *Increased conception rates in beef cattle inseminated with nanopurified bull semen.* Biology of reproduction, 2014. **91**(4).

5. Feugang, J.M., Shengfa F. Liao, Mark A. Crenshaw, Henry Clemente, Scott T. Willard, and Peter L. Ryan, *Lectin- functionalized magnetic iron oxide nanoparticles for reproductive improvement.* Journal of Fertilization: In Vitro-

IVF-Worldwide, Reproductive Medicine, Genetics & Stem Cell, 2015.

6. Sutovsky, P., *New Approaches to Boar Semen Evaluation, Processing and Improvement.* Reprod Domest Anim, 2015. **50 Suppl 2**: p. 11-9.

7. Katz, D.F., Drobnis, Erma Z., and Overstreet, James W. , *Factors Regulating Mammalian Sperm MigrationThrough the Female ReproductiveTract and Oocyte Vestments.* GameteResearch, 1989. **22**: p. 26.

8. Liu, D.Y., G.N. Clarke, and H.W. Baker, *Relationship between sperm motility assessed with the Hamilton-Thorn motility analyzer and fertilization rates in vitro.* J Androl, 1991. **12**(4): p. 231-9

.

EFFECT OF MUSCLE ENGAGEMENT AND MEASUREMENT POSITION ON ELECTRICAL IMPEDANCE OF THIGH MUSCLES

Robert Joseph Mathews and Todd Freeborn
Department of Electrical and Computer Engineering, The University of Alabama, Tuscaloosa, AL, USA

ABSTRACT

Electrical impedance measurements are being widely investigated as a means to monitor physiological change in many biological tissues, with applications for non-invasive real-time monitoring in both health and athletics. This pilot study aimed to determine if there are differences in the electrical impedance measurements collected for relaxed and tensed states of the thigh muscle, in both sitting and standing orientations. Understanding how both muscle engagement and measurement position effect the electrical impedance will be useful for systems to monitor localized muscle injury or fatigue in free-living environments, which will not have controlled conditions typical of clinical environments. For this comparison, seven sets of measurements were collected over a fourteen-day period from both right and left thighs of a single subject in four different orientations (sitting relaxed, sitting tensed, standing relaxed, standing tensed). Each set of measurements were collected using an ImpediMed SFB7, from 3 kHz to 1 MHz, with a tetra-polar electrode configuration placed on the skin surface external to the quadriceps muscles. From these results, there was an increase of the electrical impedance in the tensed state compared to the relaxed state for all orientations on most days, with the decreases (averaged using the 3 kHz to 50 kHz measurements) ranging from 2% to 6%.

Keywords: Electrical impedance, localized impedance, muscle engagement, SFB

INTRODUCTION

Electrical impedance measurements quantify the resistance of a material to an injected electrical stimulus. Applied to biological tissues, these measurements are being widely investigated as a means to monitor physiological change for non-invasive real-time monitoring in both health and athletics applications. Applications in regards to muscle monitoring have shown that: **i)** measuring the impedance across a single muscle may be a useful indicator of fatigue and recovery [1]; **ii)** changes in impedance during real-time monitoring may be useful to differentiate different muscle engagement states, supported by changes in the impedance due to muscle elongation and engagement during walking [2] and changes between relaxed and contracted states of the biceps muscle [3]; **iii)** muscle impedance varies due to injury [4,5]. This study aimed to determine if there are differences in the electrical impedance measurements collected for relaxed and tensed states of the thigh muscle, in both sitting and standing orientations. Understanding how both muscle engagement and measurement position effect the electrical impedance will be useful for systems to monitor localized muscle injury or fatigue in free-living environments, which will not have controlled conditions typical of clinical environments.

MATERIAL AND METHODS

In this study seven sets of electrical impedance measurements from a 22–year old male subject were collected over a fourteen-day period from each of the right and left thighs from four different patient orientations (sitting relaxed, sitting tensed, standing relaxed, standing tensed). These measurements were collected from a tetra polar electrode configuration, with 7 cm spacing, using an Impedimed SFB7. In this configuration, two electrodes (Kendall 133) were used to apply the electrical stimulus with two electrodes to measure the resulting voltage response. This configuration was selected to minimize the impact of the electrode impedance on these measurements. For the relaxed measurements, the subject was asked to relax their leg muscles while for the tensed measurements they were asked to tense these muscles as tightly as possible. The purpose of this was to quantify the impact that the muscle contractions had on the electrical impedance collected in this configuration. This is an important consideration if these measurements are to be used in real-time monitoring when subjects may be in a range of positions (standing, sitting, lying) and activations (relaxed, straining). This test focuses on the quadriceps, as they are a primary muscle group engaged while walking, standing, or running.

RESULTS AND DISCUSSION

The collected real and imaginary components of the impedance data (from 3 kHz to 1 MHz) for all 7 sets of measurements are given in Fig. 1, with days 1 through 7 given by blue, orange, light blue, black, red, purple, and green lines, respectively. The solid and dashed lines represent the impedances collected from left and right thighs, respectively, with the data in Figs. 1(a) and (b) collected in the sitting state and the data in Figs. 1(c) and (d) in the standing state. The real and imaginary impedances for each of the four states show the same general trends, with the real impedance decreasing towards a constant value as the frequency increases and the imaginary impedance decreasing towards a minimum (at approximately 25 kHz in these cases) after which it increases with increasing frequency. In the sitting state, the left and right thighs real impedance ranges from 21.2 Ω to 27.2 Ω at 3 kHz and 8.63 to 10.6 Ω at 1 MHz while the imaginary electrical impedance ranges from 1 Ω to 2.3 Ω at 3 kHz and -3.2 to 1.6 Ω at 1 MHz across all the days. In the standing state the left and right thighs real electrical impedance ranges from 21.2 Ω to 26.3 Ω at 3 kHz and 7.5 Ω to 10 Ω at 1 MHz while the imaginary electrical impedance ranges from 1.2 Ω to 2.3 Ω at 3 kHz and -2.5 to 1.8 Ω at 1 MHz across all the days. From Figs. 1(a) and (c), for all days there was a small (1 Ω to 2 Ω) difference between the real impedance of the right and left thighs on any given day. This same trend is observed in the imaginary impedance in Figs. 1(b) and (d) for low frequencies, though at higher frequencies this trend in differences increases; which may be a result of stray capacitances in the test setup that impact the high frequency measurements [6].

To visualize the differences each day between the relaxed and tensed muscle engagement states in the sitting and standing orientations, the percent difference for the real impedance of both legs at 5 discrete frequencies (3kHz, 10kHz, 50kHz, 100kHz, and 1MHz) are given in Fig. 2 by the dark blue, light blue, green, orange, and yellow bars, respectively. The negative values in Fig. 2 represent an increase in value based on the calculation method. From the results in Figs. 2(a) and (b) representing the sitting state for left and right legs, respectively, there is a trend of increasing real impedance ranging from 1% to 7% for each frequency when the muscle is tensed compared to the relaxed state (though days 1, 3, and 4 show the opposite behavior for the right leg and require follow-up study to investigate its cause). The increasing resistance supports the results of a previous study which reported an increase in the real impedance of the biceps brachii muscle during contraction when compared to the resting values [3]. While standing, the impedances in Figs. 2(c) and (d) again show increases ranging from 3%-7% when tensed, for most frequencies and days (except for the values at 50 kHz while standing, which showed a decrease eleven of fourteen times). Though not shown, the imaginary impedance values showed a similar trend with less consistency than the real impedance.

Follow-up studies should further investigate the effect that possible sources of error in this study may have introduced. These sources of error include **i)** electrode placement, **ii)** cable movement, **iii)** subject movement. There may have been slight placement errors introduced by the application of new electrodes on each thigh for each day of data collection. While attempts were made to minimize these errors by using a medical marker to highlight on the subject's skin the location for re-application, the error that could be introduced by this needs to be quantified further. Also, the effect of cable movement and subject movement need to be further quantified in this test configuration to validate that the changes in electrical impedance are truly representative of the muscle contractions and to ensure that the results can be consistently repeated.

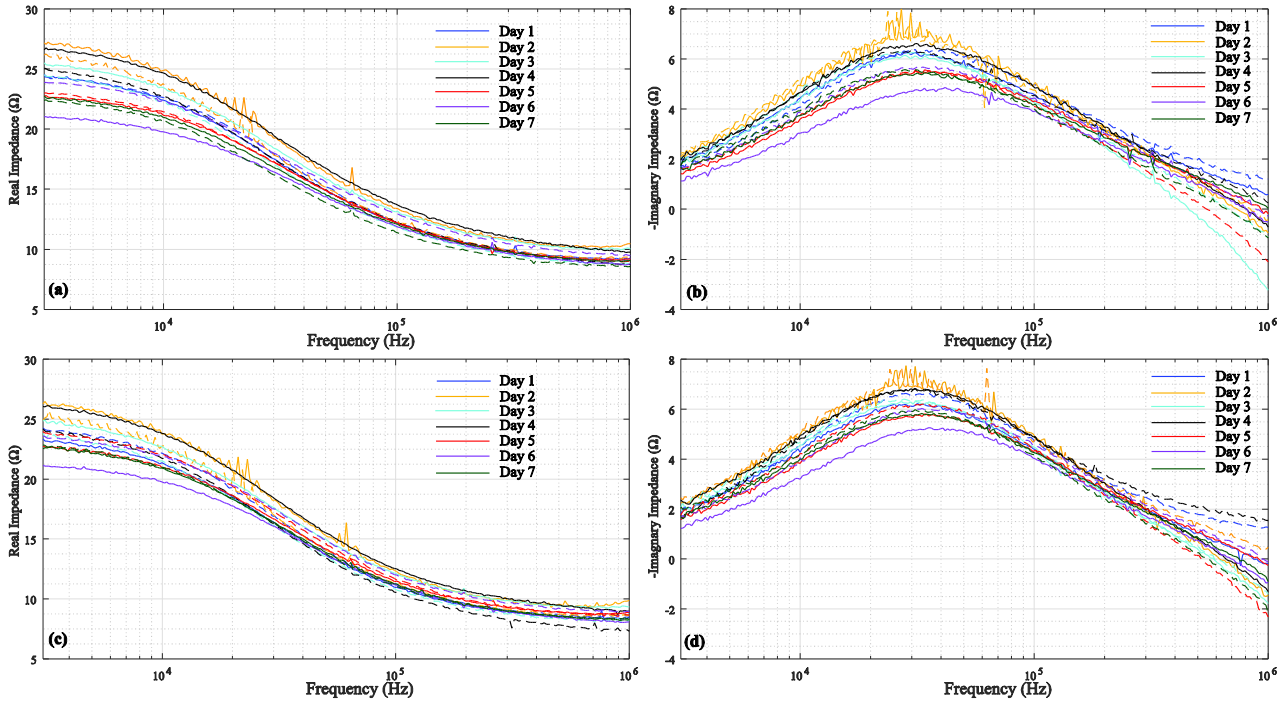

Figure 1. (a), (c) Real and (b), (d) imaginary electrical impedances collected from left (solid) and right (dashed) thighs in (a), (b) sitting and (c), (d) standing states collected for days 1-7.

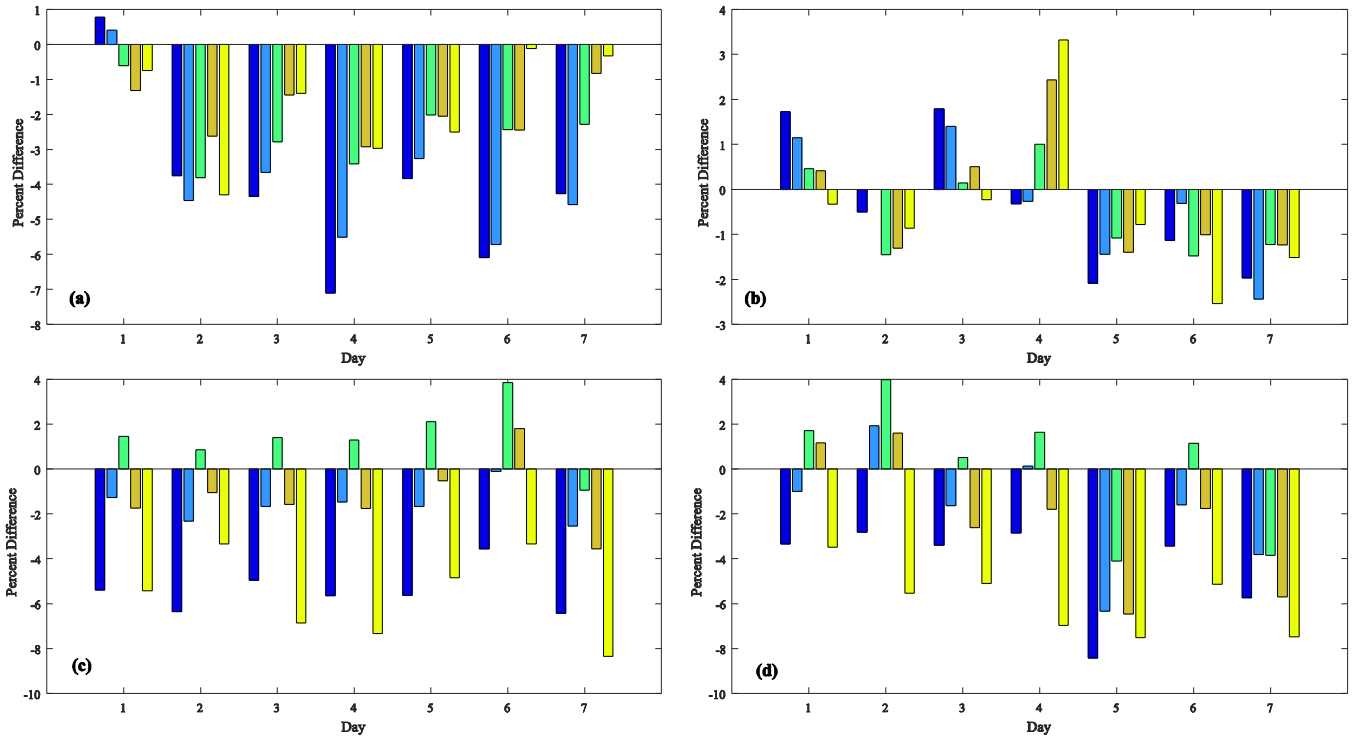

Figure 2. Percent difference of tense vs relaxed states for the real impedance in (a) left thigh sitting, (b) right thigh sitting, (c) left thigh standing, and (d) right thigh standing states for 3kHz, 10kHz, 50kHz, 100kHz, and 1MHz, respectively.

Additional follow up studies should explore if the trends observed here (increase in real impedance with muscle contraction) are consistent across larger populations with different characteristics (i.e. typical activity levels, absolute muscle strength), if they are affected by factors such as hydration and temperature (skin & ambient), and if they are consistent for different muscle groups in the body, and if they could be effectively used to monitor muscle engagement state in real-activities.

CONCLUSIONS

The typical impedance increase observed at all frequencies with muscle contraction shows that not only is there a quantifiable difference in impedance for the thigh in relaxed and tensed states, but that there is also potentially a method to differentiate between these states using only impedance data. Additionally, the decrease in impedance at 50 kHz while standing and tensed compared with the increase at that frequency while sitting and tensed indicates that certain frequencies may be used to differentiate between sitting and standing.

REFERENCES

[1] Tarulli, Andrew W. et al., "Electrical impedance myography in the assessment of disuse atrophy," *Archives of Physical Medicine and Rehabilitation*, vol. 90, no. 10, pp. 1806 – 1810, 2007.

[2] G. Hornero, D. Diaz, O. Casas, "Bioimpedance system for monitoring muscle and cardiovascular activity in the stump of lower-limb amputees," *Physiol. Measure*., vol. 34, no. 2, pp. 189-201, 2013.

[3] L. Li, H. Shin, X. Li, S. Li, P. Zhou, "Localized electrical impedance myography of the biceps brachii muscle during different levels of isometric contraction and fatigue," *Sensors*, vol. 16, no. 4, 581, 2016.

[4] L. Nescolarde, J. Yanguas, H. Lukaski, X. Alomar, J. Rosell-Ferrer and G. Rodas "Localized bioimpedance to assess muscle injury," *Physiol. Measure*., vol. 34, no. 2, pp. 237-245, 2013.

[5] L. Nescolarde, J. Yanguas, H. Lukaski, X. Alomar, J. Rosell-Ferrer and G. Rodas "Effects of muscle injury severity on localized bioimpedance measurements," *Physiol. Measure*., vol. 36, no. 1, pp. 27–42, 2015.

[6] R. Buendia, F. Seoane, R. Gil-Pita, "A novel approach for removing the hook effect artefact from electrical bioimpedance spectroscopy measurements," *J. Physics: Conf. Series*, vol. 224, 012126, 2010.

VARIABILITY OF ELECTRICAL IMPEDANCE MEASUREMENTS COLLECTED FROM HUMAN FOREARM USING MULTIPLE ELECTRODE CONFIGURATION

Shelby Critcher and Todd Freeborn

Department of Electrical and Computer Engineering, The University of Alabama, Tuscaloosa, AL, USA

ABSTRACT

Electrical impedance measurements quantify the resistance of a material to an injected electrical stimulus and have been used to detect physiological changes in biological tissues. Recently, these measurements have been applied to monitor muscle tissue towards determining if they can detect muscle fatigue. While electrodes in clinical applications can be precisely placed, their precise application for athletic monitoring may prove challenging. Therefore, it is important to understand how electrode placement impacts the measured impedance. This study collected electrical impedance measurements of the human forearm from 16 tetra-polar electrode configurations; with stimulus electrodes fixed and measurement electrodes varied along a 3 cm by 3 cm grid. Measurements from 3 kHz to 1 MHz using a Keysight SBF7 recording system were collected from a single participant on three consecutive days. Results show maximum relative deviations from <1% to 52% for the real impedance and <1% to 81% for the imaginary for all days when electrodes were moved from the reference position. The relative deviations of the real impedances showed less variability with frequency (<10% relative change across all frequencies) than the imaginary components, which in some cases exhibited errors ranging of 0.215% at 92 kHz to 80.9% at 1 MHz.

Keywords: Electrical impedance, localized impedance, electrode configuration, forearm, SFB7

INTRODUCTION

Electrical impedance measurements quantify the resistance of a material to an injected electrical stimulus and have been used to detect physiological changes in biological tissues. These measures have a real and imaginary component referred to as the resistance and reactance, respectively. In a recent study, these measurements were applied to monitor muscle tissue to see if it was possible to detect properties such as the metabolic state of the human calf muscle [1]. While electrodes in clinical applications can be precisely placed, their precise application for athletic monitoring, such as the contraction and relaxation of the bicep muscle [2], may prove challenging. Therefore, it is important to understand how electrode placement impacts the measured impedance [3]. Previous studies have shown there are numerous variables that can affect the resulting measured impedance of a biological tissue such as the position, size, and the specific type of electrodes used in obtaining these measurements [4]. These variables present a challenge when making use of bioimpedance technology. In order for this technology to expand into systems that do not require precision placement of electrodes our understanding of how these factors contribute to the variation of measurements must be improved. It must be known whether the detected changes are a result of the electrode configuration or due to physiological changes in the muscle tissue. A previous study collected measurements from the quadriceps, in a similar electrode configuration. Results from that study suggest the placement of recording electrodes vertically (from elbow to wrist) has less impact than horizontally (Fig. 1) [5]. In this study, we explore the impact of variations in a tetra-polar electrode configuration on the measured electrical impedance from 3 kHz to 1 MHz of the human forearm of a single participant.

MATERIALS AND METHODS

Electrical impedance measurements were collected from the left forearm of a 20-year-old female from 16 different tetra-polar electrode configurations. The layout of electrode configurations on the subject's forearm are given in Fig. 1(a) with the details of the pairings given in Fig 1(b). For the duration of the data collection, the subject was in a standing position with the left forearm relaxed flat on the table surface. In each configuration two current injection electrodes, labeled **i** in Fig. 1(b), were placed 21.25 cm apart and fixed for the duration of the data collection. The placement of the voltage sensing electrodes varied across two 9x9 cm grids detailed in Fig. 1(b), with each position given a numerical indicator of 1-16. Kendall H124SG foam, hydrogel electrodes (30 mm x 24 mm) were used in this experiment. Before electrode placement, the subject's skin was cleaned with a Biemarpak skin-cleaning swab. The electrical impedance measurements were obtained using an ImpediMed SFB7 set to the Bioimpedance Spectroscopy (BIS) mode;

collecting measurements at 256 frequencies from 3 kHz – 1 MHz. For each of the 16 different electrode configurations, the SFB7 was calibrated and five measurements were collected consecutively with their average used for all subsequent analyses.

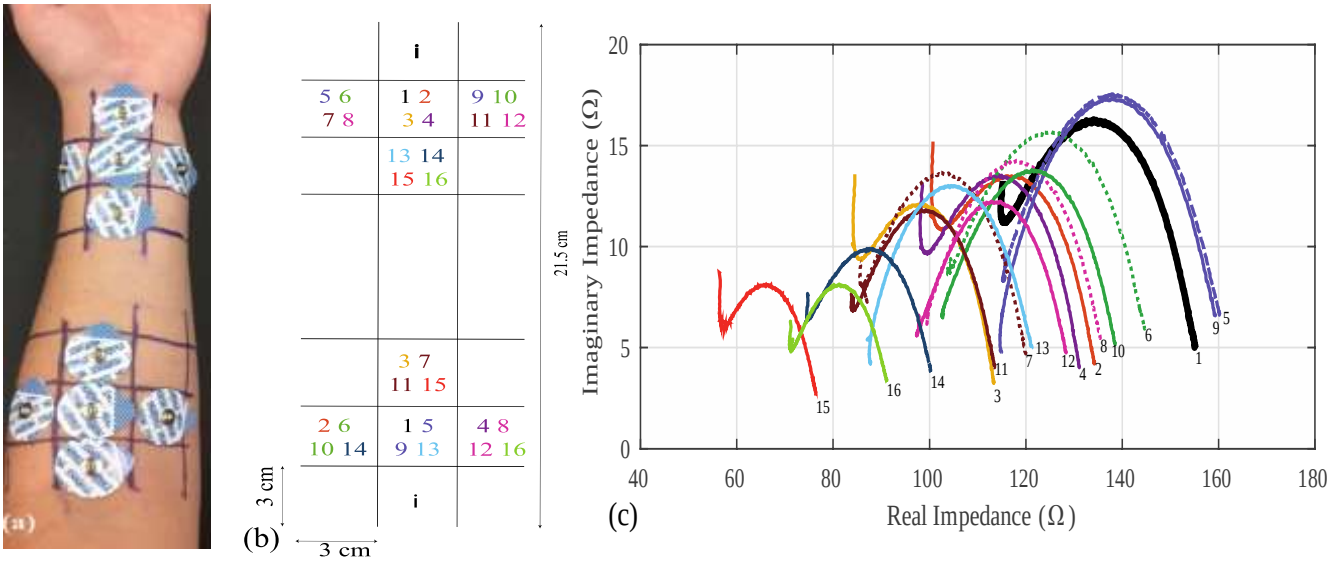

Figure 1 (a) Electrode configuration and (b) details of pairings for data collection of (c) electrical impedance from each position

.

RESULTS AND DISCUSSION

In Fig. 1(c), the real and imaginary components of the impedance are presented for each of the 16 sets of measurements. Note, that the SFB7 has a reported accuracy of +/- 1% for impedances from 50 Ω to 1100 Ω, with all collected real impedances in Fig. 1(c) within this range. Each line, labeled 1-16, corresponds to the impedance collected in the configurations detailed in Fig. 1(b). All plots show the characteristics typical of a Cole impedance [6], displaying a semi-circle behavior with the imaginary impedance decreasing towards zero at both low and high frequencies. Note also, that there is an increasing imaginary impedance component or 'hook' that is present in many of the datasets, likely a result of stray capacitances in the setup [7]. Observing the data in Fig. 1(c), the collected impedances vary significantly because of the different electrode configuration. The most significant difference occurs between configurations 15 and 5. Configuration 15 shows the smallest impedance values, wit minimum and maximum real impedances of 57.16 Ω and 76.37 Ω, respectively, and a maximum imaginary impedance of 8.126 Ω at 43.65 kHz. Configuration 5 shows the largest impedance values, with minimum and maximum real impedances of 115.3 Ω and 160.2 Ω, respectively, with maximum imaginary impedance of 17.54 Ω at 38.96 kHz.

Each of these Cole plots was produced using the calculated average of each of the five different sets of measurements collected at each respective location. The bold black line seen in Fig. 1(c), represents the resulting Cole plot of the reference position used. In Fig. 2(a), the deviation of the real component of the impedance of positions 2-16 from position 1, the reference position, are shown. Fig. 2(b) illustrates the deviation of the imaginary component. The equation used to determine the deviation of each component is given by:

$$Deviation = |\frac{Reference - Position}{Reference}| * 100 \quad (2)$$

The deviation of the real impedances in Fig. 2(a) is fairly constant with frequency, with the most extreme changes seen in configurations 16 and 12 with errors of 41.25% and 17.34%, respectively, at 3 kHz and decreasing to 38.08% and 15.36%, respectively, at 1 MHz. This same trend is not present in the deviations of the imaginary impedances given in Fig. 2(b); which at its most extreme in configuration 13 has deviations of 0.7978% at 3 kHz, which increases to 67.95% at 1 MHz. The smallest deviations seen in Fig. 2(a) compared to the reference position occurred at positions 5 and 9, with values of 0.13% and 0.004% at 135.8 kHz and 40.70 kHz;

and variations less than 1% above 28.36 kHz and 18.44 kHz. In these configurations, the voltage sensing electrodes nearest the elbow were in the same position, but the voltage sensing electrodes nearest the wrist were mirrored about the axis of the current injecting electrodes. Positions 7 and 11 also have similar deviations and have a similar mirroring pattern as positions 5 and 9. The largest deviation compared to the reference position occurred with configuration 15. In this configuration, the sensing electrodes were farthest (vertically) from the current injecting electrodes, and showed deviations of approximately 50% across the entire frequency range. The results in Fig. 2(a) suggest that moving the electrodes horizontally has less effect on the real impedance than moving the electrodes vertically. Positions with the voltage sensing electrodes in the same horizontal plane (e.g. configurations 2, 4, 5, 6, 8, 9, 10, 12) all had deviations lower than 17%, while positions where one of the sensing electrodes is positioned in a different horizontal plane (e.g. configurations 3, 7, 11, 13, 14, 15) had deviations greater than 27%. Comparing the imaginary impedances given in Fig. 2(b) there does not appear to be any immediate patterns between the electrode position and the deviation compared to the reference values.

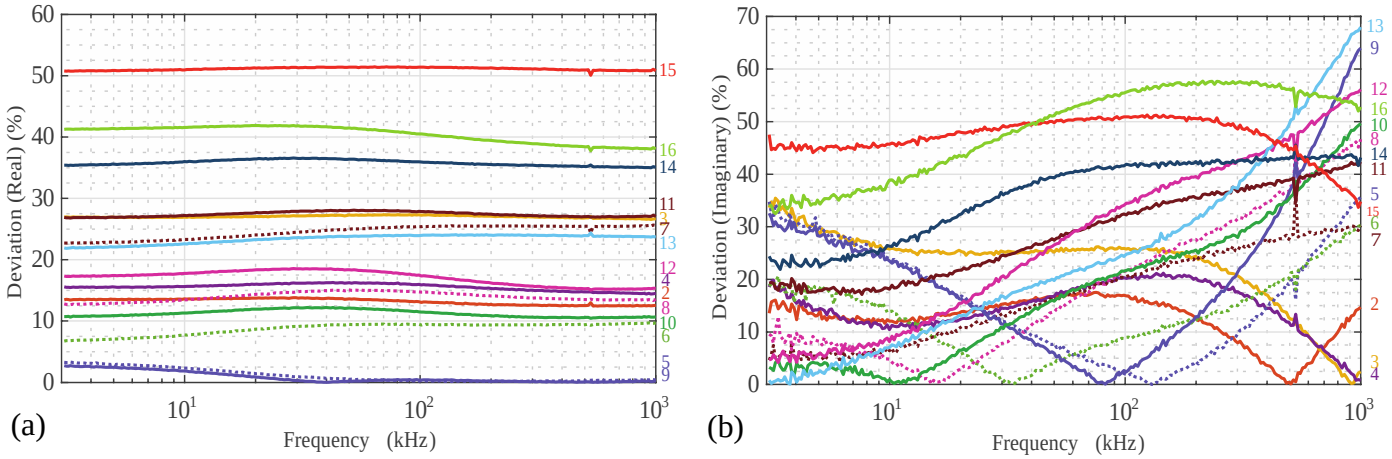

Figure 2 Percent deviation of the (a) real and (b) imaginary impedances of electrode configurations 2-16 compared to the reference position (configuration 1

.

Additional electrical impedance measurements were collected from all 16 electrode configurations for two more consecutive days; with results showing deviations from <1% to 52% for the real impedance and <1% to 81% for the imaginary. Future studies will explore these additional datasets to determine the deviations that occur as a result of collecting the same measurements on different days, which is another important aspect if these measurements are to be used in continuous monitoring. Possible sources of error in this study include movement artifacts introduced by the subject, which may have resulted in changes to the tissue state or cable positioning during the measurements. Follow-up studies are recommended to repeat this process while the patient is in different positions to explore the impact. Knowing the effects of electrode positioning may improve applications of applying electrical impedance measurements in conditions where electrodes cannot be precisely placed.

CONCLUSIONS

This experiment illustrates the variability of impedance measurements collected from a single subjects forearm due to 16 different electrode configurations. From these measurements, the real impedance showed deviations from 0.0044% to 51.44% and the imaginary impedance showing deviations from 0.014% to 67.95% when compared to a reference value. Of note were the mirroring trends observed between the set of voltage electrodes on one half of the subject's forearm.

REFERENCES

[1] E. M. Bartels, E. R. Sorensen, and a. P. Harrison, "Multi-frequency bioimpedance in human muscle assessment," Physiol. Rep., vol. 3, no. 4, pp. e12354–e12354, 2015.

[2] L. Li, H. Shin, X. Li, S. Li, and P. Zhou, "Localized electrical impedance myography of the biceps brachii muscle during different levels of isometric contraction and fatigue," Sensors, vol. 16, no. 4, 2016.

[3] S. B. Rutkove, R. A. Partida, G. J. Esper, R. Aaron, and C. A. Shiffman, "Electrode position and size in

electrical impedance myography," Clin. Neurophysiol., vol. 116, no. 2, pp. 290–299, 2005.
[4] C. a Shiffman, "Adverse effects of near current-electrode placement in non-invasive bio-impedance measurements," Physiol Meas, vol. 34, pp. 1513–1529, 2013.
[5] B. Sanchez, A. Pacheck, and S. B. Rutkove, "Guidelines to electrode positioning for human and animal electrical impedance myography research.," Sci. Rep., vol. 6, p. 32615, 2016.
[6] T. J. Freeborn, "A survey of fractional-order circuit models for biology and biomedicine," IEEE J. Emerg. Sel. Top. Circuits Syst., vol. 3, no. 3, pp. 416–424, 2013.
[7] R. Buendia, F. Seoane, and R. Gil-Pita, "A novel approach for removing the hook effect artefact from electrical bioimpedance spectroscopy measurements, " J. Phys. Conf. Ser., vol. 224, no. 1, p. 12126, 2010.

A NEW METHOD FOR EARLY DIAGNOSIS OF COLON CANCER USING FLUORESCENCE EXCITATION-SCANNING HYPERSPECTRAL IMAGING

Malvika Lall[1], Joshua Deal[1], Shante Hill[4], Paul F. Rider[5], Carole W. Boudreaux[4], Thomas C. Rich[2], and Silas Leavesley[1,2,3]

[1]Department of Chemical and Biomolecular Engineering, [2]Department of Pharmacology, [3]Center for Lung [4]Biology, Department of Pathology, [5]Department of Surgery
University of South Alabama, Mobile, AL, USA

ABSTRACT

Colon cancer is the second leading cause of cancer death in the United States. Early detection and diagnosis is a very important step in reducing morbidity and mortality making the ultimate goal of screening exams to identify lesions prior to advancement into cancer or tissue invasion. The objective of this study is to examine the potential of hyperspectral imaging for measuring spectral changes that are concurrent with changes in colon cancer compared to surrounding normal tissue. Specimen pairs of fresh normal and adenocarcinoma tissues were obtained from surgical resections of colon tissue in collaboration with the University of South Alabama Departments of Surgery and Pathology. All procedures were carried out in accordance with Institutional Review Board protocol # 13-120. The colon tissues from normal and cancerous regions were scanned by excitation scanning hyperspectral imaging using a novel microscope constructed at the University of South Alabama. Multiple fields of view (FOV) were acquired from each specimen and MATLAB and ENVI were used to correct for background signal and to draw regions of interest and extract the average spectra for each region. When comparing spectra averaged over several areas of normal colon, results demonstrated consistent spectral information images with similar peak wavelengths and shapes. However in colon cancer, extracted spectra demonstrated high heterogeneity. High heterogeneity likely indicates variation in structural organization and molecular composition that is divergent from normal tissue composition. We conclude that hyperspectral fluorescence excitation-scanning may be a viable technology for detecting abnormal changes in the colon tissue based on spectral changes in the mucosa of the colon. This information could be used to provide new methods for early diagnosis of colon cancer.

INTRODUCTION

Colon cancer is the second leading cause of cancer death in the United States. [8] Early detection is the ultimate goal of screening exams to identify lesions prior to advancement into cancer or tissue invasion. [15] The colon has four layers: the mucosa, submucosa, muscularis externa, and serosa. [22] Most colorectal cancers begin as a growth on the mucosa of the colon, called a polyp. Adenocarcinomas make up more than 95% of colorectal cancers. There are 5 stages of colon cancer from 0 to IV. [2] Using the revised AJCC sixth edition system, the 5-year colon cancer–specific survival decreased from stage I to stage IV [15], making early detection a critical step in reducing morbidity and mortality.

Traditional white light endoscopy remains the gold-standard imaging modality for colorectal screening in the United States[8]. However, studies have estimated that the miss rates for large (≥10mm) adenomas can range anywhere from 0% to 20% with increased rates for flat and small (<5mm) lesions [6], [16], [18], [19]. In an effort to improve the detection sensitivity and specificity, alternative imaging modalities including auto fluorescence imaging, chromoendoscopy and narrow band imaging were developed [8],[10],[11],[12], [23]. However in larger studies, these techniques have not shown significant improvements in sensitivity and specificity [3], [7], [14].

Spectral imaging uses the wavelength dependent nature of light-tissue interactions to analyze the different tissues in the body by the difference in their reflectance and fluorescence [1],[13]. The specificity of single wavelength fluorescence techniques is low due to the inability to differentiate between fluorophores. In hyperspectral imaging, this limitation is overcome by using images acquired over a range of wavelengths at narrow intervals to produce a spectrum[3].

Traditional biomedical fluorescence hyperspectral imaging obtains images by filtering the fluorescence emission (emission scanning) across a broad wavelength range while exciting at a single wavelength band. However this provides a low signal because the emitted light is filtered to a narrow band prior to detection which results in the need for long acquisition times. This limits its use in time sensitive procedures including video rate endoscopic procedures.[4] Hyperspectral imaging using fluorescence excitation scanning (HIFEX) can overcome the limitations of emission scanning by allowing signal from all emitted light at a particular excitation wavelength to be detected. This provides a 10-to-30 fold higher signal sensitivity than traditional spectral imaging

approaches. [4]

The goal of this study is to assess the potential of HIFEX microscopy for the early detection of differences between cancerous and normal healthy tissue in resected colorectal specimens. In the long term, it is hoped that the HIFEX microscope technology can be translated to an endoscope system for real-time detection of colorectal lesions.

MATERIALS AND METHODS

Tissue Specimens

Specimen pairs of fresh normal and adenocarcinoma were obtained from surgical resections of colorectal tissue in collaboration with the University of South Alabama Departments of Surgery and Pathology. All procedures were carried out in accordance with Institutional Review Board protocol # 13-120. Confirmation of normal tissue and adenocarcinoma were determined by histologic evaluation of H&E permanent sections. Specimens were given a de- identified label of HSI-1, HSI-2, etc., for each patient enrolled in the study.

Image Acquisition Microscope, Equipment and Hyperspectral Excitation-Scanning Image Acquisition

An inverted fluorescence microscope (TE2000-U, Nikon Instruments) with a 20x objective (10x/.25 Ph1 ADL ∞/1.2 WD 6.2, Nikon Instruments) was used as the imaging platform. Illumination light was provided by a 300W Xenon arc lamp (TITAN 300ST-K, Sunoptics Technologies). An evaluation prototype thin-film tunable excitation filter system containing 5 separate tunable filters (Sutter, VF5) was used to filter the excitation light that was illuminating the sample. After passing through the tunable filters and the liquid light guide, excitation light was reflected off of a Long-Pass Dichroic Beamsplitter (Semrock 555) through the microscope objective to the specimen. Fluorescence emission was detected through a 561nm long pass emission filter. An electron- multiplied charge-coupled device (CCD) camera (Andor Zyla sCMOS) was used to acquire images of the illuminated tissues. The movement of the microscope stage was controlled by an automated stage (PS3J100, Prior). The detailed configuration of the tunable filters is described by Favreau et. al. 2014 [4]. For hyperspectral imaging, fluorescence excitation was scanned using wavelength ranges from 340-520nm. Figure 1 shows a schematic light path used for excitation-scanning.

At least three fields of view (FOV) were located on the prepared tissue specimens and hyperspectral images were obtained. The fluorescence excitation was scanned through each excitation wavelength sequentially, and the fluorescence image was acquired at each excitation wavelength.

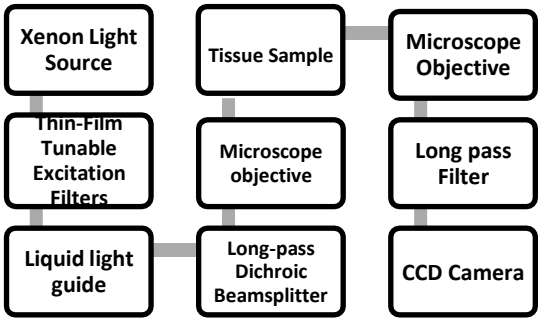

Figure 1: *Excitation scanning light path*

Spectral Correction

To account for differences because of wavelength-dependent illumination or transmission, a correction factor was used to orrect the system back to a flat spectral response using a NIST-traceable lamp (LS1-CAL-INT, Ocean Optics, Inc.) and fiber-coupled spectrometer (QE65000, Ocean Optics, Inc.) [25].

Spectral Image Collection and Analysis
Collecting Background Spectrum

A background spectrum was acquired from each specimen for use in the flat spectral correction process. For each tissue, one field of view was acquired in which some of the region was outside of the tissue. The spectrum of this region was used as a background spectrum for correcting all of the spectral image data acquired from the specimen. MATLAB and ENVI were collectively used to determine the background spectrum used to correct all the spectral image data acquired from the specimen. The stored image files were opened in MATLAB. These were converted from tiff to BSQ files for each FOV. The background ROI was defined in ENVI software, and the average spectrum of the background ROI was calculated. ImageJ was used to visualize normal and cancerous tissues. Spectra were plotted to visualize readily observable differences in the shape of the spectra.

For each FOV1 image, a region of interest was drawn in the background area (lacking tissue) using the ROI tool in ENVI, and the average spectrum of the background ROI was measured. The background spectrum was exported to Excel (Microsoft Corp.), transferred onto an excel file and saved as text files. A custom MATLAB script was used to perform background subtraction and flat spectral correction. The spectrally-corrected image file was saved in BSQ format, with a corresponding text header file that

allowed the corrected files to be opened in ENVI software.

Identifying structural features and extracting spectral data

Each spectral image stack was opened and regions of interest were manually identified according to anatomical structures in the image, as described below. The average intensity at each wavelength from each region was calculated and the intensity data was extracted as the average spectrum of each region.

The selected ROI method was used to identify structural features and extract spectral data for each ROI. ROI's were drawn based on characteristic or unique anatomical structural features seen in each image. Each region was assigned a different color. Once the spectra for both the lesional and normal tissue were generated, they were visually compared using side-by-side plots.

RESULTS

When comparing average spectra for FOV2 and FOV3 in HIS-1 normal tissue, the spectra were very similar in peak occurrences and intensities. The spectra from several different FOV's in 3 patients all appeared similar (homogeneous). The lesional tissue had different spectral patterns in different FOV's compared to the normal tissue sample. Peaks of various intensities occurred at some areas in the lesional tissue that were not present in the normal tissue. Figure 2 shows the correction of images in normal and lesional tissue. Figure 3 shows regions of interest in lesional tissue. Figure 4 and Figure 5 show the spectra for normal and lesional tissue respectively.

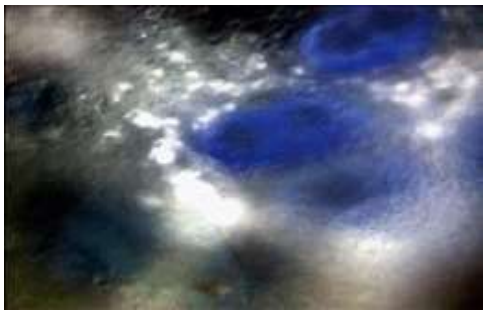

Figure 2: Correction of Image

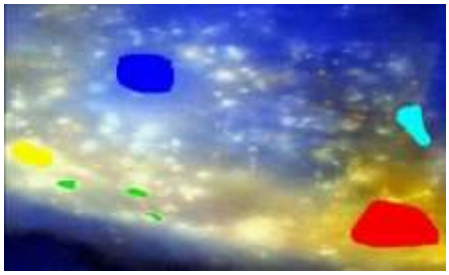

Figure 3: FOV3 HSI-1 Lesional with Regions of Interest

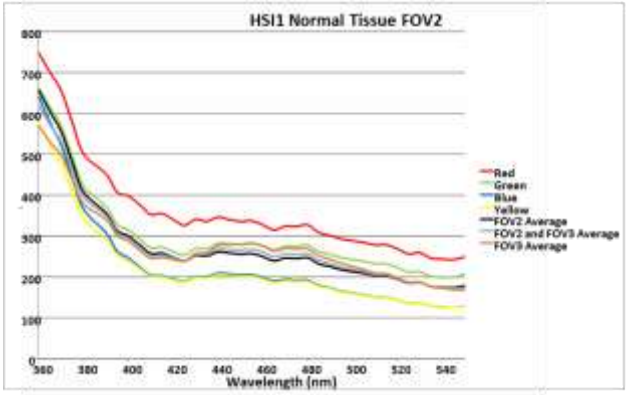

Figure 4: The black line represents the average spectra for all ROIs in FOV2 for HSI-1 normal tissue. Each color represents the corresponding ROI on the corrected image. The grey line represents the average spectra for all ROIs in FOV2 and FOV3 for normal tissue.

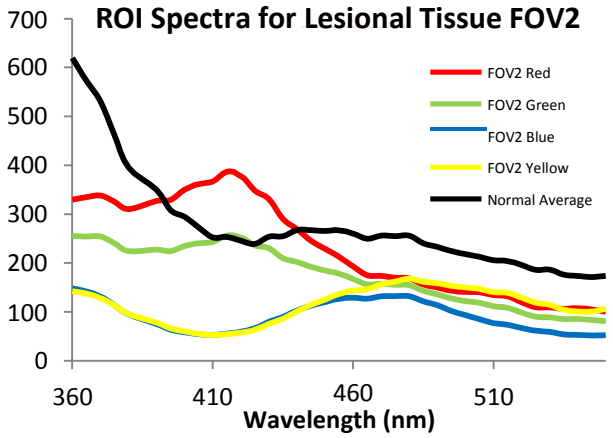

Figure 5: The black line represents the average spectra for all ROIs in FOV2 for HSI-1lesional tissue. Each color represents the corresponding ROI on the corrected image.

DISCUSSION

Hyperspectral fluorescence excitation- scanning imaging allowed measurement of fluorescence excitation spectra for normal and cancerous tissues. The overall goal of this study was to demonstrate spectral changes in colon cancer tissues compared to normal surrounding colon tissue. The normal tissue was for the most part spectrally homogeneous as the shape of the spectra was similar within different FOV's. The lesional tissues were observed to be spectrally hetero-geneous as the spectra for the different ROIs were different. Overall, the spectra for lesional tissues differed in patterns with an increased variance in the intensities when compared to the spectra from normal tissues. Hyperspectral fluorescence excitation-scanning may also be capable of producing fast acquisition times and therefore can possibly be incorporated into real- time endoscopic procedures to identify tissue types based on spectral changes.

CONCLUSIONS

This study demonstrated that differences in the spectral patterns of normal and lesional tissue could be detected using fluorescence excitation- scanning hyperspectral imaging. This supported the hypothesis that the spectral properties of normal tissue are homogenous and therefore deviations from the normal spectrum can be used to identify changes in tissue types.

ACKNOWLEDGMENTS

The authors would like to acknowledge support from: NIH grants UL1 TR001417 and P01 HL066299. The Abraham Mitchell Cancer Research Fund, and The University of Alabama at Birmingham Center for Clinical and Translational Science (CCTS).

REFERENCES

1. Akbari H, Uto K, Kosugi Y, Kojima K, Tanaka N. Cancer detection using infrared hyperspectral imaging. Cancer Sci.102(4):852-7. (2011)
2. American Joint Committee on Cancer. Colon and Rectum Cancer Staging. 7th Ed
3. Chiu H.M, Chang C.Y, Chen C.C, Lee Y.C, Wu M.S, Lin J.T, Shun C.T and Wang, H.P. A prospective comparative study of narrow-band imaging, chromoendoscopy, and conventional colonoscopy in the diagnosis of colorectal neoplasia. Gut 56, 373–379 (2007).
4. Favreau P. F, Hernandez C, Heaster T, Alvarez D.F, Rich T.C, Prabhat P and Leavesley S. Excitation-scanning hyperspectral imaging microscope. J. Biomed. Opt. 19, 046010–046010 (2014).
5. Favreau P. F, Hernandez C, Lindsey A.S, Alvarez D.F, Rich T.C, Prabhat P and Leavesley S. Thin-film tunable filters for hyperspectral fluorescence microscopy. J. Biomed. Opt. 19, 011017 (2014).
6. Hixson, L., Fennerty, M., Sampliner, R. & Garewal, H. Prospective blinded trial of the colonoscopic miss-rate of large colorectal polyps. Gastrointest. Endosc. 37, 125–127 (1991).
7. Ignjatovic, A., East, J.E., Guenther, T., Hoare, J., Morris, J., Ragunath, K., Shonde, A., Simmons, J., Suzuki, N., Thomas-Gibson, S. and Saunders, B.P. What is the most reliable imaging modality for small colonic polyp characterization? Study of white-light, autofluorescence, and narrow-band imaging. Xu, J., Murray, T. and Thun, M.J. Endoscopy 43, 94 (2011).
8. Jemal, A., Segal, R., Ward, E., Hao, Y. Cancer statistics, 2008. CA. Cancer J. Clin. 58, 71–96 (2008).
9. Kester, R. T., Bedard, N., Gao, L. & Tkaczyk, T. S. Real-time snapshot hyperspectral imaging endoscope. J. Biomed. Opt. 16, 056005–056005 (2011).
10. Machida H, Sano Y, Hamamoto Y, Muto M, Kozu, T, Tajiri H and Yoshida S. Narrow-band imaging in the diagnosis of colorectal mucosal lesions: a pilot study. Endoscopy 36, 1094–1098 (2004).
11. Matsumoto T, Esaki M, Fujisawa R, Nakamura S, Yao T, Iida M. Chromoendoscopy, narrow-band imaging colonoscopy, and autofluorescence colonoscopy for detection of diminutive colorectal neoplasia in familial adenomatous polyposis. Dis. Colon Rectum 52, 1160–1165 (2009).
12. McGill SK, Evangelou E, Ioannidis JP, Soetikno RM, Kaltenbach T. Narrow band imaging to differentiate neoplastic and non-neoplastic colorectal polyps in real time: a meta-analysis of diagnostic operating characteristics. Gut. 62(12):1704-13 (2012)
13. Miller J.C. Magnetic Resonance Spectroscopy in the Brain. Radiology Rounds. 10:7 (2012)

14. Moriichi K, Fujiya M, Sato R, Watari J, Nomura Y, Nata T, Ueno N, Maeda S, Kashima S, Itabashi K, Ishikawa C, Inaba Y, Ito T, Okamoto K, Tanabe H,Mizukami Y, Saitoh Y, Kohgo Y. Back-to-back comparison of auto-fluorescence imaging (AFI) versus high resolution white light colonoscopy for adenoma detection. BMC Gastroenterol. 22;12:75 (2012)

15. O'Connell J.B, Maggard M.A and Ko_C.Y. Colon Cancer Survival Rates With the New American Joint Committee on Cancer Sixth Edition Staging. JNCI J Natl Cancer Inst 96(19): 1420-1425. (2004)

16. Rembacken, B. Rembacken B J, Fujii T, Cairns A, Dixon M F, Yoshida S, Chalmers DM, Axon A T. Flat and depressed colonic neoplasms: a prospective study of 1000 colonoscopies in the UK. The Lancet 355, 1211–1214 (2000).

17. Rex, D. K. Maximizing detection of adenomas and cancers during colonoscopy. Am. J. Gastroenterol. 101, 2866–2877 (2006).

18. Rex D K, Cutler C S, Lemmel G T, Rahmani E Y, Clark D W, Helper D J, Lehman G A, and Mark D G. Colonoscopic miss rates of adenomas determined by back-to-back colonoscopies. Gastroenterol. 112, 24–28 (1997).

19. Saitoh Y, Waxman I, West A B, Popnikolov N K, Gatalica Z, Watari J, Obara T, Kohgo Y, and Pasricha P J. Prevalence and distinctive biologic features of flat colorectal adenomas in a North American population. Gastroenterol. 120, 1657– 1665 (2001).

20. Schoenfeld P, Lipscomb S, Crook J, Dominguez J, Butler J, and Holmes L. Accuracy of polyp detection by gastroenterologists and nurse endoscopists during flexible sigmoidoscopy: a randomized trial. Gastroenterol. 117, 312–318 (1999).

21. Seeff LC, Richards TB, Shapiro JA, Nadel MR, Manninen DL, Given LS, Dong FB, Winges LD, McKenna MT. How many endoscopies are performed for colorectal cancer screening? Results from CDC's survey of endoscopic capacity. Gastroenterol. 127, 1670–1677 (2004).

22. Stanfield C.L, Germann W.J. Principles of Human Physiology 3rd Ed (Pearson Education 2008).

23. Su M.Y, Chen-Ming Hsu, Yu-Pin Ho, Pang-Chi Chen, Chun-Jung Lin and Cheng-Tang Chiu Comparative study of conventional colonoscopy, chromoendoscopy, and narrow-band imaging systems in differential diagnosis of neoplastic and nonneoplastic colonic polyps. Am. J. Gastroenterol. 101, 2711–2716 (2006).

24. Wallace, M. B., Wax, A., Roberts, D. N. & Graf, R.N. Reflectance spectroscopy. *Gastrointestinal endoscopy clinics of North America* **19**, 233–242 (2009).

25. Leavesley, S.J., N. Annamdevula, J. Boni, S. Stocker, K. Grant, B. Troyanovsky, T.C. Rich, and D.F. Alvarez. "Hyperspectral Imaging Microscopy for Identification and Quantitative Analysis of Fluorescently-Labeled Cells in Highly Autofluorescent Tissue." *Journal of Biophotonics* 5, no. 1 (2012): 67–84. doi:10.1002/jbio.201100066

.

FUNCTIONAL ANALYSIS OF AIF-1 IN ASSOCIATION WITH CARDIAC ISCHEMIA REPERFUSION (IR)

D. Olga McDaniel[1], Allen A. Simeone[1], Kathy M. Alvarez[2], Madeleine Cunningham[2], and Larry S. McDaniel[1]

[1] University of Mississippi Medical Center, Jackson MS, and [2]University of Oklahoma Health Sciences Center, Oklahoma City OK

ABSTRACT

The mechanisms by which sterile inflammation is induced, after ischemia/reperfusion (IR) during organ procurement contributes significantly to tissue injury and may cause early organ dysfunction after transplantation. Genes associated with innate immunity are prime activators of early inflammatory responses to an allograft that lead to host-induced inflammation and organ rejection. We hypothesized that endogenous substances or damage-associated molecular patterns (DAMPs), released after allograft reperfusion such as allograft inflammatory factor 1 (AIF-1)/Daintain could promote activation of innate immune responses. This would occur through the activation of cardiac TLRs and may contribute to allograft dysfunction. We have reported expression levels of AIF-1 and TLRs during cardiac IR in a rat model of the left anterior descending artery (LAD) occlusion which generates ischemia in the left ventricle (LV). AIF-1 and TLR mRNA transcripts were significantly increased in a time dependent- manner after IR. These markers were upregulated as early as 10 minutes after reperfusion and further they were increased several-fold after 60 minutes of reperfusion in tissue and peripheral blood cells as compared to the control group. Functional activity of AIF-1 was confirmed in an *in vitro* model using human coronary vascular smooth muscle cells (CVSMC), treated with INF-γ as well as using HEK293 cells transfected with h-TLR2 or TLR4 in which the functional activity was determined by production of a pro-inflammatory cytokine such as IL-18. Thus, elucidation of the mechanisms of an induced inflammation within the myocardial cells has the potential for the development of novel anti-inflammatory strategies that could improve outcomes for cardiac allograft transplant recipients.

KEY WORDS: Allograft inflammatory factor-1, cardiac, innate immunity, ischemia, LAD, myocardium, reperfusion, IL-18, IFN-γ, toll-like receptors

INTRODUCTION

The early mechanism that triggers rejection episodes (RE) after cardiac transplantation may involve activation of the recipient innate immune response towards ischemia reperfusion injury (IRI) that occurs during cardiac procurement. Cardiac allograft transplants rarely have a 50% survival rate beyond 10-12 years (1). A number of studies have shown the importance of inflammatory responses in the development of allograft rejection (2, 3). However, limited studies have been reported for the role of innate immune responses and the target elements causing activation of early inflammatory responses (4, 5). It is speculated that the injury is often recognized as an inflammatory cause of damaged-tissue debris or molecular factors associated with unusual activation of the innate immune response, independent of host immunologic background (5). A broad range of non-pathogenic motifs could trigger the induction of inflammatory episodes in the myocardium. We have recently reported increased levels of allograft inflammatory factor-1 (AIF-1) as well as the Toll-like receptors (TLRs) in an *in vitro* model of IR, and in an *in vivo* experimental model of left anterior descending (LAD) artery occlusion (6, 7). TLRs initially, identified as a family of pattern-recognition receptors (PRR) that allow mammalian cells to recognize pathogen associated molecular patterns (PAMPs) causing activation of the immune system and inflammation (8, 9). However, increasing evidence indicated that TLRs can also be stimulated by non-infectious endogenous molecules generated by disease or IR, known as DAMPs (10- 12). The mechanism by which these molecules interact in allograft rejection remain to be determined. In this study we investigated the mechanisms by which the AIF-1 and TLRs interact in an in vitro model using primary cell lines generated from human coronary arteries and an HEK-293 cell line stably transfected with TLRs, which may help to identify the molecular pathways by which AIF-1 enhances release of inflammatory cytokines.

MATERIALS AND METHODS

Human primary cell line preparation

Monocytes: Monocytes were isolated from allograft recipient's peripheral blood mononuclear cells (PBMCs), treated with AIF-1 peptides and tested for cytokine production.

Coronary artery SMC: Cell lines from human coronary artery smooth muscles (SMC) were generated and cultured in RPMI 1640 (Gibco-Thermo Fisher Scientific, Waltham MA). The culture media was supplemented with 5% heat-inactivated FCS, 2mM L-glutamine, 100U/ml

penicillin and 100 μg/ml streptomycin. Occasionally, supplemented with 10% condition media for AIF-1 induction. Cultures were treated with 0.75 ng/ml IFN-γ (RD system Inc., Minneapolis, MN) for AIF-1 production.

HEK293-human TLR stably transfected cell lines: Transfected cells (kindly provided from Dr. Cunningham's laboratory, University of Oklahoma Health Sciences Center, Oklahoma city OK) were cultured and maintained in DMEM(Gibco-Thermo Fisher Scientific, Waltham MA), supplemented with heat inactivated 10% FBS and 100U/ml penicillin and 100 μg/ml streptomycin. Cells were treated with recombinant AIF-1 protein (My Biosource, San Diego, CA) as well as with known TLR-2 or -4 ligands (Pam3CSK4 and LPS respectively)(Invivo Gen, San Diego CA). Supernatants were harvested after 72 hours and tested for cytokine production.

Cytokine detection

Supernatants from monocyte cultures treated with AIF-1 protein, transfected cells treated with AIF-1 peptides as well as known TLR-2 and -4 ligand were collected and tested using ELISA kit from BD- Pharmingen, (Piscataway, NJ) for IL-18 production levels. The test assay was performed according to the instruction provided by the manufacturer in 96-well plates.

Measurement of AIF-1 expression

RNA was extracted from monocytes using "Pure Link" RNA kit (Life Technologies, Carlsbad, CA), and was reversely transcribed using ImProm-II Reverse Transcriptase (Promega, Madison, WI). All samples were tested by 25 cycles of semi-quantitative RT-PCR using primers for AIF-1 isoforms. There are three isoforms generated due to gene splicing. These isoforms share sequence homology. The orientation of these isoforms has been described previously (9). The 5' forward primers for isoform 1 and 2 were identical and the 3'reverse primers for isoform 1 and 3 were identical. The forward primer for isoforms 1 and 2 was 5´- ATG-GAG-TTT-GAC-CTT-AAT-GG-3´, and for isoform 3, it was 5´- ATG-AGC-CAA-ACC-AGG-TAC-AG-3´. The reverse and complementary primer for isoforms 1 and 3 was 3´-GCA-ACT-CAG-AGA-TAG-CTT-TG-5´, and for isoform 2, it was 3´- TCA-CAT-TTT-TAG-GAT-GGC-AGA-TC-5´. Primer for β-Actin were 5'- ATG-GAT-GAT-GAT-ATC-GCC-GCG-3'and 5'-CTA-GAA-GCA-TTT-GCG-GTG-GAC-GAT-3'. The values were calculated as described previously (9). Expression levels between the isoforms were determined by one-way analysis of variance. The level of significance was set at $p<0.05$ for comparison between the isoforms.

Immunohistochemistry (IHC)

The formalin fixed paraffin embedded (FFPE) human monocytes were prepared for detection of AIF-1 using IHC stain. After antigen retrieval, sections were incubated with primary antibody corresponding with AIF-1 for 1 hour at room temperature followed by the IHC staining procedure previously described (13).

RESULTS

To verify release of AIF-1 from monocytes after treatment with IFN-γ, we measured AIF-1 by RT-PCR and IHC. AIF-1 was specifically detected in monocytes by the level of mRNA expression. However, a minimal level of anti-AIF-1 stain was detected by IHC. Figure 1. Illustrates AIF-1 isoform mRNA transcript levels calculated after they were normalized to β-Actin expression levels (normalized mRNA level for each isoform=mRNA expression determined by semi quantitative RT-PCR, divided by mRNA expression for β-Actin).

To verify AIF-1recombinant protein activate TLRs, we used HEK293 cells transfected with human (h) TLR-2, h-TLR-4, h-TLR-8 and hTLR-9 and tested for cytokine production. AIF-1 treated cells demonstrated 1.25 to 4.5 fold, dose dependent increase in IL-18 secretion in HEK-293 transfected cells with TLR-2, shown in Figure 2. However, a significantly less increase was observed in cells transfected with TLR-4. Also, no production of IL-18 was observed in cells transfected with TLR-8 or TLR9 (data not shown). To investigate the impact of TLR2 on activation of human HEK293 by AIF-1, cells were incubated with a monoclonal antibody (mAb) to TLR-2 (Imgenex, San Diego CA) for 1 hour before treatment with AIF-1. The mAb to TLR2 inhibited IL-18 production, shown in Figure 2.

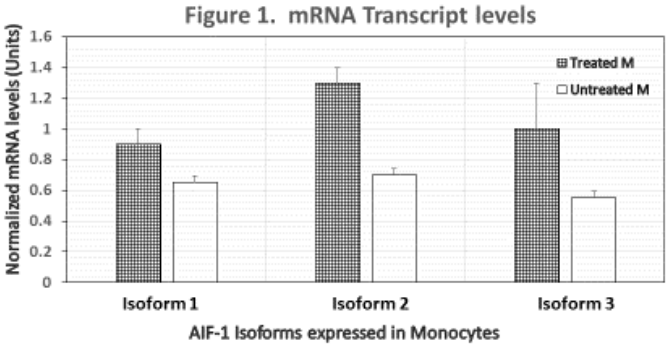

Figure 1. Illustration of levels of AIF-1 isoforms. Isoform 2 and 3 were expressed significantly greater in treated monocytes vs. untreated cells ($p<0.03$, $p<0.05$ respectively).

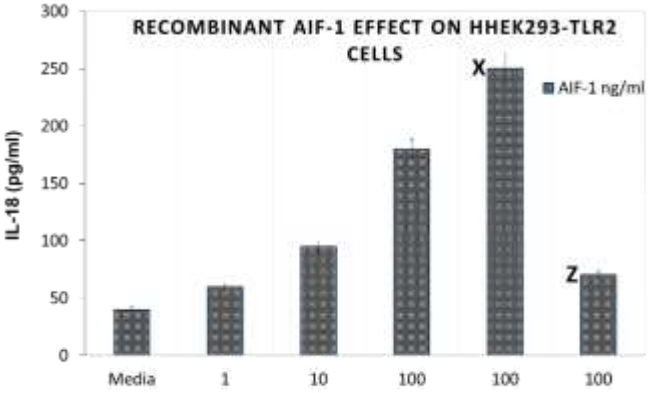

Figure 2. Illustration of AIF-1 impact on hHEK293-TLR-2 cells. ^{X}Pam3CSK4 . was used as a control ligand for TLR2 ^{Z} a TLR-2 mAb was used to inhibit the activity.

DISCUSSIONS

The practical value of this study was that AIF-1 closely associated with pathogenesis of allograft rejection and is a novel member of the cytokine network involved in the innate immunological process of host immune response to IRI. There is no information regarding AIF-1 association with TLR in the literature. Although, one study using a gene expression approach has reported the identification of AIF-1 as a potential factor involved in TLR-4 hyper-responsiveness in synovial fluids of patients with rheumatoid arthritis. Structural studies of TLR-ligand complexes are increasing, due to their significance in inflammatory immune responses and disease. It has been shown that the rate of troponin release by cardiac muscle after I/R has direct effects on myocardial protection during cardiac allograft preservation (14). Using AIF-1 protein sequence in a 3D protein database, we found a strong homology between domain 2 of human AIF-1 (sdi:160028) and cardiac Troponic C (1IH0 A). Despite numerous structural studies on the basis of ligand binding characterization of the TLRs, more knowledge is needed to understand the interaction between endogenous ligands such as AIF-1 molecule, as well as the activation of innate immune responses which may help the identification of new antagonists or agonists for clinical application.

CONCLUSIONS

Our experimental approach was effective in characterization of AIF-1 as a ligand for the TLR-2. However, using an AIF-1 antagonist, or a neutralizing TLR-2 antibody during cardiac IR in a rat model of LAD artery occlusion may further confirm the current *in vitro* study. New knowledge may help to understand the interaction between endogenous ligands and the activation of innate immune response which may guide the design of therapeutic inhibitors for clinical applications. This may help to improve transplantation outcomes.

ACKNOWLEDGEMENTS

This work was supported in part by Funds from the Transplantation Immunogenetics Laboratory (PI: D.O.M) in the Department of Surgery at UMMC.

REFERENCES

1. Lund, LH, Edwards, LB, Kucheryavaya, AY, Benden, C, et al. The Registry of the International Society for Heart and Lung transplantation: Thirty-second Official Adult Heart Transplantation Report -2015; Focus Theme: Early Graft Failure. J Heart & Lung Transplantation. 2015; 34(10): 1264–1277.
2. Wood, KJ, Goto, R. Mechanisms of Rejection: Current Perspectives. Transplantation. 2012; 93: 1-10.
3. Baker, AK, McDaniel, DO, Zhou, X, et al. Combined Analysis of Allograft Inflammatory Factor-1, Interleukin-18, and Toll-like receptor Expression and Association with Allograft Rejection and Coronary Vasculopathy. The American Surgeon, 2010; 76(8):872-878.
4. McDaniel, DO, Zhou, X, Moore, CK, Aru, G. Cardiac Allograft Rejection Correlates with Increased Expression of Toll-like receptor 2 and 4 and Allograft Inflammatory Factor-1. Transplantation Proceedings. 2010; 42(10):5235-4237.
5. Land WG. Emerging role of innate immunity in organ transplantation part II: Potential of damage-associated molecular patterns to generate immune-stimulatory dendritic cells. Transplantation Reviews. 2012; 26:73-87.
6. McDaniel DO, Zhou X, Rigney DA, et al. Allograft inflammatory factor-1 in cardiac ischemia reperfusion injury: release of molecular markers in an in vitro setting. OJOTS 2013; 3:5-12.
7. McDaniel DO, Majors L, Fang T, Zhang F, McDaniel LS. Allograft inflammatory factor-1induction during ischemia

reperfusion injury: A rat model of LAD occlusion. Int J Clinical Cardiol 2014; 1:1-6.
8. Beutler B. Inferences, questions and possibilities in Toll-like receptors signaling. Nature 2004; 430:257-263.
9. Takeda K, Akira S. Toll-like receptors in innate immunity. International Immunol 2005; 17(1): 1-14.
10. Yu L, Wang L, Chen S. Endogenous Toll-like receptor ligands and their biological significance. J Cell Mol Med 2010; 14:2592-2603.
11. Zhang P, Cox CJ, Alvarez KM, et al. Cutting edge: cardiac myosin activates innate immune responses through TLRs. J Immunol 2009; 183:27-31.
12. Yang Y, Lv J, Jiang S, Ma Z. et al. The emerging role of Toll-like receptor 4in myocardial inflammation. Cell Death Dis, 2016; 7:e2234.
13. Barker AK, McDaniel DO, Zhou X, et al. Combined analysis of allograft inflammatory factor-1, interleukin-18 and Toll-like receptor expression and association with allograft rejection and coronary vasculopathy. Am Surg 2010; 76: 872-878.
14. Ryan JB, Hicks M, Cropper JR, Garlick SR, et al. The initial rate of troponin I release post-reperfusion reflects the effectiveness of myocardial protection during cardiac allograft preservation. European J Cardio-thoracic Surgery 2003; 23:898-906.

EFFECTS OF MUSCLE FATIGUE ON ELECTRICAL IMPEDANCE OF BICEP MUSCLES DURING EXERCISES OF VARYING INTENSITY: A CASE STUDY

Tim Crenshaw and Todd Freeborn

Department of Electrical and Computer Engineering, The University of Alabama, Tuscaloosa, AL, USA

ABSTRACT

Electrical impedance measurements quantify the resistance of a material to an injected electrical stimulus and have been used to detect physiological changes in biological tissues. Previous studies have indicated that exercise induced fatigue results in a decrease of the electrical impedance of muscle tissues compared to pre-fatigue values. However, studies have failed to explore the impact of exercise intensity on this decrease, which is an important consideration if this technique is to be used for personalized, real-time fatigue monitoring for athletes during training and competition. During this case study, a single subject performed sets of bicep curls until failure on multiple days at 60%, 75%, or 90% of their assessed one repetition maximum towards inducing fatigue in their bicep muscle. Electrical impedance measurements from 5 kHz to 1 MHz were collected using a tetra-polar electrode configuration and Keysight E4990A impedance analyzer immediately pre- and post-exercise. The electrical impedance of the bicep muscle showed decreases after each of the fatigue protocols, consistent with previous research, with resistance/reactance decreases/increases of 1.5%/3%, 7.2%/15.3%, and 5.8%/15.5% immediately post the 90%, 75%, and 60% protocols, respectively, compared to pre-exercise measures.

Keywords: Impedance, bio-impedance, muscle, bicep, fatigue

INTRODUCTION

Electrical impedance is the measure of a materials resistance to an electrical stimulus. Applied to biological tissues, these measurements are being widely investigated as a means to monitor physiological change for non-invasive real-time monitoring in both health and athletics applications that include monitoring hydration status during dialysis [1], monitoring tissue damage [2,3], and muscle fatigue [4,5,6]. Previous studies have indicated that exercise induced fatigue results in a decrease of the electrical impedance of muscle tissues compared to pre-fatigue values [5,6]. However, studies have failed to explore the impact of exercise intensity on this decrease, which is an important consideration if this technique is to be used for personalized, real-time fatigue monitoring for athletes during training and competition. During this case study, a single subject performed sets of bicep curls until failure on multiple days at 60%, 75%, or 90% of their assessed one repetition maximum towards inducing fatigue in their bicep muscle. If a relationship can be found in the data, it has the potential help athletes train more effectively and protect against overtraining.

METHODS

For this study, electrical impedance measurements were collected using a Keysight E4990A impedance analyzer with a tetra-polar electrode configuration. To enable interfacing this device to the electrodes required for data collection from the study participant, a custom interface was designed that adapts the BNC-connectors of the impedance analyzer to a cable-set with the required snap-electrode connectors; this adapter is given in Fig. 1(a). To validate that this adapter did not introduce significant errors into the impedance analyzer measurements, several circuits constructed with 1% tolerance components were measured and compared to their theoretical values. For each circuit the measured error was less than 1% for frequencies below 1 MHz, above which larger errors were introduced. For this reason, the frequency range for data collection was limited to below 1 MHz.

For this study, a 23-year-old male performed a series of dumbbell bicep curls until failure on three occasions at weights of 60%, 75%, and 90% of their assessed one-repetition maximum (40 and 45 lbs. for the right and left arms, respectively). To collect the impedance measurements from the participant biceps, four Kendall 3 cm foam electrodes were placed 4.5 cm apart (center-to-center) on each bicep, given in Fig. 1(b). The electrodes labeled “I” injected the sinusoidal excitation current with 1 mA amplitude while those labeled “V” measured the resulting voltage to determine the impedance. 201 logarithmically spaced data points from 5 kHz to 1 MHz were collected. For each set of exercises at the different weights, measurements were collected from the subject’s left and right biceps while asked to stand upright and

relax their muscle. The subject then performed sets of dumbbell bicep curls until exhaustion, with two minute rests between sets, until either **i)** they were not able to perform a single repetition on a new set after their 2-minute rest or **ii)** they had completed 10 sets; after which their electrical impedance was again collected. To minimize the impact that electrode placement has on the collected impedance measurements, medical markers were used to highlight on the subject's skin their location for re-application on each day.

RESULTS

Both real and imaginary components of the measured electrical impedance from 5 kHz to 1 MHz are given in Fig. 2, with solid and dashed lines representing the pre- and post-fatigue values, respectively, with Figs. 2(a), (b), and (c) representing the measurements for the 60%, 75%, and 90% exercise-intensity, respectively. The blue/red and green/magenta lines represent the real/imaginary components for the left and right arms. Each of the pre-fatigue measurements, which were collected on different days, displayed similar impedances. Note that the corresponding weights and repetitions of the participant are given in Table 1. The real values were approximately 45 Ω at 5 kHz and decreased with increasing frequency, reaching approximately 22 Ω at 1 MHz. While the imaginary values decreased with increasing frequency from approximately -4 Ω at 5 kHz until 20 kHz, with an increase from 20 kHz until reaching a peak at 300 kHz, and finally a decrease again until reaching approximately -10 Ω to -12 Ω at 1 MHz. All plots in Fig. 2 show the same trends with the real/imaginary components of the impedance decreasing/increasing for all frequencies after the exercise protocol. The percent change of the post-fatigue values compared to the pre-fatigue values are given in Fig. 3 with the real (blue)/imaginary (red) impedance showing an average decrease/increase for the 90%, 75%, and 60% groups of 1.5%/3%, 7.2%/15.3%, and 5.8%/15.5% respectively.

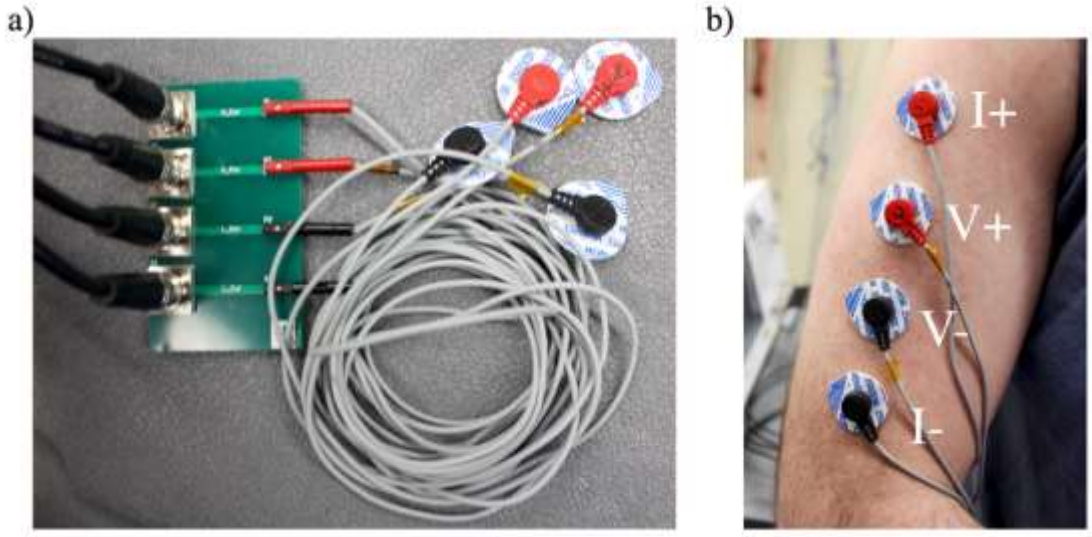

Figure 1. a) Impedance analyzer adapter and b) electrode placement on subject bicep for data collection.

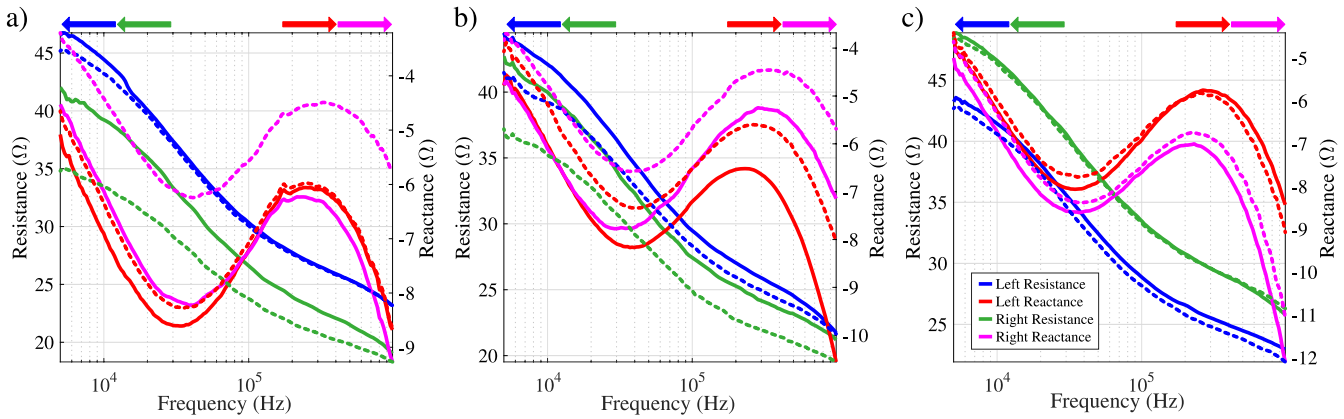

Figure 2. Pre- and post-exercise impedance measurements of both arms for the a) 60%, b) 75%, and c) 90% 1-RM exercise intensities.

Table 1. Weight and total number of repetitions performed for each set of measurements.

1-RM Group	**60%**		**75%**		**90%**	
Arm	*Left Bicep*	*Right Bicep*	*Left Bicep*	*Right Bicep*	*Left Bicep*	*Right Bicep*
Weight (lbs.)	25	30	30	35	35	40
Total Reps Performed	70	55	87	65	16	7

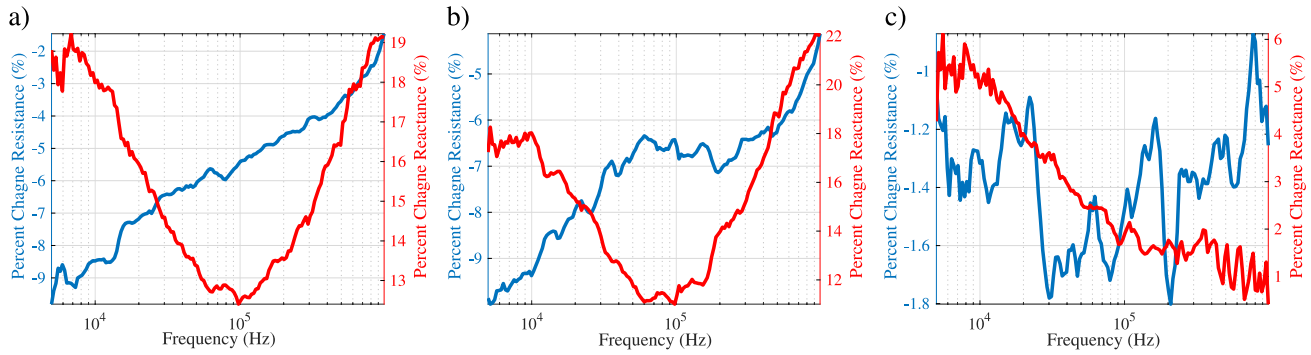

Figure 3. Average percent change of the real (blue) and imaginary (red) impedances comparing the post- and pre-exercise measurements for the a) 60%, b) 75%, and c) 90% 1-RM exercise intensities.

DISCUSSION

Impedance, because of fatigue, correlated well with increases in blood flow; which may also account for the smaller decrease in impedance for the 90% group if the lower number of repetitions at this weight did not increase the blood flow by the same amount as the 60% and 75% groups (which had a larger number of repetitions). Further studies are required to understand the underlying physiological mechanism that resulted in the different amounts of impedance variation as well as if this trend continues in a larger population of participants executing the same protocols. Additionally, when investigating if these trends continue in data collected from a larger population we need to explore if factors such as age, sex, and fitness level affect these observations. Additional measurements should be taken to examine how the impedance changes during the workout to determine if these measures can be used as an indicator of athlete performance, towards objectively monitoring training loads in real time. Finally, potential sources of error need to be further quantified including the potential noise

introduced by the use of unshielded electrode cables and the effects of perspiration and heart rate.

CONCLUSIONS

The results from this study support the results of previous studies that have investigated the effects of muscle fatigue on the electrical impedance of the bicep muscles. These results indicate that the impedance of muscle tissue decreases with muscle fatigue. Of interest in this study, are that the results indicate that the decrease in impedance was impacted by the number of repetitions performed and that a greater number of repetitions resulted in a larger decrease in impedance. While these observations are important, future studies should increase the sample size to confirm that these findings hold and to determine the underlying physiological mechanism.

REFERENCES

[1] F. Zhu, M.K. Kuhlmann, P. Kotanko, et. al. "A method for the estimation of hydration state during hemodialysis using a calf bioimpedance technique," *Physiol. Measure*., vol. 29, pp. S503-S516, 2008.

[2] L. Nescolarde, J. Yanguas, H. Lukaski, et. al. "Effects of muscle injury severity on localized bioimpedance measurements," *Physiol. Measure*. vol. 36, pp. 27-42, 2015.

[3] H. Nahrstaedt, T. Schauer, "A bioimpedance measurement device for sensing force and position in neuroprosthetic systems," *4th Eur. Conf. Int. Fed Med. Biol. Eng*., pp. 1642–1645, 2009.

[4] L. Li, H. Shin, X. Li, S. Li, P. Zhou, "Localized electrical impedance myography of the biceps brachii muscle during different levels of isometric contraction and fatigue," *Sensors*, vol. 16, no. 4, 581, 2016.

[5] T. Ikai, R. Saigou, M. Kyoso, M. Ishijima, "Dynamic electrical characteristics of the muscle with the fatigue during exercise" in *World Congress on Med. Phys. Biomed. Eng*, pp. 622-625, 2007.

[6] G. Vescio, J. Rossell, L. Nescolarde, G. Giovinazzo, "Muscle fatigue monitoring using a multifrequency bioimpedance technique" in *5th Eur. Conf. Int. Fed. Med. Biol. Eng*., pp. 1257-1260, 2011.

.

APPLICATIONS OF INERTIAL MICRO-ELECTRO-MECHANICAL SYSTEMS ON AMERICAN FOOTBALL PLAYERS AND EQUIPMENT

Derius J. Galvez and Jamel Alexander
Department of Aerospace Engineering, Mississippi State University, MS, USA

ABSTRACT

North American football players often hurt themselves because of incorrect football positions. The idea of using orientation sensing to help younger football players with football position development was studied in this research. This paper discusses how an orientation sensor can be created to help younger football players develop a better tackling position. After reviewing three inertial measurement devices, the raspberry pi coupled with a lis331 accelerometer was chosen. The MATLAB program reads the x, y, and z gravity components of the accelerometer and inputs them into the Euler angle equations. Once these angles were found, they were inserted into a flight path equation which was formulated into an orientation matrix. This allowed the sensor to measure the orientation of the football players. However, variance in the resolution of the sensor most likely occurred due to a mismatch of the input excitation voltage in the power surge which was 12 volts and the sensor's threshold voltage which was 3.3 volts. Further work must be done to enhance the signal output or sensitivity of the sensor.

Keywords: American, Football, Position, Inertia, Measurement, Devices, Equipment

INTRODUCTION

Over the past decade, more North American football (NAF) players are suffering major injuries[1]. From Pop Warner to the National Football League, players often hurt themselves because of incorrect tackling positions [2]. Head and neck injuries are usually the most severe and can have negative lasting effects on players. For young NAF players, head and neck injuries are usually a result of poor or illegal tackling techniques such as spear tackling; a technique in which a player tackles with his head down and not in an upright tackling position [2]. To properly train young football players how to tackle, youth football camps have emerged all over the United States. However, the cost of camps range from $25 per day camps to $450 per three day camps[3]. Not every family can afford camps; especially those who have multiple children playing different sports during the summer. This orientation sensor could be a safe; cost effective; self-teaching tool which would allow young players to develop proper positioning skills in football. The goal of this research was to create an orientation sensor that could be attached to a player's clothing or football equipment. The player would then get into a pre-tackling football position, and would have his stance corrected based upon the data the accelerometer would read. This device has the potential to improve the position of young football players by reducing illegal tackling habits, ultimately reducing mild and severe injuries [4]. In order to obtain accurate readings from the sensor, an ideal pre-tackling position was defined using transformation matrices.

METHODS

"It was determined an ideal pre-tackling football stance is when the player's center of gravity is low to the ground; while maintaining optimal balance (John Haneline, personal communication)." When a player is in this position, their low center of gravity allows them to achieve optimal strength when trying to tackle another player. The player has their arms positioned either in front or down by their side, while their back is straight and waist aligns 90 degrees to the ground[5]. In a real world situation, a player would be moving in order to maintain agility.

A. Raspberry Pi 2 with lis331 accelerometer and device placement

The Raspberry Pi 2 (Raspberry Pi Foundation, United Kingdom) was coupled with a lis331 accelerometer (Sparkfun Electronics, United States) and MATLAB was employed in this study as the programming language of choice [6]. The setup was powered by a 12 Volt surge protector connected to a power outlet. Post programming the orientation sensor, the readings from the accelerometer were obtained. Before the experiment, the device was strategically placed slightly below the left shoulder blade of the football player. Placement of the device on a player is very important since the correct orientation for each football player is different based upon the position of the device relative to the player. This also allows for the player a certain level of comfort in their range of motion. The full description of these orientations are labeled in Fig. 1(a) Fig. 1(b) and Fig 1(c).

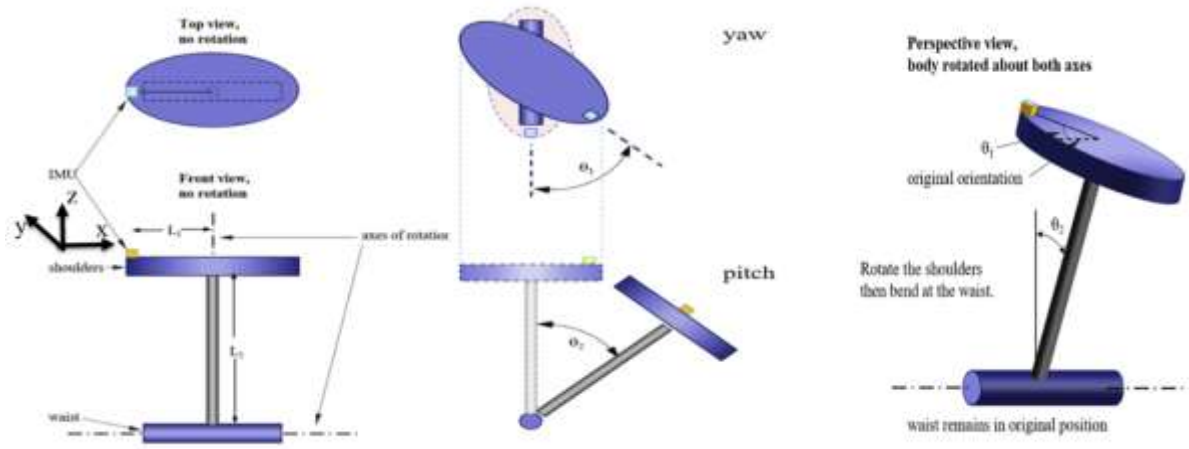

Figure 1a [left] 1b [middle] 1c [right] Device placement on player with respect to orientation angles

A suitable stance was modeled after a starting high school football player since there is no such thing as an ideal pre-tackling football stance. The player started as a defensive end and guard, which are two positions that require a similar pre-tackling football stance. To begin the experiment, the MATLAB code was initiated. Once the program was set, the wires for the device were taped onto the front of the player's shirt in a secure position to prevent shifting. The player was then asked to get into a pre-tackling stance and his orientation was recorded as the ideal stance. After that initial recording, the player was asked to move in three axial directions, which were listed in the program as x, y and z coordinates to establish set boundary conditions for the experiment; which will be used to determine if the user is out of position. The program was designed to inform the individual when they are not in the correct position or vice versa, are in a preferred orientation stance. When a player is in a good stance a positive message appears such as "Good job' or 'Perfect'. When they are out of position the program will say 'Too far to the left' or 'Too far back'. These responses depend on the orientation of player and if he or she is outside of the ideal preset boundary conditions. Once these boundary conditions were made, the device was able to be tested on other players.

B. Gravity equations

Gravity equations were necessary for expressing the components (gx, g_y, g_z) of the gravity vectors [7]. Using the gravity vectors from the accelerometer data, it is possible to relate the angles to the Earth-based inertial reference frame. Each gravity vector is related to gravity multiplied by a trigonometric function. These vectors are shown in Eq (1), Eq (2), and Eq (3).

$$g_x = -gsin(\theta) \qquad \text{Eq (1)}$$

$$g_y = gcos(\theta) * \sin(\phi) \qquad \text{Eq (2)}$$

$$g_z = gcos(\theta) * \cos(\phi) \qquad \text{Eq (3)}$$

G_x, g_y, and g_z are the values from the accelerometer data. Using those components, the angles from the gravity equations were solved and inputted into the earth-based inertial reference frame [7,8].

C. Euler Transformation Matrix

To get an accurate orientation, the position angles were solved from the gravity equation and then inserted into the Euler transformation matrix in Eq (4). The Euler transformation matrix is derived from the kinematic flight path equations used to describe the flight path of an aircraft [7]. Through the Euler transformation matrix, a relationship between the inertial reference frame of the body and the inertial reference frame of the earth is established. The coordinate system is defined based on the football player. Within this study, a point slightly below the top of the left shoulder was selected to be the body inertial reference frame while the ground was considered to be that of the earth's inertial reference frame [5]. In Eq (4) the pitch and roll angles from the gravity equations are placed inside the matrix, transforming it from the body to earth reference frame [7].

$$\begin{bmatrix} X' \\ Y' \\ Z' \end{bmatrix} = \begin{bmatrix} cos\psi cos\theta & -sin\psi cos\theta + cos\psi sin\theta sin\phi & sin\psi sin\phi + cos\psi sin\theta cos\phi \\ sin\psi cos\theta & cos\psi cos\phi + sin\psi sin\theta sin\phi & -sin\phi cos\psi + sin\psi sin\theta cos\phi \\ -sin\theta & cos\theta sin\phi & cos\theta cos\phi \end{bmatrix} * \begin{bmatrix} X \\ Y \\ Z \end{bmatrix} \quad \text{Eq (4)}$$

From this matrix, the orientation of the football player was determined. In order to get a correct position, the player's coordinate system was based on an ideal pre-tackling position.

D. Testing for Correct Position

The first test was on a 23-year-old female, with no prior football experience. She was an ideal candidate since she had never played football, considering the device and software were modeled for a young football player learning to play football for the first time. She was asked to get into her idea of a pre-tackling football position. Once she got into her assumed pre-tackling position form, the accelerometer was taped to the front of her shirt slightly below her left shoulder. She was given three tries to get the ideal position correct before the device recorded her position. Next, she was asked to get in the ideal pre-tackling position after she was assisted on the proper instructions on how to do so. This position was also done three times before the device recorded her data. Finally, she was asked to get in the ideal pre-tackling position without any assistance. This information was recorded after the third attempt.

RESULTS

The equations programmed within the orientation sensor predicted changes in position within a reasonable range. In the first trial, the results yielded a negative output for the roll ('Too far left'), pitch ('Too far forward.'), and yaw ('Don't twist left, square and centered') positions. This indicated the user's orientation did not satisfy the set boundary conditions. In the second trial, the results yielded a single positive output and two negative outputs. Roll ('Too far left.'), pitch ('Great Job!'), and yaw ("Don't twist right stay square and centered. '). The final trial also yielded a single positive output and two negative outputs. Roll ('Good Job!'), pitch ('Too far back.'), and yaw ('Don't twist right.").

Table 1. Orientation results of 23-year old female

Positions	Trial 1	Trial 2	Trial 3	Ideal Position
Roll	2.781±1.170	2.828±1.170	0.743±1.170	0.815±1.170
Pitch	1.757±1.702	-0.509±1.702	-2.407±1.702	-0.446±1.702
Yaw	1.212±2.205	1.934±2.205	-2.378±2.205	-2.031±2.205

DISCUSSION

The results were satisfactory, but did not meet initial expectations. The orientation sensor was able to differentiate a correct position versus an incorrect position. However, variance in the resolution of the sensor most likely occurred due to a mismatch of the input excitation voltage in the power surge which was 12 volts and the sensor's threshold voltage which was 3.3 volts. Using a wired accelerometer and not a Bluetooth accelerometer should also be noted as a limiting factor. Further work must be done to enhance the signal output or sensitivity of the sensor. In order to optimize the device for more accurate data, a few modifications should be noted. One consideration is to add a battery pack, to reduce input voltage into the sensor. It would also be useful to combine the accelerometer with a gyroscope, to record the data in real time. This would allow the player to look at a frame-by-frame analysis of their own position. It would also be suitable if an Android or IOS application could be paired with the device providing the player with a much more user friendly way to read their own data. The app could also have features that would model the progress of the user with respect to their practice time. The accelerometer data would transfer to the mobile app, which would then show in an easy to ready format, if the player was in the correct position or not. Finally, outer shell could be placed around the sensor, giving it a better tolerance from environmental variables.

CONCLUSIONS

An orientation sensor was evaluated in order to better aid North American Football players on how to get into proper tackling positions. Based on the results, this device has the potential to help young football players get into a correct football position reducing temporary or severe

injuries to themselves and others.

REFERENCES

[1] "The American Academy of Pediatrics Tackles Youth Football Injuries." The American Academy of Pediatrics Tackles Youth Football Injuries. American Academy of Pediatrics, 25 Oct. 2015. Web. 27 Apr. 2016.

[2] "Tackling in Youth Football." Pediatrics 136.5 (2015): n. pag. Web.

[3] "Registration Open for 2015 Nick Saban Football Camps." - *ROLLTIDE.COM*. University of Alabama, n.d. Web. 27 Apr. 2016.

[4] Barra, Allen. "America's Most Dangerous Football Is in the Pee-Wee Leagues, Not the NFL." The Atlantic. Atlantic Media Company, 31 Aug. 2013. Web. 27 Apr. 2016.

[5]Koenig, Keith personal communication

[6] Matlab, Raspberry pi support package, Software Package, Ver 2015b

[7]Napolitano, Marcello R. *Aircraft Dynamics: From Modeling to Simulation*. Hoboken, NJ: J. Wiley, 2012. Print.

[8] Rae, J. William "Flight dynamics of an American football in a forward pass," ***isea*** *Sports Engineering*, Vol. 6, 2003

BIOCOMPATIBILITY OF NOVEL COPPER-CONTAINING BIOCOMPOSITES IN QUANTIFIABLE MODEL CELL SYSTEM

Kahla St Marthe[1], Zach Norcross[1], Anik Karan[1], Neha Karekar[2], Mark A. DeCoster[1]

[1]Biomedical Engineering Department, Louisiana Tech University, Ruston LA, USA
[2]Molecular Science and Nanotechnology Department, Louisiana Tech University, Ruston, LA, USA

ABSTRACT

Biomaterials demonstrate great promise for use as tools in a wide range of biomedical applications. Specifically, the use of these materials for the treatment and study of nervous system disorders is becoming increasingly important as the diversity of synthesized materials increases. Biomaterial scaffolds can be used as bridges, cell carriers, and targeted drug delivery vehicles, for transporting regenerative and therapeutic agents to damaged neuronal circuits. Our lab has recently discovered a novel, copper-containing and amino acid (cystine)-based high aspect ratio structure material (CuHARS) with potential for drug delivery due its degradability and low agglomeration in physiological conditions. Here, we used a quantifiable model cell system to show that delivery of moderate levels of CuHARS has little effect on cell function. More specifically, we have shown that exposure of increasing concentrations of the CuHARS from 2 to 50µg/ml, results in a dose-dependent diminishing viability and capacity of PC12 cells to extend neurites in response to the biological cue i.e. nerve growth factor. We have also exposed astrocytes, primary neurons and microglia to this material to study cytotoxicity of the material with naturally occurring brain cells. Cell viability results using CuHARS material with our quantifiable system indicates that CuHARS are biocompatible, and this demonstrates their utility in neuronal experiments. For example, as an additive step in engineering CuHARS, due to the cystine content of our biocomposite, these novel materials could be functionalized with growth factors or antibodies for targeted delivery in the brain.

Keywords: biomaterials, CuHARS, biocomposite, biocompatible, biodegradable, toxicity, nervous system, PC12

INTRODUCTION

The advent of biomaterials has impacted many scientific areas and expanded functionalities across a variety of applications. Recently, the possibility of developing materials as interfaces between brain cells and devices as therapeutic or diagnostic tools has been explored and a number of advances have been made [1]. Development of therapeutic agents geared towards neuronal recovery and regeneration after damage due to injury or neurodegenerative diseases has been a major issue in neuroscience. As a result, biomaterial platforms are being developed to aid in the diagnosis and treatment of such issues. Many biomaterials used in applications such as drug delivery could require large amounts of the material to be administered to the cells or brain region of interest, therefore it is important that the cytotoxic effect of moderate to high concentrations of these materials is investigated [2].

Our lab has recently developed a high-aspect ratio structure (CuHARS) copper containing biocomposite which is synthesized in an aqueous solution, and scales from the nano to the micro in size as confirmed using electron microscopy. The CuHARS biocomposites contain copper, and cystine as the organic component [3]. These materials, once generated, are stable without agglomeration, for months to years under refrigeration when remaining in water. The discovery of this material has opened up the possibility of creating functionalized biomaterials with growth factors (for neuronal recovery and regeneration) or antibodies for targeted delivery in the brain. Interactions between the CuHARS and different cell types have been studied and as a result, we are interested in evaluating the biocompatibility of this material. In this study, we investigated the cytotoxic effects of the CuHARS material on PC12 cells as a model for neuronal development. One property of PC12 cells is their quantifiable, rapid and reversible response to nerve growth factor (NGF). On exposure to NGF, PC12 cells develop neurite-like extensions up to 1cm in length [4]. We examined and quantified the specific effects that our CuHARS biocomposite have on cultured PC12 cells and studied their ability to respond to the biological cue NGF as compared with control cells. The main objective of this study is to examine the cytotoxicological effects of our previously developed copper containing biocomposite (CuHARS) which is intended for use in neurological cell culture systems as drug delivery vehicles of a variety of drugs including NGF.

METHODS

Synthesis of CuHARS. CuHARS were synthesized using a modified version of the method previously described[5]. Briefly, L-cystine is weighed in an antistatic weighing boat and dissolved in 1M NaOH at 7.29mg cystine per 100µl NaOH. Immediately after dissolving with NaOH,

dilute with 21µl of the cystine salt into an 80cm2 flask containing 20.37ml RO H2O and mix thoroughly. Ensure that the flask is capped and place it into an oven at 37°C for 30 minutes then add 672µl of freshly prepared 2mg/ml cupric sulfate. Mix thoroughly then place the mixture back into the oven for 5 hours. After the 5 hours, immediately place the flask into a 4°C refrigerator for 7-10 days to ensure that the structures completely develop [6].

Cell Culture. PC12 rat pheochromocytoma cells (ATCC**)** were cultured in RPMI 1640 (Sigma) supplemented with 10% horse serum (HS), 5% fetal bovine serum (FBS) and 1% penicillin/streptomycin (Sigma). The cells were passaged when reaching 70-80% confluency and split 1/3 in tissue culture dishes. **Primary Neural Cell Culture**: Cortical brain cells were obtained by performing cervical disarticulation of Outbred Sprague-Dawley newborn rats (age ≤48hrs) in adherence to protocols approved by Louisiana Tech University's Ethics and Animal Care Committee as described previously [7].

Cell exposure to CuHARS. PC12 cells were plated at ~20,000 cells/well into 24 multi-well plates (cell culture treated, CellStar**)** at a volume of 500µl per well in RPMI 1640 (Sigma) supplemented with 10% horse serum (HS), 5% fetal bovine serum (FBS) and 1% penicillin/streptomycin in a humidified incubator. Primary astrocytes and neurons were plated from primary neural mixed cultures. These cells were then plated into a 48 multi-well plate (cell culture treated, CellStar) at a density of 20,000 and 100,000 cells per well respectively and maintained in a 37^0 C, 5% CO2 humidified incubator. CuHARS biocomposite were added into the media at concentrations ranging from 5 to 50 µg/ml. Simultaneously, NGF (100 ng/ml) was added into the PC12 media to induce the differentiation of PC12 cells.

MTT Assay. For MTT experiments, PC12 media was made with RPMI without phenol red. Briefly, the cells were incubated with varying CuHARS concentrations for 6, 12, 24 and 48 hours respectively, the media was aspirated and replaced with 3-(4, 5-dimethylthiazol-2-yl)-2,5-diphenyltetrazolium bromide (Sigma). One hundred µl MTT stock solution (5 mg/ml) was added to each well, followed by incubation for 1 h at 37 °C. 300 uL of each well was added to a 96 well plate for spectroscopy. Thermo Scientific Multiskan Spectrum plate reader analyzed the wells at a wavelength of 570 nm.employed in this study as the programming language of choice [6].

RESULTS AND DISCUSSION

MTT, a common method of evaluating the cytotoxic effect of biomaterials in cell culture was done. The MTT assay is used to investigate the metabolic activity of a cellular population. The metabolic activity is determined by the extent to which the mitochondrial succinatetetrazolium reductase system converts the yellow dye (MTT) to a purple-colored formazan. The color density formed indicates the metabolic activity of the population and is used to assess the cytotoxic effects of any material. In our studies, we used this method to evaluate the potential adverse effects of the biocomposite material in PC12 cells since it contains copper. The assay was done after exposure for 6, 12, 24 and 48 hours. Exposure to increasing concentrations of CuHARS biocomposite resulted in a dose-dependent diminishing viability of PC12 cells using MTT method. At very low to moderate concentrations, cell viability was not significantly affected, however at a concentration of 50µg/ml cell viability significantly decreased. Essentially, the metabolic activity of PC12 cells decreased in a concentration dependent manner (Figure 1). At high concentrations, excess copper can induce apoptosis in PC12 cells [8]. This may account for the increased mitochondrial toxicity of the CuHARS material at a concentration of 50µg/ml.1(c).

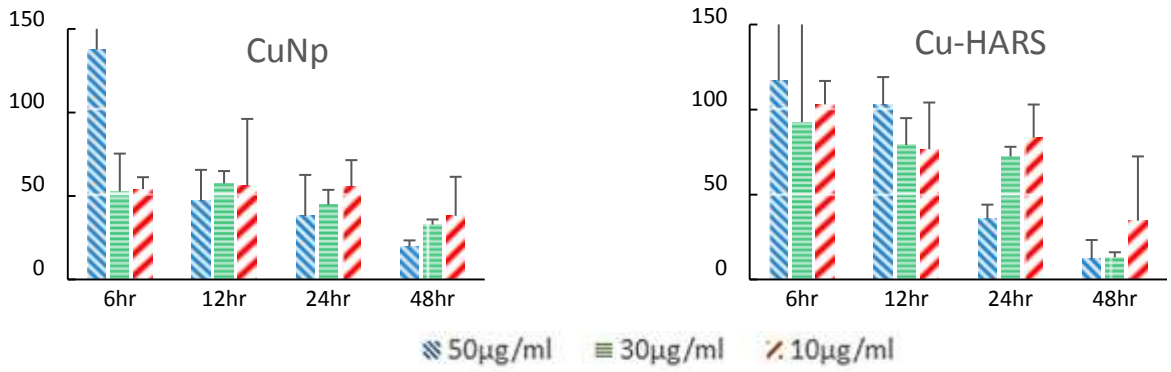

Figure1. Effect of varying CuHARS concentration on mitochondrial toxicity of PC12 cells A) Copper Nanoparticle (CuNP) treatment. B) CuHARS treatment. Y: Axis values=Relative Absorbance normalized to the controls (no treatment).

The most obvious effect that exposure to the CuHARS has upon the cells is their ability to generate neurites. The average number of neurites that sprouted from each [remaining] live cell was measured at each of the four concentrations and compared with media only control (Fig. 2 A). The data from these evaluations, plotted in Fig. 2A, shows the effect of CuHARS on the generation of neurites. Of the live cells evaluated, those exposed to 5, 10, 25 and 50µg/ml CuHARS concentrations on average produced 2.42, 1.72, 1.43, 0.72 neurites per cell (n= 30 cells/condition), respectively, as compared with 2.79 in the control cells. An inverse correlation between the level of CuHARS exposure and the ability of the cells to respond normally to NGF and extend neurites into the periphery is seen. Fig. 2B shows the typical PC12 cell line in culture; Fig. 2(C) shows NGF-stimulated PC12 cells in culture with arrows showing the location of its neurites and Fig. 2(D) shows NGF-stimulated cells in culture with 2.5µg/ml CuHARS.

These findings confirm previous reports that the presence of intracellular copper containing nanoparticle constructs can result in significant changes in cell behavior and viability [8]. In future experiments, we plan to use copper chelators to decrease the toxicity of the copper released from the CuHARS material. Current research indicates that copper deficiency plays a crucial role in many neurological disorders [8]. Treatment of these diseases may include the need for copper to supplement therapy. CuHARS promise to be a biocompatible organic copper particle that is capable of drug targeting. To evaluate the mechanism of cell death in PC12 cells induced by high CuHARS concentrations, two important enzymes will be measured. Lactate dehydrogenase (LDH) release measures the membrane damage, a hallmark of necrosis, while caspase activation is an indicator of apoptosis.

Figure 2.A): Effect of CuHARS exposure on neurite outgrowth of NGF induced PC12 cells at different CuHARS concentrations. (B+C+D) Phase contrast images of PC12 cells 4DIV (B) without NGF (Scale bar =100µm) (C) with 100ng/ml NGF/+NGF (Scale bar =100µm) (D) after adding 2.5µg/ml CuHARS at 6DIV (+NGF, Scale bars =35.0µm)

CONCLUSIONS

To evaluate the particle-induced neurotoxicity effect of our novel CuHARS material, we used PC12 and primary neural cells. Our studies demonstrate that CuHARS can elicit concentration and time dependent cytotoxicity in PC12 cells. The findings suggest that exposure of cells to CuHARS has lower mitochondrial toxicity than other copper containing materials such as CuNP [8]. Given their relatively lower toxicity, we project that the CuHARS material will be a key biomaterial for treating neurodegenerative diseases by acting as the vehicles of drug and growth factors delivery to neuronal cells. This work has also shown

that exposure to increasing concentrations of CuHARS results in a dose- dependent diminishing ability of PC12 cells to differentiate in response to nerve growth factor. The results of our model system may act as a caveat for the use of CuHARS in neuronal experimental. These results further imply that a need for more research on the effects of cellular CuHARS internalization is both warranted and necessary. Failure to fully evaluate biomaterials on a case-by-case basis may lead to lack of parameter control in *in-vitro* application.

ACKNOWLEDGMENTS

This material is based upon work supported by the National Science Foundation under Grants #1547693 and #1632891. Any opinions, findings, and conclusions or recommendations expressed in this material are those of the authors and do not necessarily reflect the views of the National Science Foundation.

REFERENCES

1. P. Fattahi, G. Yang, G. Kim, and M. R. Abidian, "A review of organic and inorganic Biomaterials for neural interfaces,"*Adv Mater*, vol. 26, no. 12, 2014.
2. T. R. Pisanic, J. D. Blackwell, V. I. Shubayev, R. R. Fiñones, and S. Jin, "Nanotoxicity of iron oxide nanoparticle internalization in growing neurons," *Biomaterials*, vol. 28, no. 16, pp. 2572–2581, 2007.
3. Deodhar, Sneha, et al. "High-Aspect Ratio Bio-Metallic Nanocomposites for Cellular Interactions." IOP Conference Series: Materials Science and Engineering 64.1 2014.
4. [Tischler AS, Greene LA. Nerve growth factor-induced process formation by cultured rat pheochromocytoma cells. *Nature*, 258(5533):341-2., 1975
5. Kelly K, Wasserman J, Deodhar S, Huckaby J, DeCoster MA. " Generation of Scalable, Metallic HighAspect Ratio Nanocomposites in a Biological Liquid Medium." *J. Vis.* Exp (101) , e52901, doi: 1. 3791/52901., 2015
6. [Milam D, Deodhar S, DeCoster MA. "Synthesis and Post synthesis Optimization of Novel Copper Biocomposites and Exploration of Potential Applications." *Biomedical Engineering Conference(SBEC).*2016
7. Daniel B, DeCoster M.A. "Quantification of sPLA2 induced early and late apoptosis changes in neuronal cell cultures using combined Tunel and DAPI staining. "Brain Res Protoc, 13:144:50, 2004.
8. P. Xu, J. Xu, S. Liu, G. Ren, and Z. Yang, "In vitro toxicity of nanosized copper particles in PC12 cells induced by oxidative stress," *Journal of Nanoparticle Research*, vol. 14, no. 6., 2012.

IN VIVO EVALUATION OF THE EFFECT OF RESONANCE FREQUENCY ON DELIVERING INSULIN NON-INVASIVELY USING ULTRASOUND

Khaldon Lweesy*, Hadeel Najjar, Sarah Hajeer, and Sarah Attari

Biomedical Engineering Department, College of Engineering, Jordan University of Science and Technology, Irbid, Jordan

ABSTRACT

Single element ultrasound atomizing circular transducers with different resonance frequencies were studied for the purpose of non-invasively delivering insulin transdermally, in order to overcome the daily pain and the risk of contamination associated with injection. Frequencies ranging from 20 kHz to 2.1 MHz were tested for this purpose. Each transducer was housed with plexiglas material which included a reservoir to hold insulin during the experiments. For each transducer, twenty white rats (weight: 200–240g) were used and divided into four groups (two control and two exposure). The rats were anesthetized by intramuscular injection of 0.5 ml of a mixture of Kitamine and Xylazine after overnight fasting. Ultrasound was delivered in pulses for a duration of 20 minutes, and the blood glucose level was measured every 10 minutes through a period of one hour. The blood samples for the strips were taken from the tail (through the jugular vein). For each transducer, the skin was closely examined after ultrasound exposure for any signs of injury to notice the thermal effects if existed. For the control experiments, the same setup was followed up except that the power generator was turned off. Ultrasound transducers in the kHz range performed better that those in the MHz range; with the best performance achieved at a frequency of 40 kHz. A 40% reduction in Glucose level was achieved at 40 kHz while the reduction was only 5% at a frequency of 2.1 MHz.

Keywords: drug delivery, ultrasound, non-invasive, transdermal, insulin

INTRODUCTION

Diabetes mellitus disease is one of the most common diseases worldwide and is a source of a lot of complications for millions of patients. According to the American Diabetes Association, about 29.1 million Americans (9.3% of the population) had diabetes in 2012. The prevalence in seniors with diabetes is even higher where about 25.9% seniors (age 65 and older) had diabetes in the same year. Most diabetic patients take daily dosages of insulin as a treatment. The insulin is provided to the body through injection which causes pain to the patients and the used needles may cause contamination especially for older patients.

Conventional method for insulin delivery is injection. An attractive alternative method to injection is delivering insulin transdermally. However, the stratum corneum stands as a barrier that prevents the drug from penetrating through the skin. The use of ultrasound on the skin makes it more permeable and allows delivering many substances through it [1]. Previous studies used light-weight compact cymbal transducers to deliver insulin transdermally [2–7]. In these studies various *in vivo* and *ex vivo* animal experiments were performed and showed that the blood glucose level was decreased as a result of delivering insulin transdermally with the help of pulsed ultrasound energy. The resonance frequency that was investigated was fixed at 20 kHz [1, 8–10]. More resonance frequencies have to be investigated in order to find the optimal value for delivering insulin. In this study, transducers with resonance frequencies ranging from 20 kHz to 2.1 MHz were tested.

METHODS

A cubic box made of 3 mm thickness Plexiglas material was used as housing for each transducer (figure 1). The Plexiglas housing included a reservoir for insulin that comes in direct contact with the skin during the experiment. The animals used in this study were twenty white rats weighting (200 –240) g.

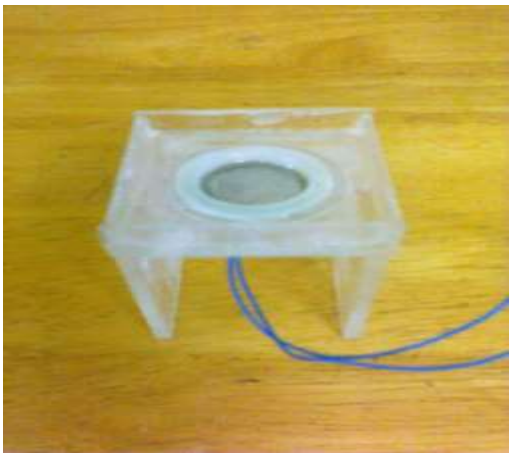

Figure 1: the housing of the transducer

The hair of the abdomen was clipped with an electric shaver. Any sign of skin disruption or rash was

unacceptable. The bare surface area was at least 4 × 4 cm^2. Before performing the experiment, each rat was anesthetized by intramuscular injection of 0.5 ml of a mixture of Ketamine and Xylazine after overnight fasting. Some rats in the ultrasound experiment needed a larger dose of anesthetizing agents because they resisted Ketamine in the second use. The bare area of the skin to be used was gently washed with warm water and dried naturally. Ultrasound was exposed to the skin by a piezoelectric oscillating element attached to the Plexiglas housing. Three milliliters of insulin and six milliliters of normal saline were filled inside the reservoir directly between the skin and the ultrasound transducer. A Function generator and a power amplifier were used to drive the ultrasound transducers. Ultrasound was delivered in pulses for durations of 20 minutes, and the blood glucose level was measured every 10 minutes through a period of 50 minutes. Then the drug and the ultrasound element were removed and the skin was closely examined after ultrasound exposure for any signs of injury for each element to notice the thermal effects if existed. Blood glucose level was measured by a Humasens glucometer. The blood samples for the strips were taken from the tail (through the jugular vein). For control experiments, the drug and ultrasound element were applied as described previously with the power generator turned off, and the blood glucose level was measured each 10 min for the duration of 50 minutes. Four fasted rats were injected with 0.1 U of insulin to compare the result between the injection and the ultrasound exposure. The amount of insulin which was injected to the rats was calculated depending on the weight of the rat.

RESULTS

The change in the blood glucose level as a result of the ultrasound delivery was recorded and compared with the control measurements for the three groups. Figures for the blood glucose level versus time were plotted for each frequency. The ultrasound exposure results were compared with the control results both exact values and normalized functions. Figures 2, 3, and 4, show plots for these comparisons for the resonance frequencies 40 kHz, 1.65 MHz, and 2.1 MHz, respectively.

Linear trend lines were drawn in each series to compare the results. The 40 kHz resonance frequency transducer was found to be the most effective one followed by the 1.65 MHz transducer. The 2.1 MHz transducer was found to be ineffective. Figure 5 shows a comparison of the three transducers.

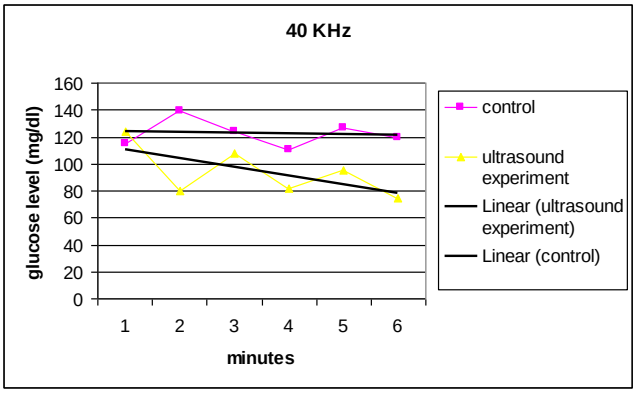

Figure 2: comparison for glucose level between control and 40 KHz ultrasound

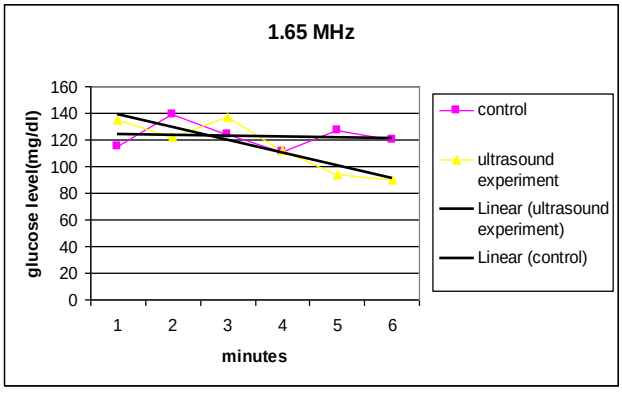

Figure 3: comparison for glucose level between control and 165 KHz ultrasound

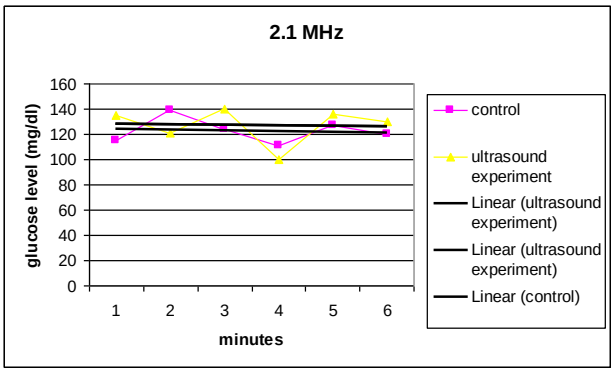

Figure 4: comparison for glucose level between control and 2.1 MHz ultrasound

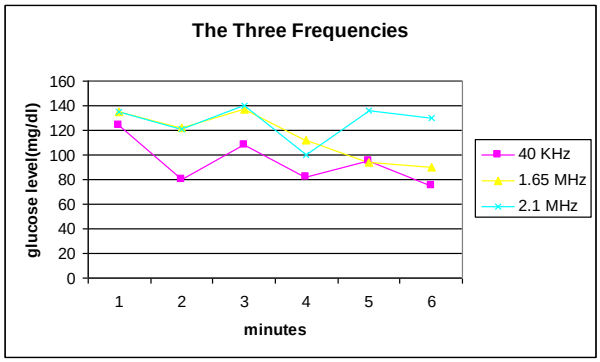

Figure 5: comparison for glucose level for three ultrasound frequencies

DISCUSSION

Diabetes is a disease that affects millions of people worldwide. It is one of the leading causes of death in both developed and developing countries. Currently the method of choice to deliver insulin to the body is using injection. The pain and the possible contamination that associate with injection make it of special need to find a painless and contamination-free method to deliver insulin to the body. Noninvasive insulin delivery using ultrasonic transducers has many advantages over the injection method; it saves the pain of repeating injection of needles especially for old people and kids and also it reduces the risk of viral infection that can be caused by contaminated needles. Many published research articles proved this concept; however most of the research done in this area focused on a single frequency (around 20 kHz) to perform this task. In this study, frequencies in the range 20 kHz to 2.1 MHz were investigated. Only three frequencies were completely tested: 40 kHz, 1.65 MHz, and 2.1 MHz. The 40 kHz transducer performed the best. The thermal effect that happens during the skin exposure of ultrasound is considered a drawback for using ultrasound in transdermal drug delivery. However, the 40 kHz frequency transducer, which was found to have the best performance, resulted in the lowest heating effect.

CONCLUSIONS

The results reported herein showed that using ultrasound waves for insulin delivery is effective. When comparing the glucose measurements for the ultrasound experiment with the control one in each group the decrease in glucose level was clear when using ultrasound transducers where for the control experiments the glucose measurements were random and did not always decrease.

When comparing the frequencies used, it was found that the transducer with 40 KHz frequency gave the best performance for delivering insulin transdermally. The 1.65 MHz transducer performed well, though it was outperformed by the 40 kHz transducer. The performance of the 2.1 MHz transducer was bad. It can be concluded that the frequency of ultrasound waves is an important factor in using ultrasound in transdermal insulin delivery. Lower frequencies (in the kHz range) are more effective in making the skin more permeable to insulin.

REFERENCES

[1] E. Maione, K.K. Shung, R.J. Meyer, J.W. Hughes, R.E. Newnham, N.B. Smith, “Transducer design for a portable ultrasound enhanced transdermal drug delivery system”. IEEE Trans. Ultrason. Ferroelectr. Freq. Contr., Vol. 49, No. 10, 2002, 1430–1436.

[2] E.J. Park, J Dodds, N.B. Smith, “Dose comparison of ultrasonic transdermal insulin delivery to subcutaneous insulin injection”. Int J Nanomedicine, Vol. 3, No. 3, 2008, 335-41.

[3] E.J. Park, J. Werner, N.B. Smith, “Ultrasound Mediated Transdermal Insulin Delivery in Pigs Using a Lightweight Transducer”. Pharmaceutical Research, Vol. 2, No. 7, 2007, 1396-401.

[4] N.B. Smith, S. Lee, K.K. Shung, “Ultrasoundmediated transdermal in vivo transport of insulin with low-profile cymbal arrays”. Ultrasound Med. Biol., Vol. 29, No. 8, 2003, 1205–1210.

[5] S. Lee, R.E. Newnham, N.B. Smith, “Short ultrasound exposure times for noninvasive insulin delivery in rats using the light weight cymbal array”. IEEE Trans. Ultrason. Ferroelectr. Freq. Contr., Vol. 51, No. 2, 2004, 176–180.

[6] Snyder, S. Lee, R.E. Newnham, N.B. Smith, “Ferroelectric transducer arrays for transdermal insulin delivery”. J. Mater. Sci., Vol. 41, No. 1, 2006, 211– 216.

[7] S. Lee, V. Nayak, J. Dodds, M. Pishko, N.B. Smith, "Glucose measurements with sensors and ultrasound". Ultrasound Med. Biol., Vol. 31, No. 7, 2005, 971–977.

[8] R.E. Newnham, Q.C. Xu, S. Yoshikawa, "Transformed stress direction acoustic transducer". US Patent 4,999,819, 1991.

[9] R.E. Newnham, Q.C. Xu, S. Yoshikawa, "Metalelectroactive ceramic composite actuators". US Patent 5,276,657, 1994.

[10] R.J. Meyer, A. Dogan, C. Yoon, S.M. Pilgrim, R.E. Newnham, "Displacement amplification of electroactive materials using the cymbal flextensional transducer". Sens. Actuators, Vol. 87, No. 3, 2001, 157–162.

THE INFLUENCE OF PHYSICAL ACTIVITY AND FRUIT AND VEGETABLE CONSUMPTION ON ADULT OBESITY

Shelia Baity and Elgenaid Hamadain
University of Mississippi Medical Center, Jackson, MS, USA

ABSTRACT

Obesity is an epidemic that leads to severe chronic health complications and is preventable by physical activity and consumption of fruits and vegetables. The objective of this study was to compare behavioral risk factors associated with adult obesity among six selected states according to the most recent Gallup-Health survey were at the range of leanest to most obese states to explain the differences in obesity levels among six states of which Colorado and Hawaii was considered the leanest; Maine and Georgia as an average state; and Louisiana and Mississippi the most obese state. Data was collected from the Behavioral Risk Factor Surveillance System (BRFSS). We hypothesized that multiple factors including daily physical activity, life style, healthy food consumption, education, and household income may have impact on individual's obesity status and wellbeing. The results confirmed that there was a significant difference among the six states with respect to prevalence of obesity ($p < 0.05$). Results also indicates a significant difference in weekly physical activity among the six selected states ($p < 0.05$). There was a direct association between an increase rates of physical activity and reduction of the prevalence of obesity. Fruit and vegetable consumption was also significant ($p < 0.05$). Results indicate that as people consume five or more servings per day significantly impacted obesity rates. In addition, there was a significant difference among the income groups ($p < 0.05$). As mean household income went up, prevalence of obesity went down. Results on children Grade 9-12 demonstrated a fair positive and significant correlation ($r = 0.669$, $p < 0.05$) between watching TV three hours or more and the prevalence of obesity. Obesity tends to worsen from children to adults if intervention is not provided. No significant difference between males and females was observed for all the six states. Differences between the six selected states were significant ($p < 0.05$) for education level. Overall, as the education level rose, the prevalence of obesity declined, therefore, suggesting that individuals with higher education may make a better choice in their life style and may have impact on the overall health outcome including obesity status. In conclusion, physical activity and consumption of healthy food have vital impact on the prevalence of obesity. An increase in physical activity and consumption of fresh fruits and vegetables may help to battle obesity and eliminating the consequences of being obese.

Keywords: Obesity, Physical Activity, BMI, Fruit, Vegetables, Environment

INTRODUCTION

Obesity is a chronic condition caused by multiple factors including genetic, environmental and behavioral/social. The later includes dietary patterns, physical activity, and inactivity. Obesity is defined based on Body Mass index (BMI), a measurement of weight as compared to height. It has become a public concern in the United States due to the link between obesity and major common diseases such as cardiovascular disease (CVD), diabetes, and cancers. The obesity epidemic continues to rise nationally especially in the state of Mississippi. Over the past decade or so, the obesity rates for adults have been gradually increased. The statistical survey have shown that approximately 68% of adults were overweight or obese, and 34% were obese in 2007-2008 (1). Obesity arises from an imbalance of energy input, energy consumption, and energy output (2). The environment factors include an excessive food intake lack of physical activities and social habits promotes unfit life style leading to the obesity disorder (3). The influence of physical activity and consumption of healthy food including fruit and vegetable on obesity has been studied with various findings. As stated by Wang et al. (4), the total cost of health care is attributed to obesity. The prevalence of overweight has been projected to double every decade and that may account for 16-18% of the total US health care expenditure by 2030. According to Wang et al. (5), the continued rise in obesity projects 65 million more obese adults in the USA by 2030, causing an additional 6-8.5 million cases of diabetes and 5.7-7.3 million cases of CVD. Thus, the aim of this study was to compare behavioral risk factors including dietary patterns, physical activity and inactivity associated with obesity among the population in the leanest vs. the states with average status and the most obese states to investigate the differences associated with obesity.

METHODS

The purpose of this investigation was to compare the prevalence of adult obesity in six states (Colorado, Hawaii, Maine, Georgia, Louisiana, and Mississippi) as affected by physical activity, trends in fruit/ vegetable consumption, and social economic status (education level, household income, gender). The study utilized data

collected through the CDC's Behavioral Risk Factor Surveillance System (BRFSS) (6). The BRFSS was established in 1984 by the CDC and is a national annual telephone survey overseen by the CDC but conducted monthly by each state, the District of Columbia, Puerto Rico, the U.S. Virgin Islands, and Guam. More than 350,000 adults are interviewed each year, making the BRFSS the largest telephone health survey in the world. States use BRFSS data to identify emerging health problems, establish and track health objectives, and develop and evaluate public health policies and programs. Many states also use BRFSS data to support health-related legislative efforts. Data was collected from the BRFSS site included the following variables: Body Mass Index (BMI), percent obesity, fruits and vegetable consumption, physical activity, gender, education level, and median household income for all six selected states for the years of 1996-2012. Data was transferred to SPSS software for statistical analysis. Statistical techniques used to analyze the data include: descriptive statistics (means ± standard error), frequency distribution tables and one-way analysis of variance. The multiple comparison test Tukey was used for means seperation. Graphical representation of the results was displayed using Excel software. All tests of significance were reported and discussed at the 5 % level of significance ($\alpha = 0.05$).

RESULTS

Results indicate that there was a statistically significant difference among the six selected states ($P < 0.05$) with respect to percent mean obesity (Table 1). The lowest percent mean obese value was for Colorado (15.94 %), while Mississippi had the largest mean value (27.5%) followed by Louisiana (26.5%), though the difference between Mississippi and Louisiana was not significant.

Table 1. Percent Mean Obese Values ± SE for the Six Selected States 1995-2011

STATE	%MEAN OBESE ± SE	95% CI	*GROUPINGS
COLORADO	15.94 ±1.0491	13.457-18.418	A
HAWAII	17.74 ±1.2024	14.894-20.581	AB
MAINE	21.05 ±1.2602	18.070-24.030	BC
GEORGIA	22.98 ±1.9859	18.279-26.710	CD
LOUISIANNA	26.53 ±1.7184	22.465-30.588	CD
MISSISSIPPI	27.50 ±10.8776	23.060-31.940	D

*****Means followed by same letter groupings are not significantly different with the respect to the percent mean obese values according to Tukey Multiple Comparison Test.

Figure 1 displays the amount of exercise done by the participants monthly for each state broken down by year (1996-2012). Results indicated that as the physical activity increaed the rate of obesity decreased (e.g, Colorado had the highest percent participation in physical activity per month (81.3 %), while they had the lowest obesity rates (15.9%). As predicted, the states with the highest rate, of obesity (Louisiana and Mississippi) have the least percent participatin in exercise (66 %). Hence, as the amount of exercise or physical activity increased the percent obesity in the selected six states decreased.

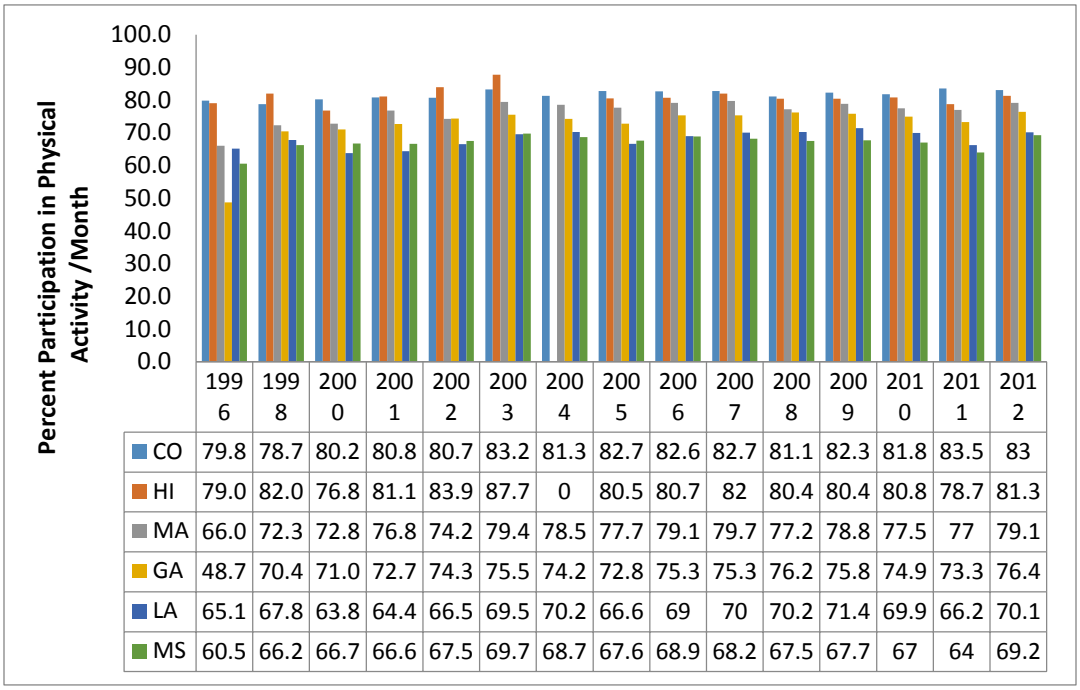

	1996	1998	2000	2001	2002	2003	2004	2005	2006	2007	2008	2009	2010	2011	2012
CO	79.8	78.7	80.2	80.8	80.7	83.2	81.3	82.7	82.6	82.7	81.1	82.3	81.8	83.5	83
HI	79.0	82.0	76.8	81.1	83.9	87.7	0	80.5	80.7	82	80.4	80.4	80.8	78.7	81.3
MA	66.0	72.3	72.8	76.8	74.2	79.4	78.5	77.7	79.1	79.7	77.2	78.8	77.5	77	79.1
GA	48.7	70.4	71.0	72.7	74.3	75.5	74.2	72.8	75.3	75.3	76.2	75.8	74.9	73.3	76.4
LA	65.1	67.8	63.8	64.4	66.5	69.5	70.2	66.6	69	70	70.2	71.4	69.9	66.2	70.1
MS	60.5	66.2	66.7	66.6	67.5	69.7	68.7	67.6	68.9	68.2	67.5	67.7	67	64	69.2

Fig 1. Percent of People Who Participated in Physical Activity/Month Broken by Year (1996-2012)

There was a significant difference (Table 2) among the selected six states with respect to mean exercise per month ($p < 0.05$). Colorado was significanly higher in the percent exercised per month in comparison to Georgia, Louisiana, and Mississippi. There was no significant difference between Colorado and Hawaii, which was the second leanest state after Colorado and Maine which. Figure 2 demonstrates that physical activity has a significant impact on percent obesity. Exercise will help in the decrease of obesity when done on a regular consistent basis.

As shown in Figure 2, the decrease in physical activity was associated with increased percentage obesity. The leanest and middle states had the highest percentage of individuals with physical activity and the lowest percentage of obesity.

Table 2. Percent Physical Activity/ Month in the Six Selected States

STATE	% MEAN EXERCISE / MONTH ± SE	95% CI	*GROUPINGS
COLORADO	81.29 ±.5841	79.906-82.669	A
HAWAII	80.79/ ±.7652	78.978-82.597	A
MAINE	75.11 ±1.6736	71.155-79.070	AB
GEORGIA	70.48/ ±3.1942	62.922-78.028	BC
LOUISIANNA	67.59 ±.9137	65.427-69.748	C
MISSISSIPPI	66.76 ±.9669	64.476-69.049	C

* Means followed by the same letter groupings are not significanlty different with respect to mean percent exercise in the past month values according to Tukey Multiple Comparison Test.

Figure 2. Mean Percent Obese Vs. Mean Percent Physical Activity per Month

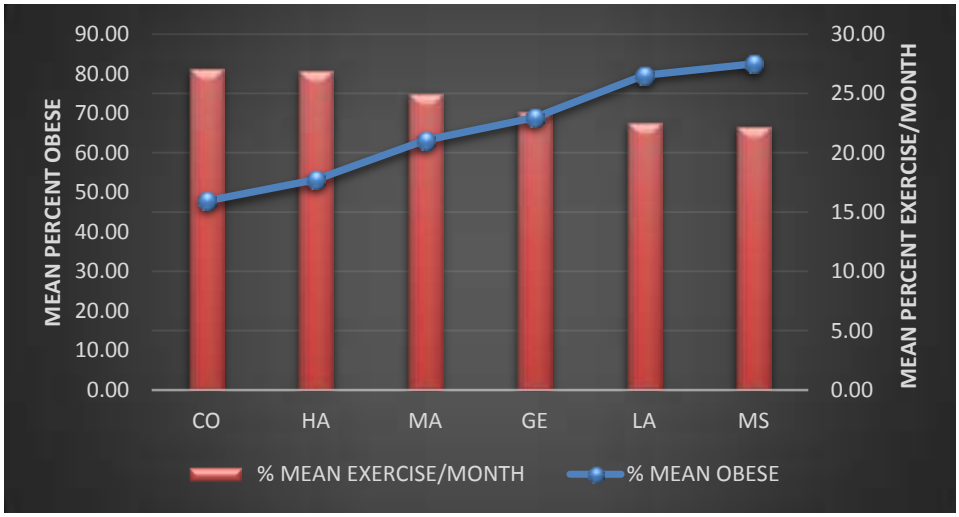

Table 3 represents percent mean fruit and vegetable consumption (> five serving per day) averaged over the study years. ANOVA results indicate a significant difference among the six selected states ($p < 0.05$). It is evident that the consumption of fruits and vegetables has impacted the obesity rates and prevalence. For example, Mississippi has the highest obesity prevalence, but shows the least amount of fruits and vegetable consumption, although it was not significantly different from Louisiana. In comparison, Main has the highest value of fruit and vegetable consumption; however, the difference was not significant from either Hawaii or Colorado. Also, there was a fluctuation in Mississippi in the consumption of fruits and vegetables from 1996 to 2009 (Figure 3).

Table 3. Percent Mean Fruit & Vegetable Consumption (> Five Serving per Day) For Six Selected States

STATE	MEAN PERENT CONSUMPTION ± SE	95% CI	*GROUPINGS
MAINE	27.35 ± 0.575	25.992-28.708	A
HAWAII	24.96 ± 1.010	22.574-27.351	AB
COLORADO	24.85 ± 0.3684	23.979-25.721	AB
GEORGIA	23.00 ± 0.469	21.891-24.109	B
LOUISIANNA	17.68 ± 0.539	16.399-18.951	C
MISSISSIPPI	17.63 ± 0.428	16.614-18.636	C

*Means followed by the same letter grouping are not significantly different with respect to percent fruits and vegetables consumption according to Tukey Multiple Comparison Test.

.

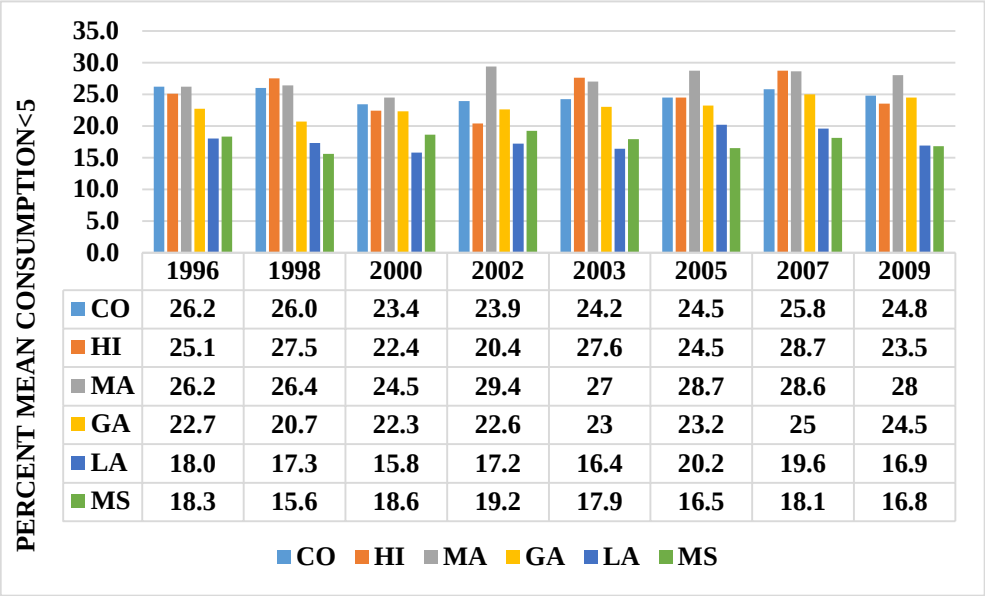

	1996	1998	2000	2002	2003	2005	2007	2009
CO	26.2	26.0	23.4	23.9	24.2	24.5	25.8	24.8
HI	25.1	27.5	22.4	20.4	27.6	24.5	28.7	23.5
MA	26.2	26.4	24.5	29.4	27	28.7	28.6	28
GA	22.7	20.7	22.3	22.6	23	23.2	25	24.5
LA	18.0	17.3	15.8	17.2	16.4	20.2	19.6	16.9
MS	18.3	15.6	18.6	19.2	17.9	16.5	18.1	16.8

Figure 3. Fruits/Vegetable Consumption ≥ Five Servings Per Day

It is apparent that adequate amounst of fruit and vegetable consumtion impacts obesity rates in these six selected states. Consumption of fruits and vegetables is influenced by a variety of interacting, environmental and individual decisions. It was thought the distance to a grocery store could be a factor in the consumption of fruits and vegetables. However, it was found that distance to the nearest grocery was not significant in intake of fruits and vegetables(8). Figure 4 demonstrates the impact of fruit and vegetable consumption in association with the level of obesity reduction. As indicated earlier, as fruit and vegetable consumption goes up the percent obesity in the state goes down. Mississippi and Louisiana had the least consumption of fruits and vegetables and the highest percent of mean obesity as compared to the other selected states.

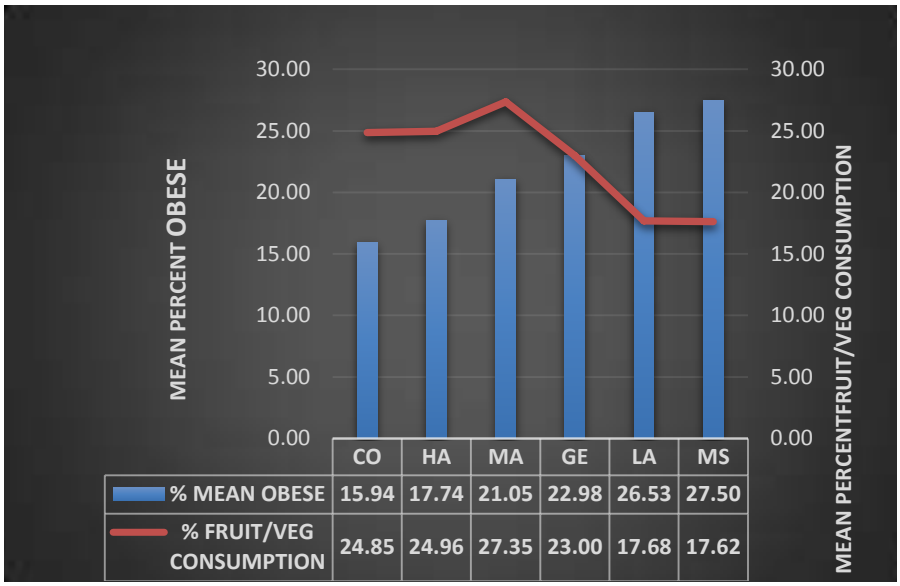

	CO	HA	MA	GE	LA	MS
% MEAN OBESE	15.94	17.74	21.05	22.98	26.53	27.50
% FRUIT/VEG CONSUMPTION	24.85	24.96	27.35	23.00	17.68	17.62

Figure 4. Mean Percent Obese Vs. Means Percent Fruit/Vegetable Consumption

DISCUSSION

Six states were selected based on the lowest to the highest levels of leanest/obesity to explore the impact of physical activity, vegetable and fruit consumption, household income, gender, and education on the level of obesity. Physical inactivity has become a global pandemic which requires global action (7). This is one of the contributing factors in the development of obesity which has been outshined by the excess availability of high technology devices that require sometimes a minimal physical activities like running, walking, playing outside sports, bike riding or swimming, which requires energy consumption and weight loss. A weekly physical activity is needed to maintain a healthy weight and to fight off diseases by improving the immune system functions. This was apparent from our results that a greater percentage of population in the state of Mississippi were presented with a least physical activity and the highest obesity rates as compared with Colorado or other states under the study. Fruit and Vegetable consumption was an important variable that is needed to help maintain a healthy weight and help the body to guard against diseases. Within the six selected states, it was confirmed that consumption of fruits and vegetable had clear impact on the prevalence of obesity. Mississippi having the highest obesity rate had the least amount of fruit and vegetable consumption. There was a fluctuation in Mississippi from 1996 to 2009 in the consumption of fruits and vegetables. Factors that could cause this fluctuations is at least 4 folds: the availability of fruits and vegetables in the markets; the pricing that may affect the ability of the consumers to pay, the consumers taste for fruit and vegetable (decision making) and access to grocery stores and the distance the consumer has to travel (8). The data showed as the education level rises the prevalence of obesity levels decline in all the six selected states. Obesity rates did not differ significantly between males and females, and that was consistent for all the six selected states. More efforts is needed to inspire people to become more active in their daily life. In addition, there should be facilitators to encourage regular consumption of healthy food such as fruits and vegetables and make them accessible and affordable to people.

CONCLUSIONS

Overall, physical activity and consumption of healthy food such as fruits and vegetables are important factors in an individual's daily life and may contributes in part to a healthy life and minimize adult obesity. More governmental programs are needed to teach young parents the need to prevent obesity in their children, which impacts the prevalence of obesity later in adult life. Factors that facilitate physical activity and consumption of fruit and vegetables are essential in dealing with obesity.

ACKNOWLEDGEMENTS

The authors would like to acknowledge the SBEC for the invitation to publsih this research. The authors appreciate the reviewers' critical comments and extensive revisions.

REFERENCES

(1) Mitchell,N., Catenacci, V., Wyatt, H.R., Hill, J.O. 2013. Obesity: overview of an epidemic. Psychiatr Clin North Am, 2011, 34(4):717-732.

(2) Prentice, A.M., Jebb, S.A. 1995. Obesity in Britain: Gluttony or sloth? British Medical Journal.12 (311), 437-439.

(3) Hill, James. O; Peters, John C. 1998. Environmental Contributions to the Obesity Epidemic. *Science*, New Series. 280: 1371-1374

(4) Wang Y, Beydoun MA, Liang L, Caballero B, Kumanyika SK. Will all Americans become overweight or obese? Estimating the progression and cost of the US obesity epidemic. Obesity (Silver Spring) 2008; 16: 2323-2330.

(5) Wang CY, McPherson K, Marsh T, Gortmaker S, Brown M, (2011) Health and economic burden of the projected obesity trends in the USA and the UK. Lancet; 378:815- 25

(6) BRFSS Centers for Disease Control and Prevention (CDC). *Behavioral Risk Factor Surveillance System Survey Data*. Atlanta, Georgia: U.S. Department of Health and Human Services, Centers for Disease Control and Prevention, 2009

(7) KohlHW 3rd Craig CL, Lambert EV,et al, The pandemic of physical activity: global action for public health. Lancet 2012;380:294-305

(8) Gase ln., DeFosset AR., Smith LV., Kuo T. (2014). The association between self-reported grocery store access. Fruits and vegetable intake, sugar-sweetened beverage consumption, and obesity in a racially diverse low-income population Frontiers in Public Health V.2 229, 1-7.

COLORECTAL CANCER SURVIVAL IN THE DELTA AND NON-DELTA REGIONS OF MISSISSIPPI

Deirdre B. Rogers, Ellen S. Jones, Elgenaid I. Hamadain, and Jessica Bailey
School of Health Related Professions, University of Mississippi Medical Center
Jackson, MS, USA

ABSTRACT

Introduction: Colorectal cancer is the second most common cancer in Mississippi affecting both males and females. Mississippi ranks second in the country for incidence and mortality from colorectal cancer based on 2013 data. Geographic region or neighborhood can have an impact on survival. To date, there have been no studies comparing the colorectal cancer survival between the Delta and non-Delta regions of Mississippi. **Methods:** A retrospective cohort research design was used to study data collected by the Mississippi Cancer Registry. The data set included colorectal cancer cases diagnosed between 2003 and 2011 with passive follow-up through 2011. Relative survival was analyzed by Delta and non-Delta region for Mississippi with stage and race included in the survival model. **Results:** The non-Delta region was significantly more likely to be diagnosed with advanced stage disease than the Delta region, 61.2% and 58.2%, respectively. The non-Delta region (63.53%) had significantly higher survival compared to the Delta region (59.55%). Whites in the non-Delta region (65.14%) had significantly higher survival than blacks (60.0%). Also, whites in the Delta region (62.10%) had significantly higher survival than blacks (56.73%). Adding stage to the model did not eliminate the difference in survival between regions nor between races in each region. **Discussion**: The data suggests a relationship exists between race, stage, and region with regard to colorectal cancer survival. Race and stage do impact survival, but are not the only reason for the survival differences between the Delta and non-Delta regions. Stage and region do not completely account for the survival differences between the races. The relationship of other factors such as treatment should also be considered.

Keywords: colorectal, Delta, Mississippi, region, survival

INTRODUCTION

Colorectal cancer is the second most common cancer in Mississippi affecting both males and females accounting for 1,649 new invasive cases and 615 deaths in 2013 [1]. Mississippi ranks second in the country for incidence and mortality from colorectal cancer based on 2013 data [2]. In Mississippi, mortality rates in whites have declined since 1975, but the mortality rates for blacks have been stable since 1991 [3].

Prior studies addressing colorectal cancer survival covered only limited sections of the United States, predominantly those funded by the National Cancer Institute's (NCI) Surveillance, Epidemiology, and End Results (SEER) program. Registries in the SEER program are not similar to Mississippi in race/ethnicity, with fewer blacks and more "other" race [4]. Understanding the influence of geography on survival in Mississippi and the relationships of age and socioeconomic status (SES) will inform treatment, education and screening programs statewide.

Geographic region or neighborhood can have an impact on survival [5, 6]. Distance and location of medical services are examples of ways that geography can impact disease outcomes [5]. The Mississippi Delta has no American College of Surgeons Commission on Cancer approved hospitals. Finally, SES is strongly associated with health [7]. Low SES groups and disadvantaged minorities are less likely to reduce behaviors that are detrimental to health such as smoking, poor dietary habits, and alcohol abuse and are less likely to begin healthier behaviors such as exercise [7]. Additionally, residential segregation in the United States is such that blacks live in poorer conditions than whites in similar SES groups [7]. These neighborhood conditions can limit access to safe places to exercise and access to nutritious foods in local grocery stores and increase exposure to marketing of alcohol and tobacco products [7]. Residential segregation can also limit access to quality education, jobs, and medical care [7].

Chien et al. [8] sought to determine if the pattern of colorectal cancer in space varies according to stage of disease at diagnosis using 9,038 cases of colorectal cancer diagnosed between 1992-2005 collected from the SEER-Medicare linked data sets for Atlanta, GA and Detroit, MI. For colon cancer in both Atlanta and Detroit, increased risk of death was associated with black race, increasing age, having received chemotherapy. In addition in Detroit, increased risk of death was associated with greater number of comorbidities and disease history. Differences did

exist in survival by stage across the census tracts in both Atlanta and Detroit. Stressors associated with place may amplify the effect of stage due to oxidative stress and increased inflammation. These could be related to location due to people not participating in healthy behaviors and having high body mass indices [8].

Fitzgerald et al. [6] studied a sample of 176,011 colorectal cancers aged 40 or older diagnosed between 1992 and 2002 from the NCI SEER Cancer Program. The county of residence at diagnosis for each case was classified as metropolitan, urban, or rural. The study found that a survival advantage was experienced by those living in metropolitan counties with < 1 million people when compared to rural counties and larger metropolitan counties. This may be the result of access to care, social or economic barriers and healthcare delivery. African American race and lower SES were also associated with a survival disadvantage with African American race being the biggest driver of the disparity in outcome [6].

METHODS

The aim of this study was to analyze the relative survival in patients diagnosed with colorectal cancer in Mississippi to determine: 1. the survival difference between the Delta and non-Delta regions of the state and 2. if region impacted the disparity in relative survival between blacks and whites. A retrospective cohort research design was used to study data collected by the Mississippi Cancer Registry. The data set included colorectal cancer cases diagnosed between 2003 and 2011 with passive follow-up through 2011. Only the first primary colorectal cancer for each individual was used in the analysis. Life tables were obtained from the CONCORD-2 Working Group from the London School of Hygiene and Tropical Medicine [9].

The study population included black or white adults ages 18-99. Cases obtained solely from other state cancer registries and from the Veterans Administration and military hospitals, as well as, cases identified by autopsy and by death certificate were excluded from the data. Delta counties included the 18 counties of Bolivar, Carroll, Coahoma, DeSoto, Holmes, Humphreys, Issaquena, Leflore, Panola, Quitman, Sharkey, Sunflower, Tallahatchie, Tate, Tunica, Warren, Washington, and Yazoo. The other 64 Mississippi counties were designated as the non-Delta.

Relative survival was calculated for Delta/non-Delta regions for both whites and blacks using the strel2 command in Stata 14 using a complete approach. The strel2 command is based on the maximum likelihood estimation of net survival and excess survival proposed by Estève and colleagues in 1990 [10]. The complete approach was chosen over the preferred cohort approach to relative survival because there would be too little data for the analysis if only the 2003 through 2006 data was used for the cohort approach. Calculation of excess hazards and net survival in the proposed research for analysis of Delta/non-Delta regions. Additionally, a separate analysis was conducted including stage of disease. The same analysis was also conducted with the addition of race to the model. Finally, analysis was done using both race and stage in the model. Excess hazards were compared using the 95% confidence intervals. Overlapping confidence intervals indicated no significant difference in hazards.

RESULTS

Table 1 provides the descriptive statistics for the study. The table includes the patient case counts, the row percentages, the column percentages, and the p-values for the χ^2 tests of significance. Blacks (27.2%) were significantly more likely to live in the Delta region than whites (15.1%). The Delta region (41.8%) had higher percentages of local stage (localized) disease than the non-Delta region (38.8%) while the non-Delta region (61.2%) had a higher percentage of advanced stage disease than the Delta region (58.2%). Blacks in the Delta region (43.2%) had a higher proportion of local stage disease than those living in the non-Delta Region (36.7%). In contrast, blacks in the non-Delta region (63.3%) had the higher proportion of advanced stage compared to those in the Delta (56.8%).

Table 2 provides the five-year relative survival estimates. The non-Delta region (63.53%) showed a significantly higher five-year relative survival rate from colorectal cancer than the Delta region (59.55%). This survival difference could be seen within the first year after diagnosis. The difference in the five-year relative survival rate was significantly lower for patients with localized disease living in the Delta (86.95%) compared to those living in the non-Delta area (88.49%). Also, patients living in the Delta region (43.31%) with advanced stage disease had significantly lower five-year relative survival than those living in the non-Delta region (48.10%). The difference in survival for advanced disease was still evident beginning in the first year after diagnosis, but the survival was similar for local disease through most of the first two years after diagnosis.

The five-year relative survival for blacks living in the non-Delta region (60.06%) was significantly higher than for blacks living in the Delta region (56.73%). Whites in the non-Delta region (65.14%) had significantly higher five-year relative survival than whites living in the Delta region (62.10%). In both the Delta and non-Delta regions, whites had significantly higher survival than blacks. This survival difference appeared in the second year after diagnosis. Region did not mediate the difference in relative survival between blacks and whites.

Table 1. Descriptive Statistics Key: Frequency, Row %, Column %

	Delta	non-Delta	Total	P-value
Overall	2,032 19.3	8,491 80.7	10,522 100.0	
Stage				
Local	799 20.2 41.8	3,160 79.8 38.8	3,959 100.0 39.4	0.016
Advanced	1,112 18.2 58.2	4,983 81.8 61.2	6,095 100.0 60.6	
Total	1,911 19.0 100.0	8,143 81.0 100.0	10,054 100.0 100.0	
Race				
White	1,032 15.1 50.8	5,819 84.9 68.5	6,851 100.0 65.1	<0.001
Black	999 27.2 49.2	2,672 72.8 31.5	3,671 100.0 34.9	
Total	2,031 19.3 100.0	8,491 80.7 100.0	10,522 100.0 100.0	
Race and Stage				
White				
Local	398 15.1 40.5	2,231 84.9 39.8	2,629 100.0 39.9	0.656
Advanced	584 14.7 59.5	3,378 85.3 60.2	3,962 100.0 60.1	
Total	982 14.9 100.0	5,609 85.1 100.0	6,591 100.0 100.0	
Black				
Local	401 30.2 43.2	929 69.8 36.7	1,330 100.0 38.4	<0.001
Advanced	528 24.8 56.8	1,605 75.2 63.3	2,133 100.0 61.6	
Total	929 26.8 100.0	2,534 73.2 100.0	3,463 100.0 100.0	

Table 2. Five-Year Relative Survival and 95% Confidence Intervals

	Delta		non-Delta	
	Survival %	**95% CI**	**Survival %**	**95% CI**
Overall	59.55	(58.03, 61.04)	63.53	(62.22, 64.81)
Stage				
Local	86.95	(86.19, 87.68)	88.49	(87.84, 89.10)
Advanced	43.31	(41.46, 45.15)	48.10	(46.43, 49.74)
Race				
White	62.10	(60.60, 63.55)	65.14	(63.86, 66.40)
Black	56.73	(55.11, 58.31)	60.06	(58.60, 61.48)
Race and Stage				
White Local	87.72	(86.96, 88.43)	88.98	(88.34, 89.59)
Black Local	85.88	(85.02, 86.70)	85.88	(85.02, 86.70)
White Advanced	45.77	(43.87, 47.65)	49.84	(48.17, 51.48)
Black Advanced	40.35	(38.40, 42.29)	44.54	(42.76, 46.31)

Controlling for stage of disease at the time of diagnosis did not eliminate the differences that exist in the five-year relative survival between blacks and white in the Delta and non-Delta regions. Figure 1 shows the survival curves for advanced disease, and figure 2 shows the survival curves for local disease. For the Delta Region, whites (45.77%) had significantly higher survival than for blacks (40.35%) for advanced stage disease. For local stage disease, the five-year relative survival for whites (87.72%) was significantly higher than the relative survival for blacks (85.88%). The five-year relative survival for advanced stage colorectal cancer in whites living in the non-Delta region (49.84%) was significantly higher than for blacks (44.54%). Also, for local stage disease, the five-year relative survival for whites living in the non-Delta region (88.98%) was significantly higher than for blacks (87.32%). For both regions for advanced disease, the survival difference was still apparent within the first year, but for local disease, survival remained similar between the races for more than the first year. Similar survival was seen into the third year after diagnosis for the Delta and into the second year after diagnosis for the non-Delta region. For local disease, the difference in survival between whites living in the Delta and non-Delta regions and for blacks living in the Delta and non-Delta regions was attenuated. The within race differences between region persisted for advanced disease. Survival for both race groups with advanced disease was similar through the first year after diagnosis. For both local and advanced disease Delta whites had equivalent survival to non-Delta blacks.

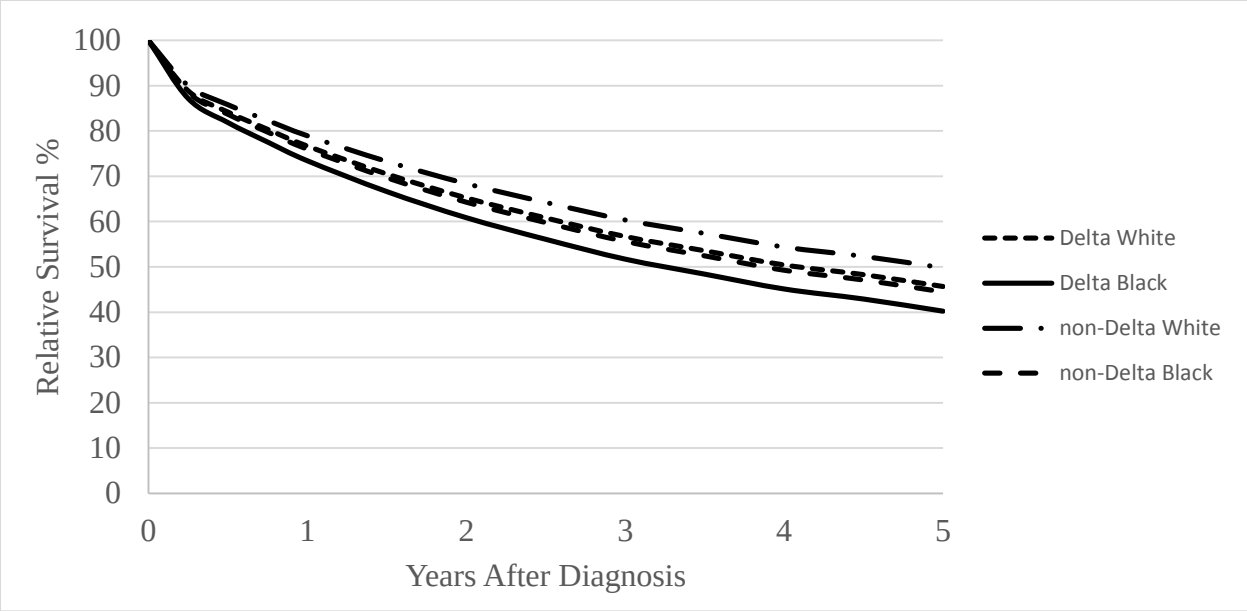

Figure 1. Relative Survival by Region and Race in Advanced Stage Disease. This figure represents the relative survival percentages for whites and blacks in the Delta and non-Delta regions by years after diagnosis for advanced stage disease.

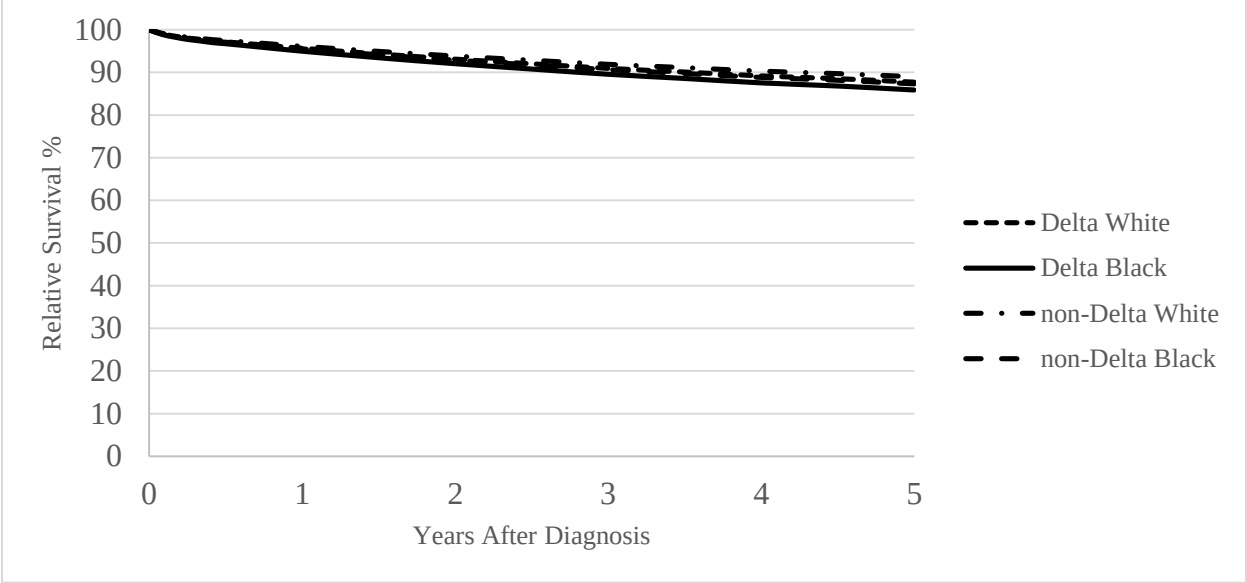

Figure 2. Relative Survival by Region and Race in Local Stage Disease. This figure represents the relative survival percentages for whites and blacks in the Delta and non-Delta regions by years after diagnosis for local stage disease.

DISCUSSION

The aim of this study was to analyze the relative survival in patients diagnosed with colorectal cancer in Mississippi to determine: 1. the survival difference between the Delta and non-Delta regions of the state and 2. if region impacted the disparity in relative survival between blacks and whites. To address the first part of the study aim, he Delta region had significantly lower survival than the non-Delta region. This is consistent with other studies conducted in the Unites States showing that place does impact colorectal cancer survival. Inclusion of stage alone in the model only extended the survival difference between the Delta and non-Delta regions for local disease but not for advanced disease. To address the second part of the study aim, whites had significantly higher survival rates than blacks in both the Delta and non-Delta regions. This is also consistent with

other studies in the Unites States that show place does not completely account for racial differences in survival. Inclusion of stage of disease in the survival model with race and region only attenuated the within race differences between regions for local disease. Inclusion of stage of disease in the survival model with race and region did extend the period of statistically similar survival beyond the first year after diagnosis for local disease, but not for advanced disease Race and stage do impact survival, but are not the only reason for the survival differences between the Delta and non-Delta regions. Stage and region do not completely account for the survival differences between the races.

One strength of the study was the comprehensive data available from the Mississippi Cancer Registry. A second strength of the study is the use of life tables that are specific to Mississippi and stratified by race, sex and age. This allows for more accurate estimation of background mortality compared to the use of United States life tables. Thus, the results of this study are more useful in informing public health and the healthcare community in Mississippi.

One limitation of the study is that patients who were diagnosed and treated solely in another state or in a Veterans Administration or military facility were excluded from the dataset due to stipulations placed on the Mississippi Cancer Registry for use of data from those entities for research. Only patients diagnosed between 2003 and 2006 participated in the full five years of the survival analysis since these patients would have been the only ones that could have been followed for a full five years after diagnosis. The later years contributed to the earlier survival times. Changes in screening or treatment would not be reflected in the later survival times. Lastly, in each analysis where both race and stage were included in the model, the survival breaks could not be done for each month in the first year which could compromise the assumption of proportional hazards between breaks.

Analysis of the cancer registry for treatment patterns compared to the established treatment guidelines would illuminate whether treatment differences exist between the race groups and regions. Further, if differences in treatment patterns are found, a qualitative study to determine the factors that are associated with these differences would be needed. Additionally, since the Delta and non-Delta regions both consist of rural and urban counties, another study of the impact rural and urban areas on colorectal cancer survival would be warranted. Urban areas tend to have a greater density of specialists allowing for greater access to screening and treatment than available in rural areas.

CONCLUSIONS

Earlier stage of disease at diagnosis leads to better survival. This study suggest that public health and the healthcare community need to work to improve the colorectal screening rates in Mississippi since the prevalence of advanced stage disease is higher in Mississippi than local stage disease. Survival is also a measure of treatment outcomes. Promotion of established treatment guidelines for all stages of colorectal cancer are imperative to ensuring that every patient receives the best care possible. The lack of an American College of Surgeons Commission on Cancer approved hospital and low numbers of specialty physicians in the Mississippi Delta make this more challenging. Ensuring appropriate treatment can be done through promotion of clinical trials, especially in the black population, which is traditionally underrepresented in clinical trials. Additionally, removing barriers to obtaining treatment is also important to ensuring that all patients receive the care they need regardless of race, stage of disease, or region of the state in which they lives. These barriers can be financial, transportation, or access to care. Lastly, Mississippi leads the nation in many chronic diseases. Rates of chronic diseases tend to be higher in the black population. These comorbidities can prevent a patient from being able to undergo certain treatments or reduce the patient's ability to recover from treatment. Managing these chronic illnesses is essential to improved health to both prevent colorectal cancer and increase the chance of survival.

ACKNOWLEDGMENTS

The authors would like to acknowledge the Mississippi Cancer Registry for the use of the cancer incidence data which is funded by a grant from the Centers for Disease Control and Prevention and funds from the Mississippi State Department of Health and the University of Mississippi Medical Center. The content of this manuscript are solely the responsibility of the authors and do not necessarily represent the views of the Mississippi Cancer Registry or its funding agencies.

REFERENCES

[1] Mississippi Cancer Registry (2016, March). *Cancer-rates.info* [Online]. Available: http://www.cancer-rates.info/ms/index.php

[2] U.S. Cancer Statistics Working Group. (2016, August). *United States cancer statistics: 1999-2013 incidence and mortality web-based report* [Online]. Available: http://nccd.cdc.gov/uscs/

[3] National Cancer Insititute (2016, June). *State cancer profiles.* Available: http://statecancerprofiles.cancer.gov/index.html.

[4] R.S. Kirsner, F. Ma, L. Fleming, D. G. Federman, E. Trapido, R. Duncan, and J. D. Wilkinson, "The effect of Medicare health care delivery systems on survival for patients with breast and colorectal cancer," *Cancer Epidemiol Biomarkers Prev* vol. 15 no. 4, pp. 769-773, Apr 2006.

[5] N. Wan, F. B. Zhan, Y. Lu, and J. P. Tiefenbacher, "Access to healthcare and disparities in colorectal cancer survival in Texas." *Health and Place* vol. 18, pp. 321-329, Nov 2011.

[6] T. L. Fitzgerald, C. S. Lea, J. Brinkley, and E. E. Zervos, "Colorectal cancer outcome inequalities: Association between population density, race, and socioeconomic status," *Rural Remote Health,* vol. 14, pp. 2668. Jul 2014.

[7] D. R. Williams and P. B. Jackson, "Social sources of racial disparities in health," *Health Affairs* vol. 24, no. 2, pp. 325-334, Mar 2005.

[8] L. Chien, M. Schootman, and S. L. Pruitt, "The modifying effect of patient location on stage-specific survival following colorectal cancer using geosurvival models," *Cancer Causes Control* vol. 24, pp. 473-484, Jan 2013.

[9] C. Allemani, H. K.Weir, H. Carreira, R. Harewood, D. Spika, X.Wang, F. Bannon, J. V. Ahn, C. J. Johnson, A. Bonaventure, R. Marcos-Gragera, C. Stiller, G. A. e Silva, W. Chen, O. J. Ogunbiyi, B. Rachet, M. J. Soeberg, H. You, T. Matsuda, M. Bielski-Lasota, H. Storm, T. C.Tucker, M. P. Coleman, and the CNCORD Working Group, "Global surveillance of cancer survival 1995-2009: Analysis of individual data for 25 676 887 patients from 279 population-based registries in 67 countries (CONCORD-2)," *Lancet* vol. 385, no. 9972, pp. 977-1010, Mar 2015.

[10] M. Hills, B. Rachet, and M. Falcaro (2014). "strel2: A command for estimating excess hazard and relative survival in large population-based studies." The Stata Journal vol. 14, no. 1, pp. 176-190, Jan 2014.

ANTICOAGULANT EFFECTS ON PURE PLATELET-RICH PLASMA

Sofia E. M. Galdames[1], Andréa A. M. Shimojo[1], Ângela C. M. Luzo[2], and Maria H. A. Santana[1]

[1]Department of Engineering of Materials and Bioprocesses, School of Chemical Engineering and the [2]Haematology and Hemotherapy Center, Umbilical Cord Blood Bank, University of Campinas, Campinas, SP, Brazil

ABSTRACT

Platelet-rich plasma (PRP) is frequently used to restore adequate number of platelets and thus maintain hemostasis. Nowadays, PRP has been widely used in regenerative medicine as an important tool. However, different protocols of preparation affect the properties of PRP, making result comparison more difficult. We investigated the effects of anticoagulants on blood cells and on plasma partitioning behavior after centrifugation, adopting a standardized protocol. P-PRP type (rich in platelets and poor in leukocytes) was prepared with one centrifugation cycle (100xg, 10 min), using a range of hematocrit of 30% to 45% from 10 healthy donors. Results show that anticoagulants primarily affected the morphology of the red blood cells (RBC) and the centrifugal portioning of plasma. As a consequence, different RBC packing levels and PRP volumes were obtained upon centrifugation. This study demonstrates how important is the standardized protocol and also that the investigated anticoagulants affected the preparation of P-PRP.

Keywords: centrifugation; PRP; anticoagulant

INTRODUCTION

PRP is a concentrated autologous platelet product and a new approach to regenerative medicine. It is able to release a great number of bioactive molecules, growth factors, chemokine, cytokines and interleukins involved in immunomodulation and healing processes, apoptosis and cell survival [1]. Although, the precise way of action is still not completely understood, PRP has been widely used in various surgical fields including orthopedic, dental and maxillofacial surgery. Moreover, great majority of clinical published articles are performed with few numbers of patients, who were not randomized leading to a low evidence grade. Despite encouraging published results, there is still a lack of studies about the standardization of PRP preparation process toward diminishing the great variability in PRP composition.

Anticoagulants are a class of drugs that prevent the blood clotting by blocking reactions that are part of the coagulation cascade. Heparin, CIT (sodium citrate) and ACD-A (citric acid- sodium citrate- dextrose solution A) are the most commonly used anticoagulants for preserving and storing human blood and its derivatives [2, 3]. In the case of PRP, CIT and ACD-A are preferred because they are nontoxic and biocompatible. Besides, the reversal anticoagulant process is simpler. Within this context, we have expanded upon previous findings by studying the effects of ACD-A and CIT on centrifugal plasma partitioning. The results of the centrifugation experiments were analyzed in terms of RBC packing, the volume of P-PRP in the supernatant and the recovery efficiencies of platelets and plasma. The results obtained will broaden the knowledge of the effects of anticoagulants on the preparation of PRP. Furthermore, these results will facilitate selecting the appropriate anticoagulants to utilize when collecting blood that will be used to prepare PRP with the best quality.

METHODS

The experiments using human blood were approved by the Ethics Committee of the Faculty of Medical Sciences of Unicamp (Campinas; CAAE: 0972.0.146.000-11).Ten healthy blood donors of ages ranging from 20 to 40 years were selected based on the results of their clinical laboratory tests.

The blood was collected into different vacuum tubes. In case of CIT, we used 3.5-mL tubes (Vacuette, Brazil) containing 0.5 mL of 3.2% sodium citrate (w/v) in a volumetric ratio 9:1 blood: sodium citrate. Otherwise, for ACD-A was used 8.5-mL tubes containing 1.5 mL of anticoagulant (BD Vacutainer, USA). For standardization purpose, the blood collected with ACD-A was transferred and centrifuged in 3.5-mL tubes.

P-PRP was prepared according to Perez *et al.* (2013 and 2014). Briefly, whole blood (WB) was centrifuged using a Rotina 380R centrifuge (Hettich Zentrifugen, Germany) at 100 ×g for 10 min at 25°C. An equal volume of both anticoagulated blood samples was used, 3.5-mL. Afterward, the P-PRP in the supernatant was carefully collected using an automatic pipet (200-µL), leaving an approximately 0.1-cm-thick layer above the buffy coat to minimize the concentration of white blood cells in the preparation. The collected P-PRP was transferred to empty tubes and its volume was accurately measured. The concentrations of platelets and other cells in the WB and P-PRP samples were determined using an ABX Micros ES 60 hematologic analyzer (Horiba ABX Diagnostics, France). The measurements were performed in triplicate.

The recovery efficiency of platelets E(Pt) and plasma E(Pl) were calculated using eqs. 1 and 2, respectively, according to Perez *et al.* (2013).The presented values were the mean values of triplicate measurements for each donor.

$$E(Pt) = \frac{(Nº\ Pt_{PRP} \times V_{UL})}{(Nº Pt_{WB} \times V_{WB})} \times 100 \quad \text{(eq.1)}$$

$$E(Pl) = \frac{V_{UL}}{(1 - H_{WB}) \times V_{WB}} \times 100 \quad \text{(eq.2)}$$

where Nº Pt was the number of platelets.mm^{-3}, V_{UL} was the volume of the supernatant or upper layer (UL) obtained through centrifugation, V_{WB} was the volume of WB and H_{WB} was the hematocrit as a percentage of the WB volume.

The platelet concentration factor (F_C), calculated using eq. 3, was the ratio between the concentration of platelets (Nº Pt.mm^{-3}) in the P-PRP and in the respective WB sample [4, 5].

$$F_C = \frac{Nº Pt_{PRP}}{Nº Pt_{WB}} \quad \text{(eq.3)}$$

The assays were performed in triplicate unless otherwise noted, and the results were presented as the mean values ± standard deviation (SD). Data were analyzed using analysis of variance (ANOVA), considering a p-value of ≤ 0.05 to indicate significant differences.

RESULTS

The results showed that the volume of PRP obtained from blood anticoagulated using CIT was higher than that of blood anticoagulated using ACD-A. The better definition of the interfaces made it easier to manually separate the PRP from the RBC- or WBC-containing layers.

Figure 1A shows that the concentration of RBC in the bottom layer (BL), the H_{BL}, was higher in CIT-containing WB samples than in those containing ACD-A in the case of the WB from all 10 donors and throughout the entire range of hematocrits (30% to 45%). Therefore, for WB samples from the same donor subjected to the same centrifugation conditions (volume, xg and t), the bottom layer of CIT-treated WB was more tightly packed, due to the CIT-induced shrinkage of the RBC. In contrast, the bottom layer of ACD-A- treated WB was more loosely packed. A linear relationship between the measured values was observed; indicating that H_{BL} (CIT) values were 12% greater than those obtained using ACD-A (Figure 1B).

Regarding the recovery efficiency values, which were calculated using equations 1 and 2; were equal for ACD-A and CIT treated WB for majority of donors, five of eight (Figure 1C).

However, in most cases, E(PI) values were higher for CIT-treated WB than for ACD-A-treated WB ($p<0.05$) (Figure 1D). Additionally, the platelet concentration factors calculated using eq. 3 were approximately 8% higher for ACD-A-treated WB than for CIT-treated WB. Therefore, the concentration of platelets in the PRP samples prepared using ACD-A was higher than that in the PRP samples prepared using CIT.

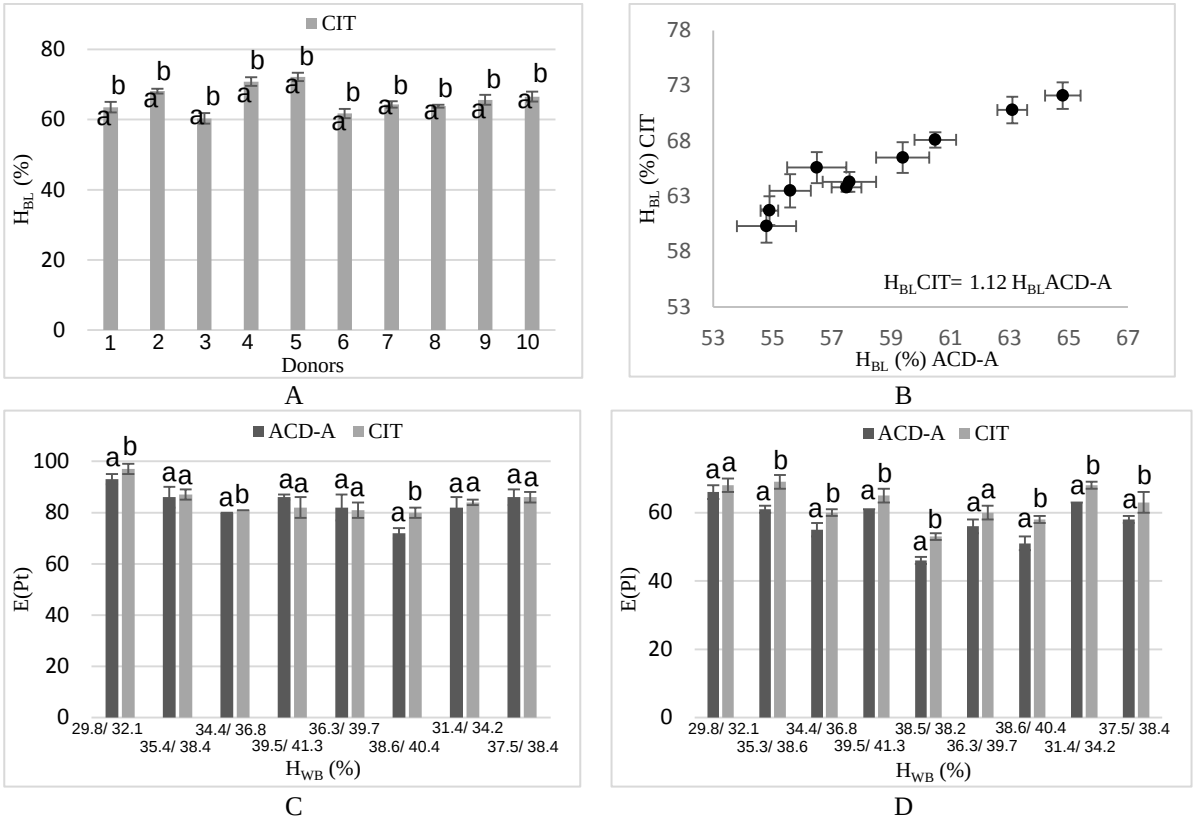

Figure 1 (A) Hematocrit percentage of bottom layer (H_{BL}), n=10; (B) Correlation between H_{BL} of CIT and ACD-A after centrifugation n=10. (C) Recovery efficiency of platelets E(Pt), n=8; (D) Recovery efficiency of plasma E(Pl), n=9. The WB samples were obtained from healthy donors with ages ranging from 20 to 40 years old. The values are the mean values ± standard deviation for triplicate measurements. Different letters (a or b) at the top of the bars indicate significant differences among the values ($p<0.05$).

DISCUSSION

Centrifugation is the first step in preparing platelet-rich plasma. Upon centrifugation, the WB is fractioned into the three following layers dispersed in plasma: a bottom layer containing RBC; an intermediate layer containing mainly WBCs and a supernatant or upper layer (UL), which is the initial PRP preparation. The percentage of RBC in WB directly affects the volume of the upper layer (V_{UL}). Thus, the higher the hematocrit of WB, which is the volume occupied by the RBC, the lower will be the volume of the upper layer or PRP.

Comparing ACD-A and CIT upon centrifugation, the results showed that for WB samples from the same donor subjected to same centrifugation conditions, the bottom layer of CIT-treated WB was more tightly packed due to the CIT-induced shrinkage of the RBC [6]. In contrast, the bottom layer of ACD-A- treated WB was more loosely packed due to the morphological changes in RBCs. The differences in the platelets counts were due to the differences in size distributions of the platelets from the different donors as well as the experimental errors. However, these differences are consistent with those observed for the H_{BL} values, due to the differential partitioning of plasma among the layers.

In this same context, Shimizu *et al*. (1984) compared two anticoagulants, ACD and CPD. They obtained different PRP volume and number of platelets for each anticoagulant. Beside, Stokol *et al*. (2007) compared CIT and EDTA. The results showed that the precision of the platelet count was significantly affected by platelet aggregation occurrence. Finally, Callan *et al*. (2009) studied the effects of CIT and ACD-A on mammals blood and PRP. The authors observed that the platelet count in the whole blood was lower when ACD-A was used rather than CIT, although the difference was not significant.

Further, we can say that a favorable centrifugation must maintain platelet integrity by preventing premature activation of platelet, thus obtaining a PRP with good quality, in other words, with high biological regeneration activity. To analyze the quality of PRP, it is necessary to study the biological effects (growth factors release and cellular proliferation) *in vitro*. That will be the next step of our studies.

CONCLUSIONS

The anticoagulants affect the preparation of PRP and the cell membranes. CIT and ACD-A have different pH and chemical composition. It is necessary to standardize the centrifugation protocol and considering the anticoagulant effect for obtain a PRP with high quality and the best biological efficiency.

ACKNOWLEDGEMENTS

We are grateful to *CAPES* (*Fundação Coordenação de Aperfeiçoamento de Pessoal de Nível Superior*) for support and financial assistance as well as to all of the donors who made this work possible.

REFERENCES

[1] P.C. Kreuz *et al*. "Platelet-Rich Plasma preparations types show impact on chondrogenic differentiaiton, migratiom and proliferation of Human subchondral mesenchymal progenitor cells". *Arthroscopy: The Journal of Arthroscopic & Related Surgery*, vol. 31, no. 10, pp. 1951-1961, Oct. 2015.

[2] T. Stokol and H.N. Erb. "A comparison of platelet parameters in EDTA- and citrate-anticoagulated blood in dogs". *Veterinary Clinical Pathology*, vol. 36, no. 2, pp. 148-154, 2007.

[3] M.B. Zurcker and J.B.A. Borrelli. "Reversible Alterations in Platelet Morphology Produced by Anticoagulants and by Cold". *Blood*, vol. 9, no. 6, pp. 602-608, 1954.

[4] A.G.M. Perez *et al*. "Prediction and modulation of platelet recovery by discontinuous centrifugation of whole blood for preparation of Pure Platelet- Rich Plasma". *BioResearch Open Access.*, vol. 2, no.4, pp. 307-314, Aug. 2013.

[5] A.G.M. Perez *et al*. "Relevant aspects of centrifugation step in the preparation of Platelet-Rich Plasma". *ISRN Hematology*, pp. 1-8, Mar. 2014.

[6] W. I. Rosenblum. "In vitro measurements of the effects of anticoagulants on the flow properties of blood: the relationship of these effects to red cell shrinkage". *Blood*, vol. 31, pp. 234-241, Feb. 1968.

[7] T. Shimizu *et al*. "High Yield of Platelet-Rich from CPD Blood Compared to ACD Blood". *Tohoku J. exp. Med*., vol. 143, pp. 381-382, 1984.

[8] M.B. Callan, F.S. Shofer and J.L. Catalfamo. "Effects of anticoagulant on pH, ionized calcium concentration, and agonist induced platelet aggregation in canine platelet rich plasma". *Am J Vet Res.*, vol. 70, no. 4, pp. 472–477, Apr. 2009.

PREVALENCE AND TRENDS OF EARLY CHILDHOOD CARIES EXPERIENCE AND UNTREATED CARIES IN THE MISSISSIPPI HEAD START POPULATION

Kristin Nalls, Elgenaid Hamadain, and Denise Krause
University of Mississippi Medical Center, Jackson, MS, USA

ABSTRACT

Early Childhood Caries (ECC) is defined as "the presence of one or more decayed, missing, or filled tooth surfaces in any primary tooth in a child 71 months of age or younger". ECC is the most common childhood disease. It is linked to periodontal disease and increased likelihood of chronic and inflammatory disease in adulthood, poor academic performance and poor quality of life for the children who are affected, and their families [2]. ECC disproportionately affects low-income and minority children. Head Start (HS) is a federally established preschool program aimed to identify and provide support for low-income children and their families. Due to the federal mandates for the HS grantees, children participating in these programs are in a position to receive increased access to dental care through oral screenings and referrals to dentists for oral health treatment. Studies have shown that HS enrollees are almost three times more likely to obtain a dental screening than those enrolled in other preschool centers. Even with these parameters in place, a great amount of tooth decay is still present in HS children. There is a need to evaluate present interventions as a starting point for oral health reform in this underserved population**.** The purpose of this study is to investigate and report the demographics and the current oral health status of Mississippi HS Children (MSHSC), as well as to identify any statistical differences with national prevalence reported by The National Health and Nutrition Examination Survey (NHANES). The study used the oral screening data from the Mississippi State Department of Health's (MSDH) *Make a Child's Smile Program* for the time period 2009-2014 and data retrieved from NHANES to examine prevalence of caries experience and untreated caries over the study time period, and to compare the oral health status of MS Head Start Centers (MSHSCs) to national reported levels. The majority of study subjects were African American (AA), between the ages of 3 and 5 years, displaying a burden of caries experience and untreated diseases significantly higher than the reported national average ($p < 0.01$). Age and race, but not gender, had a significant impact on the disease. The prevalence of caries experience and untreated caries were significantly higher as compared with the national average rates ($p < 0.01$). The researchers conclude that caries experience and untreated caries continue to be a significant problem in MSHSCs. Further research is needed to develop more effective interventions and oral health policies.

INTRODUCTION

Low-income and minority populations are historically underserved and suffer disproportionately in many areas of health, including oral health. Dental caries, or tooth decay, is the most common of oral diseases and is highly prevalent across all age groups. Prevalence is particularly high in low-income, minority preschool age children [1]. In this population of children, dental caries is considered Early Childhood Caries (ECC), as defined by the Centers for Disease Control and Prevention. ECC is defined as "the presence of one or more decayed, missing, or filled tooth surfaces in any primary tooth in a child 71 months of age or younger" [2]. In its most recent findings, the National Health and Nutrition Examination Survey (NHANES) has reported that roughly 23% of U.S. children between the ages of two and five have experienced dental caries and that ECC prevalence is two times higher in African American and Hispanic children than Caucasian non-Hispanics between the ages of two and eight [3]. The Centers for Disease Control and Prevention has reported that preschool age children in low-income families are two times more likely to suffer from untreated tooth decay than those in higher income families [4].

Head Start (HS) is a federally supported preschool program aimed to identify and provide support for low-income children and their families. The purpose of HS and Early Head Start (EHS) is to "promote the school readiness of low-income children" by two guiding principles: 1) providing a stable and thriving educational environment and 2) assessing and addressing health and nutritional needs for optimal learning, social growth, and cognitive development [5]. Oral health is one of the issues that HS programs must address in order to ensure that the overall health mission is enforced. Due to the federal mandates for HS grantees, children participating in these programs are in a position to receive increased access to dental

care. Studies have shown that HS enrollees are almost three times more likely to receive a dental screening than those enrolled in other preschool centers [6]. HS enrollees are also more likely to have state issued dental coverage than other children with similar backgrounds. However, there seems to be little difference in rates of caries experience and untreated disease between the HS participants and children of similar demographics that attend other preschool and daycare programs. It was indicated that access to dental services is limited to oral health assessment and referral.

There is limited published literature that describes the linkage of preventive and restorative care beyond oral health assessment for HS participants. A HS survey conducted by the Mississippi State Department of Health for the 2007-2008 academic year found that dental decay was a significant health problem for Mississippi's Head Start Children. Fifty-six percent of children (N=2,128) had caries experience. Forty-one percent had untreated tooth decay and 7% had urgent treatment needs related to pain, swollen tissue, or inability to eat [7]. This report indicated that intervention is still needed to address the oral health issues in Mississippi Head Start (MSHS) programs. In response, the Mississippi State Department of Health (MSDH) initiated the Make a Child's Smile (MACS) program, which provides oral screening, implementation of fluoride regimen for prevention, and referrals as needed for those MACS participants with treatment needs (8). Although the program has been in existence over a decade, there has not been any significant improvement in the oral health status of MSHS participants.

Specific aims of this study were to investigate the impact of the MACS program by: 1) reviewing the oral health status of MSHS participants, 2) determining the prevalence of caries experience and untreated caries, as well as the significance of observed trends of caries experience and untreated caries, and 3) comparing the oral health status of the study subjects to national prevalence as reported by the NHANES survey. We hypothesized that: 1) there will be no difference in percentage of children with caries experience, untreated caries, and early urgent treatment across the study period (2009-2014), and 2) the prevalence of caries experience and untreated caries will be significantly higher than the reported national prevalence for these oral health indicators.

METHODS

Data Collection: This is a retrospective study using data retrieved from the MSDH on all participants from 2009 to 2014 (N=45,107). Parents of the participants provided dental histories of their children and signed the consent document. Licensed dental hygienists approved by the MSDH were designated to perform screening at the Head Start Centers (HSCs) across the state. Participation in MACS was voluntary. Results of the oral screening were provided to the HSCs to share with participating families. Dental history and oral health screening data were kept in a secure electronic database at the MSDH. Name and any information that may identify the participants were removed and a unique code or ID was assigned that can be linked to the parental consent document. This study was exempt by the University of MS Medical Center (UMMC) and MSDH Institutional Review Boards (IRBs).

Data preparation: The original data file retrieved from the MSDH contained 45,107 records, each representing a child who participated in the MACS program. Participants either attended a Mississippi Head Start Center (MSHSC) or other day care centers that participated in the program from 2009-2014. Parameters for oral screening include screen date, caries experience and untreated caries. Out of the original data, 6,157 records were excluded due to incomplete data information. An additional 5,318 records were removed because screening did not take place at a HSC. Children's ages were determined using the date of birth at the time that the screening took place. Two thousand three hundred five participants over the age of six years were also excluded from the study. The remaining 31,327 records were used for determination of frequency distribution of caries experience and untreated caries using the SPSS statistical program.

Data Analysis: Of the 45,107 study records from MACS database, 31,327 were used for determination of the prevalence of caries experience and untreated caries. The NHANES national comparison data for prevalence of caries experience and untreated caries among children between the ages of 2 and 5 years were obtained from the National Institute of Dental and Craniofacial Research (NIDCR) [9]. Data analysis was performed using SPSS. Demographic characteristics, such as age, gender, and race were stratified by the year that oral screening was performed. Significance of the frequency distribution between the variables were tested by Chi square. The standard prevalence rate (SPR) for caries experience and untreated caries between the MACS data vs. expected prevalence rates from the NHANES were calculated. The standard error (SE) and 95% confidence interval for upper and lower limits were calculated (SPR ± SE). The SPR was significant if the graphed line did not cross over x=1. A binominal test was executed using SPSS to test whether the prevalence of the disease and untreated caries in the

MACS data were significantly different than the national average.

RESULTS

Demographic Characteristics of the Study Population: The total study population was 49.9% female and 50.1% male. Detailed characteristics are shown in Table 1. Of the total study subjects, 81.5% were African American (AA), 13.8%, Caucasian (CAU), 4.5% Hispanic, and 0.2% Asian. The race distribution of the sample was consistent for all years except 2009, where there were 3% more males than females. The majority of children in the study group were AA, followed by CAU. There was a very small number of Asian and Hispanics in the study group (Table 2.).

Table 1: Gender Distribution for Head Start Children Stratified by Year

Gender	2009 n (%)	2010 n (%)	2011 n (%)	2012 n (%)	2013 n (%)	2014 n (%)	TOTAL n (%)
Female	243 (**48.5**)	3206 (**50.1**)	3836 (**49.9**)	4032 (**49.4**)	2862 (**50.3**)	1448 (**50.1**)	15627 (**49.9**)
Male	258 (**51.5**)	3197 (**49.9**)	3845 (**50.1**)	4128 (**50.6**)	2828 (**49.7**)	1444 (**49.9**)	15700 (**50.1**)
TOTAL	**501**	**6403**	**7681**	**8160**	**5690**	**2892**	**31327**

Table 2: Race Distribution of Head Start Children Stratified by Year

Race	2009 n (%)	2010 n (%)	2011 n (%)	2012 n (%)	2013 n (%)	2014 n (%)	TOTAL n (%)
Asian	0 (**0.0**)	10 (**0.2**)	15 (**0.2**)	17 (**0.2**)	8 (**0.1**)	2 (**0.1**)	52 (**0.2**)
African American	457 (**91.2**)	5336 (**83.3**)	6235 (**81.2**)	6718 (**82.3**)	4457 (**78.3**)	2325 (**80.4**)	25528 (**81.5**)
Hispanic	9 (**1.80**)	227 (**3.5**)	359 (**4.6**)	369 (**4.5**)	305 (**5.4**)	159 (**5.5**)	1428 (**4.5**)
Caucasian	35 (**7**)	830 (**13**)	1072 (**14**)	1056 (**13**)	920 (**16.2**)	406 (**14**)	4319 (**13.8**)
TOTAL	**501**	**6403**	**7681**	**8160**	**5690**	**2892**	**31327**

Most HS enrollees, with the exception of Early Head Start Programs, were between the ages of 3 and 5 years. Early Head Start Programs serve children from birth to 3 years of age. The majority of study subjects in the HS group were between the ages of 3-4 and 5-6 (52.4% and 45.4% respectively). Only 670 (2.2%) were between the ages 0.5-2 years (Table 3).

Table 3: Age Distribution of Head Start Children Stratified by Year

Age	2009 n (%)	2010 n (%)	2011 n (%)	2012 n (%)	2013 n (%)	2014 n (%)	TOTAL n (%)
0.5-2	0 (**0**)	148 (**2.4**)	139 (**1.8**)	144 (**1.8**)	165 (**2.9**)	74 (**2.5**)	670 (**2.2**)
3-4	405 (**80.9**)	3357 (**52.4**)	4035 (**52.5**)	4513 (**55.3**)	2890 (**50.8**)	1210 (**42**)	1641 (**52.4**)
5-6	96 (**19.1**)	2898 (**45.2**)	3507 (**45.7**)	3503 (**42.9**)	2635 (**46.3**)	1608 (**55.5**)	14247 (**45.4**)
TOTAL	**501**	**6403**	**7681**	**8160**	**5690**	**2892**	**31327**

Prevalence of Caries Experience: Prevalence of caries experience was above the national rate (27.9%) for each year as presented in Figure 1. Variation between the lowest and the highest prevalence was 4.4 points across the study period. There were statistically significant differences in caries experience as compared by year ($p<0.01$). The overall average prevalence for caries experience was 41.2% per 100 children. Again, this was significantly higher than the national average of 27.9% prevalence

for children between the ages of 2 and 6 years of age as shown in Figure 2. Except for 2012, all other study years using the MACS data were found to be statistically significant (>1 at 95% CI).

Figure 1: Prevalence of Caries of Head Start Children Screened by Year

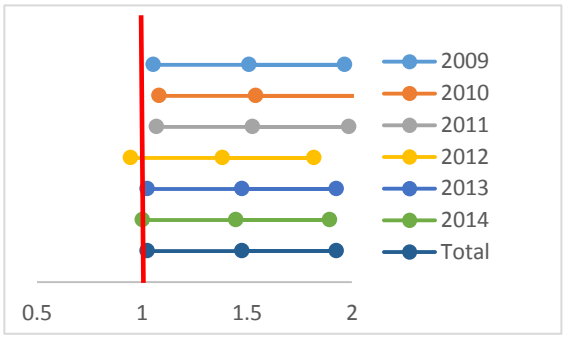

Figure 2: Caries Experience Prevalence Significance by Year (SPR* ± CI) *CI 95%

Prevalence of Untreated Caries: Prevalence of untreated caries was also greater than the national average (20.48%), except for years 2012 and 2014, as shown in Figure 3. Variations in the prevalence of untreated caries were within 7.5 points across the study period. The highest prevalence was 25.5% in 2009, and the lowest was 18.0% in year 2014. Differences were statistically significant in comparison by year ($p<0.01$). There was higher prevalence of untreated caries in the MACS dataset when compared with the national rates, however the difference was not statistically significant. Variations across the study period are illustrated showing the standard prevalence rates (SPR) and confidence intervals (CI) as demonstrated in Figure 4.

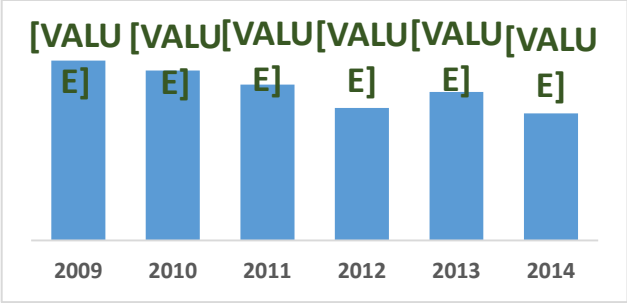

Figure 3: Percentage of Untreated Caries of Head Start Children by Year

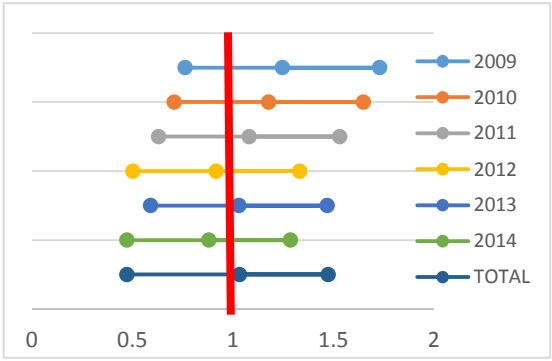

Figure 4: Untreated Caries Prevalence Significance by Year (SPR* ± CI) *CI 95%

Comparison of the Prevalence of Caries Experience by Gender, Race, and Age: The prevalence of caries experience was stratified by gender, race, and age. The binominal test results demonstrated that the percentages of males and females with caries experience in MACS study subjects were significantly higher than the national average (Male: 46.62% vs. 44.43% Female: 41.23% vs. 39.8%). Significant differences for both males and females were observed ($p<0.01$). Similarly, the percentages of AA and CAU study subjects with caries experience were significantly higher than the national average (AA= 65.22% vs. 43.34%, CAU= 39.10% vs. 38.56%, $p<0.01$). Furthermore, the percentage of children ages 2-5 in the MACS study with caries experience (33.13%) was significantly higher than the national average (27.90%). Binomial tests were performed only

for the 3-4 years age group due to limitations of the data in the NHANES age range group ($p<0.01$).

Comparison of the Prevalence of Untreated Caries by Gender, Race, and Age: The prevalence of untreated caries was stratified by gender, race and age. Percentages of untreated caries in the MACS children were significantly lower than the national average (Male: 21.09% vs. 24.16%, Female: 21.29% vs. 21.66%, $p<0.01$). Binomial test results for untreated caries in both CAU and AA groups in the MACS study were significantly lower than the NHANES data (CAU=14.66% vs. 19.47%, AA=22.62% vs. 27.58%, $p<0.01$). The percentage of children with untreated caries in the MACS data was significantly lower than the national average for children ages 2-5 years (20.07% vs. 20.48%). Binomial tests were performed only for the 3-4 years age group due to limitations of the NHANES data ($p<0.01$).

DISCUSSION

Early childhood caries (ECC) disproportionally affects low income and minority children. Early detection can reduce life-threatening consequences and may help to improve quality of life for children who are affected and their families. The highest prevalence of caries is reported in African and Southeast Asia (50% to 80%), and the lowest in European countries (1% to 32%) (10). In the U.S. overall, the prevalence of caries in children ages 2-5 years is approximately 23-24% (10). The MSDH initiated the MACS program to improve the oral health of Mississippi's underserved children. The goal of this study was to evaluate the outcomes and successes of the MACS program using national comparisons.

We found that the majority of participants in the MACS program were African American (AA: 81.5%), between the ages 3-5 years (52%). Forty one percent of the study subjects had a burden of caries experience and 21% experienced untreated disease (cavities). In comparison, the MACS data was significantly higher overall than the NHANES data reported by the NIDCR (27.90% and 20.48% respectively). These findings were tested for statistical significance using Chi square and Binomial tests. Variations for age and race, but not gender, were statistically significant. This was in agreement with the literature showing that there is increased risk of ECC development for minorities and increased prevalence of caries as children age [11,12]. Literature also confirms an increased risk of ECC with preschool aged children, especially those of lower income families and minority [13, 14].

The MACS program was established after the initial MSDH oral screening of MSHSCs results revealed high levels of caries and untreated caries, which needed urgent treatment. Even with the MACS program providing oral screenings, fluoride varnishes, and referrals to dental providers, prevalence of caries experience and untreated caries remained relatively unchanged over the study period. This indicates that the current treatment measures are not adequate for improving the oral health conditions of these children. Considering variations of the prevalence of caries experience (4.4 points across the study time frame), as well as changes in prevalence of untreated cavities (decreased every year from 2009 to 2012, then an increase in 2013 and decrease in 2014), suggests that screening children and giving referrals to dentists for follow-up treatment in this program may be effective in facilitating linkage to needed dental care for the HS population. Findings from the comparison of caries experience and untreated caries prevalence to national averages by gender, race, and age, indicate that while caries experience was statistically higher by each strata, untreated caries prevalence was statistically lower. These data suggest that while the development of ECC in this population is still high, the MACS program may be effectively providing linkage to dental care for treatment. Further interventions could be done to follow-up and ensure that these children get linked to a dental home. Linkage to dental care and possible establishment of a primary care dentist may have a positive impact on improving overall oral health throughout life, prevention of diseases, and better quality of life.

CONCLUSIONS

Most oral diseases, though common, are preventable. Early childhood caries (ECC) is the most common childhood disease. It has been linked to periodontal disease, increased likelihood of chronic disease in adulthood, poor academic performance, and poor quality of life for the children who are affected, and their families. This study shows that caries experience and untreated caries are highly prevalent among preschool children, ages 3-5 years in Mississippi. As already stated, ECC has been identified as a risk factor in the later development of chronic and inflammatory illness in adulthood. This association makes ECC an important issue, especially in MS where there are high levels of chronic disease (hypertension, diabetes, obesity, etc.). Because of the accessibility and unique characteristics of children that attend Head Start programs, researchers may consider using this program to analyze the effectiveness of current dental policies and dental care delivery models that are targeted to assist the underserved children of Mississippi. Thus, a better understanding of the prevalence and trends of ECC may help to establish baseline data and emphasize the need for preventive measures for children at higher risk.

ACKNOWLEDGEMENTS

The authors would like to acknowledge the SBEC for the invitation to publish this research and appreciate all the constructive reviewer comments.

REFERENCES

[1] U.S. Department of Health and Human Services, "Oral Health in America: A Report of the Surgeon General," National Institute for Dental and Craniofacial Research, Rockville, MD, 2000.

[2] AAPD Council on Clinical Affairs, "Definition of Early Childhood Caries (ECC)," American Academy of Pediatric Dentistry, 2008.

[3] U.S. Department of Health and Human Services, "Dental Caries and Sealant Prevalence on Children and Adolescents in the United States, 2011-2012," Centers for Disease Control and Prevention and National Center for Health Statistics, 2015.

[4] National Center for Chronic Disease Prevention and Health Promotion, "Children's Oral Health," Centers for Disease Control and Prevention, 2014.

[5] Milgrom P., Weinstein P., et. al. "Empowering Head Start to Improve Access to Good Oral Health for Children from Low Income Families," *Maternal Child Health Journal*, vol. 15, no. 7, pp. 876-882, 2011.

[6] Children's Dental Health Project, "Keeping Health in Head Start: Lessons Learned from Dental Care," Washington, D.C., 2003.

[7] Mississippi State Department of Health, "Mississippi State Department of Health (MSDH) Survey of Third-Grade Children" Jackson, MS, 2005.

[8] Mississippi State Department of Health, "Mississippi State Department of Health (MSDH) Head Start Dental Survey." Jackson, MS, 2008.

[9] National Institute of Dental and Craniofacial Research, "Dental Caries (Tooth Decay) in Children (Age 2 to 11)", http://www.nidcr.nih.gov/DataStatistics/FindDataByTopic/DentalCaries/DentalCariesChildren2to11.htm#, Bethesda, MD, 2004.

[10] Early childhood caries update: A review of causes, diagnosis and treatments. J Natural Science, Biology and Medicine, vol. 4, no. 1, pp 29-38, 2013.

[11] Abanto, J., T. S. Carvalho, et al., "Impact of oral diseases and disorders on oral health-Related quality of life of preschool children." Community Dent Oral Epidemiology vol. 39, no. 2, pp 105-114, 2011.

[12] Abanto, J., Paiva, S. M., Raggio, D. P., Celiberti, P., Aldrigui, J. M., & Bonecker, M., "The Impact of Dental Caries and Trauma in Children on Family Quality of Life," Community Dent Oral Epidemiol, vol. 40, no. 4, pp. 323-331, 2012.

[13] Reed, R., York, J., Dady, N., Chaviano-Moran, R., Jiang, S., & Holtzman, J., "Head Start Oral Health Assessment," Matern Child Health Journal, vol. 20 no. 5, pp. 962-967, 2016.

[14] Roberts, R. Z., & Erwin, P. C., "Pediatricians and the Oral Health Needs of Children: One Potential Means for Reducing Oral Healthcare Inequities," J Tenn Dent Assoc, vol. 95 no 2, pp 23-27, 2015.

TAILORING GITLAB FOR COMPUTER SCIENCE PROGRAMMING COURSES

Mesafint Fanuel[1], Tzusheng Pei[1*], Ali Abu El Humos[1], Andrew Villarrubia[1], and Hyunju Kim[2]

[1] Department of Computer Science, Jackson State University, Jackson, MS, USA
[2]Department of Mathematics and Computer Science, Wheaton College, Wheaton, IL, USA

ABSTRACT

In light of the fact that teamwork is crucial in the development of new software or the maintenance of old systems; our project has built an in-house version control system using only open source products to provide students with the platform to experience collaborative development. This educational environment will instruct students on Open Source Software community. It will familiarize students with writing large scale software code and introduce them to version control tools hugely utilized in software development. Students will experience the various aspects of software development by playing different roles while allowing instructors to easily track student activities. The communities' code repository will work as a knowledge base for student projects, and thus students can reuse the code and artifacts as examples or basic frame works for their development. Progress in software engineering education can easily be measured using the historical archives of this repository, giving computer science departments and instructors insight about their students overall standing.

Keywords: version control, repository, software development, Open Source Softwar, GitLab

INTRODUCTION

A major challenge in teaching software engineering is the gap between real development activities and the materials taught in class. Being highly invested in the theoretical, most of software engineering education doesn't prepare students for the industry. Students will be introduced to the reality of software development the hard way once they graduate. The best way to tackle this mismatch is through skill oriented educational strategies. Programs students write in class settings, being few hundred lines in length, are not typical in real world development. Students need to be made proficient in writing large scale software products through team work (collaboration).

Students need not only lectures but an experience in problem modeling, algorithmic thinking, collaborating with team members, and following the software development life cycle. They need to be induced to put in thousands of hours of coding practice to master the trade of software developer. This paper reports our effort to adopt an OSS community model to educate CS students in software engineering, specifically collaborative software development. We built a client-server system to support students' software development and team activities. Students can learn from real-world code examples and team dynamics by participating in OSS projects that are hosted at the community system.

BACKGROUND

Open source software tools have been used in CS education in order to teach traditional or online CS courses, such as programming, data structures, algorithms, and software engineering [2, 8, 9]. Although such previous practices simply used OSS tools to teach the subjects, they demonstrated that the use of OSS in classrooms resulted in positive impacts.

In addition to using OSS tools several studies have also brought OSS projects to the classroom [3, 4, 10, 12]. Finding have shown that OSS projects provide students a unique opportunity in developing software in a real-world environment. By participating in these projects, students not only sharpen their coding skills, but also learn how to work with teams. They also become more familiar with intellectual property, software licensing issues and acquire working knowledge on the domains the project revolves around [1].

Nevertheless, teaching Computer Science students software engineering using open source projects brings a set of unique challenges to the classroom. The code bases of open source projects as well as the tools used to collaborate on them are complex. Students will not have the time to make concrete contributions to a project in academic terms since it will take weeks for them to even get well informed about the project.

Setting up a development environment suitable to everyone can be complicated in light of varying degrees of familiarity students have to tools and platforms. Open source Communities also have particular development methodologies and norms that one can learn only through extensive participation in them. Furthermore, class academic calendars may not overlap with a projects release schedules. This makes joint work even more

difficult.

Thus, instead of embedding students into preexisting communities it is sensible to let students create their own communities which could start out as assignments posted by the instructor. This assignment could be month long codes. And by giving software engineering courses for two semesters or more, or by crafting the appropriate educational model, students will be able to deliver dozens of large scale (1000 or more lines) of OSS software per year. This will greatly increase their coding and team work skills. Instructors will give regular grades to the students by checking the work being done on the Open source community. This paper reports our effort to establish such a teaching environment called Student-Source for such OSS benefits while minimizing the identified limitations.

THE STUDENT-CENTERED OPEN SOURCE SOFTWARE (SOSS) COMMUNITY

A fundamental paradigm shift in software engineering education will be the unintended outcome of Student-Source. By allowing students to work on semester long—even year round—projects, grades will escape the confines of the traditional classroom. By default, students will have a plethora of project code and artifacts accumulated at a central location. Thus, the community system acts as a virtual classroom, and students learn by examples and from peers. The grade they will gate will count to their senior project or to an overall course requirement.

Furthermore, Student-source will afford a different standard of instructor to student interaction. A CS student's education will not jus be theoretical but experiential. The traditional confines of the classroom will be supplemented by development activities on the community system. As students learn more throughout the year they will add a little to the OSS projects they are undertaking on the system. Students can also work on the various OSS projects taking place on the system as well.

Most development of OSS happens in university initially. The tool will make the university a hub of OSS development activity. Many projects will be started. It will be an enabler in creating a microcosm of the real software industry in the university setting. Overall Student-Source will provide active learning environment, which allows collaborative learning, intuitive learning, role playing, etc.

A. Structure and Functionalities

The front end of Student-Source contains a web site that allows user to log in or create a user account through Google OAuth authorization protocol. We implemented the Google OAuth authorization protocol along with the restriction that the domain must match one of the institution's email domains. Google OAuth gives users the ease of creating accounts automatically by just signing into our institutional email system that is supported by Gmail. These functionalities keep the scope of Student-Source within the confines of the university.

Another way we created a controlled teaching environment is by disabling public visibility level of Student-Source. Student-Source offers three visibility levels on project repositories. By visibility level we mean permission types to one's code and project artifacts. This visibility types are private visibility meaning repos are available to users explicitly given access, internal visibility gives access to any user logged in and public visibility gives access to anyone for free.

All users will be categorized as either admin or student. Each category possesses different permission levels that can access diverse functionalities of Student-Source. Students have traditional permission and control just like any conventional user of version control tools such as GitHub. They can clone project, pull projects, collaborate on projects and so forth. A list of student activities on the system appears on the student dashboard page. Various other features exist on Student source web frontend as well making the system a highly integrated and rich platform for users.

Admin users have an overall view of the system from their admins control panels. They can post announcements on Student-Source through the announcement feature. Admin rights can be given to instructors so that they can easily track everything that is happening. In future works, we seek to dissect admin and create a new user role called instructor with its own permission levels and advanced functionalities. Already our team has implemented a faculty forum page for instructors on the system.

On the backend, Student-Source is hosted on a Nginx web server, and this in turn runs on an Ubuntu 14.04 host machine. The community users can access their project repositories by using Git client or EGit, which is supported by Eclipse. EGit works with JGit (the Java implementation of Git). Currently, the server is running on a generic desktop with a quad-core processor and 4GB RAM. Student-source functionality is backed by a PostgreSQL database.

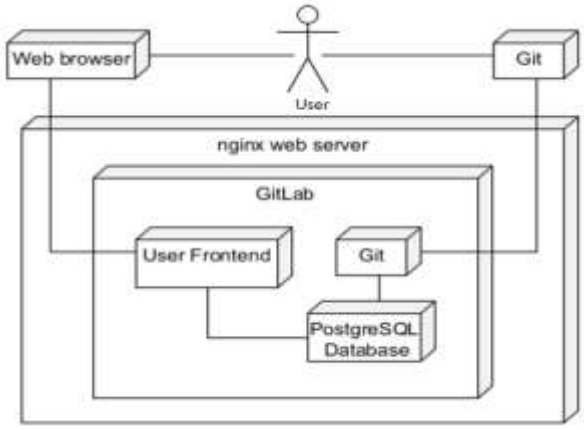

Fig. 1. The SOSS server architecture.

B. Open sources software's used

Built on top of the famous web-base Git management tool, GitLab, our Student source contains all the rich features of these management tools. These features include issue tracking, built in wiki systems, protected branches, code snippets, project importing and unlimited public and private repositories. Projects can be organized into private, internal or public and access to them can be managed with five different users setting for external users.

We decided to use GitLab because it is Git server based upon the famous source code management tool, Git. Of all the source code management tools out there such as subversion, mercurial, we found Git to be by far superior. It is the default version control system for large open source repository websites such as GitHub and Bit Bucket. Previous surveys have also shown Git to be the most preferred version control tool.

The benefits of Git include a full history of code changes so that a user can easily pull previous versions of the code, and a branch mechanism so that the user can develop and test different scenarios on the code. Additionally, its repository-to-repository interaction allows the user to share entire branches between repositories.

UTILZIING STUDENT-SOURCE

The SOSS Community system was first introduced graduate and undergraduate software engineering courses during Fall 2014 semester in the Department of Computer Science at Jackson State University. In subsequent years we have introduced the system to lower level CS and CE classes at our institution. These efforts have brought to light challenges that need to be tackled before a complete adoption and a successful application of student-source in Software engineering.

As identified earlier, it is challenging to get the student body used to the system and its corresponding collaboration tools. Currently our team uses a series of modules to be distributed in classes during our brief introductory sessions. These short modules contain a clear step by step guide on how to get started on Student-Source. While students have overall been successful in following guidelines, the experience has highlighted the need for students to grasp concepts related to Student source more successfully as a prerequisite.

Our team realizes the necessity of having deeper introductory sessions to teach students Git and basic CLI commands. An initial introduction of Git and CLI must also be followed by a short phase of familiarizing students with them. Such sessions could be held in programming labs in order not to require fundamental changes to curriculums [13]. Furthermore, these sessions specifically and student-source in general must be introduced to lower-level CS courses (e.g. programming course) so that students can utilize the system throughout the course of their CS education.

Secondly it is arduous to build a dynamic community full of open source projects and usable OSS products based purely on student initiative. An open source community needs leaders, those who initiate the projects and oversea the various projects. We have seen the tremendous role instructors will play in this area. There unique position allows them to easily be the instigators of various open source projects. By lightly integrating Student-Source into their curriculum as a supplemental material, instructors play the leading role in building up dynamic communities.

While the overall impact of our efforts had been positive, we have discovered the traditional road block to a complete adoption of the community system. A community needs leaders and the instructors are the initiators of projects on student source. We propose an educational model were instructors include Student-source as a supplemental material to there curriculum. These will motivate students to play active role in the community and build up various OSS products.

FUTURE WORK AND PLANNED ENHANCEMENTS

Moving forward, we plan to introduce a third category of users to the system, Instructors. The instructor user will make student source more fit for the educational environment. The instructor will be afforded a whole range of actions such as checking student accounts and tracking student activities.

Instructors should be able to grade students based on various development and collaborative activities students do on the system. A grading mechanism will grade

students based on the number of commits, number of insertions in the commits, number of deletion in the commits, and total line of code written by student as they are extracted from the total number of commits done by the students. Other factors such as number of collaborative task such as pulling project, adding students, commenting on work and so forth will also be factored out by the grading methodology. In conclusion, the admin controls the system, the students collaborate on the system, while instructors track student activities on the system.

ACKNOWLEDGMENT

This work has been supported through the National Science Foundation grant (HRD-1348565) on the SOSS (Student- centered Open Source Software) Community. The views and conclusions contained in this document are those of the authors and should not be interpreted as necessarily representing the official policies, either expressed or implied, of the funding agency.

REFERENCES

1. Bryan Behrenshausen, "Professors embed students directly into open source communities", http://opensource.com/education/14/8/challenges-to-open- source-computer-science-education, 2014.
2. Carrington and S. Kim, "Teaching software design with open source software", In Proc. of the 33rd ASEE/IEEE Frontiers in Education Conference, 2003, pp.9-14.
3. R. Charles and Y. Tao, "Evaluating student participation in open source software development with an annotation model", In Proc. of the 4th IASTED International Conference on Knowledge Sharing and Collaborative Engineering, 532-063, 2006.
4. Ellis, M. Purcell, and G. Hislop, "An approach for evaluating FOSS projects for student participation", In Proc. of the 43rd ACM Technical Symposium on Computer Science Education, 2012, pp.415-420.
5. Git, http://git-scm.com.
6. GitLab, https://about.GitLab.com.
7. Google Developers, "Using OAuth2.0 to access Google APIs", https://developers.google.com/accounts/docs/OAuth2.
8. S. Lakhan and K. Jhunjhunwala, "Open source software in education", Educause Quarterly, vol. 31, no. 2, 2008, pp.32-40.
9. D. Lipsa and R. Laramee, "Open source software in computer science and IT higher education: a case study", International Journal of Advanced Computer Science and Applications, vol. 2, no. 1, 2011, pp.43-54.
10. Antoine Melki, "Proprietary versus open source software in support of learning in computer science", In Proc. of the 2014 Federated Conference on Computer Science and Information Systems, 2014, pp.111-115.
11. Ian Skerret, "Eclipse community survey 2014 results", https://ianskerrett.wordpress.com/2014/06/23/eclipse-community-survey-2014-results/, 2014.
12. S. Sowe, I. Stamelos, and L. Angelis, "An empirical approach to evaluate students participation in free/open source software projects", In Proc. of IADIS International Conference on Cognition and Exploratory Learning in Digital Age, 2006, pp.304-308.
13. L. Vu, T. Tan, and P. Maneerat, "Incorporating open-source software development into computer science and software engineering education at university level", In Proc. of the 2nd Australian Undergraduate Students' Computing Conference, 2004, pp.149-164.

INCREASED GLUTATHIONE IN CAOV-3 OVARIAN CANCER CELLS FOLLOWING TREATMENT WITH THYMOQUINONE

Jennifer L. Harpole and Hamed Benghuzzi
University of Mississippi Medical Center, Jackson, MS, USA

ABSTRACT

Thymoquinone (TQ) is an antioxidant that has possible anti-cancer effects. Studies have shown that TQ can exhibit inhibitory effects on the cell proliferation of many cancer cell lines. These results indicate that TQ inhibits tumor growth, and could be used as a potential drug candidate for cancer therapy. Cancer cells are constantly exposed to oxidative stress which can be detected by changes in total reduced glutathione levels. This study investigates changes in cellular glutathione concentration following conventional and sustained delivery of TQ to the ovarian cell line, CAOVv-3. CAOV-3 cells (1 x 10^5) were plated according to standard lab protocols and subdivided into three groups of 6 wells each. Group 1 served as control and groups 2 and 3 cells were treated with either TQ (16 µM) delivered in a bolus dose or via a ceramic drug delivery system. Cells were evaluated for growth and intracellular glutathione. The results of the study revealed: (1) bolus dosing did not alter intracellular glutathione concentration over a 72 hour treatment period and (2) sustained delivery of TQ over a 72 hour period resulted in changes in intracellular glutathione which were statistically different from control untreated cells. Overall conclusion: TQ only affected glutathione levels when administered by a sustained delivery system.

Keywords: Glutathione, Thymoquinone, Antioxidant, Cancer therapy, Ovarian cancer, CAOV-3 cell line

INTRODUCTION

Cancer cells are constantly exposed to oxidative stress, and it has been shown that human tumor cell lines generate reactive oxidative species (ROS) to a much higher extent than do non-transformed cell lines [1]. The main defense mechanism in cells to counteract cellular stress is intracellular reduced glutathione. The use of natural products for suppression of cancer cells is currently on the rise; however, the mechanism of action for most products have yet to be clearly defined. Thymoquinone (TQ) is a component derived from the medial plant *Nigella sativa* that has been used for medical purposes for more than 2,000 years [2]. The seed has been used as a natural remedy to promote health and treat diseases [3]. For many years, it has been used as a traditional medicine for a wide range of illnesses including bronchial asthma, headache, dysentery, infections, obesity, back pain, hypertension and gastrointestinal problems [4]. TQ is the bioactive constituent of the volatile oil of black-seed. TQ has been shown to exert anti-inflammatory, anti-oxidant, and anti-neoplastic effects both *in vitro* and *in vivo* [3]. TQ has antioxidant effects and has been shown to protect against heart, liver and kidney damage in animal models. TQ is an angiogenesis inhibitor and has been shown to exhibit antioxidant, anti-inflammatory, and chemopreventive effects [5,6]. Studies have shown that TQ can exhibit inhibitory effects on proliferation of many cancer cell lines [2]. Yi *et al*. (2008) demonstrated that TQ inhibits tumor angiogenesis and tumor growth. He suggested that TQ could be used as a potential drug candidate for cancer therapy. Thymoquinone has been shown to kill cancer cells by a process that involves apoptosis and cell cycle arrest, while non-cancerous cells are relatively resistant to TQ [8]. A decrease in cell survival with pro-apoptotic properties have also been identified in various cancer cell lines including canine osteosarcoma cells, human colon carcinoma, breast adenocarcinoma cells, and the ovarian adenocarcinoma cells. TQ has been demonstrated as a cytotoxic agent in several multi-drug resistant human tumor cell lines. However, the underlying molecular mechanism of its anticancer properties is not well understood [9]. The literature suggest that TQ's principal mechanism of action is to induce cell cycle arrest, while other studies suggest TQ induces cell stress. The goal of this study is to determine the effects of TQ on intracellular glutathione levels when administered as a bolus dose or using a tricalcium phosphate delivery system.

METHODS

CAOV-3 cells (1 x 10^5) were plated according to standard lab protocols and subdivided into 3 groups of 6 wells each. Group 1 served as control and groups 2 and 3 were treated with TQ (16µM). The groups were terminated at 24, 48, and 72 hours. Glutathione biomarker evaluations were performed following standard lab techniques [10]. The statistical analysis was conducted using SPSS version 17.0. Analysis of variance (ANOVA) was used to compare the groups. Statistically

significant effects in ANOVA were followed up with Tukey's LSD to compare every groups mean with every other group mean.

Experimental Design

Group	Treatment	Duration (Hours)
1	CAOV-3	24, 48, 72
2	CAOV-3 + TQ-bolus	24, 48, 72
3	CAOV-3 + TQ-SD	24, 48, 72

RESULTS

Glutathione levels for CAOV-3 cells that were exposed to TQ through conventional delivery showed that the differences in the mean values among the treatment groups were not statistically different ($p>0.05$) at 24, 48, and 72 hours. Intracellular oxidative damage was assessed by determining the intracellular glutathione concentration of the CAOV-3 ovarian cancer cell following a single administration of TQ at 24, 48, and 72 hours. The data are expressed as μM glutathione normalized to cellular protein concentration as average ± SEM. A single dose of TQ did not induce intracellular oxidative stress over a 72 hour period.

Glutathione levels for CAOV-3 cells that were exposed to TQ using sustained drug delivery revealed that the differences in the mean values among the treatment groups was not statistically different ($p>0.05$) at 24 and 48 hours. However, the data showed glutathione levels for TQ were statistically significantly different ($p<0.05$) compared to the control at 72 hours. By 72 hours, there was a significant two-fold decrease in intracellular GSH concentration in cells treated with TQ when compared to the control.

DISCUSSION

Normally, antioxidants are associated with the prevention or delaying the development of cancer by inhibiting oxidative radical damage or by increasing the cellular glutathione detoxifying systems within the cells. TQ is known to induce glutathione and is thought to protect healthy cells by inducing the activity of glutathione transferase aiding in cellular detoxification. In cancer where ROS are generated at a greater rate, the addition of TQ induces more radical formation and instead of a protectant, it insults the cellular membrane inducing cytolysis and apoptosis. A review of the literature suggests that antioxidants have the ability to increase apoptosis in cancer cells by holding cells within the cell cycle and increasing the activity of various capases and p53. Work on numerous cell lines in our labs have shown positive outcomes in regards to using TQ to impair cell proliferation and induce cytolysis In this study, TQ did not increase the total cellular glutathione content of CAOV-3 cells. Glutathione is a sensitive marker of cell stress that when increased reflects the cells ability to detoxify while decreases in glutathione indicate cell death.

Ceramic drug delivery devices (CDDD) are particularly promising as delivery systems because they are capable of the storage and release of hydrophilic and hydrophobic compounds, and low and high molecular weight molecules over extended intervals. Also, these delivery systems which are capable of delivering a wide variety of chemicals and biologicals can be used in other applications including veterinary medicine, and agriculture [12]. Sustained delivery utilizes the slow release of drugs to maintain a constant dose and deliver a particular amount for the course of the day as opposed to bolus delivery as what occurs in conventional delivery. In this study the slow release of TQ showed more favorable reduction in glutathione that suggest increased cytolysis and cell death when compared with bolus dosing.

CONCLUSIONS

This study was utilized to determine if there were any effects on the cells after treatment of two different delivery methods: conventional delivery (CD) and sustained delivery (SD) of natural potential chemotherapeutic agents. Conventional delivery of TQ was not able to reduce cell numbers or deplete intracellular pools of GSH. Continuous release of similar amounts of TQ over a 72 hour period was able to hinder cell growth and reduce intracellular levels of GSH. The study suggests that natural compounds when administered in a sustained fashion has the potential to interfere with a cancers cells defense mechanisms.

ACKNOWLEDGMENTS

This project was partially supported by grant from Enzymatics (PI: Benghuzzi and Tucci). The authors would like to thank Gerri Wilson, Lisa McCammon, and mentors for their support and guidance.

REFERENCES

[1] Falck, Eva, Sandra Karlsson, Jessica Carlsson, Gisela Helenius, Mats Karlsson, and Karin Klinga-Levan. "Loss of Glutathione peroxidase 3 expression is correlated with epigenetic mechanisms in endometrial adenocarcinoma."

Cancer Cell International. 10:46 (2010): Print.

[2] Yi, Tingfang, Sung-Gook Cho, Zhengfang Yi, Xiufeng Pang, Melissa Rodriguez, Ying Wang, Gautam Sethi, Bharat B. Aggarwai, and Mingyao Liu. "Thymoquinone inhibits tumor angiogenesis and tumor growth through suppressing AKT and extracellular signal-regulated kinase signaling pathways." *Molecular Cancer Therapy*. 7.7 (2008): 1789-96. Print.

[3] Jafri, Syed H., Jonathan Glass, Runhua Shi, Songlin Zhang, Misty Prince, and Heather Kleiner-Hancock. "Thymoquinone and cisplatin as a therapeutic combination in lung cancer: *In vitro and in vivo*." *Journal of Experimental and Clinical Cancer Research.* 29:87 (2010): Print.

[4] Ragheb, Ahmed, Ahmed Attia, Walid Shehab Eldin, Fawzy Elbarby, Sna Gazarin, and Ahmed Shoker. "The Protective Effect of Thymoquinone, an Anti-oxidant and Anti-inflammatory Agent, against Renal Injury: A Review." *Saudi Journal of Kidney Diseases and Transplantation*. 20(5): 741-752 (2011): Print.

[5] "Thymoquinone." *Wikipedia*. 2010. Web. http://en.wikipedia.org/wiki/Thymoquinone

[6] Sethi, Gautam, Kwang Seok Ahn, and Bharat B. Aggarwal. "Targeting Nuclear Factor-kB Activation Pathway by Thymoquinone: Role in Suppression of Antiapoptotic Gene Products and Enhancement of Apoptosis." *Molecular Cancer Research.* 6.6 (2008): Print.

[7] Richards, La'Toya Ross, Pamala Jones, James Hughes, Hamed Beghuzzi, and Michelle Tucci. "LNCaP Cells Exposed to Ceramic Drug Delivery Treatment with Epigallocatechin-3-Gallate, Thymoquinone, and Tannic Acid." *Biomedical Sciences Instrumentaion.* (2007): Print.

[8] Shoieb, Ahmed M., Mona Elgayyar, Paul S. Dudrick, John l. Bell, and Patricia K. Tithof. "In vitro inhibition of growth and induction of apoptosis in cancer cell lines by thymoquinone." *International Journal of Oncology.* 22:107-113 (2003): Print.

[9] Gurung, Resham Lal, Shi Ni Lim, Aik Kia Khaw, Jasmine Fen Fen Soon, Kirthan Shenoy, Safiyya Mohamed Ali, Manikandan Jayapal, Swaminathan Sethu, Rajamanickam Baskar, and M. Prakash Hande. "Thymoquinone Induces Telomere Shortening, DNA Damage and Apoptosis in Human Glioblastoma Cells." PLoS ONE 5(8): e12124. doi:10.1371/journal.pone.0012124

[10] Norwood, Anne A., Michelle Tucci, and Hamed Benghuzzi. "A Comparison of 5-Fluotouracil and Natural Chemotherapeutic Agents, EGCG and Thymoquinone, Delivered by Sustained Drug Delivery on Colon Cancer Cells." *Biomedical Sciences Instrumentation.* (2007): Print.

[11] Cramer, DW, H Kuper, BL Harlow, and L Titus-Erstoff. "Carotenoids, antioxidants and ovarian cancer risk in pre- and postmenopausal women." *International Journal of Cancer* 94.1 (2001): 128-34. Web. 14 Jul 2010. http://www.ncbi.nlm.nih.gov/pubmed/11668487

[12] Benghuzzi, H. A., B. G. England, and P. K. Bajpai. "Characterization of Ceramic Drug Delivery Devices: The Effect of Various Temperatures of Incubation on the Delivery of Biologicals." *Biomedical Sciences Instrumentation.* (1992): Print.

[13] Shinto, Yoshitaka, Atsumasa Uchida, Feza Korkusuz, Nobuhito Araki, and Keiro Ono. "Calcium hydroxyapatite ceramic used as a delivery system for antibiotics." *British Editorial Society of Bone and Joint Surgery.* 74B (1992): Print.

NANOCERIA AND CATALASE CONJUGATES AS A FREE-RADICAL SCAVENGING SYSTEM

Brendan Ward[1], Dmitry Gil[1], Vladimir Ivanov[2], Vladimir Reukov[1,3]

[1]Department of Bioengineering, Clemson University, Clemson, SC
[2]Kurnakov Institute of General and Inorganic Chemistry, Moscow, Russia
[3]Institute for Biological Interfaces of Engineering, Clemson University, Clemson, SC

ABSTRACT

Reactive oxygen species (ROS), a product of cellular respiration, are present in any given aerobic organism at any time. However, ROS have been proven to play a role in the propagation of the immune response, causing cellular growth and apoptosis. Nanocrystalline cerium dioxide (nanoceria) is known for its pronounced antioxidant activity. It was shown that nanoceria possesses activity similar to that of SOD, converting free oxygen radicals into hydrogen peroxide. Catalase, a naturally occurring enzyme found in peroxisomes, can convert hydrogen peroxide molecules into water and oxygen. The goal of this project is to combine nanoceria and catalase into an ROS scavenging system to take a free radical oxygen and convert it to a water and oxygen molecule. When implemented, this system could drastically reduce the amount of ROS, ultimately decreasing its contribution to harmful effects on the immune response

Keywords: nanoceria, SOD, catalase, ROS

INTRODUCTION

Reactive oxygen species (ROS) and reactive nitrogen species (RNS) are produced intracellularly and extracellularly within the body [1], [2]. When these radicals are left unchecked, the natural antioxidant defenses in the body are unable to neutralize them, permitting oxidative damage[3]. This types of damage, known as oxidative stress, takes form in many neurodegenerative diseases including Alzheimer's disease and Parkinson's disease and also propagates atherosclerosis[3], [4]. RNS also has the potential to cause neurological damage by reacting with tyrosine proteins, modifying protein functionality[3]. Formation of RNS occurs when NO, a common compound used in cellular signaling, reacts with $\cdot O_2^{\bullet -}$ to form peroxynitrite ($ONOO^-$). Peroxynitrite is capable of traversing lipid bilayer membranes using anion channels and reacts slowly within the cytoplasm resulting in specific reactions within the cell, subtly causing detriment [5]–[7].

Catalase is one of the most efficient antioxidant enzymes found in human body; one molecule can interact with more than a million H_2O_2 molecules per second[8], [9]. However, it was shown that the activity of this enzyme lessens dramatically when exposed to superoxide free radicals through a negative feedback inhibition mechanism[10]. It can be hypothesized that the shielding action of catalase can be drastically increased if the enzyme is conjugated with the compound capable of dismasting superoxide radicals.

Cerium oxide (CeO_2) has proven to be a unique material with applications ranging from fuel cells to antioxidants [5]. Nanocrystalline cerium particles (Nanoceria) have an augmented number of surface defects that allow balancing between +3 and +4 oxidation states [11]. There is a large body of evidence suggesting that nanoceria mimics catalase effectively dismutating H_2O_2 and diminishing the effects of oxidative damage[5].

The goal of this study is to develop and characterize an antioxidant system comprised of nanoceria and CAT to effectively combat the adverse effects that oxidative stress induces.

METHODS

Materials

Catalase (from bovine liver), cerium (III) nitrate, ammonia, citric acid, and lipopolysaccharides (LPS) were obtained from Sigma-Aldrich (St. Louis, MO, USA). Amplex® Red catalase assay kit (Cat # A22180) was purchased from ThermoFisher Scientific (Waltham, MA, USA). Dulbecco's Modified Eagle Medium (DMEM), fetal bovine serum (FBS), penicillin and streptomycin were purchased from Corning Inc. (Manassas, VA, USA). RAW 264.7 (ATCC® TIB-71™) cell line was obtained from ATCC® (Manassas, VA, USA). Griess reagent was obtained from Enzo Life Sciences (Farmingdale, NY, USA).

Synthesis of Nanoceria

Synthesis of nanoceria was performed as described by *Ivanova et all* [12]. Concisely, 25ml of 0.4M cerium (III) nitrite with 2.0 g of citric acid were added to 100 ml of 3 M ammonia. This solution was kept at room temperature for several hours to allow the formation of CeO_2 to be completed. Afterwards, the solutions were rinsed thoroughly with deionized water and dried.

Nanoceria Characterization

The formation of nanoceria was confired by means of X-ray diffraction. Diffraction peaks were then compared with JCPDS database. Transmission electron microscopy (TEM) and dynamic light scattering (DLS) were used to determine particle size of the obtained samples. Thermogravimetric analysis (TA instruments, New Castle, DE, USA) was used to determine the concentration of ceria in the obtained samples.

Formation of Nanoceria-CAT Conjugate

To form the conjugate (Fig. 2), an aqueous solution of catalase (5 U/ml) was mixed with the ceria-containing aqueous solution and incubated for two hours at room temperature.

Measurement of Antioxidant Activity

The scavenging properties of the conjugate were measured using an Amplex® Red catalase assay kit provided by Thermo Fisher Scientific (Waltham, MA, USA). Griess reagent test was performed on the conjugates to evaluate their activity against reactive nitrogen species. To test the antioxidant activity of the conjugate in cell culture experiments, a suspension containing 1×10^5 cells/ml mouse macrophages (RAW 264.7) was seeded in a 24-well plate and incubated at 37^{o}C to allow attachment to the well plate. The next day the cells were challenged with 10 μg/ml lipopolysaccharide (LPS) and allowed to incubate for four hours. During each incubation period, the amount of CO_2 was set to 5%.

RESULTS

The formation of nanoceria was confirmed by means of X-ray diffraction. The results showed a cubic ceria structure with a cell parameter of about 5.45A, which corresponds to the stoichiometry of $CeO_{1.90}$. The determined size of the nanoceria particles was a 2.3±1 nm.

In the present work, the ability of ceria-CAT conjugates to dismutase hydrogen peroxide was assessed and compared with unfunctionalized ceria and catalase. All three compounds were capable of degrading hydrogen peroxide, which was not unexpected given the antioxidative nature of catalase and nanoceria (Table 1). However, it was shown that antioxidant activity of the conjugates was significantly higher than that of nanoceria and catalase alone ($p << 0.001$, n=6).

Cell culture experiments in the presence of the conjugates, ceria, and catalase were conducted in order to evaluate the ability of the compounds to deactivate RNS. The latter were generated by the macrophages activated by LPS. The results are presented in Table 2.

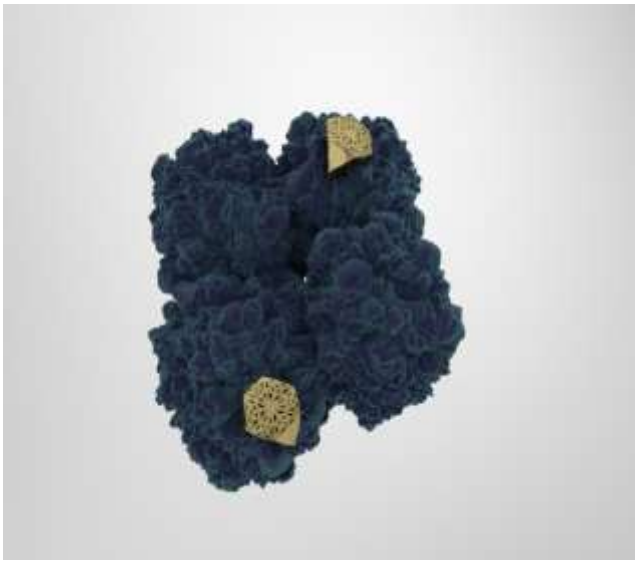

Fig. 2: CAT and nanoceria conjugate system

Table 1. The results of the Amplex Red assay conducted for catalase, nanoceria and ceria-CAT conjugates.

Sample	CAT	Ceria	Ceria-CAT
Hydrogen peroxide inhibition rate, %	26±1	73±1	80±1

Table 2. The results of the Griess test conducted for catalase, nanoceria and ceria-CAT conjugates. The absorbance at 550 nm directly corresponds to the concentration of nitric oxide.

Sample	Control, no LPS	Control	CAT	Ceria	Ceria-CAT
Absorbance at 550 nm	0.06±0.02	1.11±0.12	1.02±0.11	0.51±0.07	0.47±0.07

DISCUSSION

Potential use of nanoceria in biomedical application puts certain requirements to the form of the compound. In particular, it was shown that the particle size should be in the range of 2-3 nm, in order to anticipate pronounced antioxidant properties[13]. Moreover, it should be appropriate for dosing and possess long-term stability. Because of that, ceria colloidal solutions stabilized by citric ions were synthesized and characterized in the present work.

The results of the Amplex® Red assay shown in Table-1 prove that ceria-CAT conjugates possess pronounced antioxidant activity, effectively converting physiological relevant levels of hydrogen peroxide. Moreover, the synergetic effect of ceria and catalase is evident from the results: the activities of unfunctionalized compounds are significantly lower when compared with ceria-CAT conjugates. Therefore, the conjugate has potential to outperform both of its components by inhibiting hydrogen peroxide at a more elevated rate.

The antioxidant activity against RNS was determined in cell culture experiments (Table 2). The ceria-CAT conjugate showed a lower absorbance than that of the unfunctionalized ceria and unfunctionalized catalase. However, the absorbance level of unfunctionalized ceria is significantly closer to that of the ceria-CAT conjugate when compared to the unfunctionalized catalase. These results suggest that the activity of the conjugates is primarily driven by nanoceria, which effectively acts as a scavenger of RNS. In its turn, the activity of the catalase against RNS is low, due to the nature of this enzyme as a peroxide scavenger, not an RNS scavenger. Therefore, the approach proposed in this study requires additional optimization to be effective against RNS..

CONCLUSIONS

In conclusion, the present study deals with the antioxidant activity of ceria-CAT conjugates. It was shown that catalase and ceria can be conjugated to achieve the synergetic effect of individual components. The antioxidant activity of the conjugates was found to be significantly higher than that of ceria and catalase alone.

ACKNOWLEDGMENTS

This work was supported in part by the Clemson University Creative Inquiry Program, Institute for Biological Interfaces of Engineering, and the National Institutes of Health (5P20GM103444-08).

REFERENCES

[1] E. Naik and V. M. Dixit, “Mitochondrial reactive oxygen species drive proinflammatory cytokine production.,” *J. Exp. Med.*, vol. 208, no. 3, pp. 417–20, Mar. 2011.

[2] M. Hulsmans, E. Van Dooren, and P. Holvoet, “Mitochondrial Reactive Oxygen Species and Risk of Atherosclerosis,” *Curr. Atheroscler. Rep.*, vol. 14, no. 3, pp. 264–276, Jun. 2012.

[3] S. Gandhi and A. Y. Abramov, “Mechanism of Oxidative Stress in Neurodegeneration,” *Oxid. Med. Cell. Longev.*, vol. 2012, pp. 1–11, 2012.

[4] I. Perrotta and S. Aquila, “The Role of Oxidative Stress and Autophagy in Atherosclerosis,” *Oxid. Med. Cell. Longev.*, vol. 2015, pp. 1–10, 2015.

[5] A. Kumar *et al.*, “Behavior of nanoceria in biologically-relevant environments,” *Environ. Sci. Nano*, vol. 1, no. i, pp. 516–532, 2014.

[6] P. Pacher, J. S. Beckman, and L. Liaudet, “Nitric oxide and peroxynitrite in health and disease.,” *Physiol. Rev.*, vol. 87, no. 1, pp. 315–424, Jan. 2007.

[7] R. P. Patel *et al.*, “Biological aspects of reactive nitrogen species,” *Biochim. Biophys. Acta - Bioenerg.*, vol. 1411, no. 2, pp. 385–400, 1999.

[8] D. S. Goodsell, “Catalase,” *RCSB Protein Data Bank*, Sep. 2004.

[9] K. Rahman, “Studies on free radicals, antioxidants, and co-factors.,” *Clin. Interv. Aging*, vol. 2, no. 2, pp. 219–36, 2007.

[10] N. Shimizu, K. Kobayashis, and K. Hayashi, “THE JOURNAL OF BIOLOGICAL CHEMISTRY The Reaction of Superoxide Radical with Catalase MECHANISM OF THE INHIBITION OF CATALASE BY SUPEROXIDE RADICAL*,” vol. 259, no. 7, pp. 4414–4418, 1984.

[11] A. S. Karakoti *et al.*, “Nanoceria as Antioxidant: Synthesis and Biomedical Applications.,” *JOM (1989).*, vol. 60, no. 3, pp. 33–37, Mar. 2008.

[12] O. S. Ivanova *et al.*, “One-stage synthesis of ceria colloid solutions for biomedical use,” *Dokl. Chem.*, vol. 437, no. 2, pp. 103–106, Apr. 2011.

[13] B. Nelson, M. Johnson, M. Walker, K. Riley, and C. Sims, “Antioxidant Cerium Oxide Nanoparticles in Biology and Medicine,” *Antioxidants*, vol. 5, no. 2, p. 15, May 2016.

[14] B. Chance, “EFFECT OF pH UPON THE REACTION KINETICS OF THE ENZYME-SUBSTRATE COMPOUNDS OF CATALASE*,” 2017.

[15] E. Grulke, K. Reed, M. Beck, X. Huang, A. Cormack, and S. Seal, “Nanoceria: factors affecting its pro- and anti-oxidant properties,” *Environ. Sci. Nano*, vol. 1, pp. 429–444, 2014.

NONLINEAR FINITE ELEMENT ANALYSIS OF MICRO- LATTICE STRUCTURES FOR PATIENT-SPECIFIC IMPLANTS

Prashant Athanker and Amit Kumar Singh

Malaviya National Institute of Technology, Jawahar Lal Nehru Marg, Malviya Nagar, Jaipur, Rajasthan

ABSTRACT

The primary objective of this research paper is design and nonlinear finite element analysis of micro-lattice of Ti-6Al-4V implants using the Bauschinger effect. Micro-lattice cellular Ti-6Al-4V structures are commonly used for orthopedic application with an organized porosity and pore sizes appropriate for tissue ingrowth and organic process. In this research paper CAD model of different unit lattice structures with design variables such as strut length, strut cross-section and pore size using Intra-Lattice software were designed. Intra-Lattice software is a parametric lattice demonstrating tool and is developed based on Grasshopper, a graphic algorithm editor for Rhino CAD software. In this study, three different unit cells are presented including a Grid (simple cubic), Star (body centered cubic) and Tesseract (hypercubic) structure. The finite element analysis (FEA) technique is presented to analyze the mechanical properties of these three types of lattices-based cellular structure. For FE modeling, beam elements have been used to model the micro-lattice structures under different loading conditions (i.e. tension and compressive). The FE simulations were carried to predict the functional effectiveness and load-bearing effectiveness for the above three unit cells. In the last phase of this investigation, the unit cell topology was improved to increase the stiffness and yield stress under loading conditions. Finite Element Simulations demonstrate that the stiffness and yield strength can be enhanced by changing the unit cell geometry. The results of the above investigation will then be applied to patient-specific implants.

Keywords: Unit Cell, Lattice-Based Structures, Biomaterials, Finite Element Modeling, Bauschinger Effect

INTRODUCTION

In a lattice-based cellular structure implant, the pores size is the most important parameter for biomedical application [1]. Their mechanical properties mainly depend on the porosity, and the biomaterials used for implant fabrication. The advantages of cellular structures in common are light- weight structures, effective damping, high grade of deformation, high energy absorption capability and durability at dynamic loadings and fatigue [2]. The main complications with metallic implants in orthopedic surgery is the mismatch of the mechanical properties between bone and implant materials. Due to this mechanical divergence, bone is not sufficiently loaded and turns into stress-shielded, which ultimately leads to bone resorption [3]. Ti-based alloys demonstrate much lower elastic modulus than other metallic alloys such as Co-Cr alloy and 316L stainless steel [4]. An isotropic material is no longer isotropic after yielding and encounters kinematic hardening. For very large strain simulations, the linear kinematic hardening model can become inappropriate because of the Bauschinger effect. The nonlinear kinematic hardening is generally used for small strain, cyclic loading application. To model the Bauschinger effect and similar responses, where a hardening in tension will lead to a softening in a subsequent compression, one can use the kinematic hardening rule, shown in Figure is the 1. Results of Finite element analysis which demonstrates that the nonlinear model is superior to the linear model in the modeling of cyclic plasticity phenomena, specifically ratcheting [5]. The main objective of this paper is to design micro-lattice structures with different pore size, and subsequent nonlinear finite element analysis usin the Bauschinger effect.

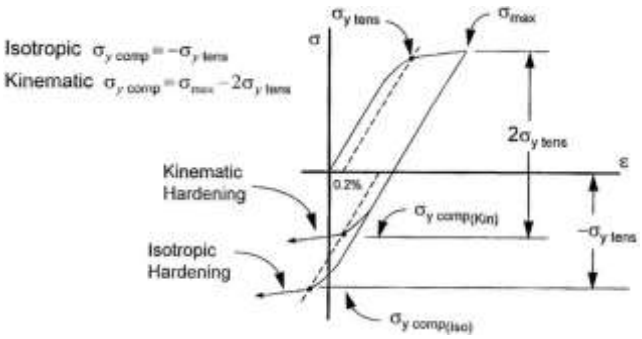

Figure 1: Bauschinger effect [7]

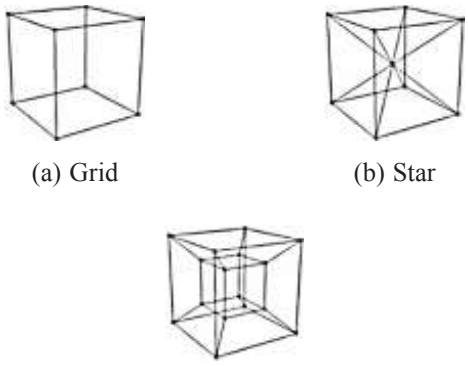

(a) Grid (b) Star

(c) Tesseract

Figure 2: Unlimited cell topologies (a) Grid, (b) Star, (c) Tesseract

MATERIAL AND METHODS

This paper aims at studying the three distinct Ti-6Al-4V micro-lattice structures (grid, star, and tesseract) which were modeled with four different pore size consideration using open-source INTRALATTICE software, developed at McGill's Additive Design & Manufacturing Laboratory (ADML, 2016). The outer wireframe of star and tesseract unit cell are same as a grid unit cell, but its internal architecture is different as shown in Figure 2. The design of four different pore sizes of three distinct micro-lattice structures with the same diameter (0.1 mm) is illustrated in Table2.

The beam elements were used to predict the Bauschinger effect. Subsequent yield in compression ($\sigma_{y\ comp}$) is decreased by the amount by which the yield stress in tension ($\sigma_{y\ tens}$) increased so that a $2\sigma_{y\ tens}$ difference between the yields is always maintained. (This is known as the Bauschinger effect). The porosity percentage of micro-lattice structures was evaluated from the weight and the apparent volume of the CAD model. Porosity = 100-[(Weight of the lattice part / The weight a dense part with the same size)*100%] [8].

Table 1: The twelve total block dimension of Ti-6Al-4V micro-lattice structure.

Sr. No.	Grid, Star, Tesseract unit cell topology Pore Size (mm)	Number of unit cell pattern in three direction Xn	n	Zn	Total lattice block dimensions approx. Length (mm)	Width (mm)	Height (mm)
1	0.75	9	9	14	7.75	7.75	12
2	1	7	7	11	7.8	7.8	12.2
3	1.25	6	6	9	8.2	8.2	12.25
4	1.5	5	5	8	8.1	8.1	12.9

RESULTS

The Ti-6Al-4V alloy stressed into the inelastic range in uniform tension is unloaded and then subjected to uniform compression in the opposite direction. From the FE simulations it is observed that the Bauschinger effect of tesseract is higher than of star for all pore sizes. The Young's modulus of elasticity (E) and density of Ti-6Al-4V material are 113.8 GPa and 4320 kg/m^3 respectively which is used as input data. The true stress-strain curve of all Ti-6Al-4V micro-lattice structures under uniform loading sequence (tension to compression) using Ansys Parametric Design Language (APDL) is shown in Figure 3.

Figure 4 (a) shows the relation of Bauschinger effect and porosity of star and tesseract micro- lattice structures. The total nodal displacement due to the uniform tension and compression of tesseract for pore size 1.25 mm is shown in Figure 4 (b) and (c).

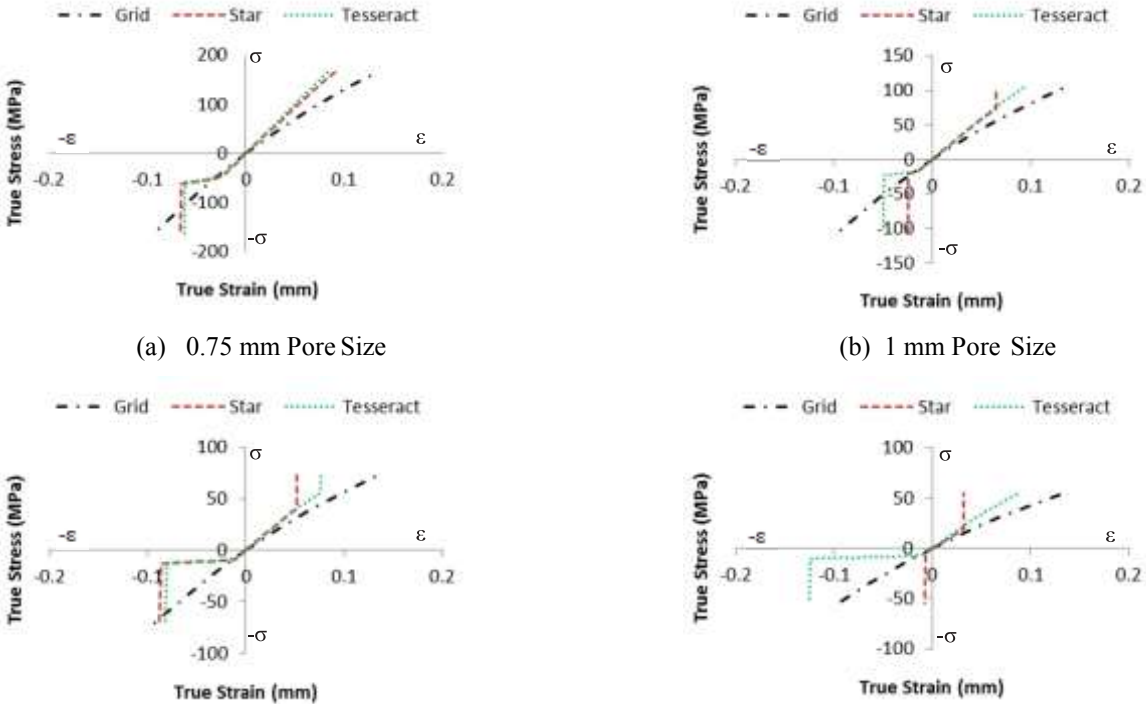

(a) 0.75 mm Pore Size (b) 1 mm Pore Size

(c) 1.25 mm Pore Size (d) 1.5 mm Pore Size

Figure 3: True stress vs. true strain curves at maximum node reaction with different pore size of structures under loading sequence (tensile to compressive): (a) 0.75 mm; (b) 1 mm; (c) 1.25 mm; (d) 1.5 mm

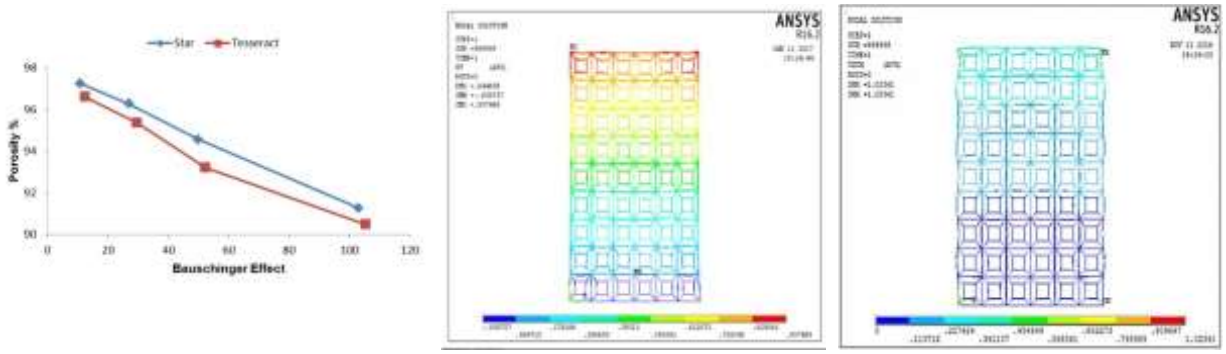

(a) (b) (c)

Figure 4: (a) Porosity % vs. Bauschinger effect; Total nodal displacement of tesseract structure of 1.25 mm pore size: (b) Tension mode; (c) Compression mode

DISCUSSION

In each case, it found that the nonlinear kinematic hardening (Bauschinger effect), predicted by the finite element (FE) analysis, the tension to compression loading sequence of micro-lattice structures has the lower porosity percentage thus implying higher Bauschinger effect, as seen in Table2.

Table 2: Star and tesseract type of micro-lattice structure and the properties of the beam element models

Sr.No.	Pore Size (mm)	Volume of dense part (mm3)	Volume of porous part (mm3)	Weight of dense part (gram)	Weight of porous part (gram)	Porosity %	Max. Tensile Stress (σ_{max}) (MPa)	Compressive Yield Stress ($\sigma_{y\,comp}$) (MPa)	Bauschinger Effect ($2\sigma_{y\,tens}$) (MPa)
Star micro-lattice structure									
1	0.75	720.75	62.92	0.0311	0.0027	91.27	166.52	63.70	102.81
2	1	742.24	40.38	0.0321	0.0017	94.56	74.65	24.88	49.77
3	1.25	823.69	30.68	0.0356	0.0013	96.28	41.98	15.09	26.89
4	1.5	846.36	23.07	0.0366	0.0009	97.27	19.18	8.57	10.61
Tesseract micro-lattice structure									
1	0.75	720.75	68.55	0.0311	0.003	90.49	165.71	60.55	105.16
2	1	742.24	50.32	0.0321	0.0022	93.22	71.89	22.12	52.17
3	1.25	823.69	38.06	0.0356	0.0016	95.38	55.19	12.74	29.45
4	1.5	846.36	28.5	0.0366	0.0012	96.63	17.55	5.31	12.24

CONCLUSIONS

Cortical bone does not illustration kinematic hardening and Bauschinger's effect. The Bauschinger effect would have transformed the yield points in tension and compression on the expense of each another, which is due to loading sequence process. We have selected an elasto-plastic model to illustrate the Bauschinger effect of different micro-lattice structure (similar, as cancellous bone structure) accumulations in tension and compression. Based on FE simulation results, it was found, the mechanical behavior and the porosity are intensely dependent on the lattice structure's architecture with uniform loading sequence. The proposed methodology illustrates how to predict a possible application for a 3D micro-lattice structure implant. Such methodology would be a favorable tool to include the loading mode dependent on type of lattice-based structure and plasticity into fracture risk investigation of bones and implant structures.

REEFERENCES

[1] C. Yan, L. Hao, A. Hussein, S. L. Bubb, P. Young, and D. Raymont, "Evaluation of light-weight AlSi10Mg periodic cellular lattice structures fabricated via direct metal laser sintering," J. Mater. Process. Technol., vol. 214, no. 4, pp. 856–864, 2014.

[2] M. Vesenjak and Z. Ren, "Yielding and post-yield behaviour of closed-cell cellular materials under multiaxial dynamic loading," Met. Mater. Int., vol. 22, no. 3, pp. 435–442, 2016.

[3] M. N. Ahsan, C. P. Paul, L. M. Kukreja, and A. J. Pinkerton, "Porous structures fabrication by continuous and pulsed laser metal deposition for biomedical applications; Modelling and experimental investigation," J. Mater. Process.Technol., vol. 211, no. 4, pp. 602–609, 2011.

[4] Y. Li, C. Yang, H. Zhao, S. Qu, X. Li, and Y. Li, "New Developments of Ti-Based Alloys for Biomedical Applications," pp. 1709–1800, 2014.

[5] T. Zhang, N. M. Harrison, P. F. McDonnell, P. E. McHugh, and S. B. Leen, "A finite element methodology for wear- fatigue analysis for modular hip implants," Tribol. Int., vol. 65, pp. 113–127, 2013.

[6] M. Muscat, D. Mackenzie, and R. Hamilton, "Evaluating shakedown under proportional loading by non-linear static analysis," Comput. Struct., vol. 81, no. 17, pp. 1727–1737, 2003.

[7] T. Matikas, "Low-cycle fatigue/high-cycle fatigue (LCF/HCF) interaction studies using a 10-to 40-kHz HCF loading device," in International Society for Optics and Photonics, 1999, pp. 98–106.

[8] X. Li, C. Wang, W. Zhang, and Y. Li, "Fabrication and characterization of porous Ti6Al4V parts for biomedical

applications using electron beam melting process," Mater. Lett., vol. 63, no. 3–4, pp. 403–405, 2009.

A NEW EXCITATION-BASED TECHNIQUE FOR ESTIMATING FRET EFFICIENCY

John Robert Griswold[1], Tom Rich[2,3], and Silas Leavesley[1,2,3]
[1]Departments of Chemical and Biomolecular Engineering, [2]Department of Pharmacology, and [3]Center for Lung Biology, University of South Alabama, Mobile, AL, USA

ABSTRACT

We have developed a novel hyperspectral imaging microscopy technique that filters excitation wavelengths and collects a bulk emission signal. We have previously shown that this excitation-based system can detect multiple fluorophores in live cells with high signal-to-noise ratios. Furthermore, this system is capable of faster acquisition times than conventional emission-based methods. This project aims to adapt our excitation-scanning technique for a new purpose: Förster Resonance Energy Transfer, or FRET. Though FRET is a ubiquitous tool in the biological sciences for measuring intermolecular distances, current spectral FRET detection methods suffer from poor signal-to-noise ratios, making it difficult to capture rapid cell-signaling events. This study's hypothesis was that excitation-scanning could provide improved signal strength for these measurements. Data were collected from HEK-293 cells transfected with a Turquoise-Epac-Venus FRET probe to monitor cyclic AMP, and treated with Forskolin, an adenylyl cyclase activator. Excitation light was provided by a Sutter VF-5 filter system connected to a 300W Xe arc lamp. Samples were excited from 380 to 490 nm, at 5 nm increments, and an image was acquired at each wavelength. Donor and acceptor excitation signals were resolved using linear unmixing and a spectral library acquired from single-labeled samples. FRET efficiency was determined by comparing donor signals at two dichroic filter cut-off wavelengths (458 and 495 nm). Results indicate that excitation-scanning could be a high-signal method for FRET estimation, but further optimization is required. If successful, this system will allow rapid acquisition of live-cell FRET image data along with simultaneous detection of other fluorescent markers.

Keywords: hyperspectral imaging, excitation, emission, Forster Resonance Energy Transfer, cyclic AMP, donor, acceptor

INTRODUCTION

Förster Resonance Energy Transfer, or FRET, is an indispensable tool in the biological sciences for measuring intermolecular distances.[1] FRET probes can be linked to sensor proteins, which change conformation when bound to certain signaling molecules. These conformational changes, in turn, lead to changes in FRET efficiencies, making FRET a spectroscopic tool for the detection of intracellular concentrations.[2]

Previous work has shown that FRET efficiencies can be measured using a technique known as hyperspectral imaging.[3] This microscopy technique requires a set of optical filters which sequentially collect a series of narrow bands of emitted light. By sampling the fluorescence emission at many narrow wavelengths we are able to reconstruct the emission spectrum of the sample. By collecting the emission spectra of single-label donor and acceptor samples and applying mathematical analysis algorithms such as linear unmixing, the emission spectrum of a FRET sample can be resolved into donor and acceptor intensity contributions. The ratio of these contributions can then be used to estimate FRET efficiency at each pixel in the image. We have shown the utility of this method in observing cyclic AMP (cAMP) gradients in the cell.[4]

Despite these promising results, there are limitations to the process outlined above; in the hyperspectral emission scanning technique, each filter collects only a small fraction of total photons being emitted at a given moment, so long acquisition times are needed to acquire sufficient signal at each wavelength. This weakness makes it difficult to use FRET to observe rapid cell-signaling processes.[5] Hence, a new method is needed for FRET detection, which can collect images with higher signal-to-noise ratios and consequently record images more rapidly without losing definition.

The goal of this research is to develop a FRET detection method called excitation-scanning hyperspectral imaging. In this approach, rather than filtering emission wavelengths at a constant excitation wavelength, the sample is excited at a range of wavelengths and a bulk emission signal is collected at each excitation wavelength. A long-pass dichroic beam splitter and long-pass dichroic filter ensure that only fluorescence signal reaches the camera. This system can distinguish fluorophores based on their excitation spectra, rather than their emission spectra. Because the entire emission signal is detected from each excitation event, higher signal-to-noise ratios can be achieved. We have already shown that excitation-scanning is an effective tool for distinguishing fluorescent labels in autofluorescent tissues.[6] Here, we describe an initial attempt to apply the excitation scanning

hyperspectral imaging approach to FRET microscopy measurements.

METHODS

The biological setup consisted of HEK 293 cells, transfected with an H188 FRET probe consisting of Venus-Epac-Turquoise. Epac is a protein that binds cAMP, triggering a conformational change, and leading to a change in FRET efficiency as described in the introduction. Cells were grown to confluency on coverslips.

Emission image data were acquired using a commercially available confocal microscope (A1+, Nikon USA) and a 60X water immersion objective (CFI Plan Apo VC 60XWI, Nikon USA) as previously described.[4]

Excitation image data were acquired using an inverted fluorescence microscope (TE-2000-U, Nikon USA, Melville, NY) equipped with an identical objective. Excitation light was generated with a 300W Xe arc lamp (Titan 300, SunOptics Technologies, Inc, Jacksonville, FL), connected to a tunable filter array (VF-5, Sutter Gmbh, St. Wendel, Germany). Light was emitted by the arc lamp, and the desired excitation wavelength was selected by the tunable filter. Light was then directed to the sample using a longpass dichroic beamsplitter. Fluorescence emission was detected using an EMCCD camera (Rolera em-c^2, Qimaging, Surrey, BC).

For each sample, timelapse hyperspectral image data were acquired for 10 minutes, with 1 scan acquired every 15 seconds. Cells were treated with 50 µM Forskolin (an adenylyl cyclase activator) at 2 minutes. For the emission scan, the sample was excited at 405 nm and emission was collected from 412 to 599 nm, in roughly 6 nm increments. Images were acquired at a rate of two frames/second. For the excitation scan, the sample was scanned from 380-490 nm, in 5 nm increments. A 495 nm and a 458 nm dichroic long-pass filter were used during excitation scanning. The camera exposure time was 50 ms.

Images were unmixed using single-label reference spectra, collected using both microscope systems and identical settings as those described above. The unmixing algorithm calculated venus and turquoise intensities at each pixel of the image collected. For emission scanning, FRET efficiency was obtained using the spectral (linear) unmixing method described in Leavesley et al.[7] Excitation-based FRET detection required a different equation that we are still optimizing.

RESULTS

Below are the preliminary results of FRET efficiency timelapse scans using emission- and excitation-based systems. In both scans, a reduction in FRET efficiency was observed, as cAMP concentration increased and probes entered the low FRET conformation.

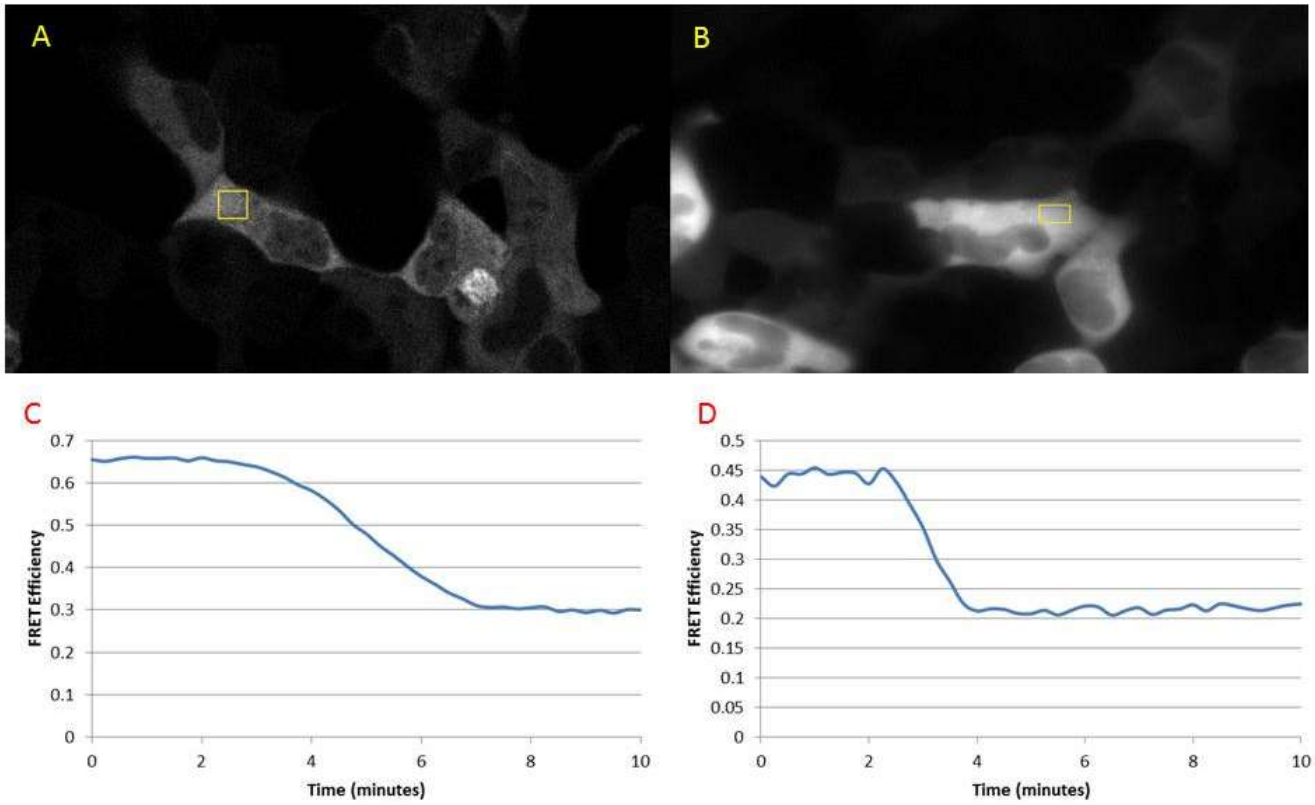

Figure 1: Results of timelapse FRET Scans. A and B show a single frame from the emission and excitation hyperspectral image data, respectively. The yellow boxes are the Regions of Interest selected for further analysis of FRET spectral image data, shown in C and D.

DISCUSSION

Our results indicate that FRET changes can be detected by using excitation scanning hyperspectral imaging microscopy. However, there are two important next steps to be taken before this technique can be adopted. First, we will need to reduce noise in the measurements, perhaps by incorporating a high-power and fast-switching speed light source. Second, we plan to install a new set of filters to allow us to measure FRET efficiency using emission and excitation methods simultaneously. This will allow us to verify FRET efficiency values for the same field of view, at the same time, for both excitation and emission scanning approaches.

CONCLUSIONS

Excitation-scanning hyperspectral imaging is a promising new method for FRET detection, though our method clearly requires significant improvement. Current hyperspectral techniques filter emission from the sample, attenuating the signal and requiring longer acquisition times. Excitation-scanning remedies this problem by filtering excitation instead, and distinguishing fluorophores by excitation signatures. This technology could offer an alternative approach for observing rapid cell-signaling events in real time.

ACKNOWLEDGMENTS

The authors would like to acknowledge support from NIH grants P01 HL066299, UL1 TR001417, S10 RR027535, S10 OD020149, and the Abraham Mitchell Cancer Research Fund. The authors also disclose financial interest SpectraCyte LLC, a startup company formed to commercialize spectral imaging technologies.

REFERENCES

[1] R. D. Mitra, C. M. Silva, and D. C. Youvan, "Fluorescence resonance energy transfer between blue-emitting and red-shifted excitation derivatives of the green fluorescent protein," *Gene*, vol. 173, no. 1, pp. 13–17, 1996.

[2] B. Ponsioen *et al.*, "Detecting cAMP-induced Epac activation by fluorescence resonance energy transfer: Epac as a novel cAMP indicator," *EMBO Rep.*, vol. 5, no. 12, p. 1176,

Dec. 2004.

[3] T. Zimmermann, J. Rietdorf, A. Girod, V. Georget, and R. Pepperkok, "Spectral imaging and linear un-mixing enables improved FRET efficiency with a novel GFP2-YFP FRET pair.," *FEBS Lett.*, vol. 531, no. 2, pp. 245–249, Nov. 2002.

[4] T. Rich *et al.*, "Real Time Four Dimensional Measurement of cAMP Gradients in Pulmonary Microvascular Endothelial Cells," *FASEB J.*, vol. 30, no. 1 Supplement, p. 1135.2-1135.2, Apr. 2016.

[5] S. J. Leavesley and T. C. Rich, "Overcoming limitations of FRET measurements," *Cytometry A*, vol. 89, no. 4, pp. 325–327, 2016.

[6] P. F. Favreau *et al.*, "Excitation-scanning hyperspectral imaging microscope," *J. Biomed. Opt.*, vol. 19, no. 4, p. 46010, Apr. 2014.

[7] S. J. Leavesley, A. L. Britain, L. K. Cichon, V. O. Nikolaev, and T. C. Rich, "Assessing FRET using spectral techniques.," *Cytom. Part J. Int. Soc. Anal. Cytol.*, vol. 83, no. 10, pp. 898–912, Oct. 2013.

MIRROR THERAPY FOR LOWER EXTREMITY RECOVERY AND GAIT IN SUBACUTE STROKE: A RANDOMIZED CONTROLLED TRIAL

Lisa J. Barnes and Kim Curbow Wilcox

Department of Physical Therapy, University of Mississippi Medical Center, Jackson, MS, USA

ABSTRACT

Stroke often leads to decreased mobility, strength, and motor control. During mirror therapy (MT), observing mirrored images of movement of the unaffected limb produces the appearance of movement on the affected side. MT has been shown to increase cortical activity in the affected hemisphere. The purpose of this study was to examine the effect of MT on lower extremity impairments in patients with sub-acute stroke. Participants were recruited upon admission to inpatient rehabilitation. Those meeting inclusion/exclusion criteria were randomly assigned to groups using computer randomization. The control group received traditional physical therapy (PT). The treatment group received traditional PT and daily MT exercises. Data was collected at admission and discharge. Thirty patients participated, ages 26 – 79 years, with 17 in the control group and 13 in the treatment group. Results indicate improved mean scores for all outcome measures at discharge. A significant difference was shown in between-group scores for lower extremity function measured by the Stroke Rehabilitation Assessment of Movement (STREAM) ($p < .05$); however, the control group had higher scores. No significant differences were found for the Functional Independence Measure locomotor score, the Timed Up and Go, or the basic mobility scores in the STREAM. Using MT as an adjunct intervention may benefit patients with subacute stroke by improving motor control and gait. However, this study did not indicate significant differences in outcomes compared to traditional physical therapy. Additional research is needed to determine the value of MT for rehabilitation of patients with subacute stroke.

Keywords: Mirror Therapy, Stroke, Lower extremity recovery

INTRODUCTION

This study was conducted by recruiting patients admitted to an inpatient rehabilitation facility for treatment following a stroke. Participants met specified inclusion/exclusion criteria, agreed to take part in the randomized controlled trial, and signed an informed consent. Inclusion criteria consisted of lower extremity recovery of at least Brunnstrom stage II, modified Ashworth score < 3, ability to follow a 3-step command in English, and unilateral involvement. Exclusion criteria included history of prior stroke, passive range of motion limitations of the hip and/or knee at less than 90 degrees, and visual deficits that would prevent observation during mirror therapy.

Thirty participants, ranging in age from 26 – 79 years ($m = 51.47$, $SD = 13.56$), were randomly assigned to either the control group or the treatment group by a computer-generated randomization process. Table 1 indicates demographic information of the participants by research group. Seventeen participants in the control group received traditional physical therapy rehabilitation interventions which included, but were not limited to, therapeutic exercise, functional mobility training, pre-gait and gait activities, electrotherapeutic modalities, and education. Thirteen participants assigned to the treatment group received traditional physical therapy interventions with the addition of MT exercises for 15 minutes per day. Mirror therapy included exercises for the unaffected lower extremity, focusing on ankle dorsiflexion, knee flexion, and hip flexion performed using a mirror to reflect movement of the unaffected lower extremity. Participants observed the mirrored image of the unaffected limb being visually overlaid on the affected side, creating the illusion of normal movement on the affected side during active exercise.

Data was collected by the research team upon admission and at discharge for statistical analysis. Standard outcome measures included in the study were the Functional Independence Measure (FIM), the Timed Up and Go (TUG), and the Stroke Rehabilitation of Movement (STREAM) lower extremity subscore and mobility subscore. This study was approved by the Institutional Review Board of the University of Mississippi Medical Center.

Table 1: Participant Demographics

N = 30	Control Group N = 17	Treatment Group N = 13
Males	10	9
Females	7	4
Right Side Lesion	12	7
Left Side Lesion	5	6
Ischemic Stroke	9	10
Hemorrhagic Stroke	8	3

RESULTS

Statistical analysis indicated that participants showed improved mean scores for all outcome measures at discharge (see Figures 1 - 3). Multivariate analysis of variance (MANOVA) indicated a statistically significant difference in between group discharge scores for lower extremity function measured by the STREAM ($p < .05$); however the control group had higher scores than the treatment group (see Figure 3). No statistically significant differences were found in the discharge scores for the FIM locomotor score ($p > .05$), the TUG ($p > .05$), or the basic mobility scores in the STREAM ($p > .05$) (see Figures 1- 3).

Figure 1: FIM Results – Mean (SD)

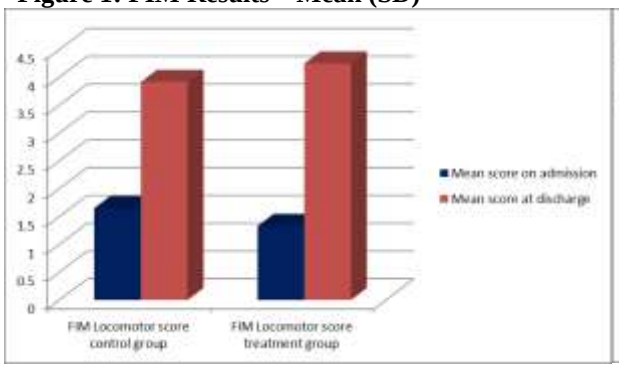

Admission 1.65 (1.06) Admission 1.33 (0.65)
Discharge 3.82 (1.38) Discharge 4.25 (0.62)

Figure 2: TUG Results – Mean (SD)

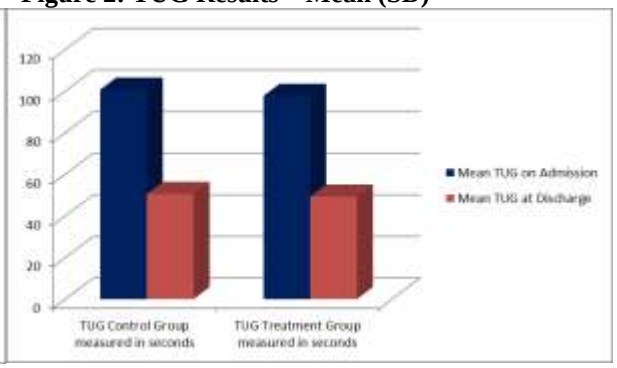

Admission 100.69 (53.42) Admission 97.75 (47.69)
Discharge 50.6 (34.88) Discharge 49.25 (15.96)

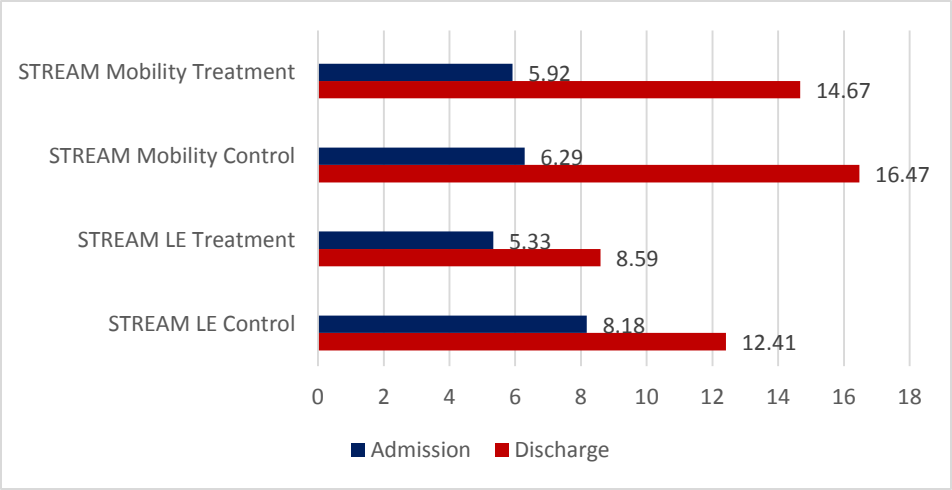

Figure 3: STREAM Results – Mean scores

DISCUSSION

Mirror therapy has been shown to be effective in the treatment of the upper extremity following stroke [5,6,7,8] but there are limited studies related to the use of MT in the treatment of the lower extremity post stroke. The small sample size and the variability of treatment sessions inherent within an inpatient rehabilitation facility were limitations of the study. Although findings from the study demonstrated no statically significant improvement in the rehabilitation of lower extremities following stroke, anecdotal reports from clinicians indicated clinical improvement in function. Additionally, participants reported enjoyment in the utilization of this treatment technique with a desire to continue incorporating the technique as part of the rehabilitation program.

CONCLUSIONS

The incorporation of mirror therapy for the lower extremity as an adjunct intervention in the rehabilitation of patients with subacute stroke may be clinically beneficial in improving lower extremity motor control and gait, but this study did not indicate significant differences in functional outcomes when compared to traditional physical therapy. Additional research is needed to determine the value of mirror therapy in the rehabilitation of patients with subacute stroke.

ACKNOWLEDGMENTS

The authors acknowledge the contributions of Boon Ong, Keri H. Moore, Amy Fountain, Gina McRae, and Pattie Stegall in the development and data collection for this study.

REFERENCES

1. Sutbeyaz S, Yavuzer G, Sezer N, Koseoglu F. Mirror therapy enhances lower-extremity motor recovery and motor functioningafter stroke: A randomized controlled trial. Archives of Physical Medicine and Rehabilitation. 2007;88:555-9.
2. Dohle C, Pullen J, Nakaten A, et al. Mirror therapy promotes recovery from severe hemiparesis: A randomized controlled trial. Neurorehabilitation and Neural Repair. 2009; 23(3):209-17.
3. Stevens JA, Stoykov MEP. Simulation of Bilateral movement training through mirror reflection: A case report demonstrating an occupational therapy technique for hemiparesis. Topics in Stroke Rehabilitation. 2004;11(1):59-66.
4. Michielsen ME, Selles RW, van der Geest JN, et al. Motor recovery and cortical reorganization after mirror therapy in chronic stroke patients: A phase II randomized controlled trial. Neurorehabilitation and Neural Repair. 2011;23:223-33.
5. Gurbuz N, Afsar SI, Ayas S, Cosar SNS. Effect of mirror therapy on upper extremity motor function in stroke patients: A randomized controlled trial. Journal of Physical Therapy Science. 2016;28:2501-6.
6. Kim K, Lee S, Kim D, Lee K, Kim Y. Effects of mirror therapy combined with motor tasks on upper extremity function and activities daily living of stroke patients. Journal of Physical Therapy Science. 2016;28:483-7.
7. Lim K, Lee H, Yoo J, Yun H, Hwang H. Efficacy of mirror therapy containing functional tasks in poststroke patients.Annals of Rehabilitation Medicine. 2016;40(4):629-36.
8. Yeldan I, Huseyinsinoglu B, Akinci B, Tarakci E, et al. The effects of very early mirror therapy on functional improvement of the upper extremity in acute stroke patients. Journal of Physical Therapy Science. 2016;27:3519-24.

AQUATIC THERAPY EFFECTS ON QUALITY OF LIFE AND FATIGUE IN MULTIPLE SCLEROSIS: A SYSTEMATIC REVIEW

Kimberly R. Willis and Lisa J. Barnes

Department of Physical Therapy, University of Mississippi Medical Center, Jackson, MS, USA

ABSTRACT

INTRODUCTION: Multiple Sclerosis (MS) is a progressive demyelinating disease affecting the central nervous system. It has been shown to cause excessive fatigue and decreased quality of life. Aquatic therapy is a water-based intervention utilizing the buoyancy and viscosity of water to improve strength, balance, and functional activities. The purpose of this review is to examine the effectiveness of aquatic therapy on decreasing fatigue and improving quality for those with MS. **METHODS**: PubMed and CINAHL databases were searched using search terms related to multiple sclerosis, aquatic therapy, and fatigue, with limitations of English language, date range 2010 - 2015, and human subjects. Inclusion criteria were patients with MS, aquatic therapy, and outcome measures assessing fatigue. Exclusion criteria were systematic reviews and case studies. Selected articles were scored using the PEDro and the Centre of Evidence Based Medicine (CEBM) 2011 criteria. **RESULTS**: Four articles were reviewed with an average PEDro score of 4.75 The CEBM scores were: two level II, one level III, and one level IV. Results of the article review suggested that aquatic therapy may be beneficial in improving quality of life and reducing fatigue in patients with MS.**CONCLUSION**: Aquatic therapy using total body interventions showed improvements in quality of life and functional movements in patients with MS. Evidence supported the use of aquatic therapy for the reduction of fatigue in those with higher initial fatigue levels. Aquatic therapy may be beneficial as an adjunct therapeutic activity as a means to decrease fatigue and improve perceived quality of life.

Keywords: Multiple Sclerosis, Aquatic therapy, Fatigue, Quality of Life

INTRODUCTION

Multiple Sclerosis (MS) is a progressive demyelinating disease affecting the central nervous system and causing muscle weakness, fatigue, loss of balance, and difficulty performing daily activities.[1-3] Onset is usually between 20 and 50 years of age with a peak onset at approximately age 30.[1,2] Multiple sclerosis, which is more common in women, currently has no known cure and has been shown to lead to excessive fatigue and negatively impact quality of life.[1,2] Fatigue may affect people with MS in all aspects of their lives, including physical, psychosocial, and cognitive well-being.[2] Treatment, which includes aquatic therapy, focuses on improving daily functioning and overall quality of life.[2] Aquatic therapy is a water-based intervention for people to perform strength training, balance activities, and to address performance of functional activities.[4] Due to the buoyancy and viscosity of water, individuals with MS are able to perform physical activities with less exposure to heat under gravity-reduced conditions, thus decreasing the chance of exacerbating symptoms.[2-4] The purpose of this systematic review is to determine the effectiveness of aquatic therapy on decreasing fatigue and improving quality of life in patients with MS.

METHODS

The experiments using human blood were approved by An electronic search of the PubMed and CINAHL databases was conducted in September 2015 using search terms related to multiple sclerosis, aquatic therapy, and fatigue. The terms were searched both individually and in combination. The search was limited to articles involving human subject, written in the English language, and with dates ranging from 2010 – 2015. The electronic search resulted in 14 articles to undergo the limitations process, which left six articles to be considered in the screening. The articles were then screened for duplication between the databases, titles, abstracts, and inclusion/exclusion criteria which resulted in 4 articles to be included in the review. Inclusion criteria were patients with multiple sclerosis who received aquatic therapy as a therapeutic intervention with an outcome measure utilized to assess fatigue. Articles that were systematic reviews or case studies were excluded from the review.

The articles chosen for the review were scored using Physiotherapy Evidence Database (PEDro) and the Centre of Evidence Based Measure (CEBM) 2011. The PEDro is an 11-point scale used to evaluate the internal validity of research in physical therapy with a higher score indicating a higher quality study. The CEBM, a 5-point scale with a lower score indicating a stronger study design, was used to evaluate the level of evidence and study design.

RESULTS

Results of the electronic search and the screening process led to four articles for inclusion in the systematic review. The average PEDro score was 4.75/10, with a range of 2/10 to 7/10. Levels of evidence assessed by the CEBM scale resulted in two studies at a level II, one scored at level III, and one scored level IV. Results of the article review suggested that aquatic therapy focusing on strength, flexibility, balance, and functional mobility may be beneficial in improving quality of life and reducing fatigue in patients with MS.

In an article by Bansi *et al.* [5], fifty-two patients with MS in an inpatient rehabilitation facility were randomized into one of two groups. All participants received physical therapy and occupational therapy twice daily. In addition to standard therapeutic activities, the control group used an ergometer at 50-60 revolutions per minute (RPM) for 30 minutes a day, 5 days per week for 3 weeks. The experimental group used an aquatic bike at 50-60 RPM with water temperature at 28˚C for the same frequency and duration. Both groups had a significant increase in health-related quality of life measured by the short form-36 (SF-36) ($p < 0.05$), and a significant decrease in the Modified Fatigue Impact Scale (MFIS) physical fatigue measure ($p < 0.05$). No significant differences were noted in the Fatigue Scale of Motor and Cognitive Functions (FSMC) total score or in the Modified Fatigue Impact Scale (MFIS) total score (see Figure 1). A between-group comparison showed significant differences in FSMC total ($p < 0.05$) and the FSMC motor function scores ($p < 0.05$) with the control group showing a greater decrease in levels of fatigue.

Kargarfard *et al.* [2], studied 21 females with MS. The control group maintained individually recommended treatment and activities with no specific interventions from the study. The experimental group performed aquatic exercise sessions for 60 minutes, 3 times per week for eight weeks working on strength, flexibility, balance, and mobility at a water temperature between 28-30˚C. The experimental group showed significant within group improvement in the Multiple Sclerosis Quality of Life-54 questionnaire (MSQOL-54) after 4 weeks & 8 weeks ($p < 0.001$) and a decrease in fatigue at 8 weeks ($p < 0.05$), while the control group showed no differences in the MSQOL-54 and significant worsening of fatigue ($p < 0.001$). Between group comparisons indicated that the experimental group showed significant improvements in quality of life measured by the MSQOL-54-physical ($p < 0.001$), MSQOL-54-mental ($p < 0.001$), and a significant decrease in fatigue in the MFIS overall score ($p = 0.002$) (see Figure 1) and the MFIS physical score ($p = 0.003$) when compared to the control group.

Bayraktar *et al.* [3], studied 18 females diagnosed with MS in which the participants were allowed to choose groups by individual preference. The control group participated in a home exercise program twice a week for 8 weeks. The experimental group participated in aquatic exercises at a water temperature of 28˚C for 60-minute group sessions at the same frequency and duration to work on strength, balance, flexibility, and relaxation. The experimental group showed significant within group improvements in measures of mobility and function which may be considered indicative of improved quality of life including single limb stance measuring balance ($p = .017$), the Timed Up & Go (TUG) measuring gait velocity ($p = .028$), and the 6-minute Walk Test (6MWT) measuring endurance ($p = .050$). Additionally, the experimental group demonstrated significant improvement in levels of fatigue measured by the Fatigue Severity Scale (FSS) ($p = .009$) (see Figure 1). No within group differences were found in the control group, and no between-group comparisons were reported.

Salem *et al.* [4], used a pre-post-test design to assess 10 participants with MS who completed an aquatic exercise training program. All participants completed 60 minute aquatic exercise sessions twice per week for 5 weeks at a water temperature of 31˚C focusing on flexibility, strength, and functional mobility. Pre-post-test measurements indicated improvements in balance and mobility which may be considered reasonable aspects of assessing quality of life including the Berg Balance Scale (BBS) measuring static and dynamic balance ($p = 0.008$), the TUG ($p = 0 .001$), and the 10-Minute Walk Test (10-MWT) measuring gait speed ($p = 0.049$). Levels of fatigue measured by the MFIS indicated no significant improvement (see Figure 1).

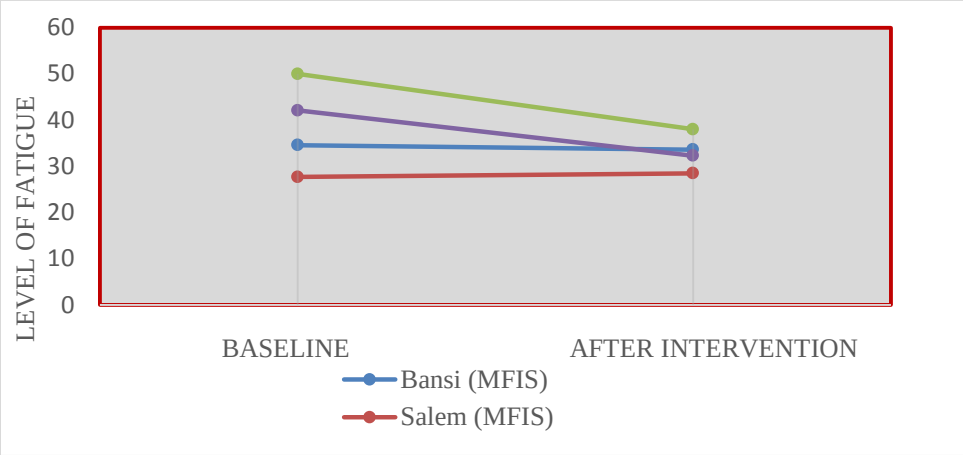

Figure 1: Effects of intervention of levels of fatigue

DISCUSSION

When comparing cycling exercises as in the article by Bansi *et al.*, [5] aquatic cycling showed no significant benefit in the reduction of fatigue when compared to land-based cycling. However other studies indicated that water-based exercises did results in improvements in fatigue levels. For example, in the two studies by Bayraktar *et al.* [3] and Kargarfard *et al.* [2], patients with MS who participated in total body water-based exercises with specific attention to the constructs of strength, balance, and flexibility did show significant improvement in fatigue levels. Studies indicated that patients who began aquatic therapy programs with higher levels of fatigue showed greater improvements in the reduction of fatigue after the intervention. Aquatic therapy also resulted in improvements in balance, endurance, and gait which may indicate an opportunity to promote a more active lifestyle in patients with MS. All studies showed some elements of improved quality of life with exercises using water-based techniques, whether through direct quality of life outcome measures, or functional outcomes that may contribute to improved quality of life.

CONCLUSIONS

Aquatic therapy which consisted of total body interventions showed improvements in perceived quality of life and measured quality of functional movements in patients with MS. This is noteworthy since MS is a disease that impairs motor control and functional mobility. Evidence supported the use of aquatic therapy for the reduction of fatigue in some instances with the most progress seen in patients suffering from higher initial levels of fatigue. Findings from this review suggest that aquatic therapy may be beneficial as an adjunct therapeutic activity for those living with MS as a means to decrease fatigue and improve perceived quality of life while living with this disease.

ACKNOWLEDGMENTS

The authors would like to acknowledge Gracy E Hewes and Natalie R Phongam for their contributions to the initial development of this project.

REFERENCES

[1] C. Goodman & T. Snyder, *Differential Diagnosis for Physical Therapists: Screening for Referrals*. St. Louis, MO: Elsevier, 2013.

[2] M. Kargarfard, M. Etemadifar, P. Baker, M. Mehrabi, and R. Hayatbakhsh, "Effect of aquatic exercise training on fatigue and health-related quality of life in patients with multiple sclerosis," *Archives of Physical Medicine and Rehabilitation*, vol. 93, no. 10, pp. 1701-1708, 2012.

[3] D. Bayraktar, A. Guclu-Gunduz, G. Yazici, J. Lambeck, H. Z. Batur-Caglayan, C. Irkec, and B. Nazliel, "Effects of Ai-Chi on balance, functional mobility, strength and fatigue in patients with multiple sclerosis: a pilot study," *Neuro Rehabilitation*, vol. 33, no. 3, pp. 431-437, 2013.

[4] Y. Salem, A. H. Scott, H. Karpatkin, G. Concert, L. Haller, E. Kaminsky, R. Weisbrot, and E. Spatz, "Community-based group aquatic programme for individuals with multiple sclerosis: a pilot study," *Disability and Rehabilitation*, vol. 33, no. 9, pp. 720-728, 2011.

[5] J. Bansi, W. Bloch, U. Gamper, S. Riedel, and J. Kesselring,. "Endurance training in MS: short-term immune responses and their relation to cardiorespiratory fitness, health-related quality of life, and fatigue," *Journal of Neurology*, vol. 260, no. 12, pp. 2993-3001, 2013.

THERAPEUTIC ULTRASOUND EFFECTIVENESS FOR NON-SPECIFIC CHRONIC LOW BACK PAIN: A SYSTEMATIC REVIEW.

Sherry T. Colson and Lisa J. Barnes

Department of of Physical Therapy, University of Mississippi Medical Center, Jackson, MS, USA

ABSTRACT

Background and Significance: Therapeutic ultrasound (US) is a commonly used intervention for physical therapy care of clients with non-specific chronic low back pain. The efficacy of passive US specific to chronic low back pain has recently been challenged. The American Physical Therapy Association (APTA) Choosing Wisely campaign stated "Don't employ passive physical agents except when necessary to facilitate participation in an active treatment program." The purpose of this systematic review is to determine the effectiveness of therapeutic ultrasound for decreasing pain and improving quality of life for patients with non-specific chronic low back pain. **Methods:** PubMed database was searched in February 2015 with no date restrictions. Search terms included back pain, lumbago, and therapeutic ultrasound. Electronic limitations were English language and Randomized Control Trials. Inclusion criteria: Age > 18 years, and nonspecific chronic low back pain for a duration > 3 months. Study quality was assessed using Physiotherapy Evidence Database scale and the 2011 Oxford Centre of Evidence Based Medicine scale. **Results:** The electronic search yielded 37 articles. Five articles met all the criteria for this review. The average PEDro score was 6/10. CEBM level of evidence scores revealed one study at level II and four studies at level III. **Conclusion:** Ultrasound combined with exercise may be more effective than exercise alone or placebo US combined with exercise to decrease pain and increase QOL measures in patients with chronic low back pain. However, US does not appear to be more effective than other modalities such as phonophoresis and electrical stimulation.

Keywords: Back pain, lumbago, therapeutic ultrasound, quality of life

INTRODUCTION

Therapeutic ultrasound (US) is a commonly used physical therapy intervention, specifically for those suffering from non-specific chronic low back pain (LBP). [1,2] The impact of therapeutic US is caused by vibrating sound waves at a level that produces heat, and the modality is delivered via continuous movement of a soundhead over the affected musculature. The increase in temperature within the tissue may decrease pain by increasing enzymatic activity and blood flow to the muscles. [3] Ultrasound is considered to be a passive modality. The efficacy of passive US specific to chronic low back pain has recently been challenged. [2, 4] The American Physical Therapy Association (APTA) Choosing Wisely campaign has stated "Don't employ passive physical agents except when necessary to facilitate participation in an active treatment program." [5] The purpose of this systematic review is to explore the effectiveness of therapeutic ultrasound for decreasing pain and improving the quality of life for patients with non-specific chronic low back pain

METHODS

An electronic search of PubMed database was conducted in February 2015 with no date restrictions. The search terms included back pain, lumbago, back pain or lumbago, and therapeutic ultrasound with terms searched in combination. This search strategy resulted in 196 articles. The resultant articles were then electronically limited to the English language and RCT's which left 37 articles to undergo the screening process. Screening of the articles by title and abstract eliminated 28 articles resulting in 9 for further consideration. The search inclusion criteria included subjects greater than 18 years of age and a diagnosis of nonspecific chronic low back pain that had been present for at least three months. Following the inclusion/exclusion screening process, five articles were chosen to be included in this review.

The articles were assessed for quality by scoring with the PEDro for internal validity, and the 2011 CEBM scale for the level of evidence and strength of the study. The PEDro scores ranged from 5/10 – 8/10 with an average score of 6/10 for a moderate level of internal validity. The CEBM scale uses a 5-point scale assessing strength of the evidence related to the study design with level I indicating the highest. The studies reviewed were RCT's with one at CEBM level II and four at level III.

RESULTS

rt Form 36 (SF-36). Within group comparisons showed that all groups had significant decreases in pain and increases is QOL measures ($p < 0.01$). Between groups comparisons revealed a significant decrease in the VAS pain scores for the experimental US and experimental

phonophoresis group when compared to the control ($p < 0.01$). However, there were no differences between the experimental US and experimental phonophoresis groups for pain. Subsets of the SF-36 that measure quality of life indicated significant improvements for the experimental phonophoresis group when compared to the experimental US group ($p < 0.05$), however there were no differences in the other QOL measures.

In an earlier study by Durmus *et al* [2] the researchers divided 59 female participants with chronic LBP into three groups that included: a control group receiving exercise alone, an experimental group receiving electrical stimulation and exercise, and a second experimental group that utilized US and exercise. Pain was measured utilizing the VAS and the PDI. Quality of life was measured using the ODQ and the SF-36. Within group comparisons revealed that all groups had a significant decrease in pain and an increase in QOL scores ($p < 0.05$). Between groups comparison showed a significant decrease in VAS pain scores in both experimental groups compared to the control group ($p < 0.05$). There were also significant improvements in SF-36 scores in both experimental groups compared to the control group. However, there were no significant differences noted between the two experimental groups for pain or QOL scores on any of the outcome measures.

Koldas *et al* [1] enlisted 55 participants with chronic LBP and assigned each participant to one of three groups. Group one received a home exercise program only. Group two received a home exercise program and participated in treadmill aerobic exercises. Group three received home exercises and a combination of hot packs, US and transcutaneous electrical nerve stimulation. The researchers utilized the VAS to measure pain, and the BDI, General Health Questionnaire (GHQ), and the Roland Morris Disability Questionnaire (RMDQ) to measure quality of life. All groups had significant improvements in pain scores ($p < 0.05$) noted upon within group comparisons. There were significant improvements in all QOL measures in the experimental US group ($p < 0.05$), and significant improvements in the GHQ in the experimental treadmill group. However, between groups comparison showed no significant difference in pain scores or QOL measures.

DISCUSSION

Three of the five studies indicated that exercise combined with other modalities such as US, electrical stimulation or phonophoresis lead to better reduction in pain levels than interventions consisting of exercise alone. Although some improvements in QOL scores were noted when these modalities were added to an exercise program, the results were inconsistent across the studies and across specific outcome measures utilized. One study simply compared the use of continuous US to a placebo US with the continuous US leading to significant improvements in pain and QOL. Interestingly, the placebo US group actually improved in both measures, possibly suggesting that the tactile sensation and slow rhythmic movement of the soundhead nay have induced a relaxation effect leading to some level of improvement.

Limitations of the studies included small sample sizes among the groups and a general lack of consistency among the studies in the manner in which comparisons were made.

CONCLUSIONS

Ultrasound combined with exercise may be more effective than exercise alone to decrease pain and increase QOL measures in patients with chronic low back pain. Ultrasound does not appear to be more effective than other passive modalities such as phonophoresis and electrical stimulation. Evidence showing the independent effects of US without other interventions, specifically exercise, seems lacking and further research is recommended.

ACKNOWLEDGMENTS

The authors would like to acknowledge Mabry L Bailey, Robert J Cooper, Jacob B Daniels, Joseph J Madden, and Tiffany A Lewallen for their contributions to the initial development of this project.

REFERENCES

[1] Koldas Dogan, S, Sonel Tur, B, Kurtais, Y, Atay MB. Comparison of three different approaches in the treatment of chronic low back pain. Clinical Rheumatology. 2008; 27(7):873-881.

[2] Durmus D, Durmaz Y, Canturk F. Effects of therapeutic ultrasound and electrical stimulation program on pain, trunk muscle strength, disability, walking performance, quality of life, and depression in patients with low back pain: a randomized-control trial. Rheumatology International. 2010; 30(7):901-910.

[3] Ebadi S, Ansari NN, Naghdi S, Jalaei S, Sadat M, Bagheri H, vanTulder MW, Henschke N, Fallah E. The effect of continuous ultrasound on chronic non-specific low back pain: a single blind placebo-controlled randomized trial. BMC Musculoskeletal Disorders. 2012; (13):192.

[4] Ansari N, Ebadi S, Talebian S, Naghdi S, Mazaheri H, Olyaei G, Jalaie S. A randomized, single blind placebo controlled clinical trial on the effect of continuous ultrasound on low back pain. Electromyography Clinical Neuro-physiology. 2006; 46(6):329-336.

[5] Five things physical therapists and patients should question [Internet]. Alexandria (VA): American Physical Therapy Association. 2014 Sept 14 [cited 2015 Apr 16]. Available from: http://www.choosingwisely.org/doctor-patient-lists/american-physical-therapy-association/

[6] Durmus D, Alayli G, Goktepe AS, Taskaynatan MA, Bilgici A, Kuru O. Is phonophoresis effective in the treatment of chronic low back pain? A single-blind randomized controlled trial. Rheumatology International. 2013; 33(7):1737-1744.

THE EFFECTS OF HIPPOTHERAPY ON GROSS MOTOR FUNCTION IN CHILDREN WITH CEREBRAL PALSY: A SYSTEMATIC REVIEW

Janet P. Slaughter and Lisa J. Barnes

Department of Physical Therapy, University of Mississippi Medical Center, Jackson, MS, USA

ABSTRACT

Background and Significance: Functional limitations can affect the proficiency of motor skills and the level of participation in daily activities in children with cerebral palsy (CP). Hippotherapy is an intervention that uses horseback riding and has been suggested to increase motor control and functional ability in children with CP. The purpose of this systematic review is to explore the effectiveness of hippotherapy as a therapeutic intervention to improve functional outcomes in children with CP. **Methods:** PubMed Database was searched through February 5, 2015. Specific search terms included those related to hippotherapy and children with CP limited to the English language. Inclusion criteria were children with CP, clinical trials, and the Gross Motor Function Measure (GMFM) as a functional outcome measure. Exclusion criterion was the use of horse simulators. **Results:** After a stepwise selection process, 5 articles remained for review. Four out of five articles showed a statistically significant improvement in gross motor function in children with CP after receiving hippotherapy as a therapeutic intervention. **Conclusion and Clinical Implications:** Evidence in all five articles demonstrated that hippotherapy led to clinically meaningful improvements in functional outcomes when compared to traditional physical therapy interventions. This systematic review supports the use of hippotherapy as a therapeutic intervention in children with CP as evidenced by consistently greater mean differences in functional outcomes for the hippotherapy groups compared to traditional physical therapy.

Keywords: Hippotherapy, Cerebral Palsy, Gross Motor Function Measure

INTRODUCTION

Cerebral Palsy (CP) is a group of disorders of movement and posture that is caused by damage to the developing fetal or infant brain [1]. The disorder itself is non-progressive; however, because of disturbances in the motor system, sensation, perception, communication, behavior, and secondary musculoskeletal impairments, it may appear to worsen at different points across the lifespan. Impairments in movement and posture lead to delay in gross and fine motor development. Secondary musculoskeletal impairments such as spinal deformity, hip dislocation, bony torsion, and muscle contractures may be caused by growth and/or abnormal muscle tone [1]. These impairments may lead to functional limitations. These limitations can affect the proficiency of motor skills and the level of participation in daily activities [2]. Hippotherapy is an intervention that uses horseback riding to facilitate postural and functional improvements [2,3]. The effects of hippotherapy on gross motor function in children with CP have been studied, and some indications of improved motor skills were found [2,3,4]. Hippotherapy is often a suggested intervention for this patient population in an effort to increase motor control and functional ability[2]. The purpose of this systematic review is to explore the efficacy of hippotherapy as a therapeutic intervention to improve functional outcomes in children with CP.

METHODS

An electronic search of the PubMed Database was searched through February 5, 2015, which resulted in 57 articles related to this topic. Specific search terms included those related to hippotherapy and children with CP in various combinations limited to the English language. These articles were screened according to the title, which eliminated 37 articles and left 20 for continued screen. Following the abstract screen 8 articles remained, and 3 of these were eliminated by the inclusion/exclusion criteria. Inclusion criteria were; children with CP, clinical trials, and use of the Gross Motor Function Measure (GMFM) as an outcome measure. Exclusion criterion was the use of horse simulators.

The five articles included in the review were scored using the PEDro scale, an 11-point scale developed to assess internal validity and the quality of methodology of clinical trials in physical therapy research. Higher PEDro scores are indicative of higher quality clinical trials, and the PEDro scores ranged from 2 to 7 with a mean of 4.8. In addition, the level of evidence was assessed using the 2011 Centre of Evidence Based Medicine (CEBM) scale, a 5-point scale in which a lower score indicates a higher level of evidence based primarily on study design. The CEBM scoring showed two studies at a level II, one study scored III, and two studies scored IV.

RESULTS

In a study by Kwon *et al.* [3], the authors randomly assigned 91 children ages 4 – 10 years into one of two groups to study the effects of hippotherapy on gross motor function. The intervention group received 30 minute sessions of hippotherapy twice a week for 8 weeks in addition to conventional physical therapy services. The control group received conventional physical therapy services in addition to 30 minutes of home-based aerobic exercises twice weekly for 8 weeks. Outcomes were assessed using the Pediatric Balance Scale (PBS), the Gross Motor Function Measure-66 (GMFM-66) and Gross Motor Function Measure-88 (GMFM-88). Results indicated that the intervention group showed significant within group improvements in the PBS ($p < 0.05$), the GMFM-66, and the GMFM-88 total, as well as in dimensions B, C, D, and E ($p < 0.01$). The control group only showed improvements in dimension B of the GMFM-88 which is related to sitting. When comparing the two groups, the intervention group showed a significant improvement in the PBS ($p < 0.05$), the GMFM-66, the GMFM-88 total, and dimensions B, C, D, and E of the GMFM-88 ($p < 0.05$) when compared to the control.

In an earlier study, Davis *et al.* [6] used the GMFM-66 to assess outcomes for 72 children with CP following hippotherapy intervention. The participants, who were 4 – 12 years of age, were randomly assigned to one of two groups. The children in the control group followed their normal routine including traditional therapies. The intervention group received 30-40 minutes of hippotherapy once per week for 10 weeks. Although no statistically significant difference was found between the two groups, the intervention group did show slightly better improvement as evidenced by the increase in the GMFM-66 scores.

In a study comparing the outcomes of thirty-two children with CP, Kwon *et al.* [4] allocated the participants, ranging in age from 4 – 10 years, into two groups. Both groups received conventional physical therapy treatment twice per week for 30 minutes each session for eight weeks. The children in the intervention group also received 30 minutes hippotherapy twice per week. The authors compared the results using the PBS, GMFM-66, and GMFM-88. The group receiving hippotherapy showed a significant improvement in PBS ($p = 0.004$), GMFM-66 total ($p = 0.003$), and GMFM-66 dimension E ($p = 0.042$) when compared to the group receiving conventional physical therapy alone. The GMFM-88 total was nearing significance in the hippotherapy group ($p = 0.054$) when compared to the control group.

In a repeated-measures time-series design, Casady *et al.* [5], followed 10 children with CP, ages 2.3-6.8 years over a 30 week period of time. The researchers used the Pediatric Evaluation of Disability Inventory (PEDI) and the GMFM-88 to assess before and after scores of the children in three 10-week phases: pre-treatment, intervention, and post-treatment. The PEDI is a measure of functional abilities in children from six months to 7.5 years of age. The children were assessed for pre and post scores of each outcome measure in the initial 10 weeks of no intervention. The intervention phase of the study consisted of 10 weeks of hippotherapy once per week for 20-30 minutes, which was also assessed using pre and post measures of the PEDI and GMFM-88. The post-treatment phase consisted of an additional 10 weeks with no hippotherapy measured in the same manner. Results showed no significant change between pretest and posttest measures in the PEDI or GMFM-88 scores during initial 10 week pre-treatment phase. During the treatment phase, significant improvements were noted between pretest and posttest measures of the PEDI and GMFM-88 scores following 10 weeks of hippotherapy ($p < 0.05$). Findings for the follow-up post-treatment phase showed no significant change between pretest and posttest measures in PEDI and GMFM 88 scores indicating that functional improvements were maintained during the 10 weeks following participating in a hippotherapy program.

In the last study explored in this review, Park *et al.* [2] recruited 55 children, ages 2-13, with spastic CP for participation in one of two study groups. The intervention group received 45 minutes of hippotherapy twice per week for 8 weeks in addition to 30 minutes of occupational therapy (OT) and physical therapy (PT) interventions once per week. The control group received 30 minutes of OT and PT once per week. The GMFM-66, GMFM-88, and the Pediatric Evaluation of Disability Inventory: Functional Skills Scale (PEDI-FSS) were used to assess outcomes of both groups. After eight weeks, within group outcomes indicated that the intervention group showed significant improvement in the GMFM-66, GMFM-88 total, and dimensions A, B, C, D, and E related to functional mobility ($p < 0.05$), as well as significant improvement in all subsets of the PEDI ($p < 0.05$). The children in the control group showed significant change in GMFM-66 and GMFM-88 total as well as dimension B, with no significant change in the scores for the PEDI. Between group comparison, indicated that the intervention group, which received hippotherapy, showed significant improvement in GMFM-66 and GMFM-88 dimension E ($p < 0.05$), as well as significant improvement in all subsets of the PEDI ($p < 0.05$) when compared to the control group.

DISCUSSION

The GMFM outcome measure is used to assess the functional mobility skills of lying and rolling (a), sitting (b), crawling and kneeling (c), standing (d), and walking, running, and jumping (e) in children with CP [3, 5]. Findings from this systematic review support the inclusion of hippotherapy as a therapeutic intervention in children with CP as evidenced by improved functional outcomes measured with the GMFM (see Figures 1 and 2). In addition to improved functional mobility, studies also indicated that hippotherapy may lead to improved balance reactions as evidenced by improved scores in the Pediatric Balance Scale. Children with CP traditionally have difficulty with balance and functional mobility skills due to tonal imbalances, decreased strength, range of motion deficits, and possible skeletal deformities that develop over time. Hippotherapy may offer an enjoyable therapeutic intervention which can lead to positive improvements in mobility and quality of life for these children.

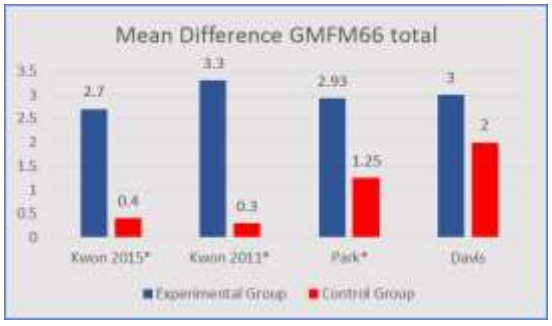

Figure 1:
Mean Difference GMFM-66 total

Figure 2
Mean Difference GMFM-88 total

CONCLUSION

In the studies explored in this review, all children who received hippotherapy as an intervention showed improvements over the duration of the intervention period. Hippotherapy led to clinically meaningful improvements in mobility and balance outcomes when compared to traditional physical therapy alone. Results found within these studies supported the use of hippotherapy as an adjunct therapeutic intervention in children with CP.

ACKNOWLEDGMENTS

The authors would like to acknowledge Victoria L. Gaskin, Hannah K. Hogue, Megan E. Laird, Anna F. Spence, and Tara N. Tharp for their assistance in gathering the information for this review.

REFERENCES

[1] P. L. Rosenbaum, N. Paneth, A. Leviton, M. Golstein, and M. Bax, "A report: The definition and classification of cerebral palsy," *Developmental Medicine and Child Neurology Suppl*, 109, pp. 8-14, 2007.

[2] E. S. Park, D. W. Rha, J. S. Shin, S. Kim, and S. Jung, "Effects of hippotherapy on gross motor function and functional performance of children with cerebral palsy," *Yonsei Med J*, vol. 55, no, 6, pp. 1736-1742, November 2014.

[3] J. Y. Kwon, H. J. Chang, S. H. Yi, J. Y. Lee, H. Y. Shin, and Y. H. Kim, "Effect of hippotherapy on gross motor function in children with cerebral palsy: A randomized controlled trial," *J Altern Complement Med*, vol 21, no 1, pp. 15-21. 2015.

[4] J. Y. Kwon, H. J. Chang, J.Y. Lee, Y. Ha, P. K. Lee, and Y. H. Kim, "Effects of hippotherapy on gait parameters in children with bilateral spastic cerebral palsy," *Arch Phys Med Rehabil*, vol 92, pp. 774-779, May 2011.

[5] R. L. Casady and D. S. Nichols-Larsen, "The effect of hippotherapy on ten children with cerebral palsy. *Pediatr Phys Ther*, vol. 16, pp. 165-172, Fall 2004.

[6] E. Davis, B. Davies , R. Wolfe, R. Raadsveld, B. Heine, P. Thomason, F. Dobson, and H. K. Graham, "A randomized controlled trial of the impact of therapeutic horse riding on the quality of life, health, and function of children with cerebral palsy," *Dev Med Child Neurol*, vol. 51, pp. 111-119, February 2009.

.

THE EFFECT OF DRY NEEDLING ON PAIN CONTROL AND POSSIBLE MECHANISM

Felix Adah, Min Huang, and Mark Weber

Department of Physical Therapy, University of Mississippi Medical Center, Jackson, MS, USA

ABSTRACT

Background and Significance: Pain is a common problem of patients seen in physical therapy clinic that attracts varying therapeutic interventions. Recently, the literature is replete with conflicting reports that dry needling (DN) can reduce pain, reduce inflammation and thereby improve function. There are conflicting reports in the literature that DN of myofascial trigger points (MTrPs) or trigger points (TrPs) is efficacious in reducing spinal pain. Therefore, the purpose of this study to evaluate the effect of DN treatment in patients with neck pain and to review the literature for possible mechanism of action of dry needling if there is a preponderance evidence of DN in pain control. **Methods:** The PubMed database was accessed through January 27, 2016 using dry needling for patients with neck or back pain. Specific search terms and combination strategies are presented. Electronic limitations included randomized control trial. Inclusion criteria included spine and/or neck regions, pain measurements, and local needling. Exclusion criteria included injections as primary interventions. Study quality was evaluated using PEDro criteria. The PEDro is a 10-point scale for assessing internal validity (higher scores indicating higher quality). The studies were also scored using the 2011 Centre of Evidence Based Medicine (CEBM) scale. This is a 5-level scale that determines a study's level of evidence based on the study's design with lower numbers indicating higher levels of evidence. The described search strategy identified seven studies meeting all requirements. The mean PEDro score of the studies was 6.57 with a range of 5 to 8. The CEBM frequency included three level II studies and four level III studies. Conclusion: The study demonstrated that DN treatment resulted in significant pain reduction and decreased sensitivity of pain in six of seven studies with the non-significant study also trending towards pain reduction. Six studies that measured ROM for an outcome measure demonstrated increased ROM of the cervical region after DN. **Discussion:** With the positive effect of DN treatment on pain reduction and increased ROM, one can deduce that patients with pain treated with DN can have an increase in function and ultimately improved quality of life. The possible mechanisms by which DN control pain are presented. The studies used in this systematic review had CEBM levels of II and III, which indicated a grade of B due to all 7 studies having CEBM levels of III or higher. **Conclusion and Clinical Implication:** DN as a modality is new in physical therapy. Chronic pain, such as neck pain, that may not respond to the traditional physical therapy (heat, exercise, and massage) may be relieved with DN treatment. It is suggested that, when considering treatment options for spinal pain and other chronic pain, DN treatment should be taken into consideration. More research is necessary to elucidate the mechanism by which DN reduces chronic pain and to carry out comparative studies between DN and other physiotherapeutic modalities.

Keywords: Dry needling, pain, myofascial trigger points, acupuncture, mechanism.

INTRODUCTION

Pain is a common problem of patients seen in physical therapy clinic that attracts varying therapeutic interventions. Recently, the literature is replete with conflicting reports that dry needling (DN) can reduce pain, reduce inflammation and thereby improve function. There are conflicting reports in the literature that DN of myofascial trigger points (MTrPs) or trigger points (TrPs) is efficacious in reducing spinal pain. The mechanism by which DN reduces pain is also not fully elucidated. The application of DN (thin filiform needles) employs different techniques, including but not limited to winding, several stabbings (pistonings) of the needle into the site, inserting the needle into the site for a certain amount of time and electrical dry needling (EDN). Irrespective of the technique of application, pain reduction of varying degrees may be observed as demonstrated in the literature. Also, Acupuncture and DN may have different philosophies but procedure of inserting the needle into the body is essentially the same and both are targeting pain reduction essentially. However, what is not very clear is the mechanism by DN affects pain control. The mechanism is complex and not fully elucidated. In this study, DN and acupuncture may not be differentiated as they could be used interchangeably in this review. It is speculated that MTrP is developed due to increased release of acetylcholine (ACh) from motor endplates and $Ca2^{+}$ resulting in continuous state of localized shortening and contractures of sarcomeres (muscle contraction) [8]. There is localized hypertonicity which then begin to cause ischemia and hypoxia [9], and subsequently, chemicals (such as bradykinin, prostaglandins, serotonin, calcitonin gene-related peptide (CGRP) and substance P) responsible for the propagation of pain and inflammation

are released. In addition, several inflammatory cytokines, such as tumor necrosis factor-α (TNF- α), interleukin-1ß (IL-1ß), interleukin-6 (IL-6), and interleukin-8 (IL-8) are released [9]. High level of H^+ ions and adenosine triphosphate (ATP) [10], are released resulting in low pH which further propagates the action of ACh (inhibition of acetylcholinesterase). The continuous presence of factors of pain and inflammation results in sensitization of the sensory afferent nerve fibers of the muscle and this may explain the point tenderness of MTrPs [10, 11, 12]. Eventually, this may lead to central sensitization of the dorsal horn neurons (which is an increase of the excitability of neurons within the central nervous system) causing pain hypersensitivity. The question is, why is DN able to mediate pain reduction in MTrPs and other tissues? Several theories are advanced in the literature. Many theories are proposed that do not present clear mechanism. Therefore, the purpose of this review is to evaluate the effect of DN treatment on spinal pain (neck) control and present possible mechanism for its action.

METHODS

In order to evaluate the effect of DN on pain control, studies of DN in pain originating from the spine were used for the study. PubMed database search was conducted. Inclusion Criteria included randomized controlled trial, spine and/or neck pain, pain measurement, and local needling. The exclusion material included acupuncture and injections. Screening strategy involved electronic screening using dry needling and (cervical pain or lumbago or lumbalgia or thoracic pain and this resulted in 57 articles. When this was filtered with randomized controlled trial, the articles narrowed to 17 in number. The study was scored by PEDro Scale, which is a 10-point scale with higher scores reflecting higher internal validity and second method of scoring is CEBM Scale with Levels I-V with higher levels reflecting stronger level of evidence based on study design. The second part that relating to the mechanism of action, the literature was reviewed for possible mechanism of action of DN.

RESULTS

The described search strategy identified seven studies meeting all requirements. The mean PEDro score of the studies was 6.57 with a range of 5 to 8. The CEBM frequency included three level II studies and four level III studies which resulted in a grade of B, see results on Table 1 and Figure 1. The study demonstrated that DN treatment resulted in significant pain reduction and decreased sensitivity of pain in six of seven studies with the non-significant study also trending towards pain reduction [5,7,6,1,3,4]. Six studies that measured ROM for an outcome measure demonstrated increased ROM of the cervical region after DN [5,7,6,1,3,2]. Rather than a ROM measure, one study used a Neck Pain Questionnaire for disability, and DN treatment significantly decreased the score [7]. A synergistic effect was observed when DN of TrPs was combined with DN of paraspinal muscles; the combined treatment improved overall ROM and general welfare more than DN treatment alone in one of the studies [1]. Another observation is that when LTRs are elicited, DN treatment was more effective in pain reduction compared to when no LTRs elicitation as reported in one of the studies [2]. Conversely, two of the studies [3,4] found DN to be less effective at reducing pain and overall ROM when compared to non-localized acupuncture [4] and laser treatment [3] respectively. With the positive effect of DN treatment on pain reduction and increased ROM, one can deduce that patients with pain treated by DN can have an increase in function and ultimately improved quality of life. The studies used in this systematic review had CEBM levels of II and III, which indicated a grade of B due to all 7 studies having CEBM levels of III or higher.

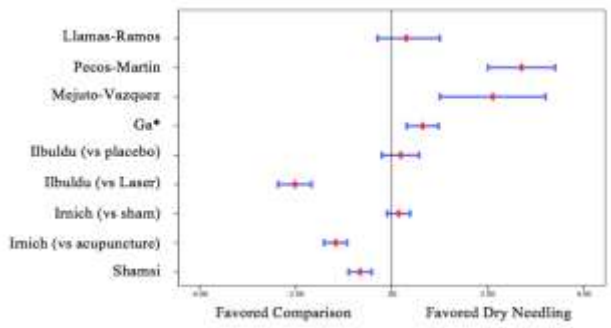

Figure 1: Immediate Post Treatment Pain Comparison of Dry Needling to
Alternate Interventions. * = 1 week post-treatment effect on pain

Study Summary Table 1.

Study	Level of Evidence	Subjects	Interventions	Outcome Measures	Results
Llamas-Ramos, R et. al [5]	II	94 subjects with chronic mechanical neck pain, randomly assigned to one of two groups	Group 1-TrP DN (n=47). Group 2-TrP MT (n=47).	-11-point numeric pain rating scale -Cervical ROM -PPT -Northwick Park Neck Pain Questionnaire for level of disability	Within Group: TrP DN and TrP MT decreased neck disability, decreased pressure pain sensitivity and increased cervical ROM ($p < 0.001$) at 1-week and 2-week follow-ups. Between Groups: TrP DN decreased pressure pain sensitivity values compared to TrP MT ($p < 0.01$). For other outcomes variables. no difference ($p > 0.01$) between the groups.
Pecos-Martin, D et. al [7]	II	72 subjects with active trigger points in lower trapezius, randomly assigned to 1 of 2 groups.	Group 1- DN MTrP in lower trapezius (n=36). Group 2: DN in the lower trapezius muscle, 1.5 cm medial to MTrP (n=36).	Visual Analog Scale (VAS) for pain, Neck Pain Questionnaire (NPQ) for disability score, and Pressure Pain Threshold (PPT).	Within Group: DN MTrP decreased neck pain, neck disability scores and decreased pressure pain sensitivity ($p< 0.001$). The control only decreased pressure pain sensitivity at 1-week and 1-month follow-ups ($p<0.001$). Between Groups: Group 1 decreased neck pain, neck disability and pressure pain sensitivity compared to Group 2 at 1-week and 1-month follow-ups ($p<0.001$).
*Mejuto-Vasquez, MJ et. al [*6]	II	17 subjects with neck pain, randomly assigned to one of two groups	Group 1-one session of TrP DN in upper trapezius muscles (n=9). Group 2-no intervention (n=8).	PPT -11-point numeric pain rating scale -Cervical ROM 10 minutes and 1 week post treatment	Within Group: Group 1 showed decreased pressure pain sensitivity values and increased cervical ROM immediately post-treatment and 1-week follow-ups ($p<0.001$). Group 2 showed no decrease in pain immediately post-treatment or at 1 week follow-ups ($p>0.01$). Between Groups: Group 1 demonstrated pain reduction, decreased pressure pain sensitivity, and increased cervical ROM compared to Group 2 ($p<0.001$).
Ga, H et.al [1]	III	40 subjects with upper trapezius myofascial pain syndrome, randomly assigned to one of two groups	Group 1-TrP DN of upper trapezius muscles (n=18). Group 2-TrP DN and paraspinal DN of upper trapezius muscles (n=22).	VAS for pain -FACES for pain -PPT -GDS-SF	Within Group: Group 1 and Group 2 decreased pain using VAS and PPT values ($p<0.001$). Both groups improved passive ROMs ($p<0.05$) except for extension ROM in Group 1 ($p>0.05$). Between Groups: No difference between groups for pain and PPT variables ($p>0.05$). Group 2 demonstrated difference compared to Group 1 for depression reduction and cervical extension increase ($p<0.05$).
Ilbundu, E et. al [3]	III	60 subjects with upper trapezius trigger points, randomly assigned to one of three groups	Group 1-Placebo laser (PL). Group 2-Dry needling (DN). Group 3-Treatment laser (L). Applications to upper trapezius muscles.	10cm-Visual Analog Scale for pain, Nottingham Health Profile (for functional assessment), and cervical ROM.	Within Group: All groups decreased pain at rest and activity ($p<0.05$) post-treatment except at six-month follow-up. Group 3 decreased pressure pain sensitivity ($p<0.001$). Flexion ROM increased with Groups 2 and 3. Extension ROM increased with Group 3 ($p<0.001$). Between Groups: Group 3 demonstrated greater decrease in pain compared to Group 1 and Group 2. Groups 2 and 3 increased flexion ROM but only Group 3 increased extension ROM ($p<0.001$). No difference was seen at six-month follow-up.
Irnich, D et. al [4]	III	36 subjects with chronic neck pain and limited mobility of cervical spine, randomly assigned to one of six treatment sequences. 34 subjects completed the trial.	Six different treatment sequences were created, each subject received a sham laser acupuncture treatment, DN, and NLA but in random sequences. Assessments were done immediately before and after treatment.	-VAS 0-100mm -ROM -Assessment of Changes of General Complaints (11 point rating scale -5=much worse, 0=no change, +5=much better)	**Within Group:** NLA demonstrated a trend showing a large decrease in pain. DN and sham treatments showed similar trends of minimally decreasing pain. **Between Group:** NLA was shown to decrease pain more effectively ($p=0.00006$) compared to DN ($p=0.7$).
Hong, CZ [2]	III	58 subjects, randomly assigned to 1 of 4 groups	Group 1– MTrP injections with 0.5% lidocaine plus elicited LTR Group 2–MTrP DN of upper trapezius muscle plus elicited LTRs Group 1a–subjects from group 1 in whom no LTR was elicited. Group 2a– subjects from group 2 in whom no LTR was elicited.	Subjective pain intensity Pain threshold of the TrP Range of motion of cervical spine	Within Group: Group 1 and Group 2 interventions reduced pain, decreased pressure pain sensitivity and increased cervical ROM ($p<0.05$) immediately after treatment and two-weeks after treatment. However, Group 1a and Group 2a interventions failed to decrease pressure pain sensitivity or increase cervical ROM ($p>0.05$) immediately after treatment. Group 1a reduced pain intensity immediately after injection ($p<0.05$). However, with LTR elicited, all outcome variables improved ($p<0.05$). Between Group: Group 1 was not statistically different from Group 2; however, 2 weeks after treatment, the reduction in pain intensity was significantly greater ($p<0.05$) in Group 1 than in Group 2.

TrP=Trigger point; MT=manual therapy; MTrP=myofascial trigger point; VAS=Visual Analog Scale; NPQ=Neck Pain Questionnare; PPT=Pressure Pain Threshold; FACES=Wong Baker Faces Scale; GDS-SF=Geriatric depression scale-short form; ROM=range of motion; DN=dry needling; NLA=non-localized acupuncture; LTR=local twitch response.

DISCUSSION

The results of this review favor DN in pain control and possible increased quality of life. The application of DN (thin filiform needles) employs different techniques, including but not limited to winding, several stabbings of the needle into the site (sometimes referred to as "pistoning"), inserting the needle into the site for a certain amount of time and electrical dry needling (EDN). Irrespective of the technique of application, pain reduction of varying degrees may be observed as demonstrated by this current review. Also, Acupuncture and DN may have different philosophies but the procedure of inserting the needle into the body is essentially the same and both are targeting pain reduction essentially. In this discussion DN refers to needling using acupuncture or dry needling techniques. However, what is not very clear is the mechanism by DN affects pain control. The mechanism is complex and not fully elucidated. In this discussion, DN and acupuncture may not be differentiated in mechanism. Several theories are advanced in the literature.

Localized Twitch Response (LTR): This is produced by repeatedly tapping a needle into sensitive loci in MTrPs which is said to cause nociceptive afferent information to be sent to the spinal cord resulting in activation of α motor neurons. Reflexive localized twitch response (LTR) may be produced to help clear the neuromuscular junction of excess ACh [13] and this continued to be reproduced until the excess ACh at the neuromuscular junction is fully depleted. There is also a reduction of CGRP and SP in LTR produced DN [09]. However, DN is said to reduce pain in tissues without neuromuscular junction needed to cause LTR [14].

Mechanotransduction: The winding or rotation of the needle in one direction or both directions and not repeated tapping of the needle in the MTrps pulls on collagen fibers causing better alignment of collagen bundles and it is said that this can stimulate the cells such as c-fibers activation via mechanotransduction [15]. Mechanotransduction can also release other receptors that may result in calcium wage propagation (CWP) and ATP release [16]. Rotation of needle after insertion is said to cause upregulation of Rho and Rac kinases. The inhibition of rho kinase prevented viscoelastic in fibroblasts which may help to reduce pain and increased remodeling of painful tissues.

Electric Dry Needling: Some clinicians perform electrical stimulation through the needles when inserted in the target tissues. This coupling of electrical stimulation and dry needling (electric dry needling -EDN) is said to lead to significant reduction in P2X3 expression (increased during injury), attenuates ATP stimuli [17] and improvement in thermal and mechanical pain thresholds [18]. EDN is said to reduce pain due to partial depletion of peripheral CGRP stores and eventually a low-level, sustained release of CGRP. Also, EDN may reduce SP released from the dorsal horn and peripheral nerve endings [19, 20, 21]. The paradoxical action of CGRP to promote inflammation and increase blood flow through vasodilation is said to lead to healing in osteoarthritis pathology. It is believed that CGRP mediates nitric oxide (NO), a vasodilator, release from endothelial cells [28, 29] and this may be effected through muscle contraction by EDN. It is also reported EDN may help to reduce systemic inflammation through activation of the hypothalamic-pituitary-adrenal (HPA) axis, and corticosterone (cortisol in human) from the adrenal cortex, prevents the production of inflammatory cytokines by inhibiting TNF- α and cyclooxygenase (cox-2) synthesis [22], thereby increasing opioid-based pain reduction. DN and EDN increases Aß fiber activation which may directly stimulate the substantia gelatinosa, thereby closing the door on pain from the periphery to the CNS [23]. Loaiza et al. [24], reported increase in blood flow because of balance between autonomic nervous system and release of NO following EDN, causing microcirculation to the knee joint. Needling is reported cause modulation of multiple bilateral cortical and subcortical limbic and paralimbic structures and the action was to decrease signal intensity in the limbic and paralimbic systems and increase signal intensity in the somatosensory cortex [25]. Biella et al [26] reports that acupuncture, a proxy for DN, "activates the left Anterior Cingulus, the Insulae bilaterally, the cerebellum bilaterally, the left Superior Frontal Gyrus, and the right Medial and Inferior Frontal Gyri. Most of the activated areas are shared with areas activated in acute and chronic pain states as described in the literature". According to the researcher [26], Acupuncture role could be as conflicting message in the pain neuromatrix, unbalancing it and then modify the perception of pain. In other words, pain is relieved by unbalancing the equilibrium of distributed pain-related central networks.

Other mechanisms: The work of Napadow et al [27], demonstrated that needling signal decreases (deactivation) of the limbic brain regions including the amygdala and the hypothalamus. The significance of this is that, the amygdala is a center in the brain for emotion expression and emotional displays that may be associated with chronic pain may be ameliorated in needling or acupuncture treatments.

CONCLUSION

With the positive effect of DN treatment on pain reduction and increased ROM seen in this study, one can

deduce that patients with pain treated by DN can have an increase in function and ultimately improved quality of life. The possible mechanisms by which DN control pain are complex and may involve decreasing inflammatory cytokines, releasing opioids, vasodilation and increased blood flow. Also, many organs or systems are involved and these includes but not limited to the cortex, the hypothalamus, the spinal cord and the limbic systems. DN as a modality is new in physical therapy. Chronic pain, such as neck pain, that may not respond to the traditional physical therapy (heat, exercise, and massage) may be relieved with DN treatment. It is suggested that, when considering treatment options for spinal pain and other chronic pain, DN treatment should be taken into consideration. More research is necessary to elucidate the mechanism by which DN reduces chronic pain and to carry out comparative studies between DN and other physiotherapeutic modalities.

REFERENCES

[1]. Ga, H., et al. Dry needling of trigger points with and without paraspinal needling in myofascial pain syndromes in elderly patients. J Altern Complement Med. 2007 Jul-Aug;13(6): 617-24.

[2]. Hong, CZ., et al. Lidocaine injection versus dry needling to myofascial trigger point. The importance of the local twitch response." Am J Phys Med Rehabil. 1994 Jul-Aug;73(4): 256-63.

[3]. Ilbuldu, E., et al. Comparison of laser, dry needling, and placebo laser treatments in myofascial pain syndrome. Photomed Laser Surg. 2004 Aug;22(4): 306-11.

[4]. Irnich, D., et al. Immediate effects of dry needling and acupuncture at distant points in chronic neck pain: results of a randomized, double-blind, sham-controlled crossover trial. Pain. 2002 Sep;99(1-2): 83-9.

[5]. Llamos-Ramos, R., et al. Comparison of the short-term outcomes between trigger point dry needling and trigger point manual therapy for the management of chronic mechanical neck pain: a randomized clinical trial. J Orthop Sports Phys Ther. 2014 Nov;44(11): 852-61. doi: 10.2519/jospt.2014.5229. Epub 2014 Sep 30.

[6]. Mejuto-Vasquez, MJ., et al. Short-term changes in neck pain, widespread pressure pain sensitivity, and cervical range of motion after the application of trigger point dry needling in patients with acute mechanical neck pain: a randomized clinical trial." J Orthop Sports Phys Ther. 2014 Apr;44(4): 252-60. doi: 10.2519/jospt.2014.5108. Epub 2014 Feb 25.

[7]. Pecos-Martin, D., et al. Effectiveness of dry needling on the lower trapezius in patients with mechanical neck pain: a randomized controlled trial. Arch Phys Med Rehabil. 2015 May;96(5):775-81

[8]. Unverzagt C, Berglund K, Thomas JJ. Dry needling for Myofascial trigger point pain: A clinical commentary. Int J Sports Phys Ther. 2015 Jun;10(3):402-18.

[9]. Gerwin RD, Dommerholt J, Shah JP. An expansion of Simons' integrated hypothesis of trigger point formation. Curr Pain Headache Rep (2004); 8: 468-475.

[10]. Shah JP, Gilliams EA. Uncovering the biochemical milieu of myofascial trigger points using in vivo microdialysis: an application of muscle pain concepts to myofascial pain syndrome. J Body Mov Her. 2008;12: 371-384. 13. Rossi SG, D

[11]. Mense S. The pathogenesis of muscle pain. Curr Pain Headache Rep. 2003; 7:419-425.

[12]. Shah, JP, Danoff, JV, Desai, MJ, et al. Biochemicals associated with pain and inflammation are elevated in sites near to and remote from active myofascial trigger points. Arch Phys Med Rehabil. 2008; 89:16-23.

[13]. Hsieh YL, Chou LW, Joe YS, et al. Spinal cord mechanism involving the remote eُوects of dry needling on the irritability of myofascial trigger spots in rabbit skeletal muscle. Arch Phys Med Rehabil. 2011;92: 1098-1105.

[14]. Qerama E, Fuglsang-Frederiksen A, Kasch H, et al. A double-blind, controlled study of botulinum toxin A in chronic myofascial pain. Neurology. 2006; 67: 241-245.

[15]. Zhang ZJ, Wang XM, and McAlonan GM. Neural acupuncture unit: a new concept for interpreting eُوects and mechanisms of acupuncture. Evid Based Complement Alternat Med 2012: 429412.

[16]. Wu SY, Chen WH, Hsieh CL et al. Abundant expression and functional participation of TRPV1 at Zusanli acupoint (ST36) in mice: mechanosensitive TRPV1 as an "acupuncture-responding channel". BMC Complement Altern Med14:96. 83.

[17]. Tu WZ, Cheng RD, Cheng B et al. Analgesic eُوect of electroacupuncture on chronic neuropathic pain mediated by P2X3 receptors in rat dorsal root ganglion neurons. NeurochemInt. 2012;60: 379-386. 120.

[18]. Cheng RD, Tu WZ, Wang WS et al. Eُect of electroacupuncture on the pathomorphology of the sciatic nerve and the sensitization of P2Xâ‚ƒ receptors in the dorsal root ganglion in rats with chronic constrictive injury. Chin J Integr Med.

2013; 19: 374-379.
[19]. Zhu LX, Zhao FY, Cui R. Eوect of acupuncture on release of substance P. Ann N Y AcadSci. 191;632: 488-489. 130.
[20]. Du J, He L. Alterations of spinal dorsal horn substance P following electroacupuncture analgesia--a study of the formalin test with immunohistochemistry and densitometry. AcupunctElectrother Res. 1992;17: 1-6. 131.
[21]. Hsieh YL, Yang CC, Liu SY et al. Remote dosedependent eوects of dry needling at distant myofascial trigger spots of rabbit skeletal muscles on reduction of substance P levels of proximal muscle and spinal cords. Biomed Res Int. 2014;982121. 132.
[22]. Lee JH, Jang KJ, Lee YT, Choi YH, Choi BT. Electroacupuncture inhibits inflammatory edema and hyperalgesia through regulation of cyclooxygenase synthesis in both peripheral and central nociceptive sites. Am J Chin Med. 2008; 34:981-988.
[23]. Kagitani F, Uchida S, Hotta H. Aوerent nerve fibers and acupuncture. AutonNeurosci. 2010; 157:2-8. 168.
[24]. Loaiza LA, Yamaguchi S, Ito M, Ohshima N. Electro-acupuncture stimulation to muscle afferents in anesthetized rats modulates the blood flow to the knee joint through autonomic reflexes and nitric oxide. Auton Neurosci. 2002; 31;97(2):103-9
[25]. Hui KK, Liu J, Makris N, Gollub RL, CHen AJ, Moore CI, Kennedy DN, Rosen BR, Kwong KK: Acupuncture modulates the limbic system and subcortical gray structures of the human brain: Evidence from fMRI studies in normal subjects. Hum Brain Mapp 2000; 9: 13-25.
[26]. Biella G, Sotgiu ML, Pellegata G, Paulesu E, Castiglioni I, Fazio F. Acupuncture produces central activations in pain regions. Neuroimage. 2001;14(1 Pt 1):60-6.
[27]. Napadow V[1], Kettner N, Liu J, Li M, Kwong KK, Vangel M, Makris N, Audette J, Hui KK. Hypothalamus and amygdala response to acupuncture stimuli in Carpal Tunnel Syndrome. Pain. 2007;130(3):254-66.
[28]. Erin N, Ulusoy O. Diوerentiation of neuronal from non-neuronal Substance P. RegulPept 152: 108-113. 123.
[29]. Langevin HM, Schnyer R, MacPherson H, Davis R, Harris RE, et al. (2015) Manual and electrical needle stimulation in acupuncture research: pitfalls and challenges of heterogeneity. J Altern Complement Med 21: 113-128. 1

THE EFFECT OF COMBINATION TREATMENTS OF EPIGALLOCATECHIN-3-GALLATE, THYMOQUINONE, AND 5-FLUOROURACIL ON FADU NASOPHARYNGEAL CARCINOMA CELLS

Sharita M. Williams, Michelle Tucci, and Hamed Benghuzzi
University of Mississippi Medical Center, Jackson, MS, USA

ABSTRACT

Nasopharyngeal carcinoma (NPC) is a rare tumor that arises from epithelial neoplasms in the nasopharynx. It is a rare malignancy in most of the world. NPC is often misdiagnosed and mistreated due to the location of the tumor and non-specific symptoms. The cancer is poorly controlled with current treatment modalities. There is a need for treatment modalities that eradicate the cancer better with lesser side effects. In this study, the FaDu squamous cell carcinoma cell line was used to determine if a combination of drugs with different cell cycle sensitivity can effectively reduce the cancer cell load. There were a total of four different combinations. One combination consisted of all three treatments: EgCg, TQ, and 5-FU. The other three combinations were as follows: EgCg + TQ, EgCg + 5-FU, and TQ + 5-FU. The combination treatments were measured at 24, 48, and 72 hours. Our results indicate that all combinations were able to reduce cell number for the duration of the experiment. The combination of two drugs specifically a natural drug plus a chemotherapeutic drug proved to be effective in eradicating cancer. In addition, the combination of all three drugs proved to be most effective in cell reduction. Since a combination of drugs target more than one phase of the cell cycle, the cells were less likely to become resistant to two or more drugs. The data suggests a natural drug can be paired with a chemotherapeutic drug to yield significant reductions in cell number producing less adverse side effects.

Keywords: nasopharyngeal, nasopharynx, FaDu, EgCg, TQ, 5-FU, natural, combination, reduction.

INTRODUCTION

NPC is an epithelial neoplasm. The cancer is often misdiagnosed and usually detected after the tumor has metastasized. The location of the tumor dictates aggressive treatments that have significant side effects. The survival rate for this type of cancer is low and the reoccurrence rate is high. The current treatments are inadequate and additional studies are needed to slow the aggressiveness of this cancer. NPC is poorly controlled with current treatment modalities and in addition, they are accompanied by many side effects. Misdiagnosis and mistreatment of NPC due to the location of the tumor and non-specific symptoms often leads to a poor prognosis. Radiotherapy is considered the main treatment for early stages of NPC. Yet, this cancer is often discovered at advanced stages. Since NPC is highly chemosensitive, efforts have been made to incorporate chemotherapy into the primary treatment of the cancer [1]. The chemosensitive nature of the NPC may allow the cells to be treated with more natural agents such as green tea (EgCg) or thymoquinone (TQ), both of which have anticancer activity. Concurrent radiotherapy and chemotherapy has been proven to prolong survival in locoregionally advanced disease [2]. Surgery, when feasible, is reserved for nodes that fail to regress after radiotherapy and chemotherapy because gaining access to the nasopharynx is difficult [3]. There are a variety of chemotherapeutic drugs used in the management of NPC, and they may be given as a single drug or in combination with two or more drugs. The literature suggests that cancer cells treated with known chemotherapeutic agent 5-FU stops division of cells in the S phase of the cell cycle [4]. The chemosensitive nature of the NPC may allow the cells to be treated with more natural agents such as EgCg or TQ, both of which have anticancer activity. Limited and conflicting information exists regarding natural agents, EgCg and TQ. Both have shown to induce apoptosis and inhibit cancer cell growth in cancer cell lines. EgCg and TQ have demonstrated to stop cells in the G_0-G_1 phase of the cell cycle and induce apoptosis [5]. One of the main problems in treating NPC is that over time the cancer cells can become resistant to chemotherapeutic drugs. The combination of two or more drugs will make it more difficult for cells to become resistant. Combination chemotherapy regimens for head and neck cancers have shown higher response rates and toxicity levels than single drugs [6]. Therefore, there is a need for treatment modalities that eradicate the cancer better than current modalities with fewer side effects and lessen chance for development of resistance.

METHODS

The IC_{50} for 5-FU, TQ, and EgCg were determined.

Cells were incubated in a 96 well plate and varying concentrations of each drug ranging from 1 x 10^{-3} M to 1 x 10^{-9} M were tested in triplicate using an MTT assay. The IC_{50} results were 3µM of EgCg and 16 µM of TQ and 5-FU. Cell cultures were exposed with 3µM of EgCg and 16 µM of TQ and 5-FU in four combinations administered by conventional methods. All cultures were incubated for 24, 48, and 72 hours. Additional cells were grown on coverslips and at the end of each time point the cells on coverslips were fixed and stained with hematoxylin and eosin. Images were taken captured using Image Pro software and the cells were evaluated for cytological changes and damage.

Groups	Treatment	Duration of Trial	Groups (N)
1	Control (cells only*)	24, 48, & 72 hours	18
2	EgCg & TQ	24, 48, & 72 hours	18
3	EgCg & 5-FU	24, 48, & 72 hours	18
4	TQ & 5-FU	24, 48, & 72 hours	18
5	EgCg, TQ, 5-FU	24, 48, & 72 hours	18

RESULTS

Cell counts are shown in Figure 1 for 24, 48, and 72 hours after FaDu cells have been treated by conventional methods with IC_{50} doses for the following combinations: EgCg + TQ, EgCg + 5-FU, TQ + 5-FU, and EgCg + TQ + 5-FU. Cells treated with a combination of EgCg + 5-FU and TQ + 5-FU showed significant reductions in cell numbers by 33% and 38%, respectively while EgCg + TQ had a 21% reduction. Combining all three compounds (EgCg + TQ + 5-FU) resulted in a 46% in cell number compared to control at 24 hours. The combination of EgCg + TQ + 5-FU reduced the cells by half after 48 hours ($p<0.05$). After 48 hours, the combination of EgCg + 5-FU had a 36% a reduction in cell number while the combination of TQ + 5-FU resulted in a 41% of cell number. The combination of EgCg + TQ showed only a modest reduction in cell number at 24 and 48 hours. After 72 hours, the combination of EgCg + TQ showed a further reduction in cell number. Accordingly, the combinations of EgCg + 5-FU and TQ + 5-FU both had significant reductions of 38%. The combination of all three compounds (EgCg + TQ + 5-FU) at 72 hours was effective in reducing the cell number by 50%. Cellular morphological changes were also evident as early as 24 hours following treatment, and by 72 hours the most noticeable nuclear changes were observed (Figure 2). Morphological changes in the TQ and 5-FU treatment groups showed evidence of cytolysis and hydropic swelling as early as 24 hours following treatment and persisted for the duration of the study.

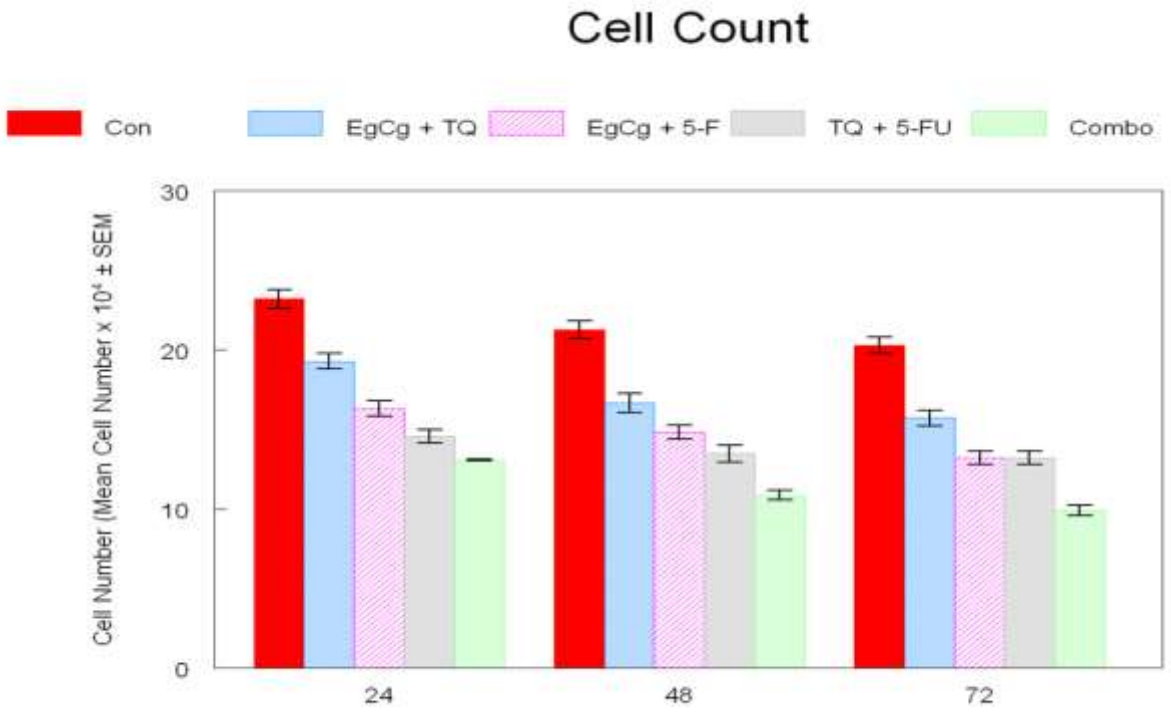

Figure 1. Cell count for cells treated with combination drugs using hemacytometer method. Data are reported as mean x 10^4 cells/mL ± SEM. The experiment was repeated 3 times and the data reflect all three experiments n= 15 wells per time point.

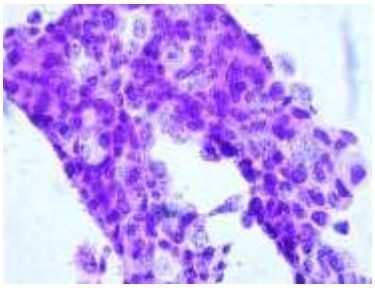

Control

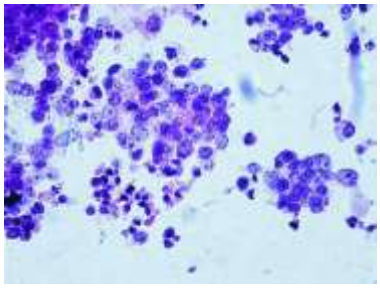

EgCg + 5-FU

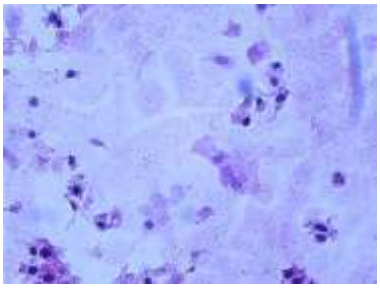

EgCg + TQ

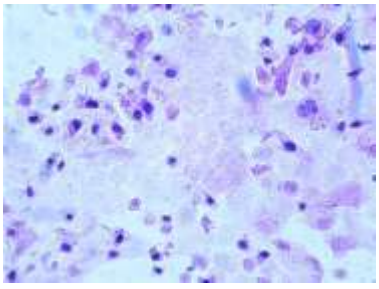

TQ + 5-FU

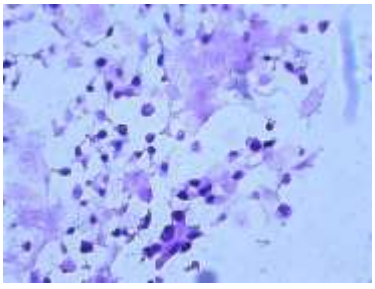

EgCg + TQ +5-FU

Figure 2. Representative of FaDu cells treated for 72 hours with a combination of drug treatments.

DISCUSSION

The dose to reduce cell numbers by 50% for each of the compounds tested was determined using a sensitive MTT assay. A least sensitive hemacytometer counting method was employed which has a higher degree of variability than the MTT assay. We were able to show a time dependent trend in decline of cell numbers indicating a decrease in cell survival with time in the combination treatments with the greatest decline seen in the combination of all three compounds. The two natural compounds combined (EgCg + TQ) had the lowest reduction at each time interval of 24, 48, and 72 hours. The two natural drugs combined possibly targeted the same phase of the cell cycle. Yet, when each natural drug was combined with the chemotherapeutic drug (5-FU) a significant reduction was observed in the two different combinations. The combination of the two natural compounds plus the chemotherapeutic drug (EgCg + TQ + 5-FU) had the greatest reduction in cell number at each time interval. The combination of a natural drug plus the chemotherapeutic drug, 5-FU, or two natural drugs plus 5-FU proved to be more effective since they each targeted different phases of the cell cycle. There was a significant reduction in cell number only after 24 hours in all combinations when compared to the control. All four combinations had over 20% reduction at 24 hours, with two having over a 30% reduction at 24 hours, and one having over a 40% reduction at 24 hours. Observing the time dependent trend higher reductions were noted in all combinations at 48 hours. EgCg + TQ slightly increased to reduce cell number at 48 hours while EgCg + TQ + 5-FU increased to reduce cells by 50% at 48 hours and EgCg + 5-FU & TQ + 5-FU reduced cell number over 35% at 48 hours. The reduction of the combination of EgCg + TQ + 5-FU at 72 hours was over 50% while EgCg + 5-FU and TQ + 5-FU both had significant reductions of 38% at 72 hours. It cannot be ruled out that the combination of natural products in combination with 5-FU induced ROS that comprised the integrity of the cell's mitochondrial membrane as evidenced by the increase in cell swelling and cytolysis observed at all time points. All three compounds have been shown at IC_{50} concentrations to induce significant ROS generation leading to activation of signaling pathway which lead to apoptosis [7-9]. Additional studies are warranted to determine the effects of the natural compounds on specific cycle targets as well as to determine changes in mitochondrial ATP generation.

CONCLUSIONS

Natural products can be paired with a chemotherapeutic drug to yield a significant reduction in cell number possibly causing less adverse side effects. EgCg or TQ can be combined with 5-FU to reduce cell number. The combination of any two drugs especially a natural product plus a chemotherapeutic drug proved to be effective in reducing FaDu cell number. The combination of EgCg + TQ + 5-FU proved to be most effective in cell reduction. Cytolysis and hydropic swelling are indicators of significant cell injury, and suggests the combination treatment increased cellular ROS. Literature suggests TQ and EgCg have the potential to halt cells in the G_0/G_1 phase of the cell cycle, while 5-FU is a known S phase specific drug. It is possible that the combination of drugs target more than one phase of the cell cycle. More research is needed in this area. Cells treated with compounds that affect more than one part of the cell cycle may be less likely to develop drug resistance.

REFERENCES

[1] Langendijk, J., Leemans, C. R., Butler, J., Berkhof, J., & Slotman, B. J. (2004). The Additional Value of Chemotherapy to Radiotherapy in Locally Advanced Nasopharyngeal Carcinoma: A Meta-Analysis of the Published Literature. *Journal of Clinical Oncology, 22*(22), 4604-4612.

[2] Chan, A., P. Teo, et al. (2002). "Nasopharyngeal Carcinoma." Annals of Oncology 13: 1007- 1015.

[3] Cho, W. (2007). "Nasopharyngeal Carcinoma: Molecular Biomarker Discovery and Progress." Molecular Cancer **6**(1).

[4] Wilkes, GM & and Barton-Burke, M. 2009 Oncology Nursing Drug Handbook. Sudbury, MA: Jones & Bartlett Publishers, 2008.

[5] Tan, M., Norwood, A., May, M., Tucci, M., & Benghuzzi, H. (2006). Effects of (-) epigallocatechin gallate and thymoquinone on proliferation of a PANC-1 cell line in culture. *Biomedical Sciences Instrumentation, 42*, 363-371.

[6] Wheeler, RH. (1990). Chemotherapy of patients with recurrent head and neck cancer. Cancer Treatment Research 52:171-193.

[7]. Mankhar M, Fatima I, Saxena R, Chandra V. Sankhar PL, and Dwivedia. (-) Epigallocatechin 3-gallate induced apoptosis in human endocarcimona cells via ROS generation and p38 MAP kinase activation. Nutritioanl Biochemistry Vol. 24, Issue 6, June 2013, pgs 940-947.

[8] El-Najjar, Chatila N., Moulkadem H. Reactive oxygen species mediate thymoqinone-induced apoptosis and activate ERK and JNK signaling. Apoptosis. February 2010, Volume 15, Issue , pp 183-185.

[9] Fu Y., Yang G., Zhu F., Peng C, Li W, Li H, Kim H-G, Bode AM, Dong Z, and Dong Z. Antioxidants decrease the apoptotic effect of 5-FU in colon cancer cells by regulating Src dependent caspase-7 phosphorylation. Cell Death and Disease (2014) 5, e983; doi10.1038/cddis.2013.509.

THE EVALUATION OF ANTIHYPERTENSIVE AGENTS USING CARDIOMYOCYTES

Shana Nelson, Michelle Tucci, and Hamed Benghuzzi

University of Mississippi Medical Center, Jackson, MS, USA

ABSTRACT

Cardiovascular disease (CVD) is the leading cause of death and hospitalization in the United States. Risk factors that lead to an increase in developing CVD include genetic, behavioral, psychosocial factors, and other underlying conditions. Hypertension is one example of underlying conditions that are risk factors and comorbidities. Treatment options for CVD and other underlying factors may affect the course of the disease. Antihypertensive drugs, such as calcium channel blockers (CCB), beta blockers (BB), or angiotensin converting enzyme inhibitors (ACEI) are used to treat hypertension. The objective of our study was to compare the cellular effects of an ACEI, captopril, on cardiomyocytes. Cardiomyocytes were grown in a tissue culture environment under normal conditions and challenged with therapeutic concentrations of captopril. Over time in culture there were significant changes in cellular protein and intracellular glutathione concentration.

Keywords: CVD, Captopril, Anti-hypertensive

INTRODUCTION

Antihypertensives are a class of drugs that are used to treat hypertension. Hypertension is an increase in the blood pressure of the arteries. Antihypertensive therapy seeks to prevent the complications of high blood pressure that lead to other cardiovascular complications, such as stroke and myocardial infarction. Angiotensin-Converting Enzyme (ACEI) Inhibitors blocks the conversion of angiotensin I to angiotensin II through competitive inhibition of the angiotensin converting enzyme. ACEIs are recommended as first line treatment option in patients with hypertension, especially if the patient is at risk or has heart failure, diabetes, and chronic kidney disease. Postmyocardial infarction patients are also prescribed ACEI. It is also used as a secondary stroke preventative measure [1]. For the purpose of this study we focused on captopril. Captopril was approved for use in the United States in 1981 and current indications are for hypertension, congestive heart failure, left ventricular dysfunction after myocardial infarction, and treatment and prevention of diabetic nephropathy. Studies show that captopril significantly reduces mortality in patients with heart failure. Captopril contains a sulfhydryl group, which may contribute to its pharmacologic action and account for some adverse reactions that occur at higher doses. The pharmacokinetics of captopril may be significantly affected by renal impairment and hemodialysis Captopril dilates arterioles, thus lowering total peripheral vascular resistance. In hypertensive patients, blood pressure is decreased with little or no change in heart rate, stroke volume, or cardiac output. However, captopril can increase cardiac output, cardiac index, stroke volume, and exercise tolerance in patients with congestive heart failure. The objective of our study was to compare the cellular effects of captopril on cardiomyocytes.

METHODS

Cell Line: American Type Culture Collection cell line H9c2 (2-1) (ATCC® CRL-1446™), is a subclone of the original cell line derived from the original clonal cell line of embryonic BD1X rat heart myocardium tissue by Kimes and Brandt [2]. Propagation of the cell line was followed by the ATCC complete growth medium (ATCC-formulated Dulbecco's Modified Eagles' Medium). Complete growth medium was prepared according to ATCC guidelines. Subculturing occurred when culture flasks were 80% confluent. Medium renewal was 2-3 times per week.

Experimental Design: This study consisted of two experimental groups that were grown in normal media. Group one served as a control containing H9c2 cardiomyocytes and media only. The remaining group contained H9c2 cardiomyocytes treated with an ACEI drug (Captopril). All groups were incubated in 24 well cell culture plates at intervals of 24, 48, and 72 hours.

Cellular Protein Determination: The Pierce BCA method is a technique utilized to determine the total protein content in both the control and experimental groups. Controls for the assay consisted of albumin calibration standards with known concentrations. For this procedure, 10 µL of cell suspension and 10 µL of aliquot standard were added to the wells of the microtiter plate. A reaction mixture was mixed using the following formula: total wells × 0.2 mL = total volume. A mixture of 50 parts Reagent A was added to 1 part Reagent B to yield the total reagent. A 200 µL aliquot of the reagent was added

to each well and placed in the incubator at 37° C for 30 minutes. When incubation was complete, the plates were read on a Spectra ELISA reader at an absorbance of 496 nm wavelength. This test will accurately measure the metabolic behavior of the H9c2 cells.

Cellular Glutathione Determination: Glutathione (GSH) is a tripeptide composed of glutamic acid, cysteine, and glycine. GSH is used as a measure of oxidative stress and cellular injury. A microtiter plate assay was used. Briefly, 50 µL of cells or standard were added to wells on 96 a well microtiter plate. Then 100 µL of a reaction mixture [1 ml of 2, 4 dinitrio-1-thiocynobenze (DNTB) (1mM), 1 ml of Nicotinamide adenine dinucleotide phosphate-oxidase (NADPH) (1 mM), 1.15 ml of buffer (100 mM phosphate buffer) and 0.02 ml of GSH reductase (200 U)] was added to each well. The microtiter plate was read at 405 nm immediately and at 30 minutes. Total reduced GSH was determined from the standard curve.

Morphological Evaluation: Representative slides were used for morphological evaluation. After each incubation phase, the cells were washed with 1 mL of phosphate buffed saline (PBS) to remove any remaining proteins. Zinc Formalin (10%) was used to fix the cells to the coverslips. The coverslips were stained using the hematoxylin and eosin staining procedure. Following staining, the coverslips were mounted cell side up to clear glass slides with mounting media. Imaging of the cells was performed using the Image- Pro Plus (Media Cybernetics, Rockville, MD).

Statistical Analysis: Experiments were performed in triplicates. Controls for each were compared to the experimental groups. The results of the experiments were expressed using the descriptive statistic of mean ± SE. Multiple comparisons were analyzed using the Dunn's Method for nonparmetric data where appropriate with SigmaPlot Version 12.0. The level of significance for this study was set at $p<0.05$.

RESULTS

Cellular Protein: Cardiomyocytes were grown in normal media. They were treated with captopril. Cellular protein was measured and shown in Table 1. Cardiomyocytes cultured in normal media showed a steady increase in protein concentration. By 72 hours, the protein concentration increased 28.7%. There is an increase in cellular protein levels over time for cells treated with captopril in normal media.

Cellular Glutathione: Cells were treated with captopril and cultured in normal media. The glutathione levels were measured and shown in Table 2. Cellular glutathione for cells treated with captopril show no significant differences at 24, 48, or 72 hours for normal media.

Table 1: Total protein levels in the media obtained from wells plated with H9c2 cells exposed to Captopril in normal media at 24, 48, and 72 hour phase (BCA assay, results expressed as Means±SE).

Group	Total Protein levels in all Phases (µL/mL)		
	24 Hours	48 Hours	72 Hours
Control	2.655±0.150	2.865±0.0999	3.543±0.136
Captopril	2.831±0.179	3.042±0.173	3.960±0.299

Table 2: GSH levels in the media obtained from wells plated with H9c2 cells exposed to Captopril in normal media at 24, 48, and 72 hour phase (results expressed as Means±SE).

Group	GSH levels in all Phases (µM/µg protein)		
	24 Hours	48 Hours	72 Hours
Control	0.624±0.0448	0.561±0.0624	0.476±0.0342
Captopril	0.500±0.0181	0.498±0.0259	0.424±0.0238

Morphological Evaluation

Cells treated with captopril for each time intervals grown in normal media are shown in Figure 1. Significant changes in nuclear area are present in cells treated with Captopril at 24-72 hours in normal media. Vacuolization was present in cells grown in normal media. Vacuoles are present in cells treated with Captopril at all time intervals in normal media. Hydropic swelling is evident in treated cells at 72 hours in normal media. Variations in cellular size are only seen in captopril treated cells cultured in normal media at 48 and 72 hours. Karyorrhexis is present in all cells treated with Captopril grown in normal media at all time intervals.

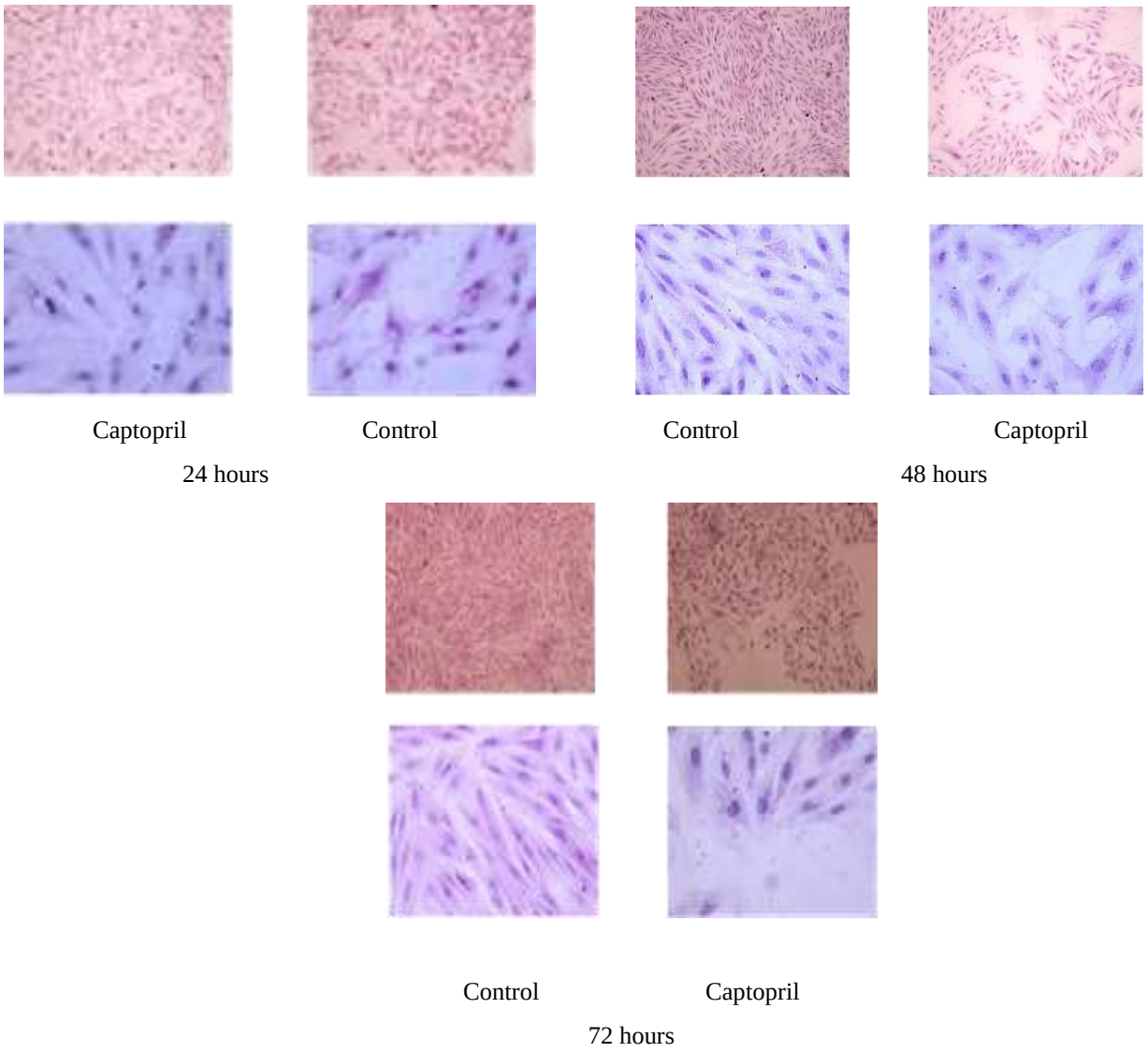

Figure 1: Representative photomicrographs of H9c2 cardiomyocytes in normal media treated with a single dose of Captopril after 24, 48, and72 hours of culture.

DISCUSSION

Many CVD patients have comorbidities that require simultaneous treatments. Hypertension is a very common condition that is often treated with captopril. This treatment has side effects that are associated with cardiovascular events. It is beneficial to have a mechanism to test the effects of such a treatment on cardiomyocytes. The effects of anti-hypertensive drugs on H9c2 cardiomyocytes grown in normal media can provide information to help in the selection of treatment options. In previous studies, captopril has proven beneficial in aiding in the treatment of diabetic patients [3].

CONCLUSIONS

The overall hypothesis of this study was that the use of an antihypertensive will cause a decrease in the growth and viability of cardiomyocytes. Our data supports the idea that the use of Captopril will cause damage to H9c2 cardiomyocytes in vitro.

REFERENCES

[1] Jones DW, Hall JE. (2004). Seventh report of the Joint National Committee on Prevention, Detection, Evaluation, and Treatment of High Blood Pressure and evidence from new hypertension trials. Hypertension, 43(1): pp.1-3.

[2] Kimes B, Brandt B. (1976). Properties of a clonal muscle cell line from rat heart. Experimental Cell Research, 98: pp. 367-381.

[3] Konzem SL, Devore VS, Bauer DW. (2002). Controlling hypertension in patients with diabetes. Am Fam Physician, 66(7): pp.1209-14.

TOWARDS THE PREVENTION OF OXIDATIVE DAMAGE VIA NOVEL ANTIOXIDANT CONJUGATES

Jeannette Rodriguez[1], Dmitry Gil[1], Vladimir Ivanov[2], and Vladimir Reukov[1,3]

[1]Department of Bioengineering, Clemson University, Clemson, SC, USA
[2]Kurnakov Institute of General and Inorganic Chemistry, Russia
[3]Institute for Biological Interfaces of Engineering, Clemson University, Clemson, SC, USA

ABSTRACT

Congestive heart failure affects 6 million Americans and results in a 35% mortality rate in the year immediately following diagnosis; one of the most common causes of heart failure is the loss of myocardial function. Success of treatment methods depend on the extent of oxidative damage to the myocardium caused by reactive oxygen species (ROS). Sufficient amount of ROS in the myocardial environment may lead to the incomplete regeneration of myocardium by myocardial stem cells. In order to decrease oxidative damage, superoxide dismutase (SOD), a class of enzymes, provides pronounced antioxidant effects. However, SOD activity is inhibited by its dismutation products. It is herein proposed that nanocrystalline cerium dioxide (nanoceria) is used with SOD to scavenge hydrogen peroxide, thereby reducing oxidative damage. Nanocrystalline ceria was synthesized using a solvothermal method and characterized by various means, including: X-ray powder diffraction, transmission electron microscopy (TEM), and dynamic light scattering (DLS). SOD-nanoceria conjugates were prepared by mixing the individual parts. The conjugates' antioxidant activity was assessed by an enzymatic activity assay and was found to have significantly higher antioxidant activity when compared to non-functional nanoceria and pure SOD.

Keywords: antioxidants, nanoceria, nanoparticles, conjugates, SOD, superoxide

INTRODUCTION

Congestive heart failure is common among the United States population, affecting six million people. Roughly 670,000 people are diagnosed with this condition each year and the mortality rate in the year immediately following diagnosis is 35% [1]. The loss of myocardial function is one of the most common causes of congestive heart failure and, in most cases, is due to a myocardial infarction. Once heart failure is diagnosed, most treatment methods focus on prevention of the progression of the disease; success of such treatment methods significantly depends on the extent of oxidative damage to the myocardium caused by reactive species. Damaged myocardium is known to conduct electrical impulses more slowly than healthy tissue and can trigger events such as lethal arrhythmias [2]. There is an increase in reactive oxygen species (ROS) and reactive nitrogen species (RNS) in the myocardium following a myocardial infarction, which may lead to unfinished regeneration of myocardial tissue.

Superoxide dismutase (SOD) is an enzyme used to catalyze the transition of superoxide radicals into oxygen or hydrogen peroxide; this enzyme is proved to decrease total oxidative damage and promote cardiac tissue regeneration [3]. The use of SOD to reduce the impact of oxidative stress has shown potential in *in vitro* and animal experiments [4, 5]. With regard to myocardial tissue damage, SOD has been shown to reduce the size of a myocardial infarction in animal studies [6]. However, considerable evidence shows that there is a lack of reproducibility of SOD therapy studies mentioned previously; this could be caused by SOD inhibition by peroxide ions formed as a result of superoxide dismutation [7].

One solution to decrease SOD inhibition is to implement a conjugated system of SOD and cerium dioxide nanoparticles (nanoceria). Due to the presence of mixed valence states of Ce^{3+} and Ce^{4+} and oxygen vacancies, ceria has many unique properties; specifically, the partial reduction of Ce^{4+} to Ce^{3+} on its surface gives nanoceria the antioxidant properties that makes it suitable for this application [8]. Studies have shown that nanocrystalline ceria is an effective ROS scavenger, thereby useful to protect against oxidative stress [9]. Nanoceria achieves this due to its large surface-to-volume ratio in its nanocrystalline state, which exhibits an abundance of oxygen vacancies with relatively high mobility [10]. Therefore, nanoceria can be used to scavenge peroxide radicals thereby decreasing the inhibition of SOD. Present work focusses on the preparation and characterization of nanoceria-SOD conjugates in an attempt to obtain robust antioxidant system.

METHODS

Ceria colloidal solution was prepared using a method described in a previous paper [11]. 25 mL of an aqueous solution of 0.4 M cerium (III) nitrate containing 2.0 g of

citric acid was prepared, then mixed with 100 mL of a 3 M ammonia solution under mild stirring. The resulting solution was kept at room temperature for 2 hours for the formation of CeO_2 to be completed. Afterwards, the solution was rinsed by large amounts of deionized water. The obtained samples were then dried and characterized using a number of techniques including: X-ray powder diffraction, transmission electron microscopy (TEM), dynamic light scattering (DLS), long-term storage experiments, and thermogravimetric analysis.

The SOD-nanoceria conjugates were prepared by adapting a method described elsewhere [12]. Briefly, an aqueous solution containing 5 U/mL SOD was mixed with the ceria solution obtained previously. This mixture was incubated at room temperature for 2 hours. The antioxidant activity of SOD-nanoceria conjugates against superoxide radicals was assessed by means of an SOD enzymatic assay. The activity of ceria nanoparticles and SOD was also assessed separately, to be used as a reference. Cell culture experiments using lipopolysaccharide (LPS)-challenged macrophages were also conducted in order to evaluate the conjugates' ability to scavenge free radicals. The SOD-nanoceria conjugates' antioxidant activity against RNS was also evaluated using cell culture experiments according to a protocol described elsewhere [13]. Mouse macrophages (RAW 264.7 cell line) were seeded in a sterile 24-well plate and incubated overnight at 37°C under 5% CO_2. Afterwards, aliquots of the samples were added to the wells and kept at 37°C for 4 hours. The cells were then LPS-challenged using an LPS concentration of 10 μg/mL and incubated for 4 hours at 37°C under 5% CO_2. The samples were then treated with Griess reagent and incubated again for 30 minutes. Then, the optical density of the resulting solution was recorded at 540 nm.

RESULTS

The obtained ceria solutions were characterized using X-ray powder diffraction to confirm the formation of ceria nanoparticles and determine the non-stoichiometry of the samples. The results show that the methodology used herein allowed us to obtain cerium dioxide with a cell parameter of 5.4426 Å, suggesting the actual composition of the compound to be $CeO_{1.90}$. The particle size determined by TEM was found to be 2-3 nm. Little to no evidence of particle aggregation was found on the micrographs and this was further confirmed by DLS, which showed that the hydrodynamic radius of the nanoceria in solution was 2.3±1 nm. Long-term storage experiments showed no observable precipitation over a 6-month period, confirming the stability of the solutions. Thermogravimetric analysis was used to determine the concentration of ceria in the samples; it was calculated to be 0.01 M.

The SOD assay used to evaluate the antioxidant activity of the SOD-ceria conjugates against superoxide radicals showed that the conjugates did effectively scavenge the radicals. It was also shown that the conjugates were superior in their scavenging ability to unfunctionalized nanoceria and pure SOD; these results are presented in **Figure 1(a)**. In the Griess experiment (see Fig. 1(b)), SOD-nanoceria conjugates effectively reduced the concentration of RNS and the efficacy of the conjugates was found to be significantly higher than that of the individual ceria and SOD ($p<<0.01$, n=4).

DISCUSSION

In order to achieve the desired antioxidant properties, the nanoceria should be stable to aggregation and appropriate for dosing with a particle size not exceeding 2-3 nm [14]. Antioxidant properties of ceria are driven by the surface-to-volume ration. The large surface area of ceria nanoparticles comes along with an abundance of oxygen vacancies that allows for the oxygen scavenging necessary to reduce oxidative stress. The synthetic approach used in this study resulted in stable ceria colloidal solutions with the desired particle size. Therefore, the pronounced antioxidant properties of ceria nanoparticles was not unexpected. At the inception of this study it was hypothesized that nanoceria would scavenge the peroxide radicals that inhibited SOD, thereby increasing the activity of SOD. The obtained results of the SOD assay and Griess experiment are indicative of this synergistic effect of nanoceria and SOD conjugates.

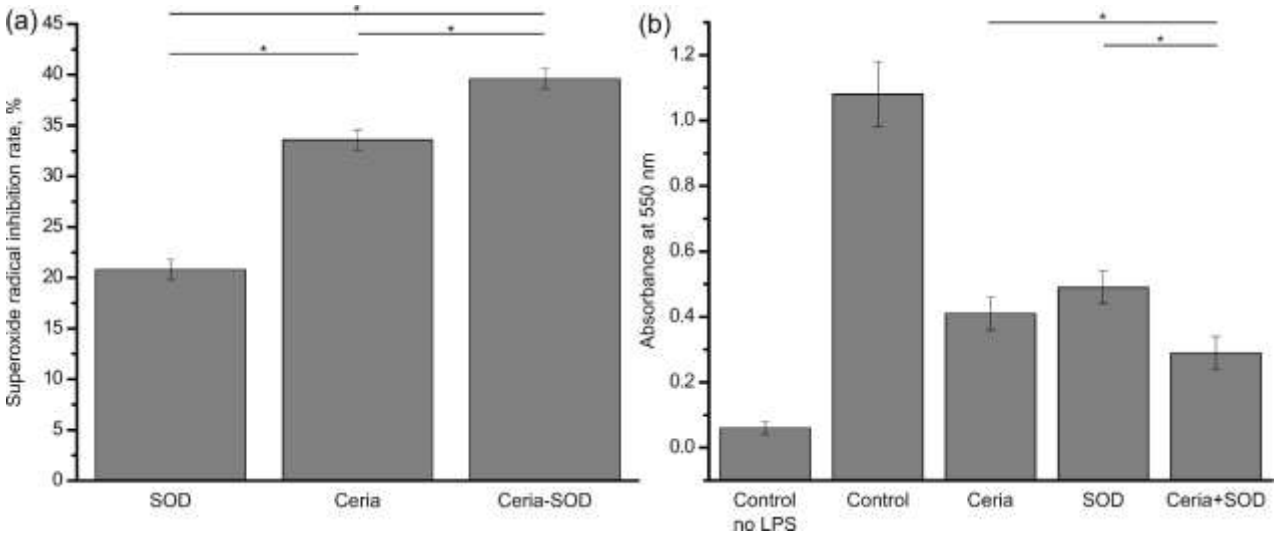

Figure 1. Results of the (a) SOD enzymatic assay and the (b) results of the Griess tests for the samples. Based on calibration curves, the percentage of superoxide radical inhibition was calculated. Note that the asterisks represent significant difference between values.

CONCLUSIONS

Present work deals with the complex antioxidant system that consists of nanocrystalline ceria and SOD. We have demonstrated in *in vitro* experiments that SOD-nanoceria conjugates are capable of reducing the concentration of reactive oxygen and nitrogen species. Moreover, the antioxidant activity of the conjugates was found to be significantly higher than that of nanoceria or SOD alone.

ACKNOWLEDGMENTS

This work was supported in part by the Clemson University Creative Inquiry Program and Institute for Biological Interfaces of Engineering.

REFERENCES

[1] Lloyd-Jones, D.M., Larson, M.G., et al. (2002). Lifetime risk for developing congestive heart failure. *Circulation Research*. [Online]. *106(24)*, 3068-3072. Available: http://circ.ahajournals.org/content/106/24/3068.short

[2] Hare, J.M. (2001, August). Oxidative Stress and Apoptosis in Heart Failure Progression. *Circulation Research*. [Online]. *89(3)*, 198-200. Available: http://circres.ahajournals.org/content/89/3/198.short

[3] McCord, J.M., & Fridovich, I. (1969, June). The Utility of Superoxide Dismutase in Studying Free Radical Reaction. *Journal of Biological Chemistry*. [Online]. *244(22)*, 6049-6055. Available: http://www.jbc.org/content/244/22/6056.short

[4] Howard, M.D., Greineder, C.F., Hood, E.D., Muzykantov, V.R. (2014, March). Endothelial targeting of liposomes encapsulating SOD/catalase mimetic EUK-134 alleviates acute pulmonary inflammation. *Journal of Controlled Release*. [Online]. *177*, 34-41. Available: http://www.sciencedirect.com/science/article/pii/S0168365914000030

[5] Shuvaev, V.V., Muro, S., Muzykantov, V.R. (2016, July). Size and targeting to PECAM vs ICAM control endothelial delivery, internalization and protective effect of multimolecular SOD conjugates. *Journal of Controlled Release*. [Online]. *234*, 115-123. Available: http://www.sciencedirect.com/science/article/pii/S0168365916303194

[6] Jolly, S.R., Kane, W.J., Bailie, M.B., Abrams, G.D., Lucchesi, B.R. (1984, March). Canine myocardial reperfusion injury. Its reduction by the combined administration of superoxide dismutase and catalase. *Circulation Research*. [Online]. *53*, 277-285. Available: http://circres.ahajournals.org/content/54/3/277.short

[7] Cassano, L.M., Gomez, L.D., Lascan, H.R., Gonzalez, C.A., Trippi, V.S. (1997, January). Inactivation and Degradation of CuZn-SOD by Active Oxygen Species in Wheat Chloroplasts Exposed to Photooxidative Stress. *Plant & Cell Physiology*. [Online]. *38(4)*, 433-440. Available: https://academic.oup.com/pcp/article/38/4/433/1839813/Inactivation-and-Degradation-of-CuZn-SOD-by-Active

[8] Heckert, E.G., Karakoti, A.S., Seal, S., Self, W.T. (2008, June). The role of cerium redox state in the SOD mimetic activity of nanoceria. *Biomaterials***.** [Online]. *29(18)*, 2705-2709. Available: http://www.sciencedirect.com/science/article/pii/S0142961208001865

[9] Grulke, E., Reed, K., Beck, M., Huang, X., Cormack, A., Seal, S. (2014, August). Nanoceria: factors affecting its pro- and anti-oxidant properties. *Environmental Science: Nano*. [Online]. *1*, 429-444. Available: http://pubs.rsc.org/en/content/articlehtml/2014/en/c4en00105b

[10] Mullins, D.R. (2015, March). The surface chemistry of cerium oxide. *Surface Science Reports*. [Online]. *70(1)*, 42-85. Available: http://www.sciencedirect.com/science/article/pii/S016757291400034X

[11] Ivanova, O.S., Shekunova, T.O., Ivanov, V.K., Shcherbakov, A.B., Popov, A.L., Davydova, G.A., Seleneva, I.I., Kopitsa, G.P., Tret'yakov, Y.D. (2011, May). One-stage synthesis of ceria colloid solutions for biomedical use. *Dokl. Chem.* [Online]. *437(2)*, 103-106. Available: http://link.springer.com/article/10.1134%2FS0012500811040070?LI=true

[12] Vertegel, A.A, Siegel, R.W., Dordick, J.S. (2004, May). Silica Nanoparticle Size Influences the Structure and Enzymatic Activity of Adsorbed Lysozyme. *Langmuir*. [Online]. *20(16)*, 6800-6807. Available:http://pubs.acs.org/doi/abs/10.1021/la047200

[13] Khanduja, K.L., Avti, P.K., Kuar, S., Pathania, V., Pathak, C.M. (2005, April). Inhibitory effect of vitamin E on proinflammatory cytokins-and endotoxin-induced nitric oxide release in alveolar macrophages. *Life Sciences*. [Online]. *76(23)*, 2669-2680. Available:http://pubs.acs.org/doi/abs/10.1021/la047200

[14] Nelson, B., Johnson, M., Walker, M., Riley, K., Sims, C. (2016, May). Antioxidant Cerium Oxide Nanoparticles in Biology and Medicine. *Antioxidants*. [Online]. *5(2)*, 15. Available: http://www.mdpi.com/2076-3921/5/2/15/htm

[15] Zholobak, N.M., Ivanov, V.K., Shcherbakov, A.B., Shaporev, A.S., Polezhaeva, O.S., Baranchikov, A.Y., Spivak, N.Y., Tretyakov, Y.D. (2011, January). UV-shielding property, photocatalytic activity and phototoxicity of ceria colloid solutions. *Journal of Photochemistry and Photobiology*. [Online]. *102(1)*, 32-38. Available: http://www.sciencedirect.com/science/article/pii/S1011134410002150

DEVELOPING AN APPARATUS TO TREAT PLANTAR FASCIITIS

John McGreevey[1], Bryce Kunkle[1], Benjamin Shumpert[2], Edward Bear[2], and Vladimir Reukov[1, 3]

[1]Bioengineering Department, Clemson University, Clemson, SC, USA
[2]Electrical and Computer Engineering Department, Clemson University, Clemson, SC, USA
[3]Institute for Biological Interfaces of Engineering Department, Clemson University, Clemson, SC, USA

ABSTRACT

Plantar fasciitis is a disorder that affects approximately 3 million people per year. The affliction is directly caused by microscopic tears in the plantar fascia tendon, causing great pain in elementary tasks such as walking and standing. The most viable non-invasive treatment is the stretch of the tendon to regain flexibility and strength while decreasing localized inflammation. In order to combat this disease, we have designed a mobile and robust apparatus that uses a stretch transducer to evaluate the amount of stretch resulting from flexion of the foot. The apparatus uses a common sock with a sensor placed such that it is parallel to the sole of the foot. Any type of flexion by the foot results in resistance values interpreted by the sensor that are relayed to a Bluetooth Low Energy (BLE) device. This device is programmed to interpret the resistance values as integers that increase with the resistance and therefore the amount of stretch by the tendon. These values are transmitted via Bluetooth to a smartphone that displays the integer values and stores the data for the purposes of tracking progress by the patient and the clinician. Furthermore, the app also tracks the patient's level of pain day-to-day and allows for programming by the patient and clinician in order to determine the optimal type and amount of stretch necessary to effectively treat the disease.

Keywords: Plantar Fasciitis, Mobile Health, Application, Plantar Fasciitis Device

INTRODUCTION

Plantar fasciitis is the inflammation of the plantar fascia tendon, which runs parallel to the sole of the foot. There are several factors that can contribute to the development of plantar fasciitis such as improper footwear, obesity, prolonged time spent on feet, and limited ankle flexion [1, 2]. The upshot of the lack of support is that microscopic tears begin to form on the tendon, which then leads to inflammation of the surrounding tissue [3]. Because of the inflammation in the tissue surrounding the tendon and the tendon's weaker mechanical structure, the patient experiences great pain in the most mundane of tasks like walking or standing. A multitude of treatments have been used on patients suffering from plantar fasciitis including inflammatory agents, walking splints, orthotic implants, shockwave therapy, and surgery [4]. Current treatments will improve the affliction but do not actively treat the disease the way that this particular project does. Specific stretches are relayed to the patient by the clinician via the app that comes with the device. The application increases patient compliance by actively relaying the stretch necessary in a patient's day-to-day life to improve the healing process.

In general, the majority of the patients who are afflicted by this disease are patients who are very active such as athletes and soldiers or patients who lead a very sedentary lifestyle [5]. As such, a proactive approach is the most effective treatment method. There are several products on the market that aim to treat the disease; however these products generally are in the form of sleeves that alleviate the pressure and mechanical forces placed on the tendon instead of actively treating the disease [6,7]. This device aims to actively involve both the patient and the clinician to develop an effective treatment method that is tailored specifically to the patient and the severity of the affliction in order to increase patient compliance. An active approach to the problem like this allows for a quicker and more efficient road to recovery for the patient. The interaction between patient and doctor is further streamlined by the smartphone application implemented with the device. A smartphone application eliminates the need for frequent face-to-face meetings between the patient and clinician regarding the necessary exercises and further treatment options.

METHODS

The device uses an athletic sock with a stretch sensor that runs parallel to the plantar fascia tendon. The stretch sensor has a base resistance value that is increased when the integrated plates on the sensor are bent or stretched apart. The stretch sensor and BLE Blend Micro are powered via an external, rechargeable power source mounted separately to the ankle. As the tendon is

stretched, the stretch sensor plates are stretched as well, resulting in an increased resistance value across the sensor. The increased resistance results in an increased voltage that is recorded by a chip mounted on the ankle of the sock. The chip is a Bluetooth low energy Blend Microchip manufactured by RedBearLab. Once the voltage is inputted into the chip, it is displayed on the app as increasing values. So as the resistance values are increased on the stretch sensor, the values on the app are increased. As the angle of the stretch sensor decreases or the plates along the sensor are further separated, the values on the app are increased. Data received from the device is stored on the app in order to track the progress of the patient's stretches.

An application is used in conjunction with the device to treat the affliction of the patient. There are several facets to the application to improve patient compliance in addition to the communication between the patient and the clinician. The application has the data from previous stretches to track progress as well as a pain level that a patient can input so that the clinician can determine effective stretches. This application is the defining characteristic of this particular device because it allows for an active treatment plan for the patient. The app in congruence with the stretches allow for a proactive approach to patient recovery.

DISCUSSION

The prototype that has been made effectively serves the purpose of what we wanted to create, but there are several ways that it can be improved. Based on the volume of data that has been recovered, we have a good understanding of what areas should be improved on for the second prototype. We will run the wires through the sock in order to better protect them and the other electronic devices that are used in the apparatus. Further, we have found a more compact power source that has a more suitable battery life while still being rechargeable.

RESULTS

A working prototype of the device has been created and tested by the members of the lab. It was found that performing the stretches on the plantar fascia increases the integers shown on the app in an expected relationship. The device does not obstruct any of the natural movements that a patient can undergo, but it is unadvised to walk around with the device in order to not damage the equipment. Instead, the device should only be used when the patient undergoes stretches and not in daily life. Furthermore, numbers recovered from improper use of the device would obfuscate the recovered data on the app and return data that is not conducive to the patient's progress. The problem with the testing of the device is that all of the volunteers from the lab do not suffer from plantar fasciitis, so while a baseline value for rest was recovered, no data for patients suffering from any degree of plantar fasciitis was given. An IRB Protocol request has been submitted to find suitable volunteers, so pertinent data will be recovered from the device. The range of the device that receives the data from the stretch sensor is in the tens of meters, which is typical of Bluetooth Low Energy devices [8].

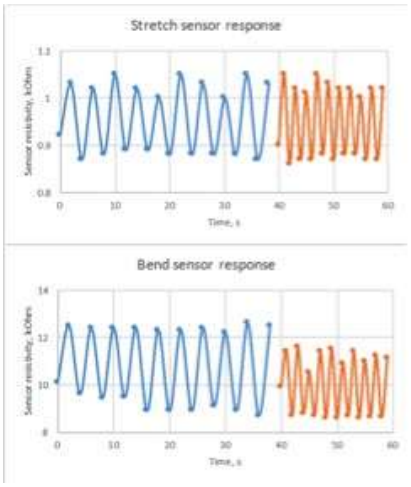

A case is currently being made to house both the power source and the BLE Blend Micro device. Currently, the chip and power source are exposed on the sock and held on via magnetic clips. We would also like to start implementing a bend sensor as well to determine if it produces data that is more suitable for the purposes of this project. Ultimately, we hope that we can manufacture an integrated circuit that performs all of the hardware functions that are performed by the prototype without the excessive bulk and the need for soldering, which can result in leads that come lose or otherwise malfunction. We are also currently working on establishing a HIPAA-compliant web server to collect and store the data

recovered from the device. This is where the patient and clinician will interact to evaluate progress and discuss further treatment plans.

There are several facets of the current prototype that will be implemented in the next version. The Bluetooth connection or the transmission of data between the device and the app is currently working optimally and efficiently. An LED on the BLE Blend Micro device activates when the Bluetooth connection is active, so it is clear to the patient when the device is active. The construction of the circuit is set up in such a way that it allows for the voltage of the stretch sensor to increase with the resistance instead of the other way around. If the sensor had been placed on the other side of the resistors used, the integers would decrease as the patient stretches. The current hardware placement will be retained until a more viable option is presented.

CONCLUSIONS

The current status of the apparatus accomplishes all of the goals initially conceived. The device effectively measures the stretch of the plantar fasciitis while simultaneously transmitting the data to the app wirelessly. Furthermore, the values displayed by the app have a positive, relatively linear relationship with the amount of stretch performed by the patient and the angling of the stretch sensor. The device does not require a large amount of power in order to effectively operate, and the current rechargeable power source has a prolonged period of sustainability before it needs to be charged again. The data recovered from the app can be stored and viewed by the users. The trials performed by the members of the lab demonstrated that the sock is intuitive, mobile, and effective. The ways that it can be further improved are relatively basic engineering principles, such as making the apparatus more efficient, compact, and user-friendly. The next step for the project is to get the IRB protocol approved to get volunteers for testing.

ACKNOWLEDGEMENTS

This research was partially supported by an IDeA grant P20GM103444 from NIH, Clemson Undergraduate Research program Creative Inquiry® and Department of Bioengineering.

REFERENCES

1. Cole C, Seto C, Gazewood J. Plantar fasciitis: evidence-based review of diagnosis and therapy. Am Fam Physician 72:2237–2242, 2005.
2. Riddle, D. L., & Schappert, S. M. (2004). Volume of Ambulatory Care Visits and Patterns of Care for Patients Diagnosed with Plantar Fasciitis: A National Study of Medical Doctors. *Foot & Ankle International*,*25*(5), 303-310. doi:10.1177/ 107110070402500505
3. Lemont, H., Ammirati, K. M., & Usen, N. (2003). Plantar Fasciitis. *Journal of the American Podiatric Medical Association*,*93*(3), 234-237. doi:10.7547/87507315-93-3-234.

THE RESPONSE OF INTERLEUKIN-STIMULATED A549 HUMAN ALVEOLAR BASAL EPITHELIAL CELLS UPON EXPOSURE TO HYDROCORTISONE IN CULTURE

Jana Bagwell[1], Hamed Benghuzzi[1], and Michelle Tucci[2]

[1]School of Health Related Professions and [2]Department of Anesthesiology
University of Mississippi Medical Center, Jackson, MS, USA

ABSTRACT

The A549 human adenocarcinoma cell line is theorized to produce chemokines in response to inflammatory cytokines. Eotaxin, a CC chemokine, may play a role in recruitment and activation of eosinophils to the site of inflammation in obstructive lung diseases such as asthma. The objective of this study was to evaluate the influence of hydrocortisone on A549 cells after exposure to cytokines, such as interleukin 1β (IL-1β). The aim of this *in vitro* model is to assess the levels of eotaxin (CCL11), when combined with hydrocortisone. To establish an environment of an inflammatory response, confluent A549 cells were stimulated separately with IL1-β in concentration variation at ten-fold serial dilution in a 96-well plate. Standard laboratory protocols and sterile techniques were followed throughout the experimentation. The cells were treated independently and allowed to incubate for 24 and 48 hours. Cellular viability and cell membrane toxicity were measured to determine overall cellular health. Eotaxin levels were determined by immunoassay. ANOVA indicated there was no significant difference in groups with IL-1β at 24 and 48 hours when comparing all treatment and non-treatment groups. The results from this study indicate that eotaxin levels are influenced by hydrocortisone in cellular model but not reduced.

Keywords: A549, asthma, interleukin 1-β, cortisol, hydrocortisone, eotaxin, CCL11

INTRODUCTION

Asthma is a hyper-reactive airway disease marked with chronic inflammatory damage of the respiratory system bronchioles. [1] The disease is marked with recurrent inflammatory spastic episodes which lead to bronchoconstriction of the bronchioles. This airway inflammation is a characteristic feature of asthma and is believed to contribute the underlying disease severity. [2] In addition, changes occur in the epithelium tissue of the airways that can lead to long term chronic tissue damage. [3] If epithelial cell injury continues, further tissue remodeling can occur leading to an over-active airway responsiveness, continued bronchospasms, and further expose irritant receptors to potential stimuli. [4, 5]

Patients with asthma have a specific pattern of inflammation in the airways that is characterized by degranulated mast cells, infiltration of eosinophils, macrophages, and neutrophils, plus an increased number of activated T-helper 2 cells. [6] Furthermore, mediators such as cytokines and chemokines work to communicate and attract cellular components. One such chemokine, eotaxin, may have a significant role in triggering activation and degranulation of eosinophils [7, 8]. Eotaxin has specific chemotaxis properties that is eosinophil-selective due to the receptor-specificity to the C-C motif receptor 3 (CCR3) [9] and has been found elevated during asthmatic bronchospasms. Currently, three eotaxin products have been identified. They are named according to their gene location on human chromosome 17; eotaxin-1 is CCL11 (C-C motif ligand) [10], eotaxin-2 is CCL24 [11], whereas eotaxin-3 is a product of gene CCL26. [12]. In this study, eotaxin-1 or CCL11 will be the focused target and referred to as merely eotaxin.

The specific aim of this study is to measure the levels of eotaxin in A549 cell culture when stimulated with a pro-inflammatory interleukin, interleukin 1-beta (IL-1β) and subsequently treated with cortisol (hydrocortisone) within cell culture. It should be noted that cortisol is a human steroid hormone, but when it is used a medication, the term hydrocortisone is used. Because cortisol has anti-inflammatory properties, the overall hypothesis of this study is to test if the level of eotaxin produced is decreased due to the presence of an endogenous anti-inflammatory substance.

METHODS

Cell Cultures A549 cells were acquired from the American Type Culture Collection (ATCC, Manassas, VA) and grown in Ham's F12K media supplemented with 10% fetal bovine serum (Sigma-Aldrich) and 1% antibiotic/antimycotic solution (Corning). Cells were transferred to a 75 cm^2 flask (Corning) and grown to confluency in a humidified 5% CO_2 incubator at 37°C. At confluency, cells were trypsinized (Hyclone EDTA-

Trypsin), removed from the flask and counted by the use of a Neubauer hemocytometer.

Plate designs: The plate design utilized a 96-well plate for stimulation of cells plus treatment with hydrocortisone (Sigma-Aldrich).Each well was initially prepared from cell stock that had a count of $9.53x\ 10^4$ cells/mL. Four rows with graduated concentrations (10.0, 1.0, 0.1, 0.0 ng/mL) of recombinant human IL-1β (Sigma-Aldrich) was added (100µL), followed by 100µL of hydrocortisone (concentration of 5.0 µg/dL). Each combination was replicated six times and allowed to incubate with termination of cells at 24 hours and 48 hours. Standard laboratory protocol was used in all collection and subsequent assays.

Cellular viability: alamarBlue® (Trek Diagnostic Systems, Inc) cell viability reagent functions as a cell health indicator by using the natural reducing power of living cells to convert resazurin to the fluorescent molecule, resorufin. The fluorescence is directly proportional to the number of living cells and corresponds to the cell's metabolic activity [13]. At the end of incubation period, fresh media (100µL) was added to cells. After 30 minutes, alamarBlue® solution (10µL), followed by incubation of one hour. A 50µL aliquot was read at 570nm and 620nm. The percent reduction was calculated in comparison to a negative control.

Eotaxin: A human eotaxin solid phase sandwich ELISA assay (Invitrogen, Camarillo, CA) was utilized to make a quantitative determination of secreted eotaxin. All final products were read at 450nm with standards ran in duplicate. Total eotaxin was determined from a standard curve. [14]

Lactate Dehydrogenase: Lactate dehydrogenase (LDH) is a cytosolic enzyme that is stored within the cell cytoplasm and released if cytotoxic events occur. LDH was quantified by adding collected media to a microtiter plate (50µL) along with 50µL of reaction mixture from LDH Cytotoxicity Assay (Pierce Biotechnology). An enzymatic reaction is measured in which LDH catalyzes the conversion of lactate to pyruvate via NAD+ reduction to NADH. Absorbance was measured at 490nm. [15]

Statistical Analysis: Analysis of variance (ANOVA) was performed using SPSS statistical software to determine differences among experimental groups, including the negative control group. All data was normalized with alamarBlue® reduction readings. Microsoft Excel was used for visualization of data.

RESULTS

No significant variation among groups was found in eotaxin levels when considering all groups (four IL-1β concentrations at both 24 and 48 hours for both treatment and non-treatment) with a p-value > 0.05 (p= 0.106). Visualization of the mean values of eotaxin (normalized with reduction of alamarBlue®) is seen in Figure 1.

Cellular health data was calculated as an overall mean from each treatment group (six replicates at 24 and 48 hours). This data is displayed as LDH (Table 1). When comparing only the 24 hour set by ANOVA, there was a significant difference between means (p=1.35E-09), with a post hoc Tukey's test indicating the LDH value of 1.0 ng/mL and 0.1 ng/mL differing within the treatment group, while only the 10.0 ng/mL IL-1β differing significantly within the 24 hour non-treatment group. When comparing means for the 48 hour set, a p-value of 8.07E-24 indicates a significant difference between all groups, but only the 0.0 ng/mL IL-1β within the treatment group and the 10.0ng/mL within the non-treatment group differ significantly. Table 1 is representation of LDH data for all groups analyzed.

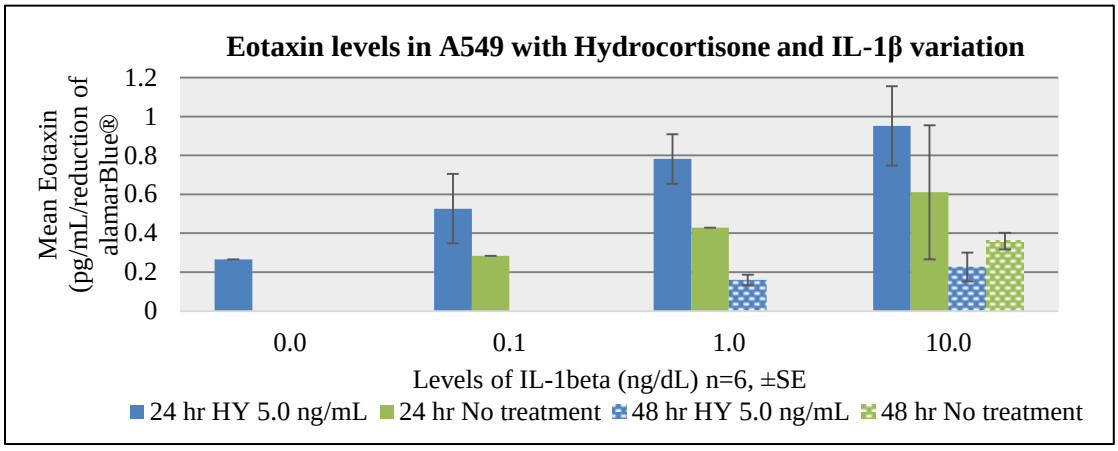

Table 1. L**DH values normalized (IU/min / reduction in alamarBlue®)**

LDH levels present in cell culture media at 24 and 48 hours. Values are expressed as the mean ± SE of all replicates/ reduction of alamarBlue®. HY = hydrocortisone; no HY = cells with IL-1β only. ****** indicates p-value is <0.05

L-1β level (ng/mL)	HY + IL-1β (24 hour)	No HY + IL-1β (24 hour)	HY + IL-1β (48 hour)	No HY + IL-1β (48 hour)
0.0	4.56±0.30	3.07±0.20	6.01±0.15**	1.47±0.11
0.1	4.98±0.22	2.60±0.27	6.54±0.28	1.66±0.18
1.0	5.91±0.36**	3.47±0.11	7.90±0.27	1.91±0.13
10.0	5.66±0.33	4.59±0.50**	8.66±0.61	2.95±0.24**

DISCUSSION

Eosinophils have been implicated in a broad range of diseases, most notably allergic conditions (e.g. asthma, rhinitis and atopic dermatitis) and inflammatory diseases. Eotaxin is a potent eosinophil-specific chemokine that is released in the respiratory epithelium after allergic stimulation. Studies have shown that A549 cells when stimulated with various cytokines, including IL-1β, produce elevated levels of eotaxin [16]. Lilly et al. (1997) showed increased eotaxin mRNA after stimulation following administration of IL-1β at doses as low as 1 ng/mL [16]. The results from our study did not see an increase in the protein levels of eotaxin secreted following IL-1β from 0.1 to 10 ng/mL with untreated cells. However, this study did indicate an increase in the protein synthesis of eotaxin following the addition of hydrocortisone, but this level of increase was not significant when statistically analyzed. Protein synthesis is a coordinate process from mRNA through translation of the complete active protein. Our findings did not indicate evidence of altered cell proliferation or increased cellular damage for the duration of the study.

Most cells in the human body have cortisol receptors, thus it acts on virtually all tissues in the body with multiple function. One of those functions include maintaining anti-inflammatory task and immunosuppression in the body. Because cortisol is a fat soluble steroid hormone, it can easily permeate into the cell to specific cell receptors. [17] It has been theorized that endogenous cortisol may be an important regulator of the allergic inflammatory response. Evidence has been found to support the theory that nocturnal exacerbation of asthma may be related to the circadian fall in plasma cortisol. [18]

Additional studies are warranted to determine the variation in the literature with this cell line regarding the production of eotaxin following cytokine stimulation. A greater eotaxin response may have been produced by elevating the IL-1β concentrations, but this would be a super-physiological environment and may not be a good model to correlate with normal human physiology parameters.

CONCLUSIONS

The results from this study indicate that eotaxin levels did not significantly decrease eotaxin levels by treatment of hydrocortisone in cellular model as hypothesized. In contrast, hydrocortisone delivery at a low physiological levels did permeate the cell membrane, but did not decrease the eotaxin levels at a statistically significant amount in the interleukin concentration parameters of this study.

ACKNOWLEDGMENTS

This project was supported by the University of Mississippi Medical Center, School of Health Related Professions Development Fund/Private Practice Plan, Jackson, MS.

REFERENCES

[1] T. Capriotti and J. P. Frizzell, *Pathophysiology: Intro concepts and clinical perspectives*. U.S. F.A. Davis Company, 2016.

[2] W. W. Busse, "Asthma diagnosis and treatment: Filling in the information gaps," *Jour of Allergy and Clinical Immunology*, vol. 128, no. 4, pp. 740–750, Oct. 2011.

[3] Y. Marandi, N. Farahi, and G. S. Hashjin, "Asthma: beyond corticosteroid treatment," *Arc of Med Sci*, vol. 9(3), pp. 521-6, 2013.

[4] C. Porth, *Ess of pathophysiology: concepts of altered health states*, 3rd ed. Philadelphia: Lippincott Williams & Wilkins, 2010.

LOW LEVEL LASER THERAPY IMPROVES MICROCIRCULATION IN SKELETAL MUSCLE VASCULAR BEDS IN ZUCKER RATS

Silu Lu, Lusha Xiang, Robert Hester, Lisa Barnes, Ham Benghuzzi, and Min Huang
University of Mississippi Medical Center, Jackson, MS, USA

ABSTRACT

Low level laser therapy (LLLT) is considered among potential alternative medical therapies. It simply applies low power energy to the body surface without inducing traumatic side effects. It has been widely used in the treatment of various medical conditions including pain, inflammation and wound healing. However, the effect of LLLT on vascular tone in skeletal muscle has not been fully elucidated, we hypothesized that LLLT induces vasodilation in skeletal muscle vascular beds. The specific aim of this study was to investigate the effect of LLLT on skeletal muscle arteriolar kinetics using Zucker rats as a model. Male Zucker rats (12-13 weeks old) were anesthetized with pentobarbital (50mg/kg, ip). The trachea was intubated to enable the rats to spontaneously breathe 30 % oxygen and 70% nitrogen. Deep esophageal temperature was maintained at 37°C by using a heat lamp. Either the right spinotrapezius muscle or mesenteric vascular beds were prepared for *in vivo* microscopy. At all times during the surgery and subsequent experiment, the vascular beds were kept at in situ dimensions and were continuously perfused with a physiological salt solution (NaCI, 6.17 mM), KCI, (2.55mM), $CaCl_2$, and 25 $NaHCO_3$, equilibrated with gases containing 5% CO_2, 95% N_2 (pH= 7.4, 35°C). Animals were allowed to stabilize for 30 minutes after surgery. A third-order arcade arteriole segment was selected for analysis. Arteriolar diameter of the spinotrapezius or mesenteric vascular beds were observed with a Nikon UM-22 microscope and measured during a control period and following LLLT (20 sec). At the end of the experiment, adenosine (10 µM) and sodium nitroprusside (10 µM) were added to the perfusate to determine maximal diameter. These experiments lasted 2-4 hours, and at the end of the experiment, the animals were euthanized by an overdose of sodium pentobarbital. Data collected from this study indicated: (I) that LLLT significantly ($P<0.05$) increased arteriole vasodilation in spinotrapezius muscle compared with basal vascular diameter, and (II) LLLT has no effect on mesenteric vascular beds compared with basal condition. In conclusion, results of this study demonstrated that LLLT induced vasodilation and improved microcirculation in skeletal muscle vascular beds. Consequently, LLLT may have the potential to improve functional outcomes in patients with neurologic deficits, soft tissue injury, pain, or wound healing through an increase in blood flow by inducing vasodilation of arterioles in microcirculation.

Keywords: LLLT, arteriole vasodilation, vessel diameter, spinotrapezius

INTRODUCTION

LLLT has been used as an alternative therapeutic method for many years. Mester *et al*. found that a low-energy (1 J/cm2) ruby laser significantly improves wound healing (4, 5, and 6). The wider application of LLLT makes understanding the mechanisms of the LLLT and developing further low-energy laser technologies and applications a necessity. Generally, the laser with the power range of 10-3 to 10-1 W is considered as low-energy laser. The wavelength is usually between 300 and 10,600 nm. Other parameters includes: 1) an interpulse interval of 1 to 500 milliseconds; 2) a total irradiation time of 10 to 3,000 seconds; 3) an intensity (power/area) of 10-2 to 10 W/cm2; 4) and a dose (power × irradiation time/area irradiated) of 10-2 to 102 J/cm2 (7). Photothermal effects of LLLT have been studied on the skin. However, a noticeable temperature increase does not occur during the low-energy or "cold" laser application on the tissue (1, 7). Other than thermal effect, there is a lack of information regarding the effect of LLLT on the microvascular reactivity. Therefore the main purpose of this study was to determine the effect of LLLT on skeletal muscle vascular function and the underlying mechanisms.

MATERIALS AND METHODS

Male Zucker rats (12-13 weeks old) were injected with pentobarbital (50mg/kg, ip). Depth of anesthesia was monitored by the palpebral reflex test. Then the trachea was intubated to enable the rat to spontaneously breathe 30 % oxygen and 70% nitrogen. Deep esophageal temperature was maintained at 37°C by using heating pad or heating lamp. Either the right spinotrapezius muscle or mesenteric vascular beds were prepared for in vivo microscopy as we have used in previously published studies (3). 2013). At all times during the surgery and subsequent experiment, the vascular beds were kept at in situ dimensions and were continuously perfused with a physiological salt solution (in mM): 118.07 NaCI, 6.17 KCI, 2.55 $CaCl_2$, and 25 $NaHCO_3$, equilibrated with gases containing 5% CO_2, 95% N_2 (pH= 7.4, 35°C). Animals were allowed to stabilize for 30 minutes after surgery. A third-order arcade arteriole segment was selected for analysis. Arteriolar diameter of the spinotrapezius or mesenteric vascular beds were observed with a Nikon UM-22 microscope and measured during a control period

and following LLLT (20 sec). At the end of the experiment, adenosine (10 µM) and sodium nitroprusside (10 µM) were added to the perfusate to determine maximal diameter. These experiments lasted 2-4 hours. For all studies the animals did not recover from anesthesia. The animals were euthanized by an overdose of sodium pentobarbital in the end of the experiment.

RESULTS AND DISCUSSION

LLLT significantly increased arteriole vasodilation in spinotrapezius muscle (19.6 ± 3 µm) compared with basal vascular diameter (15.6 ± 2 µm) (Figure 1). LLLT has no effect on mesenteric vascular beds (14± 0 10 µm) compared with basal condition (14 ± 0.80 µm) (Figure 2).

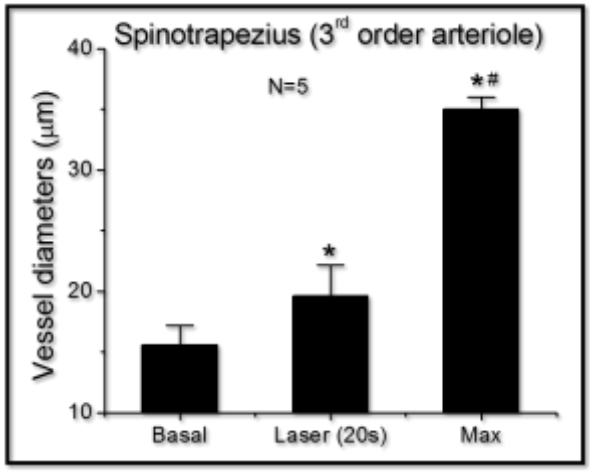

Figure 1. In spinotrapezius muscle, LLLT induces significant vasodilation compared with basal vessel diameter ($p<0.05$, n=5). Adenosine induces significant vasodilation compared with basal vessel diameter ($p<0.05$, n=5).

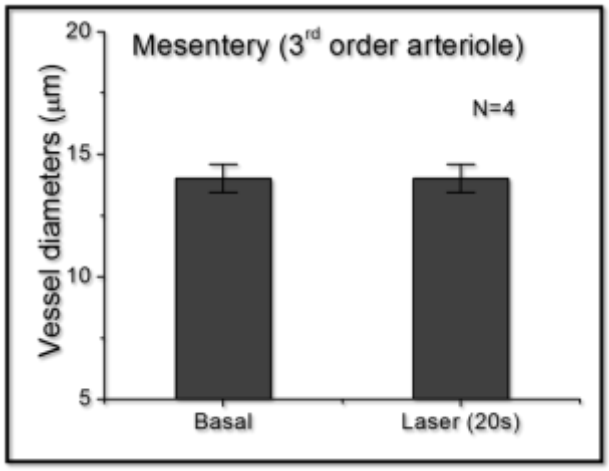

Figure 2. LLLT has no effect on vessel diameter in mesentery arterioles compared with basal vessel diameter (n=4).

Many benefits have been reported for applications with LLLT. However, these studies are complicated by discordance among the laser types used, the parameters selected, tissue type selected, and the subjects enrolled. To avoid these conflict reports, several issues mentioned above need to be addressed. To simplify the tissue type involved in current study, we exposed the third order arterial directly under the LLLT which allowed us to observe the vascular function affected by LLLT. The maximal vascular diameters have also been shown, which help us to analyze the percent change in vascular tone. In our study, LLLT did not induce maximal vasodilation. The potential mechanism of vasodilation induced by LLLT was not determined. However, the application of constant-temperature using a physiological saline solution bath during the vessel diameter measurement makes the photothermic effect less likely to be the mechanism for LLLT-induced vasodilation. In future studies, specific activator and blocker will be applied during the LLLT application to determine the role of several signal pathways, which may contribute to the LLLT-induced vasodilation. It also has been reported that LLLT has effect on the nervous system, including both the central and peripheral nervous systems (2). The use of LLLT for peripheral nerve regeneration is currently being investigated in an attempt to achieve early functional recovery. LLLT has been used in several clinical and experimental research studies on peripheral nerve injuries. However, the interaction between LLLT-induced vasodilation and its effect on nerve around the vessels has not been determined. Different arterial vessel beds have different responses to stimulants, such as ACh, NO, and electric stimulation (8, 9). In our study, we perform the vessel diameter measurement in two different vessel beds, skeletal muscle arterioles and mesentery arterioles. The LLLT induced different response in the two vessel beds. In spinotrapezius muscle, LLLT induced significant vasodilation. This vasodilatory effect was not seen in mesentery arterioles. These results suggest that the mechanisms of vasodilation in response to LLLT are different between the two vessel beds. Without further evaluation, the reason of this difference cannot be determined. In conclusion, LLLT induces vasodilation and improves microcirculation in skeletal muscle vascular beds. LLLT may have potential to improve functional outcomes in patients with neurologic deficits, soft tissue injury, pain, or for wound healing by increasing blood flow and inducing vasodilation of arterioles in the microcirculation.

CONCLUSIONS

Results of this study demonstrated that LLLT was able to induce vasodilation and to improve microcirculation in skeletal muscle vascular beds. Consequently, LLLT may

have the potential to improve functional outcomes in patients with neurologic deficits, soft tissue injury, pain, wound healing through an increase in blood flow by inducing vasodilation of arterioles in microcirculation.

REFERENCES

1. Conlan MJ, Rapley JW, Cobb CM Biostimulation of wound healing by low-energy laser irradiation. A review. J Clin Periodontol 1996; 23: 492–6. 8783057
2. Hashmi JT, Huang YY, Osmani BZ, Sharma SK, Naeser MA, Hamblin MR. Role of low level laser therapy in neurorehabilitation. PM R. 2010 Dec; 2(12 Suppl 2):S292-305.
3. Lu L, Xiang L, Clemmer JS, Gowdey AR, Mittwede PN, Hester RL. Impaired vascular KATP function attenuates exercise capacity in obese Zucker rats Microcirculation 20 (7), 662-669
4. Mester E, Korenyi-Both A, Spiry T, Tisza S The effect of laser irradiation on the regeneration of muscle fibers (preliminary report). Z Exp Chirurg 1975; 8: 258–62.
5. Mester E, Mester AF, and Mester A The biomedical effects of laser application. Lasers Surg Med 1985; 5: 31–9. 3982191
6. Mester E, Spiry T, Szende B, Tota JG Effect of laser rays on wound healing. Am J Surg 1971; 122: 532–5. 5098661
7. Schindl A, Schindl M, Pernerstorfer-Schon H, Schindl L Low-intensity laser therapy: a review. J Invest Med 2000; 48: 312–26.
8. Shawn G. Clark and Leslie C. Fuchs. Role of Nitric Oxide and Ca++-Dependent K+ Channels in Mediating Heterogeneous Microvascular Responses to Acetylcholine in Different Vascular Beds. Journal of Pharmacology and Experimental Therapeutics September 1997, 282 (3) 1473-1479;
9. Zweifach BW, Metz, DB. Regional Differences in Response of Terminal Vascular Bed to Vasoactive Agents. American Journal of Physiology Published 1 July 1955 Vol. 182 no. 155-165.

A DIETARY PHASE 2 ENZYME INDUCER IN ANIMAL MODEL OF ESSENTIAL HYPERTENSION USING AN EXTERNAL ARTERIAL CATHETER

[1]Banigesh, A, [1]Iqbal, R., [1]Murabit, A., [1]Juurlink, B., [2]Tucci, M., [2]Benghuzzi, H., and [1]Mohamed, A.

[1]Anatomy and Cell Biology, Department of Medicine, College of Medicine, University of Saskatchewan, Sk., Canada, [2]University of Mississippi Medical Center, MS, USA

ABSTRACT

It is estimated that by 2025, one billion individuals worldwide will be hypertensive. However, dietary intervention could be a simple solution for this complex multifactorial problem which is increases at an alarming rate. Previous studies in our laboratory have shown that broccoli sprouts rich in glucoraphanin, a precursor of a potent phase 2 protein inducing isothiocyanate sulforaphane, decreases oxidative stress and ameliorates hypertension using tail cuff method. In addition, in another study, pure sulforaphane ameliorates hypertension using tail cuff method. This study addressed: using the external arterial catheter (another method), can we see the same therapeutic effect of sulforaphane? After 1 week of adaptation, the 12 week old male SHRsp and SD rats were divided into two groups: (i) Corn oil (vehicle) alone (Control); (ii) sulforaphane (10 µmol/kg body weight) in corn oil. Blood pressure was determined using an external arterial catheter. The treatment lasted for 7 weeks. At the end of the treatment period, the animals were sacrificed. For comparison, age-matched normotensive Sprague Dawley (SD) rats were treated in the same manner. SHRsp control rats had significantly higher Systolic Blood Pressure (SBP) (158.4± 8.3 mm Hg) than SD control rats (108.07±3.91). Sulforaphane treatment lowered SHRsp blood pressure to 150.66 ± 8.33 (around 7 mm Hg unit). Interestingly, sulforaphane had more potential effect on diastolic BP; it reduced the diastolic BP by 47.47 mmHg unit, compared to control SD rats. There was no significant effect of sulforaphane treatment on SD rat SBP (84.35 ± 7 mm Hg) when compared with SD control rats (90.96 ±7 mm Hg). We conclude that the health benefit previously demonstrated in our laboratory is due to pure sulforaphane and the external arterial catheter BP data confirmed the results obtained by tail cuff method in previous experiment.

INTRODUCTION

The escalating health problem, hypertension, is increasing at an alarming rate. World-wide approximately one billion individuals are hypertensive (Preston, 2007). By 2025, this number is projected to increase 29%, to 1.56 billion (Kaplan & Opie, 2006; Boulanger JM & Program, 2005). Persistent hypertension is linked to an increased risk of morbidity and mortality (Preston, 2007). Clinical solutions to this complex multifactorial disease may be quiet simple (Rees, 2002). New therapeutic approach, such as the dietary intervention could attenuate the hypertension. Sulforaphane, a metabolite of glucoraphanin, is a potent inducer of phase 2 proteins. Glucoraphanin is high in broccoli sprouts shown to be protective in models of oxidative stress (Senanayake, Banigesh, Wu, Lee, & Juurlink, 2012) and inflammation (Noyan-Ashraf, Sadeghinejad, & Juurlink, 2005). The objective of this study was to determine whether the metabolite of glucoraphanin, sulforaphane, was responsible for improved blood pressure, measured by an external arterial catheter and whether this is associated with rectifying renal histology.

METHODS

Animal model: A total of 32, 12-week-old male rats, including 16 spontaneously hypertensive stroke-prone rats (SHRsp) and 16 age matched SD rats – were purchased from Charles River Laboratories (St. Constant, Quebec Canada). The rats were treated in accordance with the guidelines of the Canadian Council on Animal Care, and the Animal Care Committee at the University of Saskatchewan approved the experimental protocols. The animals were kept under standard 12 hr light/ 12 hr dark cycle and humidity condition.

Animal groups: After 1 week of adaptation, the 12 week old male SHRsp and SD rats were divided randomly into four groups then administered either sulforaphane or corn oil daily by gavage: (i) SHRsp-Corn oil (vehicle) alone (Control, n=8); (ii) SHRsp - sulforaphane (10 µmol/kg body weight, n=8) in corn oil; (iii) SD-sulforaphane (10 µmol/kg body weight,

n=8) in corn oil; and (iv) SD- Corn oil (vehicle) alone (Control, n=8); systolic and diastolic BP was determined using an external arterial catheter-BP measurement system. The gavage treatment lasted for 7 weeks. At the end of the treatment period, animals were euthanized and tissues collected and stored under -80 °C.

Statistical methods: All data are expressed as means ± SEM. Statistical significance was tested using unpaired t test with Welch's correction. Significance level was set at $p<0.05$ (one tailed). The GraphPad Prism Software version 7 was used.

RESULTS

Effect of Sulforaphane on body weights of SD and SHRsp male rats. The data for the final body weight of SD and SHRsp rats are presented in Figure 1. Sprague Dawley rats receiving control diet had initial body weights (g) which were significantly higher (276 ± 4) than body weights of the SHRsp rats (203 ± 2.16). The final body weights were also significantly higher in SD rats (729 ± 2.25) than SHRsp rats (327 ± 6.36). Sulforaphane had no effect on body weights of SD or SHRsp rats for the duration of the study (7 weeks).

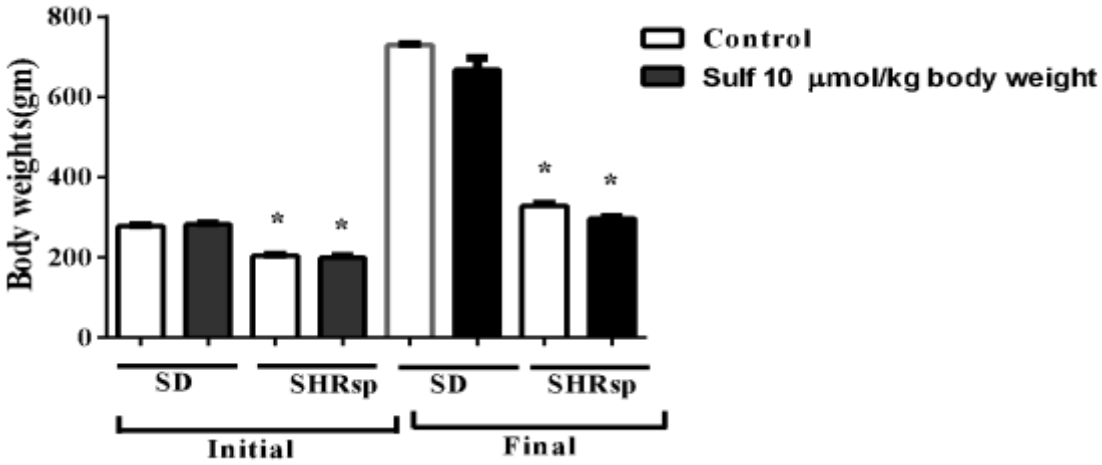

Figure1. The initial and the final Body weights (gm) of SD and SHRsp rats (n= 5-6 rats per group, data are reported as means ±SEM).

Effect of Sulforaphane on Blood pressure in SD and SHRsp male rats.

The systolic blood pressure for SD rats receiving (vehicle alone) was 108 ± 3.9 mmHg compared with the SD rats receiving sulforaphane 106.5 ± 3.67 mm Hg. Similarly, the diastolic blood pressure, for the control SD was 90.96 ± 4.86 mm Hg compared with the sulforaphane treated SD 84.35±3.6 mm Hg. Overall, SD rats fed glucoraphanin (a sulforaphane precursor) had no significant change either in systolic or diastolic blood pressure. In contrast, systolic blood pressures of sulforaphane treated SHRsp rats was 158.4 ± 8.3 mm Hg compared with 155.66 ± 7.6 mm Hg in the vehicle treated SHRsp rats, the systolic BP was reduced by 3 mm Hg by the end of the study. While the diastolic BP of sulforaphane-treated SHRsp rats was 80.47±8.02 mm Hg significantly ($P<0.05$) lower than the vehicle treated-SHRsp rats (138.4±3.14 mm Hg); lower by 58 mm Hg by the end of the study (Figure 2 A-D).

Effect of Sulforaphane on Kidney.

Sulforaphane alleviated the renal damage associated with SHRsp hypertensive animals. In the hypertensive without sulforaphane treatment, severe intimal and medial arteriolar wall thickening was seen along with glomerular atrophy. Administration of sulforaphane reduced the renal damage associated with the hypertensive state (Figure 3). In SD rats, sulforaphane treatment did not induce histological changes within the kidney tissues.

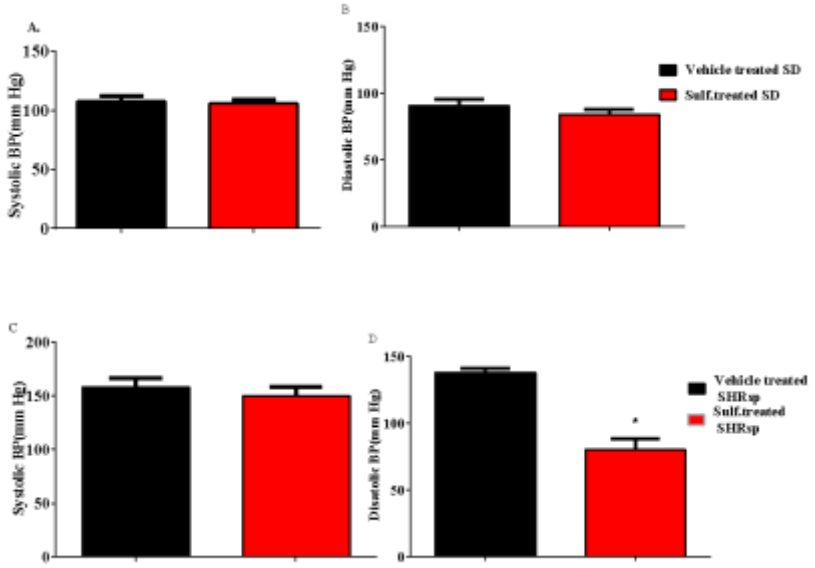

Fig 2 The systolic and diastolic BP (mm Hg) of the vehicle and the sulforaphane treated male SD (A and B) and SHRsp rats (C and D) at the end of treatment, the diastolic BP of the sulforaphane treated SHRsp is significantly lower than the vehicle treated SHRsp, $P<0.05$ *vs*. control of same age. n = 7-8 per group, mean± SEM.

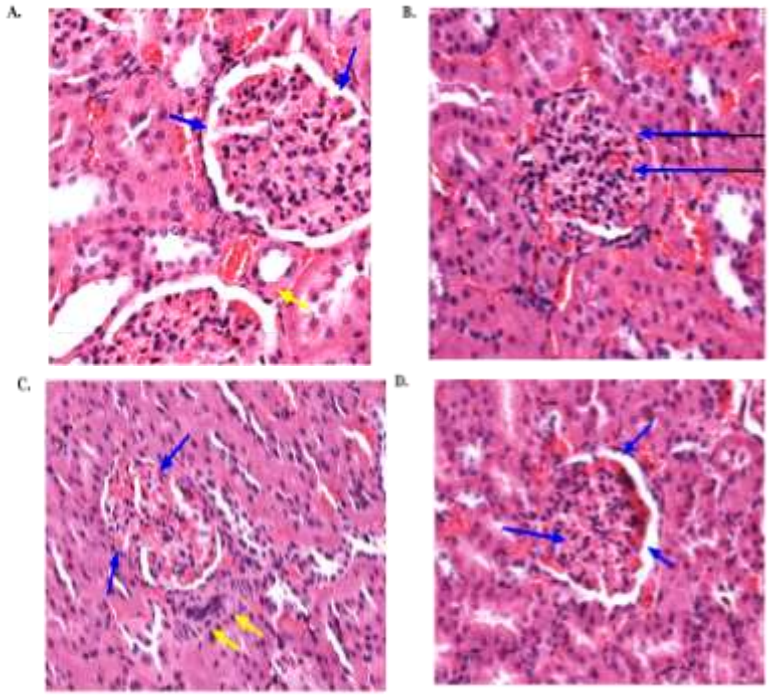

Figure 3. Kidney tissue sections from the vehicle and the sulforaphane treated male SD (A and B) and SHRsp rats (C and D) were subjected to hematoxylin and eosin staining. Images from one rat per group are shown; severe intimal and medial arteriolar wall thickening is represented by yellow arrows and Glomerular atrophy is shown with Blue arrows.

DISCUSSION

In the current study, the therapeutic potential of phase 2 enzyme inducer, sulforaphane is clearly demonstrated in SHRsp and SD rats. Treatment with phase 2 enzyme inducer, sulforaphane had no effect on body weights of SD or SHRsp rats. Sulforaphane had comparable effects in body weights among all sulforaphane treated groups throughout the experiment. From body weights prospective, our findings confirmed that chronic administration of sulforaphane had no significant effects on body weight of female SD or SHRsp rats. These findings are in agreements with those of Conaway; in A/J mice (lung cancer animal model), sulforaphane, phenyl isothiocyanate and their N-acetylcysteine conjugates treated mice had comparable body weights as compared with untreated groups (Conaway, et al., 2002). In contrast, plant food containing flavonoids (the flavonol quercetin) significantly reduces final body weight of obese and lean Zucker rats compared with the controls (Rivera, Morón, Sánchez, & Zarzuelo, 2008). In addition, phytochemicals such as green tea catechins (polyphenols) induce weight reduction (weight loss), possibly *via* inhibiting Catechol-O-methyltransferase (the enzyme that degrades norepinephrine) and fat metabolism (Shixian, VanCrey, Shi, & Kakuda, 2006). This study suggests that any beneficial effects of chronic administration of the phytochemical sulforaphane in SHRsp would be independent of body weight effects. In the kidney, treatment with sulforaphane reduced structural renal damage, minimized pathological alterations in the glomerulus and arterioles. Sulforaphane treatment shows normal looking Glomeruli with normal Bowman's capsule (Blue Arrows) (Figure: B and D), which is in agreement with the results of Noorafshan and Karbalay-Doust, (2012) and Zheng, et al., (2011). These investigators showed sulforaphane improves renal performance and minimize pathological alterations in the glomerulus.

Furthermore, treatment with sulforaphane significantly reduced diastolic BP in hypertensive rats. Our results confirmed that chronic administration of pure phase II protein inducer sulforaphane significantly lowered the blood pressure (i.e., by 7 mm Hg unit by the end of the study) in SHRsp rats compared with the age –matched SHRsp rats (Fig.2: C and D). This decrease in blood pressure was independent of animal body weight (Fig.1). In contrast, age-matched normotensive SD rats fed sulforaphane had constant blood pressure during the experimental period. This indicates that oral consumption of sulforaphane daily for 7 weeks would attenuate systolic BP in hypertensive rats while it would have no significant adverse effects on normotensive rats. Similarly, Noyan-Ashraf, Sadeghinejad, & Juurlink, (2005) and Wu, et al., (2004) using a hypertensive rat model, and 14-week administration of 200 mg/day of dried broccoli sprouts containing glucoraphanin (0.5 and 5.5 μmol sulforaphane equivalents) attenuated blood pressure. These findings suggest that the reduction of BP was due to decreasing the inflammation and oxidative stress associated with hypertension. Our results indicate that pure sulforaphane reduces BP in SHRsp rat (Fig.2: C and D). In addition to the therapeutic potential of sulforaphane in reducing BP and improving renal performance and minimizing pathological alterations in the glomerulus, one mechanism that contributed to reduction of BP and improving renal structure is possibly through reduction oxidative stress. Lopes et al.; (2015) showed that sulforaphane contributes to redox-sensitive vascular dysfunction and normalization of global kidney DNA methylation (Senanayake, Banigesh, Wu, Lee, & Juurlink, 2012) in hypertension. .Sulforaphane ameliorates the redox imbalance observed in the vasculature of stroke-prone spontaneously hypertensive rats (SHRSP) rats. Collectively, our findings indicate that sulforaphane has therapeutic potential. The results provide convincing experimental evidence that dietary compound sulforaphane can be used therapeutically to reduce BP and improve renal function. Nonetheless, future experiments investigating the therapeutic potential in different animal model of hypertension will add more weight to the dietary phase 2 enzyme inducers. This study lays the foundation for the development of new phase 2 enzyme inducers in therapeutic use to attenuate BP and prevent the pathological alterations in the glomerulus.

REFERENCES

1. Boulanger JM, H. M., & Program. *Can J Neurol Sci. 2005 Nov;32(4):403-8.*, 403-411.
2. Conaway, C., Wang, C., Pittman, B., Yang, Y., Schwartz, J., Tian, D., .Chung, F. (2002). Phenethyl isothiocyanate and sulforaphane and their N-acetylcysteine conjugates inhibit malignant progression of lung adenomas induced by tobacco carcinogens in A/J mice. *Cancer research, 65*(18), 8548-8557.
3. Kaplan, N., & Opie, L. (2006). Controversies in hypertension. *Lancet, 367*, 167-178.
4. Noorafshan, A., & Karbalay-Doust, S. a. (2012). Stereological survey of the ameliorative effects of sulforaphane and quercetin on renal tissue in unilateral ureteral obstruction in rats. *Acta Clin Croat., 51*(4), 555-62.
5. Noyan-Ashraf, M., Sadeghinejad, Z., & Juurlink, B. (2005). Dietary approach to decrease aging-related CNS inflammation. *Nutritional Neuroscience, 8*(2), 101-110.
6. Preston, R. (2007). Effects of blood pressure reduction on cardiovascular risk estimates in hypertensive

postmenopausal women. *Climacteric: the journal of the International Menopause Society, 10* (Suppl 1), 32-41.
7. Rees, J. (2002). Complex disease and the new clinical sciences. *Science (New York, N.Y.), 296*(5568), 698-700.
8. Rivera, L., Morón, R., Sánchez, M., & Zarzuelo, A. a. (2008). Quercetin ameliorates metabolic syndrome and improves the inflammatory status in obese Zucker rats. *Obesity, 16*(9), 2081-2088.
9. Senanayake, G., Banigesh, A., Wu, L., Lee, P., & Juurlink, B. (2012). The dietary phase 2 protein inducer sulforaphane can normalize the kidney epigenome and improve blood pressure in hypertensive rats. *American journal of hypertension, 25*(2), 229-235.
10. Shixian, Q., VanCrey, B., Shi, J., & Kakuda, Y. a. (2006). Green tea extract thermogenesis-induced weight loss by epigallocatechin gallate inhibition of catechol-O-methyltransferase. *J Med Food, 9*(4), 451-459.
11. Wu, L., Hossein Noyan Ashraf, M., Facci, M., Wang, R., Paterson, P., & Ferrie, A. a. (2004). Dietary approach to attenuate oxidative stress, hypertension, and inflammation in the cardiovascular system. *Current Issue, 101*(18), 7094-7099.
12. Zheng, H., Whitman, S., Wu, W., Wondrak, G., Wong, P., & Fang, D. a. (2011). Therapeutic potential of Nrf2 activators in streptozotocin-induced diabetic nephropathy. *Diabetes. , 60*(11), 3055-66.
13. Zhang et al., (2015 Dec). Downregulation of Nuclear Factor Erythroid 2-Related Factor and Associated Antioxidant Genes Contributes to Redox-Sensitive Vascular Dysfunction in Hypertension. *66*(6), 1240-1250.

ABSTRACTS

MULTIFUNCTIONAL BIOCERAMIC FOR INNOVATIVE THERAPY

Ahmed El-Ghannam, Ph.D.
University of North Carolina at Charlotte, Charlotte, NC, USA

Silica and calcium phosphate are important ingredients in synthetic bone grafts due to their significant role in new bone formation and vascularization. Of prime importance is for the synthetic bone graft to be able to present its stimulating elements in an amendable format for osteoblasts during new bone formation. Studies on Silica-Calcium Phosphate composite (SCPC) demonstrated that the silica phase provided guided cell growth and bone matrix deposition. Loading porous SCPC granules with antibiotic provided sustained release of a therapeutic dose for more than 28 days. Implantation of the antibiotic-loaded SCPC granules in a critical size calvarial defect in rabbit demonstrated the ability of the graft material to stimulate new bone formation. Moreover, on the cellular level, the SCPC-vancomycin hybrid stimulated osteoblast phenotypic expression and the released antibiotic demonstrated bactericidal effect against Staph aureus.

Session I: Biomaterials – Tissue Engineering

NANOSTRUCTURED SCAFFOLDS FOR REGENERATIVE MEDICINE AND TISSUE ENGINEERING

Jafar F. Al-Sharab and Mohammed Benalla
Northwestern State University, Natchitoches, LA 71497

There is a continuous need for new organs and tissues due to lack of donor organs necessary to help combat some the debilitating diseases. To close the gap between demand of organs and those who are indeed, regenerative medicine and tissue engineering must be utilized. In our research we utilize Electrospinning of nanofibers as a method of forming scaffolds. Due to the high charge density of polymers under the influence of electrospinning, it lends itself to the idea that a magnetic field has the capability of controlling and aligning the high-charge density fibers to the field, forming regular, aligned and thus effective scaffolds for the engineering of tissue. In this paper we will be presenting examples related to the effect of process parameters on the various properties of the fabricated fibers.

CHANGES IN NEURAL CELLS GROWN ON NOVEL HIGH ASPECT RATIO SCAFFOLD VERSUS MONOLAYER CULTURE

Kayla Ponder, Mark DeCoster, and Teresa Murray
Center for Biomedical Research and Rehabilitation Science, Ruston, LA, USA

Neural cells, such as PC12 and SH-EP1 cells, are typically grown as monolayers in tissue culture treated polystyrene dishes. Alterations in protein expression can occur when cells are grown as monolayers in dishes versus a three-dimensional (3D) environment. This can skew results for in vitro experiments making it more difficult to translate in vitro findings into in vivo models. Several strategies have been developed to culture cells in 3D, including growing them on polymer scaffolds. These have their own limitations. Here, we report on the differences in neural cells grown on tissue culture treated polystyrene versus a novel, biodegradable biocomposite containing copper that forms a high aspect ratio scaffold. This work will lay the foundation for new 3D cell culture models of neurodegeneration and regeneration.

USING POLYMER BULK DIFFUSION AS A MECHANISM FOR ADVANCING TISSUE ENGINEERING APPLICATIONS

Kelsey Phelan and Bryant Hollins
Louisiana Tech University, Ruston, LA, USA

Advances in biopolymers have long been sought to advance fields of biomedical engineering, with particular focus in biomicrofluidics and tissue engineering. We recently demonstrated that PDMS, a commonly used polymer in biological applications, can be used to intentionally leach molecules into a sample. In this work, we characterize the diffusion of fluorescein into water from the bulk PDMS, with a focus on calculating the diffusion rate of molecules from the polymer bulk into its surrounding aqueous environment. We look at diffusion from the bulk over a period of days in an attempt to formulate a fluorescein diffusion model from PDMS. Our results can guide future work in tissue engineering application studies, as we establish a framework with fluorescein for determining the properties of molecules capable of diffusion from bulk PDMS. This strategy can be used as a tool for creating self-regulating microfluidic chambers for drug discovery, cell culture, and chemical monitoring applications, as well as a substrate for guiding cell growth and migration in tissue engineering applications.

BENEFICIAL EFFECTS OF SEMEN PURIFICATION WITH MAGNETIC NANOPARTICLES

Casey Durfey[1], Sabrina Swistek1[2], Wei Tan[3], Henry Clemente[4], Peter Ryan1,[3] Scott Willard1,[2] and Jean Feugang[1]

[1.]Departments of Animal and Dairy Sciences, Mississippi State University, [2] Biochemistry, Molecular Biology, Entomology, & Plant Pathology, Mississippi State University, [3] Basic Sciences, Pathobiology and Population Medicine at Mississippi State University, [4.]Clemente Associates, Madison, CT

Semen contain both viable and non-viable spermatozoa which equilibrium affects male fertility. Current techniques for detecting non-viable spermatozoa in semen ejaculates lack specific targeting for their subtraction. Here we used magnetic nanoparticle conjugates to selectively target and remove non-viable spermatozoa, and assess the motion characteristics and viability of residual spermatozoa.

Boar semen were mixed with (nanopurified) or without (control) magnetic nanoparticle conjugates and incubated to allow specific targeting of non-viable (or moribund) spermatozoa. Afterwards, mixtures were placed against a powerful magnet trapping moribund spermatozoa and permitting elution of viable spermatozoa. Before and after incubation, sperm motion and viability parameters were respectively analyzed with a Computer-Assisted-Sperm-Analyzer and flow cytometry after specific staining to evaluate the viability status of spermatozoa. Data (mean±sem) were compared with SAS package.
The proportion of static sperm significantly decreased after purification (8.9±0.5% vs. 11.3±0.5% for the control; $P<0.05$). Motion parameters (total and progressive motility, straightness, linearity, straight line velocity or VSL, and beat cross frequency or BCF) of nanopurified spermatozoa were significantly increased, while the amplitude lateral head displacement or ALH was decreased ($P<0.05$). Sperm viability parameters (plasma and acrosome membrane integrity and mitochondrial potential) were comparable between both groups ($P>0.05$).
Findings indicate the successful removal of moribund (static) spermatozoa without impairing the viability of residual spermatozoa. Beneficial effects on sperm motion

COMPARISON OF MORPHOLOGICAL CHANGES IN MESENCHYMAL AND NASOPHARYNGEAL CANCER CELLS FOLLOWING EXPOSURE TO LOW LEVEL LASER THERAPY

David Gordy, Osasu Adah, Gerri Wilson, Felix Adah, Min Huang, Michelle Tucci, and Hamed Benghuzzi
University of Mississippi Medical Center, Jackson, MS

Low level laser therapy (LLLT) has been shown to increase cellular proliferation and cellular activity in some cell types and decrease proliferation of other cell types. The precise biochemical mechanisms underlying the therapeutic effects of LLLT are not yet well-established. From observation, it appears that LLLT has a wide range of effects at the molecular, cellular, and tissue levels. In addition, its specific modes of action may vary among different applications. Within the cell, there is strong evidence to suggest that LLLT acts on the mitochondria to increase adenosine triphosphate (ATP) production, modulate reactive

oxygen species (ROS), and induce transcription factors. LLLT has shown promise for down regulating inflammation by reducing the presence of reactive oxygen species (ROS). In normal cells, high levels of ROS are damaging to the cells and the cells have the ability to squelch the production of ROS enzymatically. Cancer cells exhibit elevated levels of ROS due to their accelerated metabolism needed for maintaining cellular proliferation. The goals of this experiment were (1) to determine the effects of LLLT for a period of 30 minutes on laryngeal cancer cell survival; and (2) to determine the effects of LLLT on mesenchymal cell survival. Both cell types are rapidly proliferating and require substantial amounts of ATP for survival. Laryngeal and MSC cell types were grown on coverslips in six well plates and treated with 830 nm laser once to mimic a 30 minute therapeutic treatment. The coverslips were harvested at 24, 48, and 72 hours following the treatment period. The results show that LLLT was effective in reducing the number of laryngeal cancer cells within the first 24 hours following treatment, and were ineffective in reducing MSC cell survival for the duration of the experiment. These findings are important since laryngeal cancer is difficult to resect, and laser therapy could be guided into the area to reduce the tumor size or used following resection.

Session II: Biomechanics – I

EFFECT OF MUSCLE ENGAGEMENT AND MEASUREMENT POSITION ON ELECTRICAL IMPEDANCE OF THIGH MUSCLES

Joseph Mathews and Todd Freeborn
The University of Alabama Tuscaloosa, AL, USA

Electrical impedance measurements are being widely investigated as a means to monitor physiological change in many biological tissues, with applications for non-invasive real-time monitoring in both health and athletics. This pilot study aimed to determine if there are differences in the electrical impedance measurements collected for relaxed and tensed states of the thigh muscle, in both sitting and standing orientations. Understanding how both muscle engagement and measurement position effect the electrical impedance will be useful for systems to monitor localized muscle injury or fatigue in free-living environments, which will not have controlled conditions typical of clinical environments. For this comparison, seven sets of measurements were collected over a fourteen-day period from both right and left thighs of a single subject in four different orientations (sitting relaxed, sitting tensed, standing relaxed, and standing tensed). Each set of measurements were collected using an ImpediMed SFB7, from 3 kHz to 1 MHz, with a tetra-polar electrode configuration placed on the skin surface external to the quadriceps muscles. From these results, there was an increase of the electrical impedance in the tensed state compared to the relaxed state for all orientations on most days, with the decreases (averaged using the 3 kHz to 50 kHz measurements) ranging from 2% to 6%.

HEAT TRANSFER MODEL OF HUMAN THIGH: IMPLICATIONS FOR TOURNIQUET USE

Luke Smith and David Nelson
University of South Alabama, Mobile, AL, USA

Tourniquets are employed to restrict blood flow to limbs incurring severe bleeding. With prolonged application, ischemic and reperfusive tissue damage can occur, leading to potential loss of limb. A decrease in temperature through cooling can potentially reduce tissue damage. Protocols to improve limb salvage outcomes can be developed using heat transfer models. A commercial thermal analysis solver (TAITherm) was used with a heterogeneous model of the human thigh as a multi-layered 3-dimensional mesh. The model monitored thermoregulation between bone, muscle, fat, and skin within the body; observing tissue cooling as a function of ambient temperature. Blood flow was restricted to the thigh to mimic the effects of tourniquet application.

When subjected to steady-state environments of varying temperature, core tissue temperatures were noticeably reduced from lack of blood flow. This difference increased with environmental temperature, with a difference of several degrees. Over a six hour period of exposure to 20°C, 30°C, and 40°C environmental temperatures, blood flow was responsible for a tissue temperature difference of 1.2, 1.5, and 3.0 degrees, respectively. We can further observe changes from additional clothing layers and body sizes with this model.

FUNDAMENTALS OF LOAD TRANSFER MECHANISMS IN BIOSTRUCTURES: A COMPLEX NETWORK APPROACH

Reena Patel[1], Guillermo Riveros[1], David Thompson[2]
[1]US Army Engineer Research and Development Center, Vicksburg, MS, USA, [2]Mississippi State University, Starkville, MS, USA

Biostructures are unique owing to the multiple functions they are designed to accomplish coupled with the complex hierarchical geometrical arrangement that makes them strong, tough, lightweight, and energy dissipative. This work presents an integrated, interdisciplinary approach that utilizes computational and experimental mechanics with complex network strategy to obtain fundamental insights into failure mechanisms of high performance, light weight, structured composites by investigating structural and material properties of the rostrum. Although computational mechanics experiments give an overall distribution of stresses in the structural systems, due to the large numbers of degrees of freedom the underlying kinematics which plays a vital role in load transfer mechanisms and the formation of the strong and weak links in the network is unknown. Towards this end, the rostrum will be formulated as a network flow problem. The nodes and edges of the rostrum's network will be extracted from the numerical model used in the computational mechanics experiments. The flow network will be weighted based on the parameter of interest, which may be stresses, energy dissipation etc. The changing kinematics of the system is input to the mathematical algorithm that will compute the maximum flow of the stresses at uniform cost. This research investigates the load transfer mechanisms for the rostrum of the paddlefish by conducting computational mechanics experiments; identify the formation of the force chains in the rostrum by employing maximum flow /minimum cut mathematical algorithm and demonstrate preliminary results of the advantages of the flow network to solve this type of engineering problems.

MECHANO-MORPHOLOGICAL AND CELLULAR DEPENDENCE ON FIBER CHARACTERISTICS IN WET-LAID SCAFFOLDS

Andrew Wood[1], Dominique Everett[1], Sanjay Kumar[2], Vinoy Thomas[1]
[1]University of Alabama, Birmingham, AL, USA and [2]Alabama State University, Montgomery, AL, USA

Fiber-reinforced materials have been used across a number of applications as a means to fabricate composites with properties similar to more massive, economically undesirable materials. In areas of biomaterials, fibers offer this increased mechanical response but also serve as a pathway to direct cellular attachment and proliferation. For continuous phases with in vivo mimicry, hydrogels are a class of materials that closely simulate the extracellular matrix found in natural biological systems. Composed of a fibrous network with large volumes of entrapped aqueous solutions, these materials are soft, ductile, and formable, but they are plagued by inherent low mechanical properties. For applications in tissue engineering, the lack of a directional cues within the hydrogels is undesired in some applications as cells require a guide for organized proliferation. In this work, we have investigated the role of poly (lactic acid) (PLA) fiber length, concentration, and surface treatment as a reinforcement phase in hydrogels matrices and the resultant mechanical and cellular responses. With increasing fiber length and concentration, we hypothesize that the mechanical properties will increase while cellular penetration into the bulk will decrease. After surface treatment, we hypothesize that the mechanical properties will increase due to greater interfacial bonding. Together, the results indicate that the wet-lay process can be optimized for a specific set of mechanical and cellular values depending on the desired application site.

VARIABILITY OF ELECTRICAL IMPEDANCE MEASUREMENTS COLLECTED FROM HUMAN FOREARM USING MULTIPLE ELECTRODE CONFIGURATION

Shelby Critcher and Todd Freeborn
The University of Alabama, Tuscaloosa, AL, USA

Electrical impedance measurements quantify the resistance of a material to an injected electrical stimulus and have been used to detect physiological changes in biological tissues. Recently, these measurements have been applied to monitor muscle tissue towards determining if they can detect muscle fatigue. While electrodes in clinical applications can be precisely placed, their precise application for athletic monitoring may prove challenging. Therefore, it is important to understand how electrode placement impacts the measured impedance. This study collected electrical impedance measurements of the human forearm from 16 tetra-polar electrode configurations; with stimulus electrodes fixed and measurement electrodes varied along a 3 cm by 3 cm grid. Measurements from 3 kHz to 1 MHz using a ImpediMed SBF7 were collected from a single participant on three consecutive days. Results show maximum relative deviations from <1% to 52% for the real impedance and <1% to 81% for the imaginary for all days when electrodes were moved from the reference position. The relative deviations of the real impedances showed less variability with frequency (<10% relative change across all frequencies) than the imaginary components, which in some cases exhibited errors ranging of 0.215% at 92 kHz to 80.9% at 1 MHz.

Session III: Biomaterials – Chemistry

PROSPECT OF BIOFLAVONOIDS AS G4/C4 LIGANDS: SPECTROSCOPIC INVESTIGATIONS.

Bidisha Sengupta
Tougaloo College, Tougaloo, MS, USA

G- and C- quadruplex (G4 and C4) forming sequences in telomeric DNA and c-myc promoter regions of human DNA are associated with tumorigenesis. Ligands that can facilitate or stabilize the formation and increase the stabilization of G4 and C4 can prevent tumor cell proliferation and have been regarded as potential anti-cancer drugs. In the present study, steady state and time-resolved fluorescence measurements provide important structural and dynamical insights into the free and bound states of therapeutically potent plant flavonoid fisetin (3,3',4',7-tetrahydroxyflavone) and quercetin (3,5, 7,3',4'-pentahydroxyflavone) in G4 and C4 DNA matrices. We have exploited dual luminescence properties of fisetin and quercetin along with their chromophores 3-HF and 7HF to examine their efficacy of binding and compare their interactions with DNA, which is one of the macromolecular targets of flavonoids in physiological systems. Following the sequence of the human telomeric DNA 5'-d (CCCTAA-)n/(-TTAGGG)n-3', two single stranded DNA oligonucleotides, 5'-d(C3TA2)3C3-3' and 5'-d(T2AG3)4-3', and their duplex were used as receptors to study the binding. Circular dichroism (CD), differential absorption, Raman spectra and thermal melting studies provide evidences for the formation of tetraplex DNAs and size exclusion chromatography (SEC) proves the binding and 1:1 stoichiometry of flavonols in the DNA matrix. Comparative analysis of binding in presence of EtBr proves that fisetin favors binding at the face of the G-quartet, mostly along the diagonal loop. Preliminary results indicate fisetin to be a prospective candidate as a G4 ligand.

STRUCTURAL KINETICS OF OXIDATIVE DNA DAMAGE FROM HYDROGEN ATOM TRANSFER

Pradip Biswas
Tougaloo University, Tougaloo, MS, USA

Elucidating the molecular pathways of oxidative DNA damage reactions by radicals is essential to assess the secondary effect of ionizing radiation, oxidants, and to design biosensors and DNA cleavage molecules. Employing a Density Functional Theory based multiscale Quantum-Mechanical-Molecular-Mechanical simulation on explicitly solvated systems of single and double stranded DNA, we reveal the molecular pathways resulting from hydrogen abstraction by OH radicals. Targeting the H4' hydrogen of the sugar moiety, we reveal how the hydrogen abstraction leads to the formation of a ketone (C4'=O4') and the break the sugar ring. The H4' abstraction dynamics further reveals that the initial energy transfer to the P-O3' and P-O5' bonds dissipates in time leaving only a permanent weakening of these bonds if no other secondary reaction is allowed. However, when the H5' hydrogen is targeted, the hydrogen abstraction alone leads to DNA cleavage at P-O5'. Results, while mimic the experimentally observed oxidative states, provide further insight into the structural kinetics essential to design biosensors and DNA cleavage molecules.

DIRECT ARYLATION POLYMERIZATION SYNTHESIS OF A SERIES OF NEW SILOLE-BENZAZOLE COPOLYMERS

Colleen Scott[3], Milind Bisen[1], Sam McKinnon[3], Dominik Stemer[2], Christine Lusbcome[2]
[1]Southern Illinois University, Carbondale, IL, USA, [2]University of Washington, Seattle, WA, USA, [3]Mississippi State University, Mississippi State, MS, USA

Electron withdrawing substituents such as fluoro and cyano groups play an important role in organic electronics, due to their ability to change the optoelectronic properties of organoelectronic materials. Particularly, difluoro-benzothiadiazole (DFBT), difluorobenzo-selenadiazole (DFBSe), difluorobenzo-triazole (DFBTA) have received much attention as they have been shown in some cases to improve the performance of optoelectronic devices. Due to the harsh reaction conditions that are usually used to prepare polymers containing these compounds, direct arylation provides an environmentally benign alternative method to prepare these high performance optoelectronic materials. Siloles are another set of compounds that have continued to generate much attention in materials science due to their unusual electronic and photophysical properties. It is well known that siloles possess lower lying LUMO energies compared to other similar heteroles such as thiophene and pyrrole. These low LUMO energies are a result of the overlap between the s* orbital on the silicon atom and the p* orbitals of the butadiene unit. Siloles are therefore being explored in p-conjugated polymers as a means of lowering the LUMO orbitals thus leading to lower band gap materials. In this presentation we will discuss the preparation of a series of p-conjugated polymers containing a silole unit copolymerized with strong electron acceptors units of the benzozole family using the direct arylation polymerization reaction, including the relatively unexplored acceptor 5,6-dicyano-2,1,3-benzothiadiazole (DCBT). These polymers possess long absorbance and emission wavelengths resulting in low band gaps – below 1.8 eV and respectable hole mobilities, ~ 3.51 x 10^{-2} cm^2/V.s.

VISUAL SENSING OF ANIONS BY SYNETHEC RECEPTORS

Alamgir Hossain, Maryam Emami Khansari, Corey R. Johnson, and Bobby Portis
Jackson State University, Jackson, MS USA

Visual sensing of anions by synthetic receptors is an active area of research, because it provides fast and direct method to identify anions which plays important roles in chemistry, biology and environment. Selective binding of anions is important from the views of both fundamental and technological aspects. Although, a several classes of synthetic receptors have been known showing high affinity for anions, synthetic anion sensors capable of visual and optical discrimination of anions are still limited. In our studies, we synthesized several types of chemical sensors using conventional synthetic protocols, and characterized by NMR, mass and elemental analysis. The new compounds were then investigated for a variety of anions in solutions, suggesting that the new receptors are capable of selective binding of anions, displaying optical and visual color change. Acknowledgements: The project described was supported by Grant Number G12MD007581 from the National Institutes of Health.

STRUCTURAL MOTION OF DI-HEME PROTEIN MAUG AND ITS FUNCTIONAL ROLE

Manliang Feng
Department of Chemistry, Tougaloo College, Tougaloo, MS

MauG is a di-heme protein that contains two distinct heme groups, a penta-coordinated high spin heme and a hexa-coordinated low spin heme The biological role of MauG is to catalyze post-translational modification of pre-MADH to synthesis mature MADH. In the catalytic reaction the penta-coordinated high-spin directly reacts with oxygen donating substrates forming a catalytically active bis-Fe(IV) species through charge-resonance. Resonance Raman spectra of MauG at various temperature reveal two structural sub-states of the high-spin heme site. The two species exhibit temperature dependent equilibrium. At lower temperature, the high spin heme is mainly 5-coordinated while at higher temperature it appears as a mixture of penta/hexa coordinated high-spin heme. The presence of two structural sub-states was further confirmed by Fourier Transformed Infrared (FTIR) spectra of ferrous MauG-CO and UV-Vis spectrophotometric titration of MauG with cyanide ions. The frequencies of the vFe-CO and vC=O point to two distinct structures of the high-spin heme that differ both in the proximal and distal structures. Titration of MauG by various ligands indicates that the affinity of the high spin heme to exogenous ligand is affected by the charge on the ligand as well as the temperature. Kd for MauG-HCN complex is 0.00073 M while that for imidazole is Kd=0.024 M at 20^{o}C. For the MauG-HCN complex Kd for HCN is 10 times smaller (higher affinity) than that measured at the room temperature. These results are all consistent with a two-structure state model. Kinetics of MauG with oxygen was conducted to elucidate the role of the two sub-states and their inter-conversion in electron-transfer and catalysis. This work is supported by NSF Research Initiation Award under HBCU-UP program (Award number: 1505446).

Session IV: Education and Research Training

INTERACTIVE BIOMEDICAL EDUCATION AND RESEARCH TRAINING

Joseph A. Cameron[1], Ibrahim Farah[1], Ramaiyer Venkatraman[1], Hilda Wells[2], Michelle Tucci[3] and Hamed Benghuzzi [4]
[1]Department of Biology, Jackson State University, Jackson, MS, USA, [2]Department of Biology, Hinds Community College, Jackson, MS USA, [3]Department of Anesthesiology, University of Mississippi Medical Center and [4]Department of Clinical Health Sciences, School of Health Related Professions, University of Mississippi Medical Center, Jackson, MS USA

In an effort to enhance the number of well-trained minority health care professionals and basic science researchers, Jackson State University, (JSU, a historically black institution) in partnership with Hinds Community College (HCC, a 2-year college) and consultant biomedical researchers/health care professionals at the University of Mississippi Medical Center, established an interactive research training Bridges to the Baccalaureate Degree Program (BBDP). The purpose of the BBDP was to increase HCC students transfer rates to 4 year institutions by providing interactive research training and biomedical education to motivate trainees to seek Baccalaureate and advanced degrees in the biomedical and health sciences areas. The program involved faculty and administrators at each institution in the planning and implementation of all programmatic aspects, including student selection, advisement procedures and program activities. HCC students (280) were recruited (94.5 % of whom were African American) and trained in interactive groups in research laboratory methodologies, responsible conduct of research concepts, literature survey mechanisms, scientific writing techniques and basic science concepts in biology, chemistry, mathematics, physics, etc., during the academic year. Students engaged in specific individualized research projects during the summer and presented their research findings at local scientific seminars and professional meetings e.g., Mississippi Academy of Sciences, ABRCMS, FASEB, and the Endocrine Society. The results show that enhanced education and research training in biomedical sciences can enhance transfer rates and advanced degrees. (GM050117)

ATTAINING STEM EXCELLENCE THROUGH RESEARCH TRAINING AT HBCU

Maricica Pacurari
Jackson State University, Jackson, MS, USA

A high percentage of high school students have intentions to choose STEM disciplines, however the realizations of such ambitions is less successful. Recent studies show that half of those choosing STEM earn a degree within 4 to 6 years after entering the college. These studies suggest that: 1) the STEM programs need to be well developed to sustain STEM students throughout the 4 year program; and 2) STEM programs must offer a comprehensive education pathway to ease student's learning and sustain student's passion for STEM. Thus, in order to attain and sustain STEM student's excellence, the entire community STEM colleges, funding agencies, local funding agencies, and high schools must collaborate to develop education pathways to engage the students starting early in high schools and continuing throughout the college years. Also, many factors that influence students sustainability in the STEM including course sequence, quality of teaching, undergraduate learning environments, and student extracurricular activities must be addressed to circumvent the effect. In order to increase STEM students' sustainability and excellence in STEM disciplines, we propose: 1) re-examination of the existing science-based curriculum and reconfiguration of course objectives to emphasize problem-based learning, and critical-thinking skills; 2) develop and implement inquiry-based courses and real-world research through undergraduate research collaborations to emphasize real-world research experience. We believe that these activities will prepare and sustain STEM students throughout the STEM education to choose STEM career. These activities will advance student's understanding of STEM disciplines and prepare them for STEM careers particularly of STEM graduates from underserved groups.

FIRST THINGS FIRST: LAYING A FOUNDATION FOR STUDENT ENGAGEMENT IN THE CLASSROOM

Gloria Miller
Jackson State University, Jackson, MS, USA

The term Student Engagement is frequently used to describe a student's willingness to participate in routine school activities, such as attending class, submitting required work, and following teachers' directions in class. Whereas disengaged students are generally passive, they do not try hard, they tend to give up easily when challenged, and they can be bored, depressed, anxious, or even angry about their presence in the classroom. Disengaged students can also be withdrawn from learning opportunities or even rebellious towards teachers and classmates. Since the college drop-out rate for first-time-in college degree-seeking students here in the United States is nearly 50%, student engagement is increasingly seen as an indicator of successful classroom instruction, and as a valued outcome of school reform. Although much is fundamental to the student, research has found that teachers actually do play a vital role in their students' motivation and engagement. It is, therefore incumbent upon the teacher to actively seek to create the conditions that foster and/or encourage student engagement. This paper will discuss some of the strategies and best practices that teachers may find useful in laying a foundation for student engagement in the classroom.

TAILORING GITLAB FOR COMPUTER SCIENCE PROGRAMMING COURSES

Mesafint Fanuel[1], Tzusheng Pei[1], Ali Abu El Humos[1], Andrew Villarrubia[1], and Hyunju Kim[2]*
[1]Jackson State University, Jackson, MS, USA and [2]Department of Mathematics and Computer Science, Wheaton College, Wheaton, IL, USA

In light of the fact that teamwork is crucial in the development of new software or the maintenance of old systems; our project has built an in-house version control system using only open source products to provide students with the platform to experience collaborative development. This educational environment will instruct students on Open Source Software community. It will familiarize students with writing large scale software code and introduce them to version control tools hugely utilized in software development. Students will experience the various aspects of software development by playing different roles while allowing instructors to easily track student activities. The communities' code repository will work as a knowledge base for student projects, and thus students can reuse the code and artifacts as examples or basic frame works for their development. Progress in software engineering education can easily be measured using the historical archives of this repository, giving computer science departments and instructors insight about their students overall standing.

ACTIVE LEARNING CLASSROOMS - TECHNOLOGICAL INNOVATION OR EDUCATIONAL EVOLUTION? A MIXED-METHODS COHORT STUDY EXPLORING THE IMPACT OF ACTIVE LEARNING CLASSROOMS ON STUDENT LEARNING OUTCOMES

Xiaoshan Gordy
University of Mississippi Medical Center Jackson, MS USA

In the past decade, increasing criticism has pointed to the inadequacy of the traditional teaching methodology as it fails to take student learning into account. Education reformers started paying more and more attention to "active learning" in recent years. Consequently, active learning classrooms (ALC) emerged in order to accommodate the new concept of learning. Are active learning classrooms more conducive to student learning than the traditional classrooms (TC)? The current study sets out to conduct a mixed-methods cohort investigation aimed at discovering whether different learning spaces result in different learning outcomes. Two consecutive courses in allied health taught by the same instructor in a newly built active learning classroom were observed and observational field notes were taken. Each class was audio/video recorded and transcribed. Final course grades earned in an active learning classroom and four-year historical grades of the same course taught by the same instructor in the traditional classrooms have been collected and compared. Student surveys and a faculty focus group interview have also been conducted. The results from both quantitative and qualitative data were analyzed to evaluate the impact of the active learning classroom on student learning outcomes. Quantitative data indicate that teaching in the ALC yields no difference in student grades from teaching in the TCs. However, qualitative data show that ALC presents greater enjoyment in learning, and both faculty and students believe that the ALC enhances group activity efficiency, deepens engagement, amplifies interaction, and fosters the development of creative ideas.

Session V: Molecular Clinical Markers

UTILIZATION OF CHEMOID® ASSAY IN THE MANAGEMENT OF MALIGNANT GLIOMAS AND DRUG DISCOVERY

Pier Paolo Claudio[1], Candance Howard[2], Jagan Valluri[3], and David Pasco[4]
[1]University of Mississippi Medical Center Jackson, MS USA, [2]University of Mississippi Center Cancer Institute, Jackson, MS, USA; [3]Marshall University Huntington, WV, USA

The prognosis of glioblastoma (GBM) treated with standard-of-care maximal surgical resection and concurrent adjuvant temozolomide (TMZ)/radiotherapy remains very poor (less than 15 months). Glioblastomas have been found to contain a small population of cancer stem cells (CSCs) that contribute to tumor propagation, maintenance, and treatment resistance. The highly invasive nature of high-grade gliomas and their inherent resistance to therapy lead to very high rates of recurrence. Administration of ineffective anticancer therapy is not only costly but more importantly burdens the patient with unnecessary toxicity and selects for the development of resistant cancer cell clones. We have developed a drug response assay (ChemoID®) that identifies the most effective chemotherapy against CSCs and bulk of tumor cells from of a panel of potential treatments, offering great promise for individualized cancer management. A prospective study was conducted evaluating the use of the ChemoID® drug response assay in 41 glioblastoma patients. Data regarding tumor response, time to recurrence, progression-free survival (PFS), overall survival (OS), odds Ratio (OR) associations of 12-month recurrence estimated for CSC, bulk tumor and combined assay responses will be discussed. Additionally, the use of the ChemoID® drug response assay as a discovery platform using natural product extracts in combination with the standard-of-care on patients' derived cancer primary cell lines will be discussed.

ACTION OF NATURAL PRODUCTS ON PATIENT-DERIVED CANCER STEM CELLS AND BULK TUMOR CELLS

David S. Pasco,[1,2,3] Pier Paolo Claudio,[1,2] Premalatha Balachandran,[1,2] and Jin Zhang[1,2]
[1]National Center for Natural Products Research, [2]Research Institute of Pharmaceutical Sciences, [3]Department of Pharmacognosy, School of Pharmacy, University of Mississippi, University, MS, USA

Genetic and epigenetic events that contribute to the transformation of normal cells into cancerous cells result in the abnormal functioning of many cell signalling pathways. This realization has led to the search for agents that target these pathways. We have utilized a battery of 13 inducible luciferase reporter gene vectors where expression is driven by enhancer elements that bind to specific transcription factors. Several thousand crude plant extracts and pure compounds were run through this screen using HeLa cells. Several compounds exhibited diverse activity profiles and were subsequently tested in the ChemoID assay against patient-derived bulk tumor cells and cancer stem-like cells. These cells were isolated from patients bearing Non-small cell lung cancer, triple negative breast cancer or Temodar-resistant Glioblastoma Multiforme. The natural products tested demonstrated either patient or tumor-type specificities for bulk vs tumor stem-like cells *in vitro*. Some natural products showed either additive or more than additive cytotoxicity in combination with many chemotherapeutic agents. Some reduced the effectiveness of certain chemotherapeutic agents. This represents an approach that could afford us an important and unique niche in the Precision Medicine Initiative – identifying patient/tumor-specific natural product-chemotherapeutic combinations that are effective against both bulk tumor cells and tumor stem-like cells.

IN VITRO ANALYSIS OF MICRORNA-181A ROLE IN LUNG INFLAMMATION

Maricica Pacurari
Jackson State University, Jackson, MS USA

Inflammation is the underlying mechanism of many lung pathologies including, lung cancer. TNFalpha is the master cytokine released during lung injury that initiates a cascade of inflammatory signaling. MicroNAs are short strands of RNAs that regulate gene expression. Using bioinformatics tools, we identified microRNA-181a novel targets Col3A1 and Notch2. Col3A1 is a component of ECM with a role in lung remodeling. Notch 2 is known to regulate epithelial progenitor cells differentiation during lung development and plays a role in NSC lung cancer.In the present study, using an in vitro system of lung cells, we investigated whether TNFalpha regulates microRNA-181a and Col3A1 and Notch2. Using A549 lung cells, we analyzed the regulation of miR-181a, Col 3A1 and Notch2 by TNFalpha using qPCR and western blot. A549 cells were exposed to TNFalpha (1 and 10 ng/ml) for 6 or 24 h. miR-181a, Col3A1 and Notch2 mRNA were analyzed. Notch 2 expression was analyzed using Notch2 antibodies. Low concentration of TNFalpha (1 ng) and short exposure (6h) slightly decreased miR-181a (0.86- vs 1.0-fold change of control). High concentration of TNFalpha (10 ng) and short exposure increased miR-181a (1.86- vs 1.0-fold

change of control). After 24h, low concentration of TNFalpha inhibited miR-181a (0.27- vs 1.0-fold change) whereas high dose of TNFalpha had no effect on miR-181a. TNFalpha significantly increased Notch2 mRNA. Immunohistochemistry showed a strong immunodetection of Notch 2 at cell periphery. Overall these data suggest that in vitro system models are suitable to study the mechanisms by which TNFalpha modulates lung inflammation and underlying pathologies.

A NEW METHOD FOR EARLY DIAGNOSIS OF COLON CANCER USING FLUORESCENCE EXCITATION-SCANNING HYPERSPECTRAL IMAGING

Malvika Lall[1,6], Joshua Deal[1,3], Shante Hill[4], Paul Rider[5], Carole Boudreaux[4], Thomas Rich[2]
[1]Chemical and Biomolecular Engineering, University of South Alabama, Mobile, AL, USA; [2]Pharmacology, University of South Alabama, Mobile, AL, USA; [3]Center of Lung Biology, University of South Alabama Mobile, AL, USA; [4]Pathology, University of South Alabama, Mobile, AL, USA; [5]Surgery, University of South Alabama, Mobile, AL, USA; [6]Biomedical Sciences, University of South Alabama, Mobile, AL, USA

Colon cancer is the second leading cause of cancer death in the United States. Early detection and diagnosis is an important step in reducing morbidity and mortality making the ultimate goal of screening exams to identify lesions prior to advancement into cancer or tissue invasion. The objective of this study is to examine the potential of hyperspectral imaging for measuring spectral changes that are concurrent with changes in colon cancer compared to surrounding normal tissue. Specimen pairs of fresh normal and adenocarcinoma were obtained from surgical resections of colon tissue in collaboration with the University of South Alabama Departments of Surgery and Pathology. All procedures were carried out in accordance with Institutional Review Board protocol # 13-120. Tissues were scanned by excitation scanning hyperspectral imaging using a novel microscope constructed at the University of South Alabama. Multiple fields of view (FOV) were acquired from each specimen and MATLAB and ENVI were used to correct for background signal and to draw regions of interest and extract the average spectra for each region. When comparing spectra averaged over several areas of normal colon, results demonstrated consistent spectral information images with similar peak wavelengths and shapes. However, in colon cancer, extracted spectra demonstrated high heterogeneity. High heterogeneity likely indicates variation in structural organization and molecular composition that is divergent from normal tissue composition. We conclude that hyperspectral fluorescence excitation-scanning may be a viable technology for detecting abnormal changes in the colon tissue based on spectral changes in the mucosa of the colon.

FUNCTIONAL ANALYSIS OF AIF-1 IN ASSOCIATION WITH CARDIAC ISCHEMIA REPERFUSION (IR)

Olga McDaniel[1], Allen Simeone[1], Kathy Alvarez[2], Madeleine Cunningham[2], and Larry McDaniel[1]
[1]University of Mississippi Medical Center, Jackson, MS, USA and [2]University of Oklahoma Health Science Center, Oklahoma City, OK, USA

The mechanisms by which sterile inflammation is induced, after ischemia/reperfusion (IR) during organ procurement contributes significantly to tissue injury and may cause early organ dysfunction after transplantation. Genes associated with innate immunity are prime activators of early inflammatory responses to an allograft that lead to host-induced inflammation and organ rejection. We hypothesized that endogenous substances or damage-associated molecular patterns (DAMPs), released after allograft reperfusion such as allograft inflammatory factor 1 (AIF-1)/Daintain could promote activation of innate immune responses through the activation of cardiac TLRs and may contribute to allograft dysfunction. We have investigated expression levels of AIF-1 and TLRs during cardiac IR in a rat model of the left anterior descending artery (LAD) occlusion which generates ischemia in the left ventricle (LV). AIF-1 and TLR mRNA transcripts were significantly increased in a time dependent- manner after IR. These markers were upregulated as early as 10 minutes after reperfusion and further they were increased several-fold after 60 minutes of reperfusion in tissue and peripheral blood cells as compared to the control group. Functional activity of AIF-1 was confirmed in an in vitro model using human coronary vascular smooth muscle cells (CVSMC), treated with IFN-g as well as using HEK293 cells transfected with h-TLR2 or TLR4 in which the end product was determined by production of IL-18 cytokine. Thus, elucidation of the mechanisms of an induced inflammation within the allograft has the potential for the development of novel anti-inflammatory strategies that could improve outcomes for solid organ transplant recipients.

SERS MONITORING OF PROSTATE CANCER PHOTOTHERMAL THERAPY USING GOLD NANOMATERIALS

Santanu Banerjee
Chemistry and Physics Department, Tougaloo College, Tougaloo, MS, USA

Prostate cancer is the most common malignancy among US men. The Southern states, including MS has one of the highest prevalence and fatality rates due to prostate cancer in the nation. Currently available treatments of radiation, surgery, and chemotherapy have severe side effects and are mostly ineffective in advanced stages. Recent advances in Nanotechnology have provided new approaches to treat this disease. We use the Surface Enhanced Raman Spectroscopy (SERS) for detection and monitoring of photothermal destruction of prostate cancer cells. Raman signal is normally quiet weak but can be enhanced over 10 orders of magnitude in gold nanoparticles and adsorbed molecules on such nanoparticles, thus making it a highly sensitive probe to detect the presence of cancer cells. We bind Rh6g attached RNA Aptamers followed by attaching anti PSMA antibodies corresponding to proteins overexpressed in the LNCaP prostate cancer cells, to join to popcorn shaped gold nanoparticles. These multifunctional gold nanomaterials selectively aggregate on LNCaP prostate cancer cells. We monitor the SERS signal of the Rh6g dye. In presence of LNCap cells we clearly see a strong SERS signal detectable to less than 100 cells per ml. The SERS signal diminishes as we perform photothermal therapy with 785 nm continuous Near Infrared Laser until all the prostate cancer cells are destroyed. This work was supported by the Mississippi INBRE, funded by an Institutional Development Award (IDeA) from the National Institute of General Medical Sciences of the National Institutes of Health under grant number P20GM103476.

Session VI: Biomechanics – II

ACCURATE DETERMINATION OF THE DYNAMIC PERMEABILITY OF THE LACUNAR–CANALICULAR SYSTEM IN HUMAN CORTICAL BONE

M. Benalla[1], L. Cardoso[2] and S. C. Cowin[2]
[1]Northwestern State University and [2]City College of New York

A new method for the experimental determination of the permeability of a small sample of a fluid-saturated hierarchically structured porous material is described and applied to the determination of the lacunar–canalicular permeability *(KLC)* in bone. The interest in the permeability of the lacunar–canalicular pore system (LCS) is due to the fact that the LCS is considered to be the site of bone mechanotransduction due to the loading-driven fluid flow over cellular structures. The permeability of this space has been estimated to be anywhere from 10−17 to 10−25 m2. However, the vascular pore system and LCS are intertwined, rendering the permeability of the much smaller-dimensioned LCS challenging to measure. In this study, we report a combined experimental and analytical approach that allowed the accurate determination of the *K*LC to be on the order of 10−22 m2 for human osteonal bone. It was found that the *K*LC has a linear dependence on loading frequency, decreasing at a rate of 2×10−24 m2/Hz from 1 to 100 Hz, and using the proposed model, the porosity alone was able to explain 86% of the *K*LC variability.

EFFECT OF MUSCLE FATIGUE ON ELECTRICAL IMPEDANCE OF BICEP MUSCLES DURING EXERCISE OF VARYING INTENSITY: A CASE STUDY

Tim Crenshaw and Todd Freeborn
The University of Alabama, Tuscaloosa, AL, USA

Electrical impedance measurements quantify the resistance of a material to an injected electrical stimulus and have been used to detect physiological changes in biological tissues. Previous studies have indicated that exercise induced fatigue results in a decrease of the electrical impedance of muscle tissues compared to pre-fatigue values. However, studies have failed to explore the impact of exercise intensity on this decrease, which is an important consideration if this technique is to be used for personalized, real-time fatigue monitoring for athletes during training and competition. During this case study, a single subject performed sets of bicep curls until failure on multiple days at 60%, 75%, or 90% of their assessed one repetition maximum towards inducing fatigue in their bicep muscle. Electrical impedance measurements from 5 kHz to 1 MHz were collected using a tetra-polar electrode configuration and Keysight E4990A impedance analyzer immediately pre- and post-exercise. The electrical impedance of the bicep muscle showed decreases after each of the fatigue protocols, consistent with previous research, with resistance/reactance decreases of 1.5%/3%, 7.2%/15.3%, and 5.8%/15.5% immediately post the 90%, 75%, and 60% protocols, respectively, compared to pre-exercise measures.

APPLICATIONS OF INERTIAL MICRO-ELECTRO-MECHANICAL SYSTEMS ON AMERICAN FOOTBALL PLAYERS AND EQUIPMENT

Derius Galvez and Jamel Alexander
Mississippi State University, Starkville, MS, USA

North American football players often hurt themselves because of incorrect football positions. The idea of using orientation sensing to help younger football players with football position development was studied in this research. This paper discusses how an orientation sensor can be created to help younger football players develop a better tackling position. After reviewing three inertial measurement devices, the raspberry pi coupled with a lis331 accelerometer was chosen. The MATLAB program reads the x, y, and z gravity components of the accelerometer and inputs them into the Euler angle equations. Once these angles were found, they were inserted into a flight path equation which was formulated into an orientation matrix. This allowed the sensor to measure the orientation of the football players. However, variance in the resolution of the sensor most likely occurred due to a mismatch of the input excitation voltage in the power surge which was 12 volts and the sensor's threshold voltage which was 3.3 volts. Further work must be done to enhance the signal output or sensitivity of the sensor.

CHARACTERIZATION AND OPTIMIZATION OF COLLAGEN-ELASTIN-LIKE POLYPEPTIDE COMPOSITE SCAFFOLDS FOR BONE TISSUE ENGINEERING

Bhuvaneswari Gurmurthy, Jason Griggs, and Amol Janorakar
University of Mississippi Medical Center Jackson, MS USA

Collagen scaffolds for guided bone regeneration (GBR) have poor mechanical properties and fail due to lack of rigidity and rapid degradation by collagenases. We have reinforced the collagen matrix with elastin-like polypeptide (ELP) and optimized the mechanical properties using a novel statistical method of response surface methodology (RSM). 2-7mg/mL collagen and 0-24mg/mL ELP were used in 11 different proportions to form the composites. Physical properties characterized by swelling ratio, differential scanning calorimetry, and FTIR spectroscopy revealed that the addition of ELP in composites reduced the residual water content. Scanning electron microscopy images of the control collagen-only hydrogels showed porous collagenous microstructure, but the ELP-collagen composites showed a dense collagenous microstructure with characteristic ELP aggregates. Mechanical properties determined by uniaxial tensile testing revealed variation with composition. Likely because of its low water content and dense microstructure, the 6:18mg/mL collagen:ELP composite had the maximum strength and modulus, but had lower toughness than many composites. Using just 5 compositions (versus the 11 we had to prepare for mechanical testing) RSM directed us to a new composition (6:12mg/mL collagen:ELP) that may have high toughness without negatively impacting strength and modulus. Overall, RSM efficiently performed optimization of composite composition by considering target levels, minimal requirements, and relative importance of the mechanical properties and predicted a new composition for future testing. Taken together, the composites prepared in this research can form good quality, rigid porous structures required for GBR as well as other tissue engineering applications.

BIOCOMPATIBILITY OF NOVEL COPPER-CONTAINING BIOCOMPOSITES IN QUANTIFIABLE MODEL CELL SYSTEM

Kahla St Marthe, Mark DeCoster, Neha Karekar, and Anik Karan
Louisiana Tech University, Rushton, LA, USA

Biomaterials demonstrate great promise for use as tools in a wide range of biomedical applications. Specifically, the use of these materials for the treatment and study of nervous system disorders is becoming increasingly important as the diversity of synthesized materials increases. Biomaterial scaffolds can be used as bridges, cell carriers, and targeted drug delivery vehicles, for transporting regenerative and therapeutic agents to damaged neuronal circuits. Our lab has recently discovered a novel, copper-containing and amino acid (cystine)-based biocomposite material with potential for drug delivery due its degradability and low agglomeration in physiological conditions. Here, we used a quantifiable model cell system to demonstrate that delivery of moderate levels of HARS has little effect on cell function. More specifically, we have shown that exposure of increasing concentrations of the HARS from 2 to 50µg/ml, results in a dose-dependent diminishing viability and capacity of PC12 cells to extend neurites in response to the biological cue i.e. nerve growth factor. We have also exposed astrocytes, primary neurons and microglia to this material to study cytotoxicity of the material with naturally occurring brain cells. The results of cell viability studies using HARS material with our quantifiable system indicate that HARS are biocompatible, and this demonstrates their utility in neuronal experiments. For example, as an additive step in engineering HARS, due to the cystine content of our biocomposite, these novel materials could be functionalized with growth factors or antibodies for targeted delivery in the brain.

AN EFFORTLESS NON-INVASIVE RESPIRATORY DIAGNOSTIC DEVICE

Jafar Vossoughi and Arthur Johnson
Fischell Department of Bioengineering
University of Maryland College Park, College Park, MD, USA

We have developed a simple inexpensive respiratory diagnostic device, the Airflow Perturbation Device (APD) that evaluates the respiratory resistance non-invasively and effortlessly while the subject normally breathes into the device, i.e. unlike other devices such as the spirometers that require considerable effort. APD detects the breathing flow and pressure. The respiratory resistance is then automatically calculated by dividing the breath pressure (in cmH_2O) by the breath flow (in L/s), resulting in respiratory resistance in $cmH_2O/L/s$. Although the device is still being enhanced, it is in its final stage of clinical trial. We have collected respiratory resistance values for over 3,500 subjects, both normal and those with asthma, COPD and vocal cord dysfunction. The competing methods consist of spirometry, plethysmography (body box), and impulse oscillometry (IOS). Spirometer is a simple inexpensive device, but requires considerable effort and is not reliable. Both plethysmograph and impulse oscillometer are expensive and very difficult to use and interpret their results. The APD is most useful in diagnosing the respiratory disorders of young children, we have even successfully used the APD in neonates.

Session VII: Modeling and Patient Safety

IN VIVO EVALUATION OF THE EFFECT OF RESONANCE FREQUENCY ON DELIVERING INSULIN NON-INVASIVELY USING ULTRASOUND

Khaldon Lweesy, Hadeel Naijar, Sara Hajeer, and Sarah Attari
Jordan University of Science and Technology, Irbid, Jordan

Single element ultrasound atomizing circular transducers with different resonance frequencies were studied for the purpose of non-invasively delivering insulin transdermally, in order to overcome the daily pain and the risk of contamination associated with injection. Frequencies ranging from 20 kHz to 2.1 MHz were tested for this purpose. Each transducer was housed with plexiglas material which included a reservoir to hold insulin during the experiments. For each transducer, twenty white rats (weight: 200-240g) were used and divided into four groups (two control and two exposure). The rats were anesthetized by intramuscular injection of 0.5 ml of a mixture of Kitamine and Xylazine after overnight fasting. Ultrasound was delivered in pulses for a duration of 20 minutes, and the blood glucose level was measured every 10 minutes through a period of one hour. The blood samples for the strips were taken from the tail (through the jugular vein). For each transducer, the skin was closely examined after ultrasound exposure for any signs of injury to notice the thermal effects if existed. For the control experiments, the same setup was followed up except that the power generator was turned off. Ultrasound transducers in the kHz range performed better that those in the MHz range; with the best performance achieved at a frequency of 40 kHz. A 40% reduction in Glucose level was achieved at 40 kHz while the reduction was only 5% at a frequency of 2.1 MHz.

THE INFLUENCE OF PHYSICAL ACTIVITY AND FRUIT AND VEGETABLE CONSUMPTION ON ADULT OBESITY

Shelia Baity and Elgenaid Hamadain
University of Mississippi Medical Center, Jackson, MS, USA

Obesity is an epidemic that leads to severe chronic health complications, and is preventable by physical activity and consumption of fruits and vegetables. The objective of this study was to compare behavioral risk factors associated with adult obesity among six different States as an attempt to explain the differences in obesity levels among the six states of the leanest Colorado and Hawaii; the middle of Maine and Georgia; and the most obese Louisiana and Mississippi. Data was collected from the Behavioral Risk Factor Surveillance System (BRFSS). First, the results confirmed that there was a significant difference among the six states with respect to prevalence of obesity ($P < 0.05$). Results also, indicates a significant difference in weekly Physical activity among the six selected states ($p < .05$). As the levels of physical activity increased, the prevalence of obesity decreased. Fruit and vegetable consumption was also significant ($p < .05$). Results indicate that as people consume five or more servings per day significantly impacted obesity rates. In addition, there was a significant difference among the income groups ($p<.05$). As mean household income went up, prevalence of obesity went down. Results on children Grade 9-12 demonstrated a fair positive and significant correlation ($r =0.669$, $p < 0.05$) between watching TV three hours or more and the prevalence of obesity. Obesity tends to worsen from children to adults if intervention is not provided. No significant difference between males and females was observed for all the six states. Differences between the six selected states were significant ($p <05$) for education level. Overall, as the education level rose, the prevalence of obesity declined supporting the fact that the more educated the people are, the better choices in life they may have generally. In conclusion, physical activity and consumption of fresh fruits and vegetables have vital impact on the prevalence of obesity. An increase in physical activity, and consumption of fresh fruits and vegetables is key to eliminating obesity. More must be done to influence people to become more active in their daily life. There should be facilitators to encourage regular consumption of fruits and vegetables and make them available for people at reasonable cost.

COLORECTAL CANCER SURVIVAL IN THE DELTA AND NON-DELTA REGIONS OF MISSISSIPPI

Deirdre B. Rogers, Ellen S. Jones, and Elgenaid I. Hamadain
School of Health Related Professions, University of Mississippi Medical Center, Jackson, MS, USA

Introduction: Colorectal cancer is the second most common cancer in Mississippi affecting both males and females. Mississippi ranks second in the country for incidence and first in mortality from colorectal cancer based on 2013 data. Geographic region or neighborhood can have an impact on survival. **Methods:** A retrospective cohort research design was used to study data collected by the Mississippi Cancer Registry. The data set included colorectal cancer cases diagnosed between 2003 and 2011 with passive follow-up through 2011. Relative survival was analyzed by Delta and non-Delta region for Mississippi with stage and race included in the survival model. **Results:** The non-Delta region was significantly more likely to be diagnosed with advanced stage disease. For both whites and blacks, the non-Delta region had significantly higher survival compared to the Delta region. For both local and advanced stages of disease, the survival differences between the races in each region remained significant. **Discussion:** Race and stage do impact survival, but are not the only reason for the survival differences between the Delta and non-Delta regions. Stage and region do not completely account for the survival differences between the races.

IMPORTANCE OF EFFECT SIZE AND SIGNIFICANCE TESTING FOR ANALYZING AND COMMUNICATING RESEARCH STUDIES

Jamil Ibrahim[1], S Ibrahim[2]
[1]University of Mississippi Medical Center, Jackson, MS, USA, [2]Arab American University, Jenin, Palestine

In research practice, the most common requests to statisticians from investigators are sample size calculations or sample size justifications. Determining sample size is one of the most important steps in designing a study. In order to have reliable and valid results, it is important to determine the right sample in combination with high quality data collection efforts. Sometimes, researchers have different opinions as to how sample size should be calculated. Statisticians usually choose from many available formulas that can be applied for different types of data and study designs. The aim of this workshop is to clarify this issue and to provide examples on how to calculate sample size. The components of sample size calculations will be discussed and what factors to consider in choosing the sample size. Other concepts related to this issue such as power analysis, confidence intervals, variability, type I error, type II error, and minimum effect size of interest will also be discussed.

PREVALENCE AND TRENDS OF EARLY CHILDHOOD CARIES EXPERIENCE AND UNTREATED CARIES IN THE MISSISSIPPI HEAD START POPULATION

Kristin Nalls, Elgenaid Hamadain, Denise Krause
University of Mississippi Medical Center, Jackson, MS USA

Background: Early Childhood Caries (ECC) is "the presence of one or more decayed, missing (due to cavities) or filled tooth surfaces in any primary tooth in a child 71 months of age or younger". ECC is the most common childhood disease, is linked to periodontal disease, poor academic performance, and increased likelihood of chronic disease in adulthood and poor quality of life for the children who are affected and their families [2]. ECC disproportionately affects low-income and minority children. Head Start is a federal preschool program aimed to identify and provide support for low-income children and their families. Due to the federal mandates for Head Start grantees, children participating in these programs are in a position to receive increased access to dental care through oral screenings and referrals to dentists for oral health treatment. Studies have shown that Head Start enrollees are almost three times more likely to obtain a dental screening than those enrolled in other preschool centers. Even with these parameters in place, a great amount of tooth decay is still present in Head Start children. There is a need to evaluate present interventions as a starting point for

oral health reform in this underserved population The **purpose** of this study is to investigate and report the demographics and the current oral health status of MS Head Start children, as well as to determine any statistical difference with national prevalence reported by The National Health and Nutrition Examination Survey (NHANES). **Methods:** The study used the oral screening data from the Mississippi State Department of Health's (MSDH) *Make a Child's Smile Program* for the time period 2009-2014 and data retrieved from NHANES to examine prevalence of caries experience and untreated caries over the study time period, and to compare the oral health status of MS Head Start Children to national reported levels. **Results:** The sample was majority African American, between the ages of 3 and 5 years of age, displaying a burden of caries experience and untreated diseases significantly higher than the reported national percentages, ($p < 0.01$). Gender was not found to have a significant impact within the sample, however, the prevalence of caries experience and untreated caries were significantly higher than the nationally reported rates, ($p < 0.01$). **Conclusions:** Caries experience and untreated caries is a significant problem in MS Head Start Children. Further research is needed to develop more effective interventions and oral health policies.

ANTICOAGULANT EFFECTS ON PURE PLATELET-RICH PLASMA

Sofia Galdames, Andrea Shimojo, Angela Luzo, and Maria Santana

Unicamp Campinas, SP Brazil

Platelet-rich plasma (PRP) is frequently used to restore adequate number of platelets and thus maintain hemostasis. Nowadays, PRP has been widely used in regenerative medicine as an important tool. However, different protocols of preparation affect the properties of PRP, making result comparison more difficult. We investigated the effects of anticoagulants on blood cells and on plasma partitioning behavior after centrifugation, adopting a standardized protocol. P-PRP type (rich in platelets and poor in leukocytes) was prepared with one centrifugation cycle (100xg, 10 min), using a range of hematocrit of 30% to 45% from 10 healthy donors. Results show that anticoagulants primarily affected the morphology of the red blood cells (RBC) and the centrifugal portioning of plasma. As a consequence, different RBC packing levels and PRP volumes were obtained upon centrifugation. This study demonstrates how important is the standardized protocol and also that the investigated anticoagulants affected the preparation of P-PRP.

APPLICATIONS OF RAMAN SPECTROSCOPY AND IMAGING IN MEDICINE

Shan Yang
Jackson State University, Jackson, MS USA

Raman scattering is a great analytical tool based on the identifying the characteristic vibrational energies of molecules presented in a material. Raman scattering based spectroscopy and imaging technologies have high potential in resolving medical problems, and the new applications are emerging continuously. In this presentation, recent studies in medical applications of Raman spectroscopy and imaging will be reported. The studies include portable Raman device for gout crystal analysis, direct Raman imaging for early tooth decay detection, and bounded and unbounded water analysis in bone. The status of these research will be presented: the portable Raman device has shown clinical trial results superior to current available clinical analysis method, the preliminary data shows Raman imaging is feasible in detection early tooth decay, and unbounded water can be discriminated from bounded water with Raman spectroscopy.

Session VIII: Drug Delivery

THERAPEUTIC GROWTH FACTOR DELIVERY USING THE ELASTIN-LIKE POLYPEPTIDE BIOPOLYMER PLATFORM

Gene Bidwell and Alejandro Chade
University of Mississippi Medical Center, Jackson, MS, USA

Therapeutic delivery of growth factors is an emerging area for treatment of a multitude of disorders, including regenerative medicine and pro-angiogenic therapy for chronic ischemia. However, free endogenous growth factors have poor pharmacokinetic and plasma stability profiles and do not make good pharmacological agents. The focus of this area of research is to develop a biopolymer delivery system to achieve a means for purification, extended plasma half-life, and tissue targeting of therapeutic growth factors. We are specifically developing isoforms of vascular endothelial growth factor (VEGF) family members for therapeutic angiogenesis in ischemic renal disease. VEGF family members were fused to the elastin-like polypeptide (ELP) biopolymer, a thermally responsive drug carrier which allows for easy purification, reduced immunogenicity, and extended plasma half-life of fused therapeutics. We demonstrated that ELP-VEGF has a long plasma half-life in a swine model. Furthermore, intrarenal administration of ELP-VEGF induced an increase in microvascular density and an improvement in renal function in a swine model of chronic renal artery stenosis. Ongoing studies are extending this approach by utilizing a kidney targeting peptide to dramatically improve renal targeting after systemic administration. The kidney targeting peptide increased renal deposition and specificity of ELP relative to the non-targeted polymer in both rat and swine models, and current studies are examining the efficacy of the kidney targeted form of ELP-VEGF via systemic administration for restoration of microvascular density and improvement of renal function in the swine renovascular disease model.

DRUG LOADED HALLOYSITE CLAY NANO TUBES AS TABLET COMPRESSION EXCIPIENT

Raghuvara Yendluri[1], Yuri Lvov[1], Melgardt De Villiers[2]
[1]Louisiana Tech University, Ruston, LA, USA and [2]University of Wisconsin Madison WI USA

Naturally formed nanotubes of halloysite clay were explored as a vehicle for delivery of anti-bacterial, anti-hypertensive, anti-cancer and cosmetic agents. Halloysite is an alumosilicate tubule material with 15 - 20 nm diameter lumen which can be used for loading and release of drugs; these biocompatible clay nanotubes may be used either in their pristine form or with chemically modifying the inner or outer surface. However, halloysite drug composites which were prepared previously were not included in any practical medical formulation. In the current study, flow and compressibility properties of halloysite such as angle of repose, Carr's index and Hausner ratio were analyseed as applied for tablets. Halloysite nanotubes were loaded with nifedipine with 5-6% loading efficiency and incorporated in to tablets at 50 wt %. Sustained drug release was studied from pristine halloysite and tablets in simulated gastric and intestinal media. Halloysite was found to be a potential compression excipient material with good to excellent flow properties. Drug release from halloysite incorporated tablets extended up to 20 hours at a sustained rate, as compared with only 3-4 hours for a standard over the counter nifedipine tablet.

IN VITRO ASSESSMENT OF A KERATOSE-PACLITAXEL DRUG COATED BALLOON

Emily Turner[1], Marzieh Atigh[1], Luke Burnett[2], and Saami Yazdani[1]
[1]Department of Mechanical Engineering, University of South Alabama, Mobile, AL, USA and KeraNetics, Winston-Salem, NC, USA

Drug coated balloons (DCB) represent a novel approach to develop a superior intervention for the treatment of peripheral artery disease (PAD). Currently, DCB are coated with antiproliferative drugs, typically paclitaxel, which combat restenosis. When coated alone, paclitaxel has poor retention due to its diffusion from the artery following treatment. Excipients have marginally improved paclitaxel retention, however retention rates are still suboptimal. Keratose, a form of keratin, is a potential paclitaxel excipient due to its biocompatibility and tunable drug release properties. The goal of this project is to evaluate keratose paclitaxel excipient in DCB. Briefly, paclitaxel-containing keratose hydrogels were formed. Keratose degradation and paclitaxel release were quantified up to 45 days. Keratose-paclitaxel DCB were coated, visualized under scanning electron microscopy (SEM), and quantified for paclitaxel dosage. Drug retention was quantified in porcine carotid

arteries 1 hour post-treatment. Results demonstrated that keratose-paclitaxel hydrogels released paclitaxel as a function of keratose concentration. SEM revealed a uniform coating comparable to commercially available DCB. Drug load averaged 2 µg/mm2. Paclitaxel retention at 1 hour was 43.6 ng/mg, which falls in the therapeutic range of paclitaxel. These studies highlight the potential of a keratose to provide a safe and controllable drug release profile for PAD treatment.

THE EFFECT OF SUSTAINED DELIVERY OF NPY RECEPTOR ANTAGONIST ON BODY WEIGHT

Jill Clayton, Michelle Tucci, and Hamed Benghuzzi
University of Mississippi Medical Center, Jackson, MS, USA

NPY is a neuropeptide that plays a major role in feeding behavior. The hyperphagia associated with menopause is thought to be a result of increased levels of NPY as estrogen declines. Female rats were ovariectomized and when the level of estrogen declined they were implanted with either empty tricalcium phosphate (TCP) delivery systems or TCP delivery devices capable of delivering 5 ng/day of a selective NPY 1 receptor antagonist. Body weights were obtained weekly, and blood was collected at 2, 4, and 8 weeks following insertion of the delivery device. The results showed a statistically significant reduction in body weight as early as two weeks in animals receiving the NPY 1 receptor antagonist when compared to ovariectomized control animals and ovariectomized animals with a sham (empty) delivery device. The blood estrogen, leptin and NPY levels were not different between the groups at any time point. The data indicates that antagonism of the NPY1 receptor may be an important target for reversal of post-menopausal weight gain.

INCREASED GLUTHATIONE IN CAOV-3 OVARIAN CANCER CELLS FOLLOWING DELIVERY OF THYMOQUINONE

Jennifer Harpole, Michelle Tucci, and Hamed Benghuzzi
University of Mississippi Medical Center, Jackson, MS, USA

Thymoquinone (TQ) is an antioxidant that has possible anti-cancer effects. Studies have shown that TQ can exhibit inhibitory effects on the cell proliferation of many cancer cell lines. These results indicate that TQ inhibits tumor angiogenesis, tumor growth, and could be used as a potential drug candidate for cancer therapy. Cancer cells are constantly exposed to oxidative stress which can be detected by glutathione levels. The glutathione assay measures glutathione peroxidase which protects the organism from oxidative damage. This study investigates the glutathione levels after the conventional and sustained delivery of TQ to the ovarian cell line Caov-3. One-hundred thousand cells were plated according to standard lab protocols and subdivided into three groups of six wells each. Group 1 served as control and groups 2 and 3 were treated with TQ (16 µM). Glutathione biomarker evaluations were performed following standard lab techniques. The results of the study revealed: (1) for conventional delivery, glutathione levels were not statistically different ($p>0.05$) following the administration of TQ at all time periods and (2) for sustained delivery, glutathione levels were statistically different ($p<0.05$) following the administration of TQ at 72 hours. Overall conclusion: TQ only affected glutathione levels when administered by a sustained delivery system.

LOCAL LIQUID DRUG DELIVERY VIA PERFUSION CATHETER FOR PERIPHERAL ARTERY DISEASE

Megan Erwin, Marzieh Atigh, Emily Turner, and Saami Yazdani
University of South Alabama, Mobile, AL, USA

One of the leading causes of morbidity in the US is Peripheral Artery Disease (PAD), a manifestation of atherosclerosis, which causes hardening and narrowing of the artery. The gold stand for treatment of PAD has been drug eluting stents. However, drug eluting stents are ineffective in the treatment of PAD due to high rates of strut fracturing and restenosis. This has led to the development of non-stent drug delivery systems to deliver anti-proliferative drugs to diseased peripheral arteries. One such novel drug delivery system is the perfusion catheter, which provides local liquid drug delivery between two occlusion balloons. The goal of this project is to evaluate the perfusion catheter as a non-stent drug delivery system. The perfusion catheter was evaluated delivering paclitaxel with different excipients using a bench top model using native, living porcine carotid arteries. Drug retention was quantified in 90 arteries using HPLC-MS at time points ranging from 1 hour to 7 days. Preliminary data indicate that the perfusion catheter successfully delivered paclitaxel to the arterial wall, including to the medial layer, and maintained drug levels up to 3 days. In conclusion, these studies demonstrate the feasibility of local liquid drug delivery using a perfusion catheter.

MORPHOMETRIC DIFFERENCES IN FIBROUS TISSUE SURROUNDING AMINO ACID COATED UHMW-PE IMPLANTED IN SOFT TISSUE

Kenneth Butler, Michelle Tucci, and Hamed Benghuzzi
University of Mississippi Medical Center, Jackson, MS, USA

Polyethylene materials used in orthopedic applications are biocompatible and non-immunogenic with host tissues. The purpose of this investigation was to determine the relationship of fibrous tissue capsule components following implantation of ultra-high molecular weight polyethylene (UHMW-PE) rinsed with saline (control) or coated with arginine-glycine-aspartic acid (RGD) or arginine-glycine-glutamic acid (RGE) into the abdominal cavity of 12 adult male rats. Implants and surrounding tissue were harvested at 90 days post-implantation. The animals were euthanized, and the UHMW-PE implants and the fibrous tissue capsules surrounding them were harvested. Microscopic examination of routinely stained sections (5 microns, Hematoxylin & Eosin) of the fibrous tissue capsules revealed macrophage, fibrocytes, and vascularity counts were highest in the saline treated group. There was a scant number of neutrophils in the saline and RGD coated groups. There were statistically significant differences (ANOVA, $p < 0.05$) of all three experimental groups compared to control with respect to macrophages, fibrocytes, and vascularity. These findings indicate that coating UHMW-PE implants with RGD and RGE limits the tissue-implant response compared to saline in soft tissue (peritoneal cavity) applications. These results provide further evidence that the intensity of the chronic inflammatory reaction to UHMW-PE can be manipulated to some extent by simple amino acid coatings that may enhance biocompatibility.

Session IX: Nutraceuticals – Tissue Engineering

IMPACT OF SOME COMMON ORGANICS ON CELLULAR GLYCOLYSIS AND THE DIFFERENTIAL SURVIVAL OF LUNG FIBROBLAST AND LUNG CARCINOMA CELL LINES

Ibrahim Farah
Jackson State University, Jackson, MS, USA

The role of energetic modulations and use of glycolytic inhibitors on cancer/normal cell survival is not clearly established in the literature. The purpose of this study was to evaluate six potential glycolytic modulators namely, Pyruvic acid, oxalic acid, Zn acetate, sodium citrate, fructose diphosphate (FDP) and sodium bicarbonate at µM concentrations on growing A549 (lung cancer) and MRC-5 cell lines. Exposed and non-exposed cells were tested with phase-contrast micro-scanning, survival/death and metabolic activity trends through MTT-assays, as well as death end-point determinations by testing re-growth on complete media and T4 cellometer counts. Results showed that oxalic acid and Zn acetate both influenced the pH of the medium and resulted in differential massive cell debris within the exposure period. Pyruvic acid, sodium citrate, sodium bicarbonate and FDP did not cause pH changes; however, they caused detectable cell disfigurement and loss of metabolic activity, viability and survival/ death end points with the resultant death of the A549 cell line. The MRC-5 cell line was differentially unaffected by exposure to pyruvic acid, sodium citrate, sodium bicarbonate, FDP and Zn acetate, underwent complete recovery and remained both attached and healthy for 6 weeks upon subculture when transferred to a new complete medium. Oxalic acid did not show

differential modulation with the consequent loss of survival and death of the MRC-5 cell line. Phase contrast, metabolic activity, cell counts as well as death end-point findings confirmed our hypothesis. These studies show the potential possibly for exploiting cellular metabolic differences in cancer control.

UNRAVELING THE MECHANISM OF ACTION(S) FOR THYMOQUINONE AND EGCG ON CANCER CELLS

Michelle Tucci and Hamed Benghuzzi
University of Mississippi Medical Center, Jackson, MS, USA

Natural products like EGCG and Thymoquinone have been shown to be effective in interrupting the growth of many different types of cancer cells. The exact mechanism of action are not currently known. We have investigated both compounds for their effectiveness in reducing cancer cell loads in numerous cell lines and each compound appears to an IC_{50} dose that is cell line specific as well as targets different signaling pathways. Overall, both compounds may be effective alone and in combination with other chemotherapeutic agents.

TRISENOX INDUCES CELL CYCLE REGULATION AND APOPTOSIS THROUGH MODULATION OF MAPK PATHWAY IN ACUTE LEUKEMIA CELLS

Sanjay Kumar and Paul Tchounwou
Jackson State University, Jackson, MS, USA

Trisenox (TX) has been used successfully in the treatment of acute promyelocytic leukemia (APL) patients alone or combination with all trans retinoic acid (ATRA). It inhibited APL cells growth at higher concentration through cell cycle regulation and apoptosis. However, TX –induced cells growth inhibition mechanisms still remain poorly understood. We hypothesized that TX induced cell growth inhibition mediated by oxidative stress, clastogenic effect and cell cycle arrest forced cells into apoptosis depended on P38 MAPK signalling cascade in APL cells. To test the hypothesis, we used both APL cell line and mice model of APL by western blotting, confocal imaging and other molecular techniques for investigation of TX induced modulation of P38 MAPK signaling cascade. We found that the phosphorylation levels of p38 and Erk modulated in HL-60 and NB4 cells treated with TX concentration dependent manner. Whereas, phosphorylation of JNK was increased in HL-60 cells, but down regulated in NB4 cells concentration dependent manner. Our specific inhibitor studied of p38 and JNK phosphorylation revealed p38 MAPK signaling pathway involved in TX induced cell cycle regulation and apoptosis in APL cells. It is a novel target for treatment of APL patients by TX and also designing of new anti-leukemic drugs.

EFFECTS OF CURLY KALE *BRASSICA OLERACEA VAR. SABELLICA* ON VIABILITY OF CULTURED MOUSE MELANOMA CELLS

Bilal Qizilbash and Ibrahim O. Farah
Department of Biology, Jackson State University, Jackson, MS USA

The challenge with many cancers is not just killing the malignant cells, but doing so in a non-toxic manner. Plants are sources of many anti-cancer compounds, many of which have been developed into chemotherapies, *e.g.* taxanes from the bark of the Pacific yew tree and vinblastine from vincas. These chemotherapies are delivered in large doses and reduce tumor growth, but have severe side effects on normal tissue. Cruciferous vegetables such as broccoli, cabbage, and kale contain anti-cancer compounds which are being isolated and examined. Some of the compounds are anti-oxidants, while others have yet to be identified. Numerous studies have been conducted on curly kale, *B. oleracea sabellica*, to identify some of the compounds responsible for the health benefits of consuming the plant, in its raw or juiced form. Much of this research focused on sulforaphane, an isothiocyanate that is also found in foods such as broccoli, brussel sprouts, and cauliflower. Sulforaphanes, among other compounds, have been shown to decrease cell proliferation, reduce inflammation, and induce protective autophagy *in vitro*. There are no studies that have examined the effect of kale juice on cells. We hypothesize that the natural context of kale's bioactive compounds may provide significant anti-cancer effects. To test this hypothesis, kale juice was prepared and added to melanoma, epithelial, and fibroblast cells. Initially, four forms of juice were tested: juice made with a blender and three juices made with an electric juicer (juiced kale, juice that was filter-sterilized, and juice that was sonicated and then filter-sterilized). Serial dilutions were tested on B16F10 melanoma cells to determine the optimum dosage for inducing cell death. There was a dose-dependent decrease in cell growth and the lowest effective concentration was chosen for all subsequent experiments. The growth rate of cells treated with an equivalent amount of unfiltered lettuce juice was not different from the untreated cells. The sonicated and filter-sterilized extract also significantly reduced growth, but had different effects on melanoma and epithelial cells. When these experiments were repeated with non-cancerous cell lines, the juiced kale was found to be non-toxic to the epithelial cells and the fibroblasts at the dosage that kills melanoma cells. Future experiments will assess the safety and efficacy of kale juice for treating melanoma *in vivo*.

GARLIC EXTRACT DESTROYS THE MEMBRANE INTEGRITY OF HUMAN LEUKEMIA (HL-60) CELLS

Sylvianne Njiki, Keara Johnson, and Clement Yedjou
Natural Chemotherapeutics Research Laboratory, NIH/NIMHD RCMI-Center for Environmental Health, College of Science, Engineering and Technology, Jackson State University, Jackson, MS, USA.

Garlic supplementation in diet has been shown to be beneficial to cancer patients. Recently, its pharmacological role in the prevention and treatment of cancer has received increasing attention. However, the mechanisms by which garlic extract induces cytotoxic effects in cancer cells remain largely unknown. The present study was designed to use HL-60 cells as a test model to determine the cytotoxic efficacy of garlic after treatment of human leukemia cells. Human leukemia (HL-60) cells were treated with different concentrations of garlic extract for 12 hr. Live and dead cells was determined by trypan blue exclusion test using the cellometer vision. In addition, the cell viability was determined by the MTT assay. Data obtained from the trypan blue exclusion test indicated that GE significantly ($p < 0.05$) reduced the viability of HL-60 cells in a concentration-dependent manner. Similar trend was observed in the data obtained from the MTT results. Finding from the present study demonstrates that at therapeutic concentrations, garlic treatment induced cytotoxic effects in HL-60 cells. **Acknowledgements**: Research supported by NIH-RCMI Grant # G1200MD007581 at Jackson State University and part by the Mississippi INBRE (NIGMS-P20GM103476).

NANOCERIA AND CATALASE CONJUGATES AS A FREE-RADICAL SCAVENGING SYSTEM

Brendan Ward[1], Dmitry Gil[1], Vladimir Ivanov[2], and Vladimir Reukov[1,3]
[1] Department of Bioengineering, Clemson University Clemson, SC USA; [2]Kurnakov Institute of General and Inorganic Chemistry Moscow Russia; [3] Institute for Biological Interfaces of Engineering, Clemson University Clemson, SC USA

Reactive oxygen species (ROS), found as a product of cellular respiration, are present in any given aerobic organism at any time. However, ROS has been proven to play a role in the propagation of the immune response, causing cellular growth and apoptosis. Nanocrystalline cerium dioxide (nanoceria) is known for its pronounced antioxidant activity. It was shown that nanoceria possesses similar activity as SOD, converting free oxygen radicals into hydrogen peroxide. Catalase, a naturally occurring enzyme found in peroxisomes, can convert hydrogen peroxide molecules into water and oxygen. The goal of this project is to combine nanoceria and catalase into an ROS scavenging system to take a free radical oxygen and convert it to a water and oxygen molecule. When implemented, this system could drastically reduce the amount of ROS, ultimately reducing its contribution to the harmful effects on the immune response.

Session X: Biomaterials

ON THE DEVELOPMENT OF GRADIENT BIOMATERIALS FOR INTERFACE TISSUE ENGINEERING

Vinoy Thomas
Department of Materials Science & Engineering, University of Alabama at Birmingham, Birmingham, AL, USA

Development of interface materials with zone-dependent properties for interface tissue engineering (ITE) and biomaterials for hard-soft interface tissues is a rapidly developing field that aims to fabricate biological tissue alternates with the goal of repairing or regenerating the functions of diseased or damaged zones at the interface of different tissue types ("interface tissues"). Notable examples of the interface tissues in the human body include ligament-to-bone, tendon-to-bone and cartilage-to-bone. Engineering interface materials requires a spatially organized material chemistry, composition and morphologies and in the case of ITE of hard-soft interfaces, cell types and signaling molecules are required additionally. Therefore, the use of conventional biomaterials (monophasic or composites) for ITE has certain limitations to help stimulate the tissue integration or recreating the structural organization at the junction of different tissue types. The advancement of 3D printing and nanotechnologies enable us to integrate and develop systems with gradients in biomaterials properties that encourage the differentiation of multiple cell phenotypes and subsequent tissue development. As an example, we focus on the fabrication of gradient scaffold/membrane for favoring the repopulation of regenerative cells for scaffold-based tissue regeneration or high throughput screening of biomaterials. Recent developments on new composite membranes with nHA gradient for potential membrane for periodontal tissue engineering by promoting the bone growth and preventing the bacterial colonization and graded-blood tubular graft for vascular tissue regeneration by promoting endothelial cells will be presented.

THE INVESTIGATION OF TOXICITY OF METAL OXIDE NANOMATERIALS

Qilin Dai
Jackson State University, Jackson, MS, USA

Metal oxide nanomaterials (MONs) in nano- photodynamic therapy (PDT) are associated with cell destruction under the light irradiation due to the ability of generating reactive oxygen species (ROS). However, some potential risks of nanomaterials in biomedical applications still remain. There are many reports about the toxicity of the metal oxide nanomaterial used in nano-PDT, but there is no systemically studies on the influence of physicochemical properties of MONs, including size, morphology and surface structure, on their toxicity. Advancing our knowledge on these issues is very urgent and critical to the development of nano-PDT. In this work, MONs with different sizes, surface structures and morphology are synthesized by chemical solution method, including CdMoO4, Zn2SnO4, Y2O3, CuO, ZnO and TiO2. ternary oxides have more freedom to tune the properties of the MONs. We synthesized ternary CdMoO4, Zn2SnO4 and indium tin oxide nanospheres and nanowires for the nanotoxicity study. The correlations between the physicochemical parameters and toxicological end-point responses of the study MONs are demonstrated in our work.

DILUTE SOLUTION BEHAVIOR OF BLOCK COPOLYMERS OF ELASTIN-LIKE POLYPEPTIDE AND POLYELECTROLYTES

Jared Cobb and Amol Janorkar
University of Mississippi Medical Center Jackson, MS, USA

Elastin like polypeptide-polyelectrolyte (ELP-PE) block copolymer coatings have been shown to promote three-dimensional spheroid arrangement of multiple cell types in in vitro cell cultures. This arrangement closely mimics cells' natural orientation within the body. This model is currently limited by the non-uniformity in both ELP-PE coating thickness and the distribution of the polyelectrolyte on the surface. This can lead to a large variation in spheroid size and an erratic scattering of spheroids across the coated surface. We have investigated the effect of important processing parameters (solvents, solutes, and temperature) on a large and small molecular weight ELP-PE block copolymer. These factors have been explored using dynamic light scattering to determine the transition temperature and radius of hydration (Rh) of the ELP-PE block copolymers. It was found that with an increase in temperature from 25 to 60°C the Rh of the polymers in solution increased, indicating that the polymers keep the inverse phase transition behaviour of the ELP. Upon addition to a 0.2M NaCl solution, the Rh for the polymers exhibited a two-fold increase in size to approximately 950 nm. As the concentration of the NaCl solution was increased to 1M, the Rh for the low molecular weight ELP-PE increased to a size of 2000 nm while the larger molecular weight ELP-PE remained at 950 nm. These studies will help determine the structural profiles of the polymers in different media, ultimately providing well characterized coating surfaces to enhance our understanding of how cells interact with the polymers based on their conformations.

INVESTIGATING ELECTROSPUN ALGINATE- AND CHITOSAN-BASED FIBERS

Kathryn Penton, William Weeks, Scarlett Salter, Amber Wilson, Tia Brown, Doug Miller, Sharon K. Hamilton
Delta State University, Cleveland, MS, USA

Recent evolutions in the field of biomaterials have focused on developing materials that can facilely interface with biological systems to treat or replace tissues or functions of the body. Natural polymers, including polysaccharides, have been investigated as suitable biomaterials to mimic the environment of body tissues and facilitate tissue regeneration. Electrospinning natural polymers, like alginate and chitosan, yields nanofibers that have shown promise as tissue scaffolds and drug delivery vehicles. However, little research has been published on the controlled delivery of drugs from polymeric nanofiber dressings. The lack of studies in this area is due in part to the difficulty of electrospinning charged polymers, like alginate and chitosan. This research has taken a two-pronged approach towards the investigation of natural polymer-based fibers. One facet focuses on the development of novel alginate- based, degradable nanofibers. It is anticipated that the degradable alginate nanofiber scaffolds can be used for drug delivery and future studies will investigate the time-release of small molecules from these fibers. Another facet focuses on the preparation of a variety of drug loaded, alginate- and chitosan-based fibers via electrospinning and the exploration of the release profiles of these novel scaffolds. This represents a first attempt to create a drug release profile catalog from negatively and positively charged natural polymer-based electrospun scaffolds. Studies from both approaches will lead to improved understanding of alginate- and chitosan-based wound healing materials, especially in the field of modern drug-laden, wound dressings.

NONLINEAR FINITE ELEMENT ANALYSIS OF MICRO-LATTICE STRUCTURES FOR PATIENT SPECIFIC IMPLANTS

Prashant Athanker and Amit Singh
MNIT Jaipur, India

The primary objective of this research paper is design and nonlinear finite element analysis of micro-lattice of Ti-6Al-4V implants using the Bauschinger effect. Micro-lattice cellular Ti-6Al-4V structures are commonly used for orthopedic application with an organized porosity and pore sizes appropriate for tissue ingrowth and organic process. In this research paper CAD model of different unit lattice structures with design variables such as strut length, strut cross-section and pore size using Intra-Lattice software were designed. Intra-Lattice software is a parametric lattice demonstrating tool and is developed based on Grasshopper, a graphic algorithm editor for Rhino CAD software. In this study, three different unit cells are presented including a Grid (simple cubic), Star (body centered cubic) and Tesseract (hypercubic) structure. The finite element analysis (FEA) technique is presented to analyze the mechanical properties of these three types of lattices-based cellular structure. For FE modeling, beam elements have been used to model the micro-lattice structures under different loading conditions (i.e. tension

and compressive). The FE simulations were carried to predict the functional effectiveness and load-bearing effectiveness for the above three unit cells. In the last phase of this investigation, the unit cell topology was improved to increase the stiffness and yield stress under loading conditions. Finite Element Simulations demonstrate that the stiffness and yield strength can be enhanced by changing the unit cell geometry. The results of the above investigation will then be applied to patient-specific implants.

FINITE ELEMENT ANALYSIS OF CYCLIC AMP DIFFUSION AND SIGNALING BETWEEN CELLS

Steven Shettlesworth, Nicholas Stone, Anh-Vu Phan, and Thomas Rich
University of South Alabama, Mobile, AL, USA

Second messengers, such as cyclic adenosine monophosphate (cAMP), are responsible for a plethora of cellular functions. The essential role cAMP signaling plays in living organisms is well understood, yet there is still much debate on the information stored within these signals. In the last decade, mathematical models have been developed for explaining concentration of cAMP gradients, including our finite element analysis (FEA) models of the diffusion, degradation and synthesis of cAMP within a single cell. In this work, we present the development of a two-dimensional FEA model of cell-cell interaction to simulate cAMP diffusion and signaling between adjacent cells. The governing equation employed in our previously developed models is also adopted in the new FEA model. The direct contact cell signaling mechanism is assumed. Some preliminary numerical results will be presented to discuss the validity of the proposed model.

Session XI: Technology For Healthcare And Education

USING iOS DEVICES AS AN INTERACTIVE LAB ENVIRONMENT

Francis Tuluri, Lattrice Evans, Terrance Eubanks, Aaron James, LaDamion Harness, and Traeshaun Hiley
Jackson State University, Jackson, MS, USA

Interactive laboratory sessions in undergraduate science and engineering disciplines, help improve the understanding of principles and theory. Using smart devices, such as smart phones and tablets for data collection and visualization facilitates performing many interactive lab activities, which are otherwise tedious and laborious for the students. Here, we describe a novel method of data collection and visualization on iOS devices by interfacing external sensor with a view to perform interactive and inquiry-based lab activities. The iOS devices (smart phone and tablets), microcontroller, WiFi module, and external sensors are interfaced to collect real time data, visualize the data trends, and publish for analysis and behavior of a subject of interest. A proto model of weather environment physical system consisting of temperature, humidity, and light sensor is designed to study real time monitoring of the environment. For example, over a period of one hour the corresponding variables are observed for the changes of a surrounding environment in a location and a certain time, and found to be 62 F to 64 F, 86% to 86.5%, and 45 to 52 (arbitrary units). The measured data are within an accuracy of 1% and the results are found to agree with the traditional data of corresponding variables. The proposed model displays the data as a dashboard in different graphical formats such as 2D plots, gauge meters among others. The study and analysis of data is simple and interesting to the students to further their learning of physical principles of dynamic systems.

AN ON-BODY CONFORMAL PRINTED ARRAY ANTENNA AT mmWAVE FREQUENCIES FOR HEALTHCARE APPLICATIONS

Saeed Latif and David Nelson
University of South Alabama, Mobile, AL, USA

On-body printed antenna is a rapidly growing research area targeted for healthcare, biomedical, public safety and military applications. Printed antennas in both microwave (MW) and millimeter wave (mmWave) frequency bands have been found useful for Wireless Body Area Networks (WBAN) and medical devices. While miniaturization, conformability and good near-field patterns have prime importance in the antenna design, the interaction of RF signals with human body and the effective signal penetration need to be assessed carefully during the design phase. An on-body 2 × 2 printed antenna array is designed at mm Wave frequencies on a flexible material. The antenna is designed such that it radiates directly into the human body. Its performance parameters including return loss, near-field patterns and radiated power are evaluated when placed on a human phantom. Measured specific absorption rate (SAR) and power density (PD) profile on an experimental phantom using a high-resolution infrared camera will be presented at the symposium.

THE USE OF COMPLEX CLINICAL DATA AND TOPOLOGICAL DATA ANALYSIS FOR PERSONALIZED MEDICINE

John Clemmer, W. Andrew Pruett, Kenneth R. Butler, and Robert L. Hester
University of Mississippi Medical Center Jackson, MS USA

Methodologies that could identify subgroups of patients that may or may not respond to a given treatment could be a revolutionary tool in personalized medicine, a new concept for treating a specific patient based on their particular health or physiology. The association between obesity and several of its comorbidities, including diabetes, hypertension, dyslipidemia, stroke, and cardiovascular disease, is well established. However, variability from patient to patient complicates the translation of these risk factors to the clinic to give actionable information about a patient's optimal treatment. Based on 36 physiological variables, we analyzed a cohort of 2700 patients from the Genetic Epidemiology of Network of Arteriopathy (GENOA) Study using topological data analysis (TDA), a new clustering algorithm tool. Variables used for the analysis included blood pressure, BMI, age, renal function, and metabolic markers. TDA clustered and separated out 6 distinct subgroups of obese patients with similar BMI but differed in over 100 variables including renal disease, serum inflammatory biomarkers, and prevalence of stroke, diabetes, and hypertension. This suggests that the association between obesity and its comorbid conditions is not always clear. These methodologies could potentially be used to discover patterns in a patient's physiology and advance personalized medicine.

VISUALIZING HEALTH IN MISSISSIPPI: THERE'S AN APP FOR THAT!

Denise Krause
University of Mississippi Medical Center, Jackson, MS, USA

Introduction. An interactive, web-based application using geographic information systems has been developed to visualize health providers, services, statistics, and outcomes in Mississippi. This user-friendly application is useful for workforce planning, recruitment, and health services and population health research. The tool was developed to assist in improving access to health care and health outcomes for all Mississippians. Methods. Data including active health professionals were collected from health professional licensure boards. These datasets, combined with other proprietary and public datasets, were prepared, processed, catalogued, and stored in our Healthy Mississippi Data Lake. An ArcGIS 10 server application was developed in JavaScript, which can run on most platforms, including mobile devices, to query and visualize the geographic distribution of the health workforce, health statistics, and health outcomes. Key findings. The application allows users to identify and query geographic locations of health professions filtering by selected criteria, to perform drive-time or buffer analyses, and to explore health-related and socio-demographic population data by selected geographic area. The application is particularly useful to medical students, the Rural Physician/Dentist Scholarship Programs, the Office of Physician Workforce, the Mississippi State Department of Health, and many other state and private organizations. Implications.

This application visually represents health in Mississippi and provides access to much needed information for state-wide health workforce planning, health services, and population health research. It is an expandable tool that enables Mississippi to become more proactive in addressing the needs for health care providers, services, and interventions to improve health.

LESSONS FROM THE FIELD: SETTING UP AND OPERATING A NETWORK OF MOLD SPORE SAMPLERS

Bruce T. Brackin[1], Fazlay Farugue[2], Martha N. Brackin[3], and Gailen D. Marshall[4]
[1]Mississippi State Department of Health, Jackson, MS, USA
[2]Department of Preventive Medicine, University of Mississippi Medical Center, Jackson, MS, USA
[3]Independent Consultant, Brandon, MS, USA
[4]Allergy & Immunology, University of Mississippi Medical Center, Jackson, MS, USA

The University of Mississippi Medical Center conducted an 18 month study to evaluate the mold spore abundance in Central Mississippi and their variations with seasons. Aeroallergens, including common fungal spores can be triggers for those with allergies, asthma and other respiratory conditions. A network of standard free standing ground-based volumetric spore traps was designed, procured, built and operated to collect mold spores samples from the study area. Common meteorological variables were also collected using weather data logging stations. Topics covered will include the site selections, gaining property owners to house stations, assistance in sample media changes, and more importantly the instrumentation related problems and their solutions. Five of the 6 sites were solar powered and air flow rates of these samplers started to vary between daylight and dark hours. Another power supply related problem was due to inefficiency of the deep cycle batteries, particularly in the colder days. An additional problem encountered when ambient temperature and pressure changed resulting in variations in air volume. This presentation will include the field data collection process and will highlight the solutions to the unanticipated problems to main data integrity required for the project.

A NEW EXCITATION-BASED TECHNIQUE FOR ESTIMATING FRET EFFICIENCY

John Robert Griswold, Naga Annamdevula, Joshua Deal, Thomas Rich, and Silas Levesley
University of South Alabama, Mobile, AL, USA

We have developed a novel hyperspectral imaging microscopy technique that filters excitation wavelengths and collects a bulk emission signal. We have previously shown that this excitation-based system can detect multiple fluorophores in live cells with high signal-to-noise ratios. Furthermore, this system is capable of faster acquisition times than conventional emission-based methods. This project aims to adapt our excitation-scanning technique for a new purpose: Förster Resonance Energy Transfer, or FRET. Though FRET is a ubiquitous tool in the biological sciences for measuring intermolecular distances, current spectral FRET detection methods suffer from poor signal-to-noise ratios, making it difficult to capture rapid cell-signaling events. This study's hypothesis was that excitation-scanning could provide improved signal strength for these measurements. Data were collected from HEK-293 cells transfected with a Turquoise-Epac-Venus FRET probe to monitor cyclic AMP, and treated with Forskolin, an adenylyl cyclase activator. Excitation light was provided by a Sutter VF-5 filter system connected to a 300W Xe arc lamp. Samples were excited from 380 to 490 nm, at 5 nm increments, and an image was acquired at each wavelength. Donor and acceptor excitation signals were resolved using linear unmixing and a spectral library acquired from single-labeled samples. FRET efficiency was determined by comparing donor signals at two dichroic filter cut-off wavelengths (458 and 495 nm). Results indicate that excitation-scanning could be a high-signal method for FRET estimation, but further optimization is required. If successful, this system will allow rapid acquisition of live-cell FRET image data along with simultaneous detection of other fluorescent markers.

Session XII: Therapeutics and Rehabilitation

MIRROR THERAPY FOR LOWER EXTREMITY RECOVERY AND GAIT IN SUBACUTE STROKE: A RANDOMIZED CONTROL TRIAL

Lisa J. Barnes and Kim Curbow Wilcox
University of Mississippi Medical Center, Jackson, MS USA

Stroke often leads to decreased mobility, strength, and motor control. During mirror therapy (MT), observing mirrored images of movement of the unaffected limb produces the appearance of movement on the affected side. MT has been shown to increase cortical activity in the affected hemisphere. The purpose of this study was to examine the effect of MT on lower extremity impairments in patients with sub-acute stroke. Participants were recruited upon admission to inpatient rehabilitation. Those meeting inclusion/exclusion criteria were randomly assigned to groups using computer randomization. The control group received traditional physical therapy (PT). The treatment group received traditional PT and daily mirror therapy exercises. Data was collected at admission and discharge. Thirty patients participated, ages 26 - 79 years, with 17 in the control and 13 in the treatment group. Results indicate improved mean scores for all outcome measures at discharge. A significant difference was shown in between-group scores for lower extremity function measured by the Stroke Rehabilitation Assessment of Movement (STREAM) ($p < .05$); however, the control group had higher scores. No significant differences were found for the Functional Independence Measure locomotor score, the Timed Up and Go, or the basic mobility scores in the STREAM. Using MT as an adjunct intervention may benefit patients with subacute stroke by improving motor control and gait. However, this study did not indicate significant differences in outcomes compared to traditional physical therapy. Additional research is needed to determine the value of MT for rehabilitation of patients with subacute stroke.

THE EFFECTS OF AQUATIC THERAPY ON FATIGUE AND QUALITY OF LIFE IN PATIENTS WITH MULTIPLE SCLEROSIS: A SYSTEMATIC REVIEW

Kimberly Willis and Lisa Barnes
University of Mississippi Medical Center, Jackson, MS, USA

Purpose/Hypothesis: The purpose of this systematic review is to determine the effectiveness of aquatic therapy on decreasing fatigue and improving quality of life in patients with MS. Methods PubMed and CINAHL databases were searched in September 2015 using search terms related to multiple sclerosis, aquatic therapy, and fatigue, both individually and in combination. Electronic limitations included English language, date range 2010 - 2015, and humans. Inclusion criteria were patients with MS, aquatic therapy, and outcome measures assessing fatigue. Exclusion criteria were systematic reviews and case studies. Results: Following the screening process, four articles were included in the systematic review. Results of the article review suggest that aquatic therapy focusing on strength, flexibility, balance, and functional mobility may be beneficial in improving quality of life and reducing fatigue in patients with MS. Conclusions: When comparing aquatic cycling to land cycling, aquatic exercise showed no significant benefit; however, total body aquatic therapy interventions showed improvements in quality of life and function with some evidence of decreased fatigue. Patients who began aquatic therapy programs with higher levels of fatigue showed greater improvements in the reduction of fatigue. One study suggested that aquatic therapy was more beneficial in reducing fatigue and improving quality of life compared to routine daily behaviors. Findings suggest that aquatic therapy may be beneficial for improving quality of life for those living with MS, and for some it may successfully decrease fatigue levels.

THE EFFECTS OF THERAPEUTIC ULTRASOUND ON ADULT PATIENTS WITH NON-SPECIFIC CHRONIC LOW BACK PAIN: A SYSTEMATIC REVIEW.

Sherry Colson and Lisa Barnes
University of Mississippi Medical Center, Jackson, MS, USA

Background and Significance: Therapeutic ultrasound (US) is a commonly used physical therapy intervention, specifically for those suffering from non-specific chronic low back pain. The efficacy of passive US specific to chronic low back pain has recently been challenged. In addition, the APTA Choosing Wisely campaign has stated "Don't employ passive physical agents except when necessary to facilitate participation in an active treatment program." The purpose of this systematic review is to determine the effectiveness of therapeutic ultrasound for decreasing pain and improving the quality of life for patients with non-specific chronic low back pain. Methods: PubMed database was searched February 2015. Relevant studies were found using a search strategy including: back pain or lumbago and therapeutic ultrasound. Electronic limitations were English language and RCT. Inclusion criteria: age > 18 years, nonspecific chronic low back pain > 3 months. Studies were scored using PEDro and the 2011 Oxford Centre of Evidence Based Medicine (CEBM) scales. Results: Five articles met all the criteria for the systematic review. The average PEDro score was 6/10. CEBM levels of evidence scores revealed one study at level II and four studies at level III. Conclusion: Ultrasound combined with exercise may be more effective than exercise alone or placebo US combined with exercise to decrease pain and increase QOL measures in patients with chronic LBP. However, US does not appear to be more effective than other passive modalities such as phonophoresis and electrical stimulation. Evidence showing the independent effects of US without other interventions seems lacking.

THE EFFECTS OF HIPPOTHERAPY ON GROSS MOTOR FUNCTION IN CHILDREN WITH CEREBRAL PALSY: A SYSTEMATIC REVIEW

Janet Slaughter and Lisa Barnes
University of Mississippi Medical Center, Jackson, MS, USA

Background and Significance: Functional limitations can affect the proficiency of motor skills and the level of participation in daily activities in children with cerebral palsy (CP). Hippotherapy is an intervention that uses horseback riding and has been suggested to increase motor control and functional ability in children with CP. The purpose of this systematic review is to explore the effectiveness of hippotherapy as a therapeutic intervention to improve functional outcomes in children with CP. Methods: PubMed Database was searched through February 5, 2015. Specific search terms included those related to hippotherapy and children with CP limited to the English language. Inclusion criteria were children with CP, clinical trials, and the Gross Motor Function Measure (GMFM) as a functional outcome measure. Exclusion criterion was the use of horse simulators. Results: After a stepwise selection process, 5 articles remained for review. Four out of five articles showed a statistically significant improvement in gross motor function in children with CP after receiving hippotherapy as a therapeutic intervention.

Conclusion and Clinical Implications: Evidence in all five articles demonstrated that hippotherapy led to clinically meaningful improvements in functional outcomes when compared to traditional physical therapy interventions. This systematic review supports the use of hippotherapy as a therapeutic intervention in children with CP as evidenced by consistently greater mean differences in functional outcomes for the hippotherapy groups compared to traditional physical therapy.

THE EFFECT OF DRY NEEDLING ON PAIN CONTROL AND POSSIBLE MECHANISM

Felix Adah, Min Huang and Mark Weber
Department of Physical Therapy, School of Health Related Professions, University of Mississippi Medical Center, Jackson, MS, USA

Background and Significance: Pain is a common problem of patients seen in physical therapy clinic that attracts varying therapeutic interventions. Recently, the literature is replete with conflicting reports that dry needling (DN) can reduce pain, reduce inflammation and thereby improve function. There are conflicting reports in the literature that DN of myofascial trigger points (MTrPs) or trigger points (TrPs) is efficacious in reducing spinal pain. Therefore, the purpose of this study to evaluate the effect of DN treatment in patients with neck pain and to review the literature for possible mechanism of action of dry needling if there is a preponderance evidence of DN in pain control. **Methods:** The PubMed database was accessed through January 27, 2016 using dry needling for patients with neck or back pain. Specific search terms and combination strategies are presented. Electronic limitations included randomized control trial. Inclusion criteria included spine and/or neck regions, pain measurements, and local needling. Exclusion criteria included injections as primary interventions. Study quality was evaluated using PEDro criteria. The PEDro is a 10-point scale for assessing internal validity (higher scores indicating higher quality). The studies were also scored using the 2011 Centre of Evidence Based Medicine (CEBM) scale. This is a 5-level scale that determines a study's level of evidence based on the study's design with lower numbers indicating higher levels of evidence. The described search strategy identified seven studies meeting all requirements. The mean PEDro score of the studies was 6.57 with a range of 5 to 8. The CEBM frequency included three level II studies and four level III studies. Conclusion: The study demonstrated that DN treatment resulted in significant pain reduction and decreased sensitivity of pain in six of seven studies with the non-significant study also trending towards pain reduction. Six studies that measured ROM for an outcome measure demonstrated increased ROM of the cervical region after DN. **Discussion:** With the positive effect of DN treatment on pain reduction and increased ROM, one can deduce that patients with pain treated with DN can have an increase in function and ultimately improved quality of life. The possible mechanisms by which DN control pain are presented. The studies used in this systematic review had CEBM levels of II and III, which indicated a grade of B due to all 7 studies having CEBM levels of III or higher. **Conclusion and Clinical Implication:** DN as a modality is new in physical therapy. Chronic pain, such as neck pain, that may not respond to the traditional physical therapy (heat, exercise, and massage) may be relieved with DN treatment. It is suggested that, when considering treatment options for spinal pain and other chronic pain, DN treatment should be taken into consideration. More research is necessary to elucidate the mechanism by which DN reduces chronic pain and to carry out comparative studies between DN and other physiotherapeutic modalities.

QUANTITATIVE MEASURES OF THE IMPACT OF EXCERCISE AMONG ELDERLY

Matt Gibson, Ham, Benghuzzi, and Michelle Tucci

University of Mississippi Medical Center, Jackson, MS, USA

Twenty percent of the US population will be over the age of sixty-five by 2030. All age groups within the greater than sixty-five population are growing, but those over the age of eighty-five are the fastest growing cohort of the US population. The specific aims of this investigation were (1) to determine if a correlation exists between maintaining a relationship with a primary care provider and heightened exercise levels among an elderly population and (2) to determine if a correlation exists between exercise among the elderly and the completion of more preventive screenings than those elderly who do not exercise. We hypothesized that those elderly who have an active relationship with a primary care provider are more prone to exercise and those elderly who exercise complete more preventive screenings. Results of this survey based investigation revealed that maintaining a relationship with a primary care physician is the norm for the vast majority of the Auburn, AL and New Orleans, LA population. Furthermore, the communication of exercise guidance during primary care physician appointments was inconsistent in the Auburn, AL population and not overwhelming in the

New Orleans, LA population. Unfortunately, the discussion of such exercise guidance during an outpatient clinic appointment has not equated to a change in exercise levels among the survey respondents in the either population. Overall conclusion: this study provided the literature with more insights regarding knowledge and awareness of the relationship between primary care and preventive healthcare consumption and exercise levels among the elderly.

Session XIII: Neuroscience

OPTIMIZING NEUROMODULATION TO ENHANCE STEPPING IN SPINAL CORD INJURY

Keith Tansey
UMMC/Methodist Rehab/Jackson VA, Jackson, MS, USA

After spinal cord injury (SCI), residual neural circuits for stepping can be augmented with afferent stimulation. We have now systematically determined how well that stimulation can be optimized to enhance stepping in patients using spinal cord and peripheral nerve stimulation. Twelve subjects with cervical or thoracic SCI of varying severity were studied in the Lokomat gait orthosis. Stimulation was provided as transcutaneous spinal cord stimulation (TSCS) or at either distal tibial or common peroneal nerve sites. Stimulation parameters that were varied included frequency (all 3 sites) and timing or duration during the gait cycle (peripheral sites). Real time forces recorded by the Lokomat guided the development of an input/output model in each subject such that stimulation parameters were eventually optimized to decrease assistance forces from the robot. Using our optimization protocol, stimulation parameters were found that improved subject generated stepping forces over random or no stimulation. At the peripheral nerve sites, we found that high frequency stimulation, delivered at the swing to stance transition, for more than 20% of the gait cycle duration improved stepping forces in most patients. With TSCS, stimulation frequencies between 30 and 50 Hz augmented stepping the best. Further analysis revealed that stimulation frequencies below 25 Hz best augmented stance and between 25 and 50 Hz best augmented swing. There was some variability between subjects and for 1/3 of them, the best TSCS stimulation was 0 Hz.

BLAST OVERPRESSURE-INDUCED VESTIBULAR DEFICITS IN RATS

Yue Yu[1], Jun Huang[1], Xuehui Tang[1], Adel Maklad[2], Dalian Ding[6], Yi Pang[3], William Mustain[1], David Sandlin[4,5], Jerome Allison[1], Wu Zhou[1,2,], Hong Zhu[1,2]*
[1]Departmant of Otolaryngology and Communicative Sciences, [2]Department of Neurobiology and Anatomical Sciences, [3]Department of Pediatric, [4]MD Program, [5]Program in Neuroscience, University of Mississippi Medical Center, Jackson MS; [6]Center for Hearing and Deafness, University at Buffalo, Buffalo, NY.

As an air-filled structure and directly exposed to the surrounding air, unprotected ears are among the most frequently damaged sites during blast exposure. Vestibular symptoms, such as dizziness and imbalance, are common complaints among the blast victims. However, little is known about how and to what extent blast overpressure damages the vestibular system. In the present study, the effects of blast shock exposure through the external ear canal on the vestibular system were studied in rats. Under isoflurane anesthesia, animals were exposed to a blast shock (peak intensity of 185 dB SPL) delivered to the external ear canal. Twenty-four hours following the exposure, single unit recording was performed on the ipsilateral superior vestibular nerve. A total of 442 afferents were recorded from 7 blast-exposed rats and 7 control rats. Blast exposure significantly reduced the baseline firing rate of regular anterior semicircular canal (AC), horizontal semicircular canal (HC), otolith organ afferents and irregular otolith organ afferents. Blast exposure also significantly reduced the sensitivity of irregular HC and AC afferents to 0.5-2Hz sinusoidal head rotation. Fluorescein-conjugated phalloidin staining, which labels the filamentous actin in sensory cilium and cuticular plate of hair cells, revealed substantial sensory stereocilia bundle damage in both crista ampullaris and macula of saccule and utricle after blast exposure. Macrophage activation was observed in brainstem of blast exposed rats indicating that blast overpressure waves entering the ear canal can impact the brain. Blast exposure, however, did not result in significant changes in gains or phases of the horizontal rotational and translational vestibular-ocular reflex (VOR). These results suggest that blast overpressure waves entering the ear canal causes damages in the peripheral vestibular system and brain that may contribute to the vestibular symptoms experienced by blast victims. Understanding the underlying mechanisms will reveal the urgency of ear protection in personnel at risk of blast exposure not just or protection of hearing and balance, but also for protecting the brain. [Supported by NIH R01DC012060 (HZ), R01DC014930 (WZ) R21EY025550 (WZ)]

NEUROPROTECTIVE AND REGENERATIVE ROLES OF THE WNT-3A PATHWAY AFTER FOCAL ISCHEMIC STROKE IN MICE

Zheng Zachory Wei1,[2], James Ya Zhang[1], Tammi M. Taylor[4*], Xiaohuan Gu[1] , and Ling Wei1,[2,3]*
[1]Department of Anesthesiology, Emory University School of Medicine, Atlanta, GA, USA; 2 Laboratories of Stem Cell Biology and Regenerative Medicine, Experimental Research Center and Neurological Disease Center, Beijing Friendship Hospital, Capital Medical University, Beijing, China; 3Department of Neurology, Emory University School of Medicine, Atlanta, GA, USA 4 Department of Biology, Jackson State University, Jackson, MS, USA

Wnt signaling is a conserved pathway involved in expansion of neural progenitors and lineage specification during development. However, the role of Wnt signaling in the post-stroke brain has not been well-elucidated. We hypothesized that Wnt-3a would play an important role for neurogenesis and brain repair. Adult male mice were subjected to a focal ischemic stroke targeting the sensorimotor cortex. Mice that received Wnt-3a (2 μg/kg/day, 1 hr after stroke and once a day for the next 2 days, intranasal delivery) had reduced infarct volume compared to stroke controls. Wnt-3a intranasal treatment of 7-days upregulated the expression of brain derived growth factor (BDNF), increased the proliferation and migration of neuroblasts from the subventricular zone (SVZ), resulting in increased numbers of newly formed neurons and endothelial cells in the penumbra. Both the molecular and cellular effects of Wnt-3a were blocked by the Wnt specific inhibitors XAV-939 and Dkk-1. In functional assays, Wnt-3a treatment enhanced the local cerebral blood flow (LCBF) in the penumbra, as well as improved sensorimotor functions in a battery of behavioral tests. Together, our data demonstrates that the Wnt-3a signaling can act as a dual neuroprotective and regenerative factor for the treatment of ischemic stroke.

INTRAUTERINE GROWTH RESTRICTION IS ASSOCIATED WITH LONG-LASTING BRAIN CHANGES

Norma Ojeda[1], Jonathan W Lee[1], Silu Lu[1], Emily C Turbeville[1], Colin B Muncie[2], Lir-Wan Fan[1]
[1]Department of Pediatrics, Division of Newborn Medicine, University of Mississippi Medical Center, Jackson, MS ,USA
[2]Department of Pediatrics, Division of Surgery, University of Mississippi Medical Center, Jackson, MS, USA

Epidemiological and experimental studies suggest that intrauterine growth restriction (IUGR) can cause neurodevelopmental impairments. Our previous studies demonstrated that IUGR alters brain size and behavioral performances in both neonatal and juvenile rats. To further examine whether IUGR has long-lasting effects on brain function, we examined brain structure and rat's behavior in 6 months old rats, exposed to IUGR. Offspring exposed to IUGR showed significantly lower birth weight compared to offspring from control dams. IUGR offspring showed motor deficits in the open field test, with brain size alteration, as indicated by the reduction of total brain, cortical, and hippocampal volume, along with the dilation of ventricles. Additionally, IUGR offspring had impairments of dendrites (MAP2+) and myelin

(RIP+), and brain inflammation, as indicated by increases in microglia and astrocytes in the brain. The current study suggests that IUGR causes long-lasting behavioral disturbances and persistent brain changes, which may be associated with brain inflammation. This model may be useful for studying mechanisms involved in the development of brain changes associated with IUGR and for developing future potential therapeutic strategies. (This work was supported by Newborn Medicine Funds from the Department of Pediatrics, University of Mississippi Medical Center.)

DEVELOPMENT OF A LONGITUDINAL IMAGING SYSTEM FOR A MURINE MODEL OF TRAUMATIC BRAIN INJURY

Chelsea Dressel and Teresa Murray
Louisiana Tech University, Rushton, LA, USA

Following traumatic brain injury (TBI), secondary injury cascades can lead to axonal damage, white matter degeneration, and persistent microglia activation in subcortical regions of mice. Current techniques, such as diffusion tensor imaging (DTI) and histology can be used to observe features related to damage, but DTI lacks cellular resolution and histology is conducted on fixed tissue, preventing longitudinal studies in the same mouse. The combination of cranial windows and multiphoton microscopy (MPM) has been used to image cells in the upper layers of the mouse cortex, but resolution rapidly degrades with imaging depth, making it difficult to observe white matter damage following TBI. In order to obtain longitudinal data related to this secondary damage, gradient refractive index (GRIN) lenses (diameter = 0.5 mm, length = 1.7 mm) attached to low profile head plates were surgically implanted into the brain of mice to acquire time-lapse images of white matter for 60 days following midline fluid percussion injury. Thy1-YFP mice were used to compare changes in white matter fiber tracts and Cx3cr1-tdTomato mice were used to compare microglial activation levels over time versus mice with sham injuries and negative controls. These longitudinal images will provide comprehensive information concerning degeneration, inflammation and remodeling of white matter following injury.

Scientific Poster Session

THE EFFECT OF DRILL HOLE LOCATION ON THE LOAD BEARING CAPACITY OF TIBIAS

Christopher Yiachos and Sabrata Saha
SUNY Downstate Medical Center, Brooklyn, NY, USA

Fracture fixation plates stabilize a fractured long bone to facilitate healing. The drill holes used to secure the implant may decrease the load bearing capacity of the bone. We investigated whether a drill hole in a compressive/tensile location had any measurable difference in load bearing capacity of tibias vs. a neutral location. Sixty-eight human cadaveric paired tibias were used. One bicortical hole was drilled into each bone in the experimental groups using a 4.1-mm drill-bit. Three groups were created: 0°/180°, 90°/270°, and 135°/315°. Each corresponded to placement of the bicortical drill hole along the circumference. Each bone underwent a four-point bend test. Maximum load bearing capacity was measured. Our results showed a statistically significant ($P<0.05$) decrease in strength of all tibias with a hole drilled at 0°/180°, and 135°/315° compared to their controls. The tibias in these groups experienced average decreases in strength of 43.4% (± 6.5%) and 35.3% (± 25.7%) respectively. Since the drill hole was bicortical, both of these holes represent compressive/tensile locations. Decrease in load bearing capacity for bones in the 90°/270° group (neutral location) was statistically insignificant ($P>0.05$). The percent difference in load bearing capacity of tibias in the 90°/270° group showed that experimental bones retained an average of 95.6% (± 8.5%) the strength of their control counterparts. We conclude from these results that holes drilled at 90°/270° from the compression or tension surface of a long bone will minimize loss of bone strength. This finding can be used to guide surgical placement of drill holes.

PHENOTYPIC SWITCH OF VASCULAR SMOOTH MUSCLE CELLS IN VASCULAR CALCIFICATION

Kelsey McArthur, Amber Kay, James Stewart, and C. LaShan Simpson
Mississippi State University, Starkville, MS, USA

One of the leading causes of death in patients with kidney disease or diabetes is cardiovascular complications. Past studies considered vascular calcification a passive process that resulted from elevated calcium-phosphate interactions. However, it is now considered an active cell-mediated process. This occurs through competition of proteins that promote calcification and inhibitors which cause arteries to harden. Current research has shown that these arteries harden analogously to bone development. It has been suggested that smooth muscle cells (SMC) in healthy arteries experience a genetic switch to osteoblast-like cells when exposed to high levels of glucose, calcium, phosphate, and cholesterol. While many researchers have recognized this anomaly, the molecular and cellular mechanisms that facilitate calcification remains unclear. Our in vitro model was developed to prompt vascular calcification and distinguish the genetic switching from healthy smooth muscle cells to osteoblast-like cells. Our goal is to use this in vitro model to examine the Wnt Signaling pathway and its relationship to the LRP5 pathway. From this, we can determine the effects these pathways have on calcification.

SYNTHESIS OF HYBRID IRON-POLYDOPAMINE NANOPARTICLES FOR IMAGING-GUIDED PHOTOTHERMAL THERAPY ON CANCER CELLS

Devin Guillory, Terriona Cowan, and Yongfeng Zhao
Jackson State University, Jackson, MS, USA

According to American Cancer Society, about 1,658,370 new cases of cancer were expected to occur in 2015 with an expected death toll of about 589,430. Magnetic resonance imaging (MRI) offers high-detailed morphological information on large regions of soft tissue. Photothermal therapy (PTT) of cancer eliminates the invasive side effects of current clinical therapies. PTT uses photo-absorbers that absorb near-IR wavelength and converts this light energy into heat energy. Magnetic resonance imaging works well in combination with PTT. Nanoparticle utilization in PTT has gained notoriety but there are safety concerns with metals. Our designed natural product nanoparticles will be metal-chelated for imaging guided PTT. Inorganic nanoparticles raise concern with high toxicity and low biocompatibility, factors not of concern with natural and naturally-derived products. These nanoparticles are usually not biodegradable and can remain in the body for extended periods of time, as well. Polydopamine (PDA) is a natural product from eumelanin, pigment found in dark hair and skin. PDA has strong photothermal capabilities; it has strong optical absorption and high photothermal efficiency. Essentially, PDA will provide photo-absorption for photothermal therapy; organic PDA also has low toxicity, high biocompatibility/degradability with shorter body retention. The approach to PTT guided by imaging requires a high-contrast component. Iron is a high-contrast agent that also has a lower toxicity retention than other metals used for MRI. Iron has shorter clearance and metabolism in the body. The proposal of this work is to produce a natural product polydopamine nanoparticle chelated with iron for magnetic resonance imaging-guided photothermal therapy.

MICROCONTROLLER SIMULATION OF AN ARTERY UNDER DEFORMATION

Ricky Greer II, Carson Schaff, Saami Yazdani, Andrew Faulk, and Jesus Estaba
University of South Alabama, Mobile, AL, USA

Treatment of peripheral artery disease is highly dependent on therapeutic drugs targeting and remaining at the disease site within the peripheral arteries. The dissipation of a drug through the arterial wall is dependent on the tortuosity and porosity of the wall membrane. These metrics are affected by peripheral movements that translate to compression, tension, and twisting of the artery in the body. To better understand how movements affect drug dissipation into arterial walls, a simulation has

been designed to mimic these movements. An Arduino microcontroller in conjunction with multiple stepper motors was designed to control the tension, compression, and twisting of a sample artery under pulsatile flow conditions. Since different arteries have different real world deformation characteristics, the system was designed to provide tension at a rate of at least 1.02 mm/s and torsion/twisting of at least 3.46°/cm. The custom Arduino code enabled the system to be adapted to various testing criteria. The developed bioreactor system will thus be used to study the impact of arterial mechanical deformation on current and next generation interventional devices.

DESIGN OF A BIOREACTOR SYSTEM WITH PERIPHERAL MOVEMENT

Carson Schaff, Ricky Greer, Saami Yazdani, Andrew Faulk, Jesus Estaba
University of South Alabama, Department of Mechanical South Alabama, Mobile, AL, USA

Peripheral Arterial Disease is the buildup of plaque in the peripheral arteries, usually in the legs. If left untreated, it can lead to health problems including heart attack and stroke. If the disease site is below the knee, a stent cannot be placed to hold the artery open due to the high fracture rates caused by cyclic motions from walking. Evidence has been presented that some drug eluting balloons do not work as well below the knee. To understand the effects that deformation has on arteries and pharmacokinetics, an ex vivo system is needed to apply the torsional and contractile movements produced from walking. This system utilizes servomotors to apply torsion and contraction/elongation to an artery. The system fits within a standard sized incubator and can be connected to a pump to allow cell culture media to pulse through it. The inlet valve allows the use of interventional devices to be deployed at a controllable position inside of the artery. The artery is surrounded with agarose to mimic the extracellular matrix and provide support. This helps eliminate kinks during the movement process. Test results agree that this system can apply accurate and repeatable movements to a live porcine artery.

MODELING THE EFFECTS OF PRESSURE AND VISCOSITY ON PENETRATION OF DRUG VIA A PERFUSION CATHETER DELIVERY SYSTEM

Brandon Rittelmeyer and Saami Yazdani
University of South Alabama, Mobile, AL, USA

The perfusion catheter is a relatively new medical device used to administer drugs locally within arteries by perfusing a drug solution into the wall of the artery. In practice, it would be desirable for the drug solution to penetrate as deeply into the wall as possible to maximize the benefit of the treatment, and this would require knowledge of the optimal combination of delivery pressure and viscosity of the drug solution. A computer model of an aortic wall with pressure-dependent geometric and material properties was used to predict drug penetration for a range of delivery pressures and drug viscosities. The results provide, for the first time, theoretical predictions of drug penetration using a perfusion catheter system, which are suitable for experimental validation.

A MATHEMATICAL MODEL TO SIMULATE REENDOTHELIALIZATION FOLLOWING STENTING

Erin McKee, John Faulk, Justin Phillips, Maria Byrne, and Saami Yazdani
University of South Alabama, Mobile, AL, USA

Drug eluting stents (DES) reduce the occurrence of restenosis but increase the risk of late stent thrombosis. Thrombosis subsequently creates reblockage of the artery requiring additional clinical procedures. Late stent thrombosis occurs as endothelial regrowth is inhibited due to an anti-proliferative drug coating, such as Paclitaxel, on the implanted stent. Although smooth muscle cells are the main target, anti-proliferative drugs are not cell type specific. The regrowth rate of endothelial cells post DES remains unknown. One way of determining the regrowth of endothelial cells, in conjunction with the DES, is to create a mathematical model and simulation. This model and simulation could determine factors that may reduce or even prevent stent thrombosis. A computer simulation, which models individual endothelial cell behavior, was implemented and defined by varying parameters carried out by a specific algorithm. Our goal was to simulate the anti-proliferative drugs concentration into the artery over time and due to fluid flow establish a gradient of concentration ratios. With this simulation, we have some insight as to how the endothelial cells interact with varying levels of anti-proliferative drugs. This mathematical model can potentially assist in identifying the ideal dosage and release kinetics of anti-proliferative drugs on DES and possibly eliminate stent thrombosis associated them.

ALTERED GENOMIC EXPRESSION IN THE HIPPOCAMPUS IN DEPRESSION

Gouri Mahajan[1], Eric Vallender[1], Michael Garrett[1], Lavanya Challagundla[1], JC Overhoerls[3], G Jurjus[2], Lesa Dieter[2], Hamed Benghuzzi[1], Craig Stockmeier[1]
[1]University of Mississippi Medical Center, Jackson, MS, USA, [2]Case Western Reserve University, Cleveland, OH, USA, [3]Louis Stokes Cleveland VA Medical Center, Cleveland, OH, USA

Major Depressive Disorder (MDD) has a lifetime prevalence of 17% among US adults, and the available pharmacotherapies are not effective for many depressed patients. Suppression of neurogenesis -related genes may underlie the decrease in hippocampal volume noted with increasing duration of illness. Tissue punches were collected from the dentate gyrus from 23 subjects with MDD (medication-free) and 24 age-matched psychiatrically normal controls. Whole transcriptome paired-end RNA-sequencing was performed using an Illumina NextSeq 500 to quantify expression of mRNA in a region of hippocampal neurogenesis. A Cuffdiff bioinformatic algorithm was used in an initial analysis to statistically compare the two cohorts. Controlling for false discovery, 32 genes were differentially expressed. The following genes were decreased in expression in MDD: several with inflammatory function (e.g. ISG15, IFI44L, IFI6 related to interferon function; NR4A1) and the GABA(B)R1 gene. The following genes were increased in expression in MDD: two genes with cytokine function (SOC3, CCL2), two genes inhibiting angiogenesis (ADM, ADAMTS9) and the KANSL1 gene, a member of the histone acetyltransferase (HAT) complex. Gene Ontology analysis will be used to identify altered gene products in terms of biological processes, cellular components and molecular functions. Additional bioinformatic analyses will also be performed to assess the impact of potentially confounding factors such as postmortem interval, age, gender, death by suicide, duration of depression, and age of onset of depression. qRT-PCR will also be used to validate altered gene expression in MDD. Supported by COBRE P30 GM103328

OPTIMIZING QUALITATIVE MAGNETIC RESONANCE IMAGING (qMRI) FOR BRAIN IRON DEPOSITION ASSESSMENT IN ALZHEIMER'S DISEASE.

Edward Florez, Kenneth Butler, Alyson Stacks, Majid Khan, Ali Fatemi
University of Mississippi Medical Center, Jackson, MS, USA

Deposition of iron in the brain has been associated with chronic neurodegenerative diseases such as Alzheimer's disease. Purpose: To assess the iron deposition more accurately using our proposed T2 weighted MR imaging technique. Materials and Methods: As a first stage, this project used phantoms that were housed in a flat-bottomed plastic vessels, containing the following set of iron standard concentrations typically found in the brain: 1, 1.5, 2, 2.5 and 3ml. MRI imaging protocol was executed using our phantoms on the Siemens Skyra 3.0T scanner. Based on the resulting images, a calibration curve was calculated and a relationship between T2 weighted MRI signal and the iron concentration was found. A map of iron concentrations using the polynomial function of second degree through an image processing algorithm in MATLAB® was done. Finally, twenty real MRI images from the brain (IRB approved retrospective T2 weighted images) were analyzed through our algorithm. These images included normal and volunteer patients with Cognitive impairment. Results: In this preliminary study, results clearly shows the high level of iron in brain

areas directly related to patients who have been diagnosed with cognitive impairment. Conclusions: Brain iron deposition map, as extra routine procedure performed in MRI images, allows to identify iron deposition in particular areas of the brain which are directly associated with degenerative diseases such as Alzheimer's disease. It could also be used as a tool to recognize patients with an advanced stage or high-risk, as well as an accurate indication for implementing a convenient therapy.

THE EFFECT OF COMBINATION TREATMENTS OF EPIGALLOCATECHIN-3-GALLATE, THYMOQUINONE, AND 5-FLUOROURACIL ON FADU NASOPHARYNGEAL CARCINOMA CELLS

Sharita Williams, Hamed Benghuzzi, and Michelle Tucci
University of Mississippi Medical Center, Jackson, MS, USA

Nasopharyngeal carcinoma (NPC) is a rare tumor that arises from epithelial neoplasms in the nasopharynx. It is a rare malignancy in most of the world. NPC is often misdiagnosed and mistreated due to the location of the tumor and non-specific symptoms. The cancer is poorly controlled with current treatment modalities. There is a need for treatment modalities that eradicate the cancer better with lesser side effects. FaDu squamous cell carcinoma cell line was used to test combination treatments of natural (EgCg and TQ) drugs and a chemotherapeutic (5-FU) drug to determine if combining drugs with different cell cycle targets would be more effective at destroying cancer cells than one drug that only targets one phase of the cell cycle. There were a total of four different combinations. One combination consisted of all three treatments: EgCg, TQ, and 5-FU. The other three combinations were as follows: EgCg + TQ, EgCg + 5-FU, and TQ + 5-FU. The combination treatments were measured at 24, 48, and 72 hours. There were significant reductions in cell number at each time increment. The combination of all three drugs proved to be most effective in cell reduction. EgCg or TQ can be combined with 5-FU to reduce cell number. The combination of two drugs specifically a natural drug plus a chemotherapeutic drug proved to be more effective than single individual drugs in eradicating cancer. Natural drugs can be paired with a chemotherapeutic drug to yield significant reductions in cell number producing less adverse side effects.

THE EVALUATION OF ANTIHYPERTENSIVE AGENTS USING CARDIOMYOCYTES

Shana Nelson, Hamed Benghuzzi, and Michelle Tucci
University of Mississippi Medical Center, Jackson, MS, USA

Cardiovascular disease (CVD) is the leading cause of death and hospitalization in the United States. Risk factors that lead to an increase in developing CVD include genetic, behavioral, psychosocial factors, and other underlying conditions. Hypertension is one example of underlying conditions that are risk factors and comorbidities. Treatment options for CVD and other underlying factors may affect the course of the disease. Antihypertensive drugs, such as calcium channel blockers (CCB), beta blockers (BB), or angiotensin converting enzyme inhibitors (ACEI) are used to treat hypertension. The objective of our study was to compare the cellular effects of an ACEI, captopril, on cardiomyocytes. Cardiomyocytes were grown in a tissue culture environment under normal conditions and challenged with therapeutic concentrations of captopril. Over time in culture there were significant changes in cellular protein and intracellular glutathione concentration.

DEVELOPMENT OF A PORTABLE NEAR INFRARED CAMERA FOR SELF DIAGNOSIS OF DIABETIC ULCERS

Vladimir Reukov, Margarita Portillo, Katherine Bryant, Silas Adams, Rebecca Schrody, Elizabeth Gaston, Colin Fair, Ben Glace, Omar Abdeladl, Alex Giron, and Ben Sleeper
Clemson University, Clemson, South Carolina, USA

Venous blood accumulation, or high levels of deoxygenated blood within a tissue, can indicate poor blood circulation and increased risk of ulceration. This condition is associated with Peripheral Arterial Occlusive Disease, or diabetic foot ulceration, which is classified as the most common cause for lower extremity amputation. Due to the loss of sensation, ulcers can form without the patient's' knowledge. Regular inspection of the afflicted area by a physician is the best prevention method for this condition. To simplify the process of examination, a low-cost system for self-monitoring by patients was developed. A near infrared camera was built utilizing a Raspberry Pi System and optical filters in conjunction with MATLAB to detect venous blood in tissues. Tests to optimize the best wavelength and imaging conditions were conducted to determine the optimal settings for the device. Further development includes the creation of an interface to allow data sharing between patients and physicians possible.

GENDER DIFFERENCES IN THE ANTINOCICEPTIVE EFFECT OF OPIOID AGENTS, ALONE OR IN COMBINETION WITH NON-OPIOID AGENTS

Xiaoli Dai, Ike Eriator, and Claude Brounson
University of Mississippi Medical Center, Jackson, MS, USA

Opioids are the most powerful analgesics available to date. However, the use of strong opioids such as morphine is often limited by their intolerable adverse side effects, which motivate the continuing search for new treatment regimen to reduce its side effects. Rational combinations of analgesics with different actions, such as an opioid plus a non-opioid agent, can achieve improved efficacy and safety compared with equianalgesic doses of the individual drugs. We investigated morphine, tramadol alone or in combination with non-opioid agents - mediated antinociceptive effect and gender differences in acute pain model in mice. Experiments were conducted in adult NIH Swiss male and female mice with 6-8 mice per treatment group. Morphine and a weak mu receptor agonist tramadol were administered to mice alone and in combination with non-opioid agents that including antidepressant, NMDA receptor antagonist and GABA receptor antagonist respectively. Mouse tail-flick response latencies to heat stimuli were determined before drug administration and 30 min after morphine, tramadol administration. Results showed that there are gender differences in the antinociceptive effect of opioid agents in combination with non-opioid agents in mice tail-flick test.

TOWARDS THE PREVENTION OF OXIDATIVE DAMAGE VIA NOVEL ANTIOXIDANT CONJUGATES

Jeannette Rodriguez[1], Dmitry Gil[1], Vladimir Ivanov[2], and Vladimir Reukov[1,3]

[1]Department Of Bioengineering, 301 Rhodes Hall, Clemson University, Clemson, SC,, USA; [2]Kurnakov Institute Of General And Inorganic Chemistry, 31 Leninsky Pr-T, Moscow, Russia;

[3]Institute for Biological Interfaces of Engineering, 301 Rhodes Hall, Clemson University, Clemson, SC,, USA

Congestive heart failure affects 6 million Americans and results in a 35% mortality rate in the year immediately following diagnosis; one of the most common causes of heart failure is the loss of myocardial function. Success of treatment methods depend on the extent of oxidative damage to the myocardium caused by reactive oxygen species (ROS). Sufficient amount of ROS in the myocardial environment may lead to the incomplete regeneration of myocardium by myocardial stem cells. In order to decrease oxidative damage, superoxide dismutase (SOD), a class of enzymes, provides pronounced antioxidant effects. However, SOD activity is inhibited by its dismutation products. It is herein proposed that nanocrystalline cerium dioxide (nanoceria) is used with SOD to scavenge hydrogen peroxide, thereby reducing oxidative damage. Nanocrystalline ceria was synthesized using a solvothermal method and characterized by various means, including: X-ray powder diffraction, transmission electron microscopy (TEM), and dynamic light scattering (DLS). SOD-nanoceria conjugates were prepared by mixing the individual parts. The conjugates' antioxidant activity was assessed by an enzymatic activity assay and was found to have significantly higher antioxidant activity when compared to non-functional nanoceria and pure SOD.

DEVELOPING AN APPARATUS TO TREAT PLANTAR FASCIITIS

Jack McGreevey, Benjamin Shumpert, Eddie Bear, Bryce Kunkle, Jushawn Macon, and Vladimir Reukov
Clemson University, Clemson, SC, USA

Plantar fasciitis is a disorder that affects approximately 3 million people per year. The affliction is directly caused by microscopic tears in the plantar fascia tendon, causing great pain in elementary tasks such as walking and standing. The most viable non-invasive treatment is the stretch of the tendon to regain flexibility and strength while decreasing localized inflammation. In order to combat this disease, we have designed a mobile and robust apparatus that uses a stretch transducer to evaluate the amount of stretch resulting from flexion of the foot. The apparatus uses a common sock with a sensor placed such that it is parallel to the sole of the foot. Any type of flexion by the foot results in resistance values interpreted by the sensor that are relayed to a Bluetooth Low Energy (BLE) device. This device is programmed to interpret the resistance values as integers that increase with the resistance and therefore the amount of stretch by the tendon. These values are transmitted via Bluetooth to a smartphone that displays the integer values and stores the data for the purposes of tracking progress by the patient and the clinician. Furthermore, the app also tracks the patient's level of pain day-to-day and allows for programming by the patient and clinician in order to determine the optimal type and amount of stretch necessary to effectively treat the disease.

LOCALIZATION OF THE EPILEPTOGENIC FOCUS FROM EEG FREQUENCY BANDS BY NETWORK CONNECTIVITY ANALYSIS OF SEIZURES OF TEMPORAL LOBE ORIGIN

Jousha Adkison[1], Bharat Karumuri[2], Ioannis Vlachos[1], and Leonidas Iasemidis[2]
Department of Mathematics and Statistics, Louisiana Tech University, Ruston, LA, USA and Department of Biomedical Engineering, Louisiana Tech University, Ruston, LA, USA

Identification and resection of the epileptogenic focus constitutes a potential treatment for abatement of recurrent seizure activity in patients with refractory epilepsy. Analysis of the epileptogenic focus via functional brain networks may assist in this direction. In order to measure the interactions between brain sites and construct functional brain networks, successive 3sec non-overlapping intracranial electroencephalographic (iEEG) segments from multiple brain regions during typical seizures from 9 patients with temporal lobe epilepsy were analysed in the frequency domain using the Generalized Partial Directed Coherence (GPDC) measure, along with surrogate data analysis, to determine the statistically significant connections between the nodes of the network. We subsequently employed the topological measure of Betweenness Centrality (BC) to quantify the importance of each node in each constructed network. The obtained BC values were then averaged over frequencies (the traditional frequency bands [alpha],[beta],[gamma],[delta],[theta] and the full frequency band (0-50Hz)) and all available ictal EEG segments per patient. The brain site with the maximum averaged BC value estimated from the [delta] band (0-4Hz) was found to be within the clinically assessed epileptogenic focus in all 9 patients, whereas the ones from other bands, including the full frequency band, did not have the same level of success (e.g. the one estimated from the full frequency band was located within the focus in only 6 of the 9 patients). These results indicate the importance of considering specific frequency bands, especially the lowest ([delta]) frequency band, in brain network analysis of ictal periods for robust localization of the epileptogenic focus.

THE RESPONSE OF INTERLEUKIN-STIMULATED A549 HUMAN ALVEOLAR BASAL EPITHELIAL CELLS UPON EXPOSURE TO HYDROCORTISONE IN CULTURE

Jana Bagwell, Michelle Tucci, and Hamed Benghuzzi
University of Mississippi Medical Center, Jackson, MS USA

The A549 human adenocarcinoma cell line is theorized to produce chemokines in response to inflammatory cytokines. Eotaxin, a CC chemokine, may play a role in recruitment and activation of eosinophils to the site of inflammation in obstructive lung diseases such as asthma. The objective of this study was to evaluate the influence of hydrocortisone on A549 cells after cytokine exposure, such as interleukin 1β (IL-1β) and interleukin 4 (IL-4) in culture. The objective of this study is to assess the levels of eotaxin (CCL11), when combined with hydrocortisone. Confluent A549 cells were stimulated separately with IL1-β and IL-4 in concentration variation at ten-fold serial dilution in a 96-well plate. Standard laboratory protocols and sterile techniques were followed throughout the experimentation. The cells were treated independently and allowed to incubate for 24 and 48 hours. Cellular viability, oxidative stress and cell membrane were measured along with analysis of cellular morphology to determine overall cellular health. Eotaxin levels were determined by immunoassay. ANOVA indicated there was no significant difference in groups with IL-1β at 24 and 48 hours when comparing all treatment groups. Only the 48 hours IL-4 group had a significant difference in groups, with the highest eotaxin level in the hydrocortisone group combined with 10.0 ng/dL of IL-4. The results from this study indicate that eotaxin levels are influenced by hydrocortisone in cellular model but not reduced. In this study, hydrocortisone had an increased influence on eotaxin levels when A549 cells were subjected to IL-4 at higher levels.

NEONATAL EXPOSURE TO INTERLEUKIN-1B ENHANCES ADULT VULNERABILITY OF NIGROSTRIATAL DOPAMINERGIC SYSTEM TO ROTENONE NEUROTOXICITY

Lir-Wan Fan[1], Lu-Tai Tien[2], Jonathan W Lee[1], Silu Lu[1], Rick CS Lin[3], Xiaoli Dai[4], Norma B Ojeda[1], Abhay J Bhatt[1], ***Renate D Savich[1], and*** *Yi Pang[1]*
[1]Department of Pediatrics, Division of Newborn Medicine, University of Mississippi Medical Center, Jackson, MS, USA
[2]School of Medicine, Fu Jen Catholic University, New Taipei City, Taiwan
[3]Department of Neurobiology and Anatomical Sciences, University of Mississippi Medical Center, Jackson, MS, USA
[4]Department of Anesthesiology, University of Mississippi Medical Center, Jackson, MS, USA

Early life brain inflammation has been proposed to play important roles in the development of neurodegenerative disorders in adult life. Our previous studies showed that interleukin-1β (IL-1β), a proinflammatory cytokine, plays an important role in mediating dopaminergic neuronal injury in the neonatal rat brain. To examine whether neonatal IL-1β exposure enhances dopaminergic neuron susceptibility to rotenone neurotoxicity at adult ages, Sprague-Dawley male rats at postnatal day 5 (P5) were pre-treated with IL-1β (1 μg/kg) via intracerebral injection, and then challenged with rotenone through subcutaneous mini-pump infusion (1.25 mg/kg per day for 14 days) at P70. A single IL-1β exposure resulted in motor function deficits during the developmental period but were spontaneously recoverable by P70. Single IL-1β exposure also suppressed tyrosine hydroxylase (TH) expression in the substantia nigra (SN) at P70. A low dose of rotenone treatment resulted in Parkinsonism-like symptoms including bradykinesia, akinesia and rigidity in rats with neonatal exposure to IL-1β, but not in those without the neonatal IL-1β exposure. Neonatal IL-1β exposure also enhanced adult susceptibility to rotenone-induced loss of dopaminergic neurons as indicated by reduced numbers of TH+ cells and Fluoro-Gold (FG)+ nigrostriatal projecting neurons in the SN of P98 rats. These results suggest that perinatal neuroinflammation may enhance adult susceptibility to develop neurodegenerative disorders triggered by environmental toxins at an ordinarily non-toxic or sub-toxic dose. Our model may be useful for studying mechanisms involved in the pathogenesis of nonfamilial Parkinson's disease. (Supported by NIH Grant NIH/NINDS R01NS080844, and Newborn Medicine Funds from the Department of Pediatrics, University of Mississippi Medical Center)

MINOCYCLINE AMELIORATES BRAIN INJURY, AND IMPROVES SENSORIMOTOR BEHAVIORAL PERFORMANCE IN NEONATAL RATS EXPOSED TO SYSTEMIC LIPOPOLYSACCHARIDE

Silu Lu[1], Jonathan W Lee[1], Lu-Tai Tien[2], James P Shaffery[3], Yi Pang[1], Norma B Ojeda[1], Abhay J Bhatt[1], Renate D Savich[1], and Lir-Wan Fan
[1]Department of Pediatrics, Division of Newborn Medicine, University of Mississippi Medical Center, Jackson, MS, USA
[2]School of Medicine, Fu Jen Catholic University, New Taipei City, Taiwan
*[3]Department of **Psychiatry and Human Behavior**, Animal Behavior Core, University of Mississippi Medical Center, Jackson, MS, USA*

Inflammation plays an important role in brain injury in neonatal human and animal models. Our previous studies have shown that systemic administration of endotoxin lipopolysaccharide (LPS) induces brain injury and behavioral deficits in the neonatal rats, which is associated with activation of microglia. The objective of the current study was to determine whether minocycline, a putative suppressor of microglial activation, ameliorates LPS-induced brain inflammation, brain damage, and neurological dysfunction. Intraperitoneal (i.p.) injection of LPS (2 mg/kg) was performed in P5 rat pups and minocycline (45 mg/kg) or vehicle was administered (i.p.) 5 min after LPS injection. The control rats were injected (i.p.) with sterile saline. Neurobehavioral tests were performed and brain injury was examined on P6. Our results showed that minocycline protected against LPS-induced neurobehavioral impairments, including reduction of mean latency times in wire hanging maneuver and hind-limb suspension. Minocycline treatment also provided protection against LPS-induced brain damage, including loss of oligodendrocytes as well as reduction of white matter size. Minocycline significantly attenuated LPS-induced increment in the number of activated microglia and concentration of IL-1beta in the neonatal rat brain and serum. These results suggest that minocycline may provide protection against systemic LPS exposure-induced brain injury and neurobehavioral disturbance, and that the protective effects are associated with its ability to attenuate LPS-induced microglial activation. (Supported by NIH grant NIH/NINDS R01NS080844, and Newborn Medicine Funds from the Department of Pediatrics, University of Mississippi Medical Center)

IL-1 RECEPTOR ANTAGONIST PROTECTS AGAINST LONG-LASTING LEARNING IMPAIRMENT AND HIPPOCAMPAL INJURY IN ADULT RATS FOLLOWING NEONATAL EXPOSURE TO LIPOPOLYSACCHARIDE

Lu-Tai Tien[1], Ku-Mao Lan[1, 2], Yi Pang[3], Silu Lu[3], Abhay J Bhatt[3], Lir-Wan Fan[3]
[1]School of Medicine, Fu Jen Catholic University, New Taipei City, Taiwan
[2]Department of Anesthesiology, Chi-Mei Medical Center, Taiwan
[3]Department of Pediatrics, Division of Newborn Medicine, University of Mississippi Medical Center, Jackson, MS, USA

We have previously reported that neonatal lipopolysaccharide (LPS) exposure resulted in an increase in interleukin-1β (IL-1β) content, injury to the hippocampus, and cognitive deficits in juvenile male and female rats, as well as female adult rats. The present study aimed to determine whether an anti-inflammatory cytokine, interleukin-1 receptor antagonist (IL-1ra), protects against the neonatal LPS exposure-induced inflammatory responses, hippocampal injury, and long-lasting learning deficits in adult rats. LPS (1 mg/kg) or LPS plus IL-1ra (0.1 mg/kg) was injected intracerebrally to Sprague-Dawley male rat pups at postnatal day 5 (P5). Neurobehavioral tests were carried out on P21, P49, and P70, while neuropathological studies were conducted on P71. Our results showed that neonatal LPS exposure resulted in learning deficits in rats at both developmental and adult ages, reduced hippocampal volume, and reduced number of Nissl+ cells in the CA1 region of the middle dorsal hippocampus of P71 rat brain. Those neuropathological and neurobehavioral alterations by LPS exposure were associated with a sustained inflammatory response in the P71 rat hippocampus, indicated by increased number of activated microglia as well as elevated levels of IL-1β. Neonatal administration of IL-1ra significantly attenuated LPS-induced long-lasting learning deficits, hippocampal injury, and sustained inflammatory responses in P71 rats. Our study demonstrates that neonatal LPS exposure leads to a persistent injury to the hippocampus, resulting in long-lasting learning disabilities related to chronic inflammation in rats, and these effects can be attenuated with an IL-1 receptor antagonist. (Supported by NIH Grant NIH/NINDS R01NS080844, Newborn Medicine Funds from the Department of Pediatrics, University of Mississippi Medical Center, grants NSC102-2320-B-030-011 and MOST103-2320-B-030-005-MY3 from the National Science Council of Taiwan, and a grant CMFJ10006 from Chi-Mei Medical Center in Taiwan)

LOW LEVEL LASER THERAPY IMPROVES MICROCIRCULATION IN SKELETAL MUSCLE VASCULAR BEDS IN ZUCKER RATS

Lu, Silu ; Xiang, Lusha; Hester, Robert L; Barnes, Lisa; *Benghuzzi, Ham: and Huang, Min*
University of Mississippi Medical Center, Jackson, MS, USA

Purpose/Hypothesis: It has been reported that low level laser therapy (LLLT) can reduce pain, inflammation and increase wound healing. But there is a lack of information regarding the effect of LLLT on the microvascular reactivity. Therefore the main purpose of this study was to determine the effect of LLLT on skeletal muscle vascular function and the underlying mechanisms. We hypothesized that LLLT induces vasodilation in skeletal muscle vascular beds in Zucker rats. Number of Subjects: Five 12-13 weeks old Zucker rats were used in this study. Arteriolar diameter of the spinotrapezius (n=5) or mesenteric vascular beds (n=5) were observed for analysis. Materials/Methods: Zucker rats (12-13 weeks old) were injected with pentobarbital (50mg/kg, ip). Depth of anesthesia was monitored by the palperbral reflex test. Then the trachea was intubated to enable the rat to spontaneously breathe 30 % oxygen and 70% nitrogen. Deep esophageal temperature was maintained at 37°C by using heating pad or heating lamp. Either the right spinotrapezius muscle or mesenteric vascular beds were prepared for in vivo microscopy as we have used in previously published studies (Lu et al, 2013). At all times during the surgery and subsequent experiment, the vascular beds were kept at in situ dimensions and were continuously perfused with a physiological salt solution (mM): 118.07 NaCI, 6.17 KCI, 2.55 CaCI2, and 25 NaHC03, equilibrated with gases containing 5% C02, 95% N2 (pH= 7.4, 35°C). Animals were allowed to stabilize for 30 minutes after surgery. A third-order arcade arteriole segment was selected for analysis. Arteriolar diameter of the spinotrapezius or mesenteric vascular beds were observed with a Nikon UM-22 microscope and measured during a control period and following LLLT (20 sec). At the end of the experiment, adenosine (10 iJM) and sodium nitroprusside (10 iJM) were added to the perfusate to determine maximal diameter. These experiments lasted 2-4 hours. For all studies the animals did not recover from anesthesia. The animals were euthanized by an overdose of sodium pentobarbital in the end of the experiment. Results: LLLT significantly increased arteriole vasodilation in spinotrapezius muscle (19.6 ± 3 1Jm) compared with basal vascular diameter (15.6 ± 2 1Jm). LLLT has no effect on mesenteric vascular beds (14 ± 1 IJm) compared with basal condition (14 ± 0.81Jm). Conclusions: LLLT induces vasodilation and improves microcirculation in skeletal muscle vascular beds. Clinical Relevance: LLLT may have good potential to improve functional outcomes in patients with neurologic deficits, soft tissue injury, pain, wound healing by increasing blood flow by inducing vasodilation of arterioles in the microcirculation.

EVALUATION OF ANISOTROPIC DIFFUSION FILTERING ALGORITHMS FOR ANALYSIS OF 3-DIMENSIONAL MICROSCOPY IMAGE DATA OF FÖRSTER RESONANCE ENERGY TRANSFER PROBES

Kenny Trinh, Naga Annamdevula, Rachel Sweat, Thomas Rich, and Silas Leavesley
University of South Alabama Mobile, AL, USA

Förster Resonance Energy Transfer (FRET) has been utilized for many different applications in cellular imaging including protein folding, signaling studies, and enzyme kinetics measurements. However, traditional FRET microscope approaches have been limited to 2 spatial dimensions. A large factor preventing FRET experiments from being extended into 3 dimensions is that approaches to measure FRET probes have commonly had poor signal strength, as compared to single label assays. The low signal-to-noise ratio (SNR) of FRET measurements often results in compromises being made between the quality of images acquired, the resolution, the imaging speed, and the ability to perform 3-dimensional imaging. The goal of this work was to evaluate the ability of post-acquisition image processing algorithms for improving the quality of FRET microscopy images. Specifically, we evaluated 2 general classes of smoothing functions: Gaussian smoothing (a standard smoothing algorithm available in MATLAB) and Perona-Malik anisotropic diffusion (available on MATLAB Central, authored by Daniel Lopes), using a range of settings. Experiments were performed using a cyclic AMP FRET reporter (Turquoise-Epac-Venus H188 FRET probe) expressed in either pulmonary microvascular endothelial cells or HEK 293 cells. All image data were acquired using a Nikon A1R spectral confocal microscope. We found that simple smoothing algorithms can be used to increase the SNR. However, by increasing the SNR the resolution of the cell's boundaries is reduced. We also evaluated Perona-Malik algorithms for non-linear smoothing. By applying anisotropic diffusion 3D FRET image data, we were able to increase the SNR while preserving accurate discrimination of the cell's boundaries.

ADIPOGENIC DIFFERENTIATION OF HUMAN ADIPOSE DERIVED STEM CELLS ATOP AN ELASTIN-LIKE POLYPEPTIDE-POLYELECTROLYTE COATED SURFACE

Sarah Fitzgerald and Jared Cobb
University of Mississippi Medical Center, Jackson, MS, USA

In today's society, obesity has become an epidemic that ultimately causes a variety of potentially deadly metabolic diseases. Therefore, it is important to study the behavior of adipocytes (fat cells) on the cellular level, to more efficiently combat the problem of obesity. Current three-dimensional in vitro model for adipocyte culture, which primarily uses collagen based hydrogels to encapsulate adipocytic cell conglomerates, allows for better intracellular communication compared to two-dimensional monolayer cell culture. However, the conglomerate size and adipose-specific cell function are diminished due to the compressive forces placed on cells by the hydrogels. Such forces do not exist on adipocytes in vivo. Elastin-like polypeptide polyelectrolytes (ELP-PE) have been tested and used in the past for several different cell types, in which positively- charged polyelectrolytes encourage cells to form three-dimensional spheroids while tethering themselves to the surface of a cell plate. We hypothesize that adipocytes grown on an ELP-PE coated surface would show an uninhibited growth from any scaffold-generated compressive forces, and thus grow larger and function better than in the current collagen hydrogel based model. To investigate this, we will use culture surfaces coated with ELP-PEs prepared using PEs of different molecular weights conjugated to ELP. Human Adipose-derived stem cells will be differentiated and matured into adipocytes atop these coatings and their growth will be monitored using optical microscopy. The adipocyte functionality will be tested using DNA assay, total protein assay, and triglyceride assay. Overall, our research will provide a proven cell culture model for future studies involving adipocytes.

QUANTITATIVE ASSESSMENT OF SEMINIFEROUS TUBULE ALTERATION ASSOCIATED WITH LONG-TERM EXPOSURE TO SUSTAINED DELIVERY OF ANDROGENS

Hamed Benghuzzi[1], Michelle Tucci[1], Kenneth Butler[1], Ibrahim Farah[2] and Joseph A. Cameron[2]
[1]University of Mississippi Medical Center, Jackson, MS and [2]Jackson State University, Jackson, MS

The specific aim of this study was to assess, morphometrically, the seminiferous tubules area and germ layers upon the exposure to sustained delivery of androgen through tricalcium phosphate lysine devices (TCPLD). A total of 105 adult Male rats (270-280 gm) were randomly divided into three equal groups. Group 1 animals were implanted with Tricalcium Phosphate Ceramic Delivery Devices (TCPLD) loaded with 40 mg androgen by following standard lab protocols. Groups 2 and 3 animals served as a sham group (empty devices), and an intact control group. For the treatment and sham groups, serum testosterone, LH and FSH levels were monitored at periodic intervals of 1, 3, 6, 9, and 12 months. Histopathological evaluation of testicular tissues (H&E) was conducted for each phase following standardized lab procedures. Results of this study indicated that: (i) endogenous testosterone and gonadotropin (LH/FSH) levels were suppressed (<0.2 ng/mL) for a 1-year period by the sustained delivery of androgen compared to control and sham groups, (ii) a decrease in the luminal areas of seminiferous tubules retrieved from treated group ($P<0.05$), (iii) an arrest of germ layers at the secondary spermatocyte at the end of the 3 month treatment and continued for the rest of the study, and (iv) spermatogonia were intact and exhibited normal N/C ration for treated animals compared control group. Overall conclusion obtained from this study indicated that androgen loaded TCPL delivery devices can be used to induce azoospermia without any untoward side effects.

DEVELOPMENT OF A NEW FUZZY C-MEANS CLUSTERING ALGORITHM FOR AUTOMATIC DETECTION OF OSA USING P-WAVE SHAPE AND TIME CHANGES

Khaldon Lweesy
Jordan University of Science and Technology, Irbid, Jordan

This paper describes the development and implementation of a new fuzzy c-means (FCM) clustering algorithm to automatically detect obstructive sleep apnea (OSA) stages from regular electrocardiogram (ECG) recordings based on shape and time changes of the P-wave. ECG signals from 25 subjects known to have OSA symptoms were recorded, pre-processed, and segmented to extract the P-waves; then three P-wave parameters were extracted: the P-wave duration, the P-wave dispersion, and the time interval from the peak of the P-wave to the R-wave. The new FCM clustering algorithm was then applied to the three parameters taken two at a time then taken the three together. Applying the new proposed FCM clustering algorithm using the parameter combination of the P-wave duration and the time from the peak of the P-wave to the R-wave resulted in a good performance with sensitivity, selectivity, specificity, and accuracy values of 87.7 ± 2.9, 86.9 ± 2.8, 87.1 ± 2.1, and 87.4 ± 1.1, respectively. A better performance was achieved when applying the new proposed FCM clustering algorithm to the three parameters taken together; the sensitivity, selectivity, specificity, and accuracy values were 89.2 ± 1.1, 88.3 ± 0.9, 89.8 ± 1.3, and 89.1 ± 1.4, respectively.

AUDITORY PROCESSING IMPAIRMENT PREDICTS PERCEIVED HEARING PROBLEM IN INDIVIDUALS WITH NORMAL PURE-TONE THRESHOLDS

Charles Bishop, Mary Johnson, Lauren McNichol, Christopher Spankovich, and Elgenaid Hamadain
University of Mississippi Medical Center, Jackson, MS USA

Normal pure tone threshold sensitivity does not necessarily indicated normal hearing. The auditory processing of a sample of 1322 participants of the Jackson Heart Study, a prospective epidemiological study of cardiovascular disease and health disparities in African

Americans, was assessed between 2008 and 2013. Here we present cross-sectional data on participants with normal pure tone thresholds with and without perceived hearing loss and relationship to central auditory processing outcomes, Quick Speech-in-Noise (SIN) and Dichotic Digits. The results suggest that perceived hearing problems, despite

A DIETARY PHASE 2 ENZYME INDUCER IN ANIMAL MODEL OF ESSENTIAL HYPERTENSION USING AN EXTERNAL ARTERIAL CATHETER

[1]Banigesh, A, [1]Iqbal, R., [1]Murabit, A., [1]Juurlink, B., [2]Tucci, M., [2]Benghuzzi, H., and [1]Mohamed, A.
[1]Anatomy and Cell Biology, Department of Medicine, College Of Medicine, University of Saskatchewan, Sk., Canada [2] University of Mississippi Medical Center, MS, USA

By 2025, one billion individuals Worldwide are hypertensive. However, dietary intervention could be a simple solution for this complex multifactorial problem which increases at an alarming rate. Previous studies in our laboratory have shown that broccoli sprouts rich in glucoraphanin, a precursor of a potent phase 2 protein inducing isothiocyanate sulforaphane, decreases oxidative stress and ameliorates hypertension using tail cuff method. In addition, in another study, pure sulforaphane ameliorates hypertension using tail cuff method. The question this study addressed: using the external arterial Catheter (another method), can we see the same therapeutic effect of sulforaphane? After 1 week of adaptation, the 12 week old male SHRsp and SD rats were divided into two groups: (i) Corn oil (vehicle) alone (Control); (ii) sulforaphane (10 µmol/kg body weight) in corn oil. BP was determined using an external arterial catheter. The treatment lasted for 7 weeks. At the end of the treatment period, the animals were sacrificed. For comparison, age-matched normotensive Sprague Dawley (SD) rats were treated in the same manner. SHRsp control rats had significantly higher Systolic Blood Pressure (SBP) (158.4± 8.3 mm Hg) than SD control rats (108.07±3.91). Sulforaphane treatment lowered SHRsp blood pressure to 150.66±8.33(around 7 mm Hg unit). Interestingly, sulforaphane had more potential effect on diastolic BP; It reduced the diastolic BP by 47.47 mmHg unit, comparing with the control SD rats. There was no significant effect of sulforaphane treatment on SD rat SBP (84.35± 7) when compared with SD control rats (90.96 ±7). We conclude that the health benefit previously demonstrated in our laboratory is due to pure sulforaphane and the external arterial catheter BP data is in parallel confirmed the results obtained by tail cuff method in previous experiment.

THE EFFECTS OF ACUTE AND CHRONIC FLUOXETINE ADMINISTRATION ON ADULT RAT TESTES

Gerri A. Wilson, Michelle A. Tucci and Hamed A. Benghuzzi
University of Mississippi Medical Center, Jackson, MS, USA

The effects of acute and chronic ingestion of the SSRI fluoxetine on testicular cells were investigated in Sprague Dawley adult male rats. The animals were exposed to either 10 or 20 mg/kg fluoxetine administered via cookie dough for two or 16 weeks. Fluoxetine administration of either dose did not result in changes in body weight over time. The wet weights of the reproductive organs were normalized to body weight and then compared to their respective controls. Differences between the groups were apparent as early as two weeks in the epididymis of the high dose groups when compared with the low dose group and control. The epididymal weights in the high group were larger than control and statistically greater than low dose treatment. By 16 weeks there were no differences in the normalized epididymal weights between the groups. Normalized testicular weights were statistically higher in the high dose group after four months when compared to both the low and control animals. Histomorphometric analysis of the testicular cell population showed decreases in the number of both primary and secondary spermatocytes and spermatid for both doses when compared to control at two and 16 weeks. Overall, long-term ingestion of either dose for 16 weeks causes a significant decrease in spermatogenesis in seminiferous tubules of the testes, which can impact fertility. Assessment of the reproductive hormones testosterone, FSH, and LH are being investigated to determine the role of the SSRI on the hypothalamic-pituitary-gonadal axis.

THE RESPONSE OF CONNECTIVE TISSUE FOLLOWING SINGLE DOSE OR SUSTAINED ADMINISTRATION OF PRP

Jessica Gilbert[1], Jeremy Stokes[2], Joseph A. Cameron[1], Hamed Benghuzzi[2], David Black[2], and Michelle Tucci[2]

[1]Jackson State University, Jackson, MS, USA and [2]University of Mississippi Medical Center, Jackson, MS, USA

Tendon ruptures and lacerations requiring suture repair can have post-operative complications that limit function. Appropriate care must include early range-of motion exercises to prevent adhesions and loss of motion and limited early weight bearing because of potential loss of excursion or even rupture. Refinement in repair technique has increased the immediate post-operative strength of the tendons, lessening the risk of rupture. However, no surgical technique or adjunct treatment exists that effectively prevents adhesions or decreases recovery time. Platelet rich plasma is rich in growth factors and has the potential to increase the repair potential and decrease the time to complete tissue healing. In this study, forty eight Sprague Dawley rats were used to investigate the effects of a single bolus dose of PRP or continuous delivery of PRP on healing of a surgically induced trauma and repair of the Achilles tendon. The injury and repair process did not induce untoward harm to the animal's behavior or ability to move freely and independently within the cage. It did not hamper the animal's ability to access food. After two weeks, a single bolus dose of PRP resulted in an increased tissue response compared to injury alone. Sustained release of the PRP induced a significant increase in the number of adipocytes present within the tissue. After eight weeks the initial increase in tissue response seen in the single dose PRP treatment was no longer evident and no differences were detected compared to the injury alone group. The Sustained PRP group still had an increase in the number of adipocytes present along with a much larger portion of fibrotic tissue at the wound site. Overall, it appears that both timing and dose are critical factors that must be taken into consideration when using PRP to enhance healing.